

GEOLOGICA ULTRAIECTINA

Mededelingen van de
Faculteit Aardwetenschappen
Universiteit Utrecht

No. 182



Cycling of Phosphorus and Manganese in the Arabian Sea during the Late Quaternary

Sjoerd J. Schenau

GEOLOGICA ULTRAIECTINA

Mededelingen van de
Faculteit Aardwetenschappen
Universiteit Utrecht

No. 182

**Cycling of phosphorus and Manganese in the Arabian Sea
during the Late Quaternary**

Sjoerd J. Schenau

ISBN 90-5744-040-7

Cycling of phosphorus and manganese in the Arabian Sea during the Late Quaternary

De fosfor en mangaan cycli in de Arabische Zee tijdens het Laat Kwartair

(met een samenvatting in het Nederlands)

Proefschrift

ter verkrijging van de graad van doctor
aan de Universiteit Utrecht
op gezag van de Rector Magnificus Prof. Dr. H.O. Voorma
ingevolge het besluit van het College voor Promoties
in het openbaar te verdedigen
op maandag 6 december 1999 des middags te 12.45 uur

door

Sjoerd Johannes Schenau

geboren op 25 oktober 1971, te Gorinchem

Promotor: Prof. Dr. C.H. van der Weijden
Department of Geochemistry, Utrecht University
Utrecht, The Netherlands

Co-promoter: Dr. G.J. de Lange
Department of Geochemistry, Utrecht University
Utrecht, The Netherlands



The research described in this thesis was carried out at the Department of Geochemistry, Institute of Paleo-environments and Paleoclimate Utrecht (IPPU), Utrecht University, Budapestlaan 4, PO Box 80021, 3508 TA Utrecht, The Netherlands. This study was supported by The Netherlands Organization for Scientific Research (NWO).

“Se il discorrere circa un problema difficile fusse come il portar pesi, dove molti cavalli porteranno più sacca di grano che un caval solo, io acconsentirei che i molti discorsi faccessar più che un solo; ma il discorrere è come il correre, e non come il portare, ed un caval barbero solo correrà più che cento frisoni”.

Galileo

“alleen voor jullie, zonen van wetenschap en wijsheid, hebben wij dit werk geschreven. Studeert aandachtig in dit boek en zoekt onze bedoeling bijeen, die wij verspreid over verschillende plaatsen hebben uiteengezet; en wat op één plaats door ons verborgen is gehouden, hebben wij op een andere duidelijk gemaakt, zodat het voor jullie onthuld wordt, als jullie wijs zijn.”

Heinrich Cornelius Agrippa von Netteshein,
De occulta philosophia, III, 65

Contents

Chapter 1: Introduction and summary	9
--	----------

Part I: OMZ Variability in the Arabian Sea

Chapter 2: Oxygen Minimum Zone controlled Mn redistribution in Arabian Sea sediments during the Late Quaternary	21
--	-----------

Chapter 3: A 27 kyr record of monsoon variability and Oxygen Minimum Zone intensity from the Oman Margin coastal upwelling area	45
--	-----------

Part II: Sedimentary P cycling in the Arabian Sea

Chapter 4: Phosphogenesis and active phosphorite formation in sediments from the Arabian Sea Oxygen Minimum Zone	65
---	-----------

Chapter 5: A novel chemical method to quantify fish debris in marine sediments: implications for interpreting phosphorus burial records	93
--	-----------

Chapter 6: Phosphorus regeneration versus burial in sediments of the Arabian Sea	113
---	------------

Chapter 7: Factors controlling the Phosphorus burial efficiency in Arabian Sea sediments during the Late Quaternary	135
--	------------

List of abbreviations	157
-----------------------	------------

References	159
------------	------------

Samenvatting in het Nederlands (summary in Dutch)	175
---	------------

Acknowledgements	182
------------------	------------

Curriculum Vitae	183
------------------	------------

1

Introduction and Summary

“But the largest number of [marine] animals and those of the largest size are in the Indian Sea, among them whales covering three acres each, and sharks 100 ells long : in fact in those regions lobsters grow to 6 ft. long, and also eels in the river Ganges to 300 ft.”

Plinius Maior, *Naturalis Historia*, Book IX. II.4.

The Arabian Sea has been known for its high marine productivity for a long time. The Greek soldiers in the army of Alexander the Great, who in the fourth century BC were the first Europeans known to sail the Arabian Sea, noticed the high abundance of marine life in comparison to the Mediterranean Sea. They observed how particularly during the solstices “rushing whirlwinds and rain-storms and tempests hurling down from mountain ridges upturn the seas from their bottom, and roll with their monsters up from the depths in great multitudes” (*Plinius Maior, Naturalis Historia*). This was probably the first time that increased marine productivity was related to the period of the monsoons. For periods exceeding written history, local and regional fisheries have harvested the high stocks of tropical tunas (*Sharp, 1992*). Only during the last century has the Arabian Sea been exploited

Chapter 1

commercially. The total marine fishery catch in the western Indian Ocean has increased from ~ 0.5 million ton in 1950 to nearly 3.7 million ton in 1997 (FAO, 1999), making this region an important fishing area. Large resources of mesopelagic fish and tunas are still under-exploited (Sharp, 1992; FAO, 1997).

The high marine biomass in the Arabian Sea is the result of monsoon induced upwelling of nutrient-rich water masses offshore Oman and Somalia (e.g. Qasim, 1982). It has still not been adequately established which nutrient(s) limit(s) productivity in the present-day oceans (e.g. Codispoti, 1989). Recently, iron bioavailability has been identified to limit phytoplankton growth in some open ocean environments (e.g. Martin et al., 1990; Coale et al., 1996). Nitrate is the limiting nutrient in most coastal waters (Howarth, 1988), due to a low supply by rivers and losses by denitrification in water column and sediment. In the Arabian Sea, present-day phytoplankton production in the surface waters is thought to be nitrogen limited as well (Woodward et al., 1999). Phosphorus (P) has, in contrast to nitrogen, no important gaseous phases in the natural environment, and the oceanic mass balance of phosphorus is solely governed by input from fluvial and eolian sources, and burial in sediments (e.g. Froelich et al., 1982; Delaney, 1998). Phosphorus is a structural and functional component of all organisms. It is present in cell constituents like nucleic acids, nucleotides, phosphoproteins, and phospholipids, and plays a central role in the storage, transport and utilization of energy. These properties make phosphorus an essential nutrient to the biosphere. On geological time scales, phosphorus availability is considered to be the main factor controlling net primary productivity in the oceans, because shortages of nitrogen are ultimately replenished by nitrogen fixation from the atmosphere (Holland, 1978; Broecker and Peng, 1982; Howarth et al., 1995; Tyrell, 1999). Marine productivity determines the burial of organic carbon, and thus controls the atmospheric CO₂ and O₂ concentrations. The bioavailability of phosphorus in the oceans may potentially play an important role in climate change (Broecker, 1982; Van Cappellen and Ingall, 1996). Furthermore, detailed knowledge of the marine phosphorus cycle provides a better understanding of the biogeochemical cycling of carbon, nitrogen, sulphur, and other biophile elements on geological time scales.

This thesis investigates phosphorus and manganese cycling in the Arabian Sea during the Late Quaternary, using sediment records recovered during the Netherlands Indian Ocean Programme (NIOP) in 1992. The **first part** is concerned with the reconstruction of Late Quaternary variability in paleoproductivity and oxygen minimum zone intensity. Special attention is given to manganese and sulphur accumulation patterns in order to trace back variations in bottom water oxygen content of the deep basin and continental slope. In the **second part** of this thesis P cycling in the Arabian Sea sediments is investigated. Pore water fluxes and solid-phase P speciation results are combined to assess the diagenetic processes controlling the benthic regeneration and burial of P. The contrasting environmental conditions that characterized the Arabian Sea in past and present provide an excellent opportunity to elucidate the mechanisms that govern P removal from the oceans, and to determine the potential role of P cycling on changes in paleoproductivity over geological time scales.

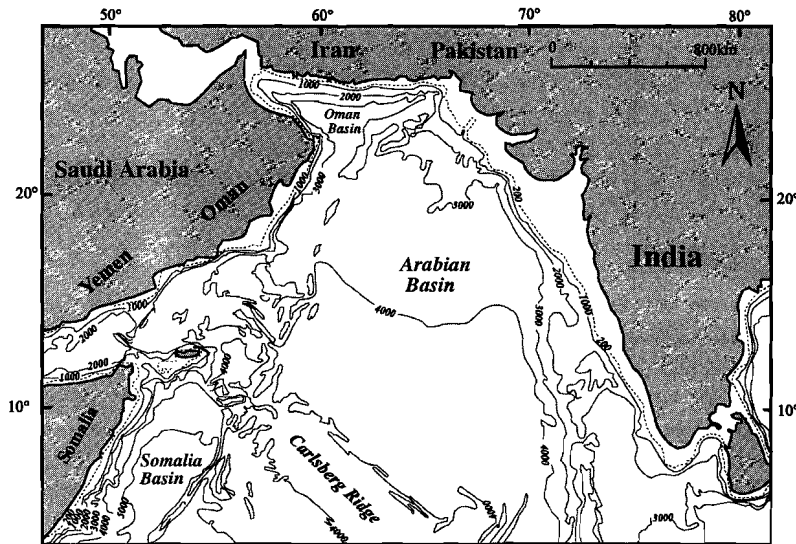


Figure 1. Map of the Arabian Sea.

Climate and hydrography of the Arabian Sea

The Arabian Sea is a semi-enclosed basin in the northwestern Indian Ocean (Fig. 1). Its climate and hydrography are controlled by the monsoonal wind system (e.g. Wyrski, 1971; Slater and Kroopnick, 1984). During Northern Hemisphere summer (May - September) differential heating between the continent and the ocean leads to the development of a low pressure cell over the Himalayas and the Tibetan Plateau. The strong pressure gradient between Asia and the southern Indian Ocean initiates strong southwestern winds (SW monsoon). These winds, which are concentrated in a narrow jet stream parallel to the coasts of Oman, Yemen and Somalia (Findlater jet), induce offshore Ekman transport of the surface waters, resulting in coastal upwelling (e.g. Wyrski, 1971; Currie, 1973). In addition, the positive (cyclonic) curl of wind stress over the Arabian Sea causes upward Ekman pumping northwest of the jet axis, which drives open-sea upwelling over a 400-km-wide area (e.g. Smith and Bottero, 1977; Bauer et al., 1991). Upwelling also occurs on the west coast of India as the result of local winds that have a southward direction (Sharma, 1978). Coastal and open-sea upwelling carries cold, nutrient-rich water masses to the ocean surface, stimulating high rates of biological productivity throughout the northern Arabian Sea (Qasim, 1982; Brock et al., 1992; Jochem et al., 1993). During the SW monsoon, primary productivity rates vary from $2.5 \text{ gC m}^{-2} \text{ d}^{-1}$ offshore Oman to $0.5 \text{ gC m}^{-2} \text{ d}^{-1}$ in the more oligotrophic central Arabian Basin (Owens et al., 1993). For the Northern Hemisphere winter (November - April) the situation is reversed. High atmospheric pressure over the

Chapter 1

Asian continent induces northeastern trade winds, which are generally weaker than the SW monsoon. These winds cause onshore Ekman transport which suppresses upwelling and productivity (Slater and Kroopnick, 1984). The alternating six-monthly change in wind direction results in a prominent seasonal contrast in primary productivity (e.g. Banse, 1987), and biogenic and lithogenic fluxes through the water column (Nair et al., 1989, Ittekkot et al., 1992). Estimates for annual primary productivity in the northern Arabian Sea vary between 200 and 400 gC m⁻²y⁻¹ (e.g. Kabanova, 1968; Qasim, 1982; Codispoti, 1991; Olsen et al., 1993; Jochem et al., 1993). This makes the Arabian Sea is one of the most productive areas of the world.

The Arabian Sea is characterized by an intense Oxygen Minimum Zone (OMZ) between 150 and 1250 m water depth (e.g. Wyrki, 1971; Slater and Kroopnick, 1984). Oxygen concentrations in the OMZ are lowest in the northeastern part of the Arabian Sea (< 4.5 μM; e.g. Morrison et al., 1999), and increase slightly in an southeastern direction (Wyrki, 1971). The pronounced oxygen deficiency at mid-water depths induces high rates of denitrification in the central part of the Arabian Sea (Deuser, 1978; Naqvi, 1987). Sporadically, free hydrogen sulphide has been detected in the OMZ (Ivanenkov and Rozanov, 1961), but these reports should be questioned (Deuser et al., 1978; Farrenkopf et al., 1997). The low mid-water oxygen concentration is caused by the combination of high oxygen consumption rates invoked by high downward fluxes of organic matter, a strong thermo-stratification of the upper 200 m of the water column, a sluggish deep water ventilation, and the relatively low dissolved oxygen content of the water sources (Indian Ocean Central Water, Persian Gulf Water, Red Sea Water) at intermediate depth (Wyrki, 1973; Slater and Kroopnick, 1984; Swallow, 1984, Olsen et al., 1993). High marine productivity and the oxygen depleted waters of the OMZ strongly affect the nature of the sediments underlying the Arabian Sea. Sediments are frequently laminated and rich in organic matter where the OMZ impinges on the continental slope (Shimmield et al., 1990; Von Rad et al., 1999; Van der Weijden et al., 1999). In the deeper part of the Arabian Basin, where bottom waters are well oxygenated, sedimentary organic matter concentrations are generally lower.

The unique characteristics of the Arabian Sea make this region an important study area for the mechanisms of wind-driven upwelling (e.g. Currie et al., 1973; Swallow, 1984; Currie, 1992), the influence of upwelling on the global carbon dioxide budget (e.g. Ittekkot et al., 1992; Shimmield, 1992), paleoclimatic reconstructions (e.g. Clemens and Prell, 1990; Sirocko et al., 1993; Emeis et al., 1995; Clemens et al., 1996; Reichart et al., 1997; 1998; Von Rad et al., 1999), and the nature of organic carbon accumulation in oxygen depleted waters (preservation vs. production; Pedersen et al., 1992; Paropkari et al., 1992; Calvert et al., 1995; Reichart, 1997; Van der Weijden et al., 1999).

Sequential extraction techniques

Application of various sequential extraction techniques constitutes a prominent element of this thesis. Sequential extractions are commonly used to study the sedimentary cycling of

several key elements, such as S, N, P, Ca, Mg, Sr, Ba, Mn, and Fe (*e.g. Lord, 1982; Canfield, 1989; Huerta-Diaz and Morse, 1990; Ruttenberg, 1992; Ruttén, et al., 1999*). This technique is based on the principle that different solid-phase fractions show dissimilar reactivity to a series of reagents. Sediment samples are washed sequentially with a series of solvents to extract the specific fractions, in which the most reactive phases are removed first.

The sedimentary manganese speciation is highly susceptible to the (past) redox conditions in water column and sediment (*e.g. Calvert and Pedersen, 1993; De Lange et al., 1994; Ruttén et al., 1999*). In **Chapter 2** a 6-step sequential extraction scheme is presented to distinguish the three main Mn fractions in marine sediments, namely 1) Mn carbonates, 2) Mn oxides, and 3) a residual fraction, consisting of Mn associated with aluminosilicates and pyrite. Application of this extraction scheme provides an important tool to determine paleoredox conditions and the nature of sedimentary Mn spikes.

As a consequence of the low P concentrations in marine sediments, sequential extraction techniques are the only available methods to obtain detailed solid-phase information on the composition of sedimentary P (*Ruttén, 1992*). *Lucotte and d'Anglejan (1985)* developed a detailed sequential extraction scheme that distinguishes 1) easily exchangeable P, 2) P associated with iron oxides, 3) apatite, and 4) organic P. This scheme was extended and modified by *Ruttén (1992)* for marine sediments (SEDEX method), enabling the separation between authigenic and detrital apatites. The SEDEX method has been applied successfully to many different marine environments (*e.g. Ruttén and Berner, 1993; Filippelli and Delaney, 1996; Slomp et al., 1996; Louchouart et al., 1997; Eijssink et al., 1998*). In **Chapter 5** the SEDEX method has been modified to allow, for the first time, the separation of P associated with biogenic apatite (fish debris) from authigenic apatite. Up to now, handpicking, which is very time consuming, was the only method to semi-quantify their presence (*Suess, 1981; De Vries and Pearcy, 1982*). Distinction between these two apatite phases has three advantages. Firstly, it enables evaluation of importance fish debris burial in the marine phosphorus cycle. Secondly, it allows reconstruction of the deposition history of fish debris in sediment records. Thirdly, application of this extraction scheme improves the determination of authigenic apatite burial rates.

The results of this thesis show that the 2 M NH₄Cl extraction can be applied for multiple usage, namely to distinguish biogenic apatite (paleo-productivity indicator, **Chapter 5**), and Mn carbonates (paleo-redox indicator, **Chapter 2**), Ca-carbonates (*De Lange et al., 1986*), and barite (paleo-productivity indicator; *Ruttén and De Lange, in prep., Chapter 5*).

OMZ Variability in the Arabian Sea

The monsoonal climate system of the northern Indian Ocean has been subject to large variations during the Late Quaternary. The intensity of monsoon-induced upwelling is primarily controlled by precessional driven changes in summer insolation, that alter the surface low-pressure over the Asian continent (*e.g. Clemens and Prell, 1990; Clemens et al.,*

Chapter 1

1991; Anderson and Prell, 1993). Sediment core studies have revealed that fluctuations in paleoproductivity exhibit a strong 23-kyr signal (e.g. Shimmiel, 1992; Emeis et al., 1995, Reichart et al., 1998). The intensity of the Indian summer monsoon is also affected by glacial-interglacial climate variations (e.g. Prell, 1984). In the Arabian Sea, glacial periods are characterized by relatively high mass accumulation rates and an overall low primary productivity rates in comparison to interglacial periods (Emeis et al., 1995; Reichart et al., 1998). As a result of the differences in the organic carbon rain rate and deep convective overturn, the intensity and extension of the OMZ has varied considerably during the Late Quaternary (Altabet et al., 1995; Reichart et al., 1998; Den Dulk et al., 1998).

Manganese is a key element for the determination of past variations in bottom water oxygen (BWO) conditions (e.g. Calvert and Pedersen, 1993; De Lange et al., 1994). In **Chapter 2** Late Quaternary Mn sedimentation is investigated in Arabian Sea sediments, in order to reconstruct past variations in OMZ intensity. The presence of Mn carbonates in the sediments of the deep Arabian Basin indicates that bottom waters have remained oxygenated for at least the last 185 kyr. At particular depth intervals Mn enrichments have been observed, which occur in the basal part of organic rich layers. The timing of the Mn spikes corresponds to periods of enhanced reactive Mn fluxes to the deep basin. A vertical extension of the OMZ resulted in enhanced remobilization of reactive Mn from continental margin sediments into the water column, and its subsequent removal to the deeper, more oxygenated environment. During glacial periods, only small vertical shifts of the base of the OMZ are needed (100-300 m) to produce the observed Mn remobilization. Mn records from deep basin sediments in the Arabian Sea can thus be used as a proxy to trace back variations of the redox conditions of the intermediate waters through time.

During the last two decades, climate studies of the Indian Ocean monsoon have focussed on the Oman and Yemen upwelling area (e.g. Prell, 1984; Shimmiel et al., 1990; Sirocko et al., 1993; Emeis et al., 1995). In **Chapter 3** sub-Milankovitch variability in monsoon intensity is studied on the Oman Margin. A high-resolution geochemical record, combined with micropaleontological data shows high-frequency variations in sea surface productivity caused by changes in the intensity of summer monsoon induced upwelling. Changes in aridity on the Arabian Peninsula varied synchronous with the summer monsoon, periods with minimum monsoon intensity being driest. The local OMZ, which presently impinges on the Oman continental margin, was reconstructed using laminations, redox sensitive elements, aragonite preservation and sulphur diagenesis. OMZ intensity varies together with summer monsoon strength, being weakest during periods of minimum summer monsoon intensity. The oxygen depleted waters of the OMZ caused iron oxides reduction in the water column and/or sediment water interface. As a consequence, pyrite formation in continental margin sediments of Oman was limited by the availability of reactive iron. Correlating summer monsoon variability to the northernmost part of the Arabian Basin indicates that minima in summer monsoon intensity coincided with maxima in winter monsoon strength. Furthermore, the record from the Oman Margin again confirms the link between sub-Milankovitch variability in high and low latitude climate.

Sedimentary P cycling in the Arabian Sea

Phosphorus is ultimately removed from the oceans by accumulation in sediments. The flux of particulate P arriving at the sediment water interface consists of a reactive and a non-reactive fraction. Only the first may potentially be mobilized and become available again for utilization in the biosphere (Krajewski, 1994). Reactive phosphorus is delivered to the sediment by three major sources, namely 1) organic matter, 2) iron oxides, which have a high sorption capacity for phosphate, and 3) fish debris (e.g. Froelich et al., 1988; Van Cappellen and Berner, 1988; Van Cappellen and Ingall, 1994; Fig. 2). Non-reactive phosphorus, primarily consisting of detrital apatite, usually represents only a small fraction relative to the total accumulating P flux (Ruttenberg and Berner, 1993; Filippelli and Delaney 1996). Upon burial, the quantity and form of reactive P sequestered in sediments is strongly affected by early diagenetic processes (e.g. Krom and Berner, 1981, Sundby et al., 1992; Delaney, 1998). Organic matter degradation, iron oxide reduction, and dissolution of fish debris result in the release of phosphate to the porewater (Fig. 2). Interstitial phosphate either diffuses back to the bottom water, is incorporated in the benthic biomass, or precipitates as carbonate fluorapatite (CFA; phosphogenesis). Authigenic apatite has been identified as a potentially important sedimentary sink of reactive phosphorus in the oceans (Ruttenberg and Berner, 1993). Particularly sediments from upwelling areas are often characterized by high authigenic phosphorus contents; when they contain over 5 wt% P_2O_5 , they are classified as phosphorites (e.g. Cook, 1984).

For the evaluation of P cycling in the oceans it is important to determine the extent and environmental conditions controlling phosphogenesis. In **Chapter 4** phosphogenesis and phosphorite formation are investigated in the Arabian Sea surface sediments located within the present-day oxygen minimum zone. Porewater characteristics and the downcore increase of a solid-phase Ca-phosphate mineral, indicate that phosphogenesis is currently occurring in these sediments. Application of a diagenetic model revealed that phosphogenesis on the Pakistan Margin is induced by a high rate of organic matter degradation and, probably, fish debris dissolution. Early diagenetic iron cycling does not significantly affect sedimentary P cycling in these environments. Furthermore, model results indicate that dysoxic rather than fully anoxic bottom waters are more effective in promoting early diagenetic phosphogenesis. The highest rate of authigenic apatite formation was observed in a boxcore taken on the Oman Margin, where it contributes to the formation of a Holocene phosphorite deposit. This is the first time Holocene phosphorite formation is reported for this upwelling area. Phosphorites are presently forming on the Oman Margin as a result of a) deposition of older, reworked material from the continental shelf, that has undergone an earlier phase of phosphogenesis, b) a high Holocene input of reactive P (fish debris and degradable organic matter), c) a relatively low sediment accumulation rate, and d) the absence of winnowing (at this specific location).

Deposition and burial of fish debris is generally considered to play an unimportant role in the marine P cycle (e.g. Froelich et al., 1982). In **Chapters 5, 6, and 7** the burial and regeneration of P associated with fish debris (P_{fish}) is studied in Arabian Sea sediments. In

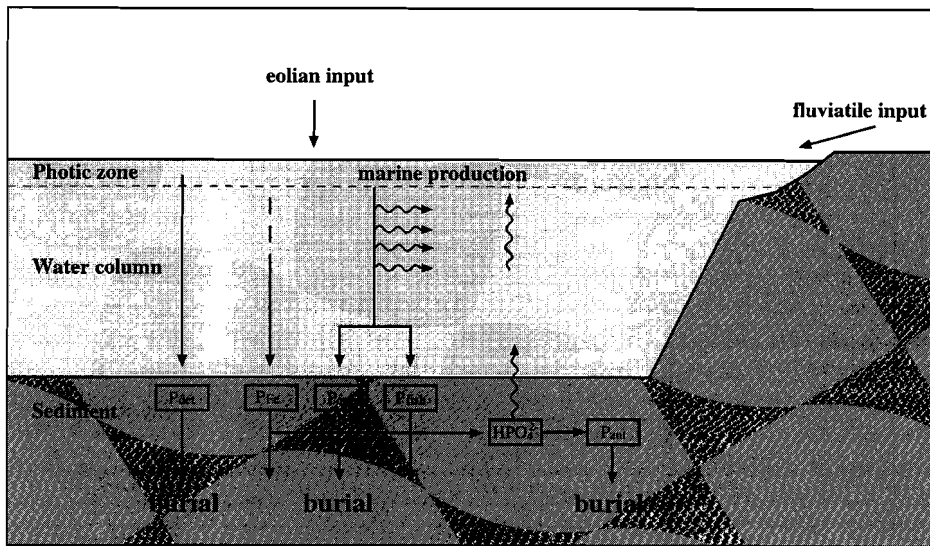


Figure 2. Simple representation of the marine phosphorus cycle. Phosphorus is supplied to the oceans by fluvial and eolian transport. In the surface waters the nutrient phosphate is incorporated in soft and hard tissues of marine organisms. These biogenic particles eventually sink to the seafloor. Most of the particulate organic P (P_{org}) or P associated with fish debris (P_{fish}) is regenerated during transit through the water column, and only a small fraction reaches the sediment surface. An additional source of sedimentary P is phosphate scavenged by settling detrital iron oxides (P_{Fe}). Upon burial, phosphate may be released to the porewater by organic matter degradation, iron oxide reduction, or fish debris dissolution. The remobilised phosphate diffuses back to bottom water, or is incorporated into an authigenic apatite phase (P_{CFA}). The remaining sedimentary P fraction is buried and removed from the oceanic P cycle. The non-reactive P fraction, primarily consisting of detrital apatites (P_{det}), does not actively participate in the oceanic P cycle. The phosphate regenerated in the sediment and water column is ultimately transported back photic zone, where it will fuel new marine production.

recent surface sediments, preservation of fish debris is significantly higher in sediments located above 1200 m water depth than it is for deeper sediments (**Chapter 5**). The distribution of P_{fish} contents in surface sediments is predominantly governed by the extent of fish debris regeneration, which is related to differences in water depth and sedimentation rate. Additionally, the low bottom water oxygen concentrations may cause enhanced preservation of fish debris in continental slope sediments. In **Chapter 6** the solid-phase P speciation and benthic phosphate fluxes in recent Arabian Sea sediments are discussed. Benthic phosphate fluxes are highest in the continental slope sediments of the Arabian Sea, underlying low bottom water oxygen concentrations. Organic matter degradation and phosphate desorption from iron oxides do not produce sufficient phosphate to explain these high benthic P fluxes. The potentially high deposition of fish debris in the Arabian Sea, and a good correlation between benthic P fluxes and P_{fish} accumulation rates indicate that benthic P fluxes in these

sediments are to a large extent governed by early diagenetic dissolution of fish debris. The burial history of P_{fish} during the Late Quaternary has been investigated in two sediment cores, one from the Pakistan Continental Margin, the other from the deep Arabian Basin (**Chapter 7**). The average solid-phase P speciation in these environments is very similar: phosphorus associated with fish debris and P associated with authigenic apatite each constitute approximately 30% of the total P inventory, whereas P associated with iron oxides, organic P, and detrital apatite constitute only minor fractions. Downcore variations in total solid-phase P concentration are primarily related to changes in the contribution of the P_{fish} fraction (**Chapter 5**). On the continental slope, changes in P_{fish} contents concur with alternations in paleoproductivity, as inferred from geochemical and paleontological proxies. In these marine environments the P_{fish} (and thus solid-phase P) content is a better paleoproductivity proxy than the organic carbon and barite concentration. In sediment records from the deep basin, on the other hand, sedimentary phosphorus contents are less suitable as a paleoproductivity indicator, due to higher regeneration rates of fish debris.

Over the past decade, there has been considerable interest in the environmental factors regulating the burial efficiency of P in the oceans. *Ingall and Jahnke (1994)* have shown that benthic regeneration of reactive phosphorus is more extensive under oxygen-depleted bottom waters, resulting in a lower P burial efficiency. Enhanced loss of P from sediments during long time periods of bottom water anoxia (i.e. exceeding the oceanic P residence time) will lead to an increased supply of P into the photic zone and promote new primary productivity, provided that P is the biolimiting nutrient (*Ingall et al., 1993; Ingall and Jahnke, 1994; 1997, Van Cappellen and Ingall, 1994*). The positive feedback between water column anoxia, benthic P generation, and marine productivity may explain the often observed occurrence of organic-rich sediments under anoxic bottom water conditions (*Ingall and Jahnke, 1994, 1997*). In **Chapters 6 and 7** the environmental factors controlling P burial in the Arabian Sea are discussed. A sharp decrease of the reactive P accumulation rate in the surface sediment with increasing water depth, in combination with constant primary productivity rates throughout the Arabian Sea indicates that P burial in continental slope sediments located within the OMZ is more efficient than in deep basin sediments (**Chapter 6**). Consequently, no direct evidence was found in Arabian Sea sediments for more efficient P burial in oxic relative to dysoxic bottom water conditions. The effectiveness of P burial is primarily regulated by differences in P regeneration occurring in the water column and at the sediment water interface.

In **Chapter 7** the response of sedimentary P burial to changing primary productivity and bottom water redox conditions during the Late Quaternary is studied. The phosphorus burial efficiency is generally lower during periods of increased productivity in both continental slope and deep marine sediments. This may be explained by a) the partial decoupling of the P export flux, consisting primarily of particulate organic P, and the P burial flux, consisting primarily of biogenic and authigenic apatite, and b) the lack of higher rates of phosphogenesis during periods of increased P deposition. Higher oceanic primary productivity induces more efficient oceanic P cycling. Over geological time scales this process may induce higher productivity (assuming that P availability is limiting productivity in the oceans), thus creating a positive feedback loop. In the Arabian Sea, this feedback mechanism may also be active on sub-Milankovitch time scales, as P regenerated on the

Chapter 1

continental margins of the Oman and Somalian coastal upwelling areas is transported to the photic zone relatively fast.

Part I:

OMZ Variability in the Arabian Sea

“The earth is round like a sphere, and the waters adhere to it and are maintained on it through natural equilibrium which suffers no variation”.

Al Edrisi, The Book of Roger, Sicily, 1154 AD

2

Oxygen Minimum Zone controlled Mn redistribution in Arabian Sea sediments during the Late Quaternary

S.J. Schenau, G.J. Reichart, and G.J. de Lange

Abstract - Manganese cycling in the Arabian Sea is strongly influenced by the presence of an intense Oxygen Minimum Zone (OMZ). In this study we have investigated Late Quaternary Mn burial in Arabian Sea sediments, comparing records from the deep basin and the continental slope. A selective sequential extraction procedure has been used to characterize the solid-phase Mn speciation. The presence of Mn carbonates in the sediments of the deep Arabian Basin indicates that the bottom waters have remained oxygenated for at least the last 185 kyr. At particular sediment depth intervals Mn enrichments have been observed with concentrations up to 3750 ppm, consisting primarily of Mn carbonates. These early diagenetic Mn spikes, which occur in the basal part of organic rich layers, have been formed during periods of enhanced reactive Mn fluxes to the deep basin. Periods of increased downward fluxes of reactive Mn are associated with a vertical extension of the OMZ, which caused dysoxic conditions in the bottom water impinging on slope sediments previously being oxic and located below the OMZ. Remobilization of reactive Mn into the water column, which has subsequently been removed to the deeper, more oxygenated environment, has resulted in the formation of the Mn enrichments in deep basin sediments. Relocation of Mn from continental slope sediments is evidenced by Mn depletion in organic-rich intervals. During glacial periods only small vertical shifts of the base of the OMZ are needed (100 – 300 m) to produce the observed Mn remobilization. The largest OMZ extensions have occurred during interglacial stage 5, which have been related to maximum productivity during interglacial precession minima. The results of this study indicate that Mn records from deep basin sediments in the Arabian Sea can be used as a proxy to trace back variations in redox conditions of the intermediate waters through time.

Introduction

The hydrography of the Arabian Sea is strongly effected by the monsoonal wind system. During Northern Hemisphere summer a strong southwest monsoon causes coastal and open-sea upwelling off Somalia and Oman (*e.g. Slater and Kroopnick, 1984*). The upwelling waters are rich in nutrients, and cause high seasonal productivity throughout the Arabian Sea (*e.g. Qasim, 1982*). High downward fluxes of organic matter into subsurface waters, in combination with a sluggish water circulation owing to the semi-enclosed configuration of the Arabian Basin, result in an intensive Oxygen Minimum Zone (OMZ) between 150 and 1250 m water depth, with oxygen concentrations lower than 2 μM (*Van Bennekom and Hiehle, 1994*). The low oxygen concentrations indicate that, besides denitrification (*Naqvi, 1987*), also Mn oxide reduction occurs in the water column. A maximum in the Mn^{2+} concentration (4.6-6.5 nM) has been observed at ~ 800 m water depth, coinciding with the OMZ (*Saager et al., 1989*). Dissolved manganese is removed at the base of the OMZ by vertical diffusion and oxidative scavenging (*Martin and Knauer, 1984*), and laterally where the OMZ expands into more oxygenated waters (*Dickens and Owen, 1994*). Consequently, Mn cycling in the Arabian Sea is strongly influenced by the presence of the OMZ.

Since upwelling areas play an important role in the global organic matter

accumulation and thus fixation of CO₂, the development of upwelling systems through geological time has received much attention (e.g. *Andersen and Gardner, 1989; Clemens and Prell, 1990; Summerhayes et al., 1992*). Sediment records from the Arabian Sea reveal strong fluctuations in paleoproductivity and OMZ intensity, which have been linked to variations in orbital parameters (e.g. *Clemens and Prell, 1990; Reichart et al., 1998*). Variations in the monsoonal activity are primarily controlled by the 23-kyr precession cycle, resulting in high organic matter accumulation rates and an intensified OMZ during late summer insolation maxima (*Reichart et al., 1998*). Superimposed on the 23-kyr cyclicity is the glacial/interglacial cyclicity. In the Arabian Sea, glacial periods are characterized by relatively high mass accumulation rates, low primary productivity and a weakened OMZ compared to interglacial periods (*Emeis et al., 1995; Reichart et al., 1998*).

Manganese burial records have frequently been used to reconstruct past variations in bottom water oxygen (BWO) conditions, because Mn is highly susceptible to changes in redox conditions in water column and sediment (e.g. *Calvert and Pedersen, 1993; De Lange et al., 1994; Schenau et al., 1999*). In the surface sediments of deep basins underlying oxygenated bottom waters, Mn accumulates as (hydr)oxides (MnO₂ or MnOOH; e.g. *Finney et al., 1988*). When organic matter accumulation rates are low and of low degradability, Mn (hydr)oxides can be preserved till considerable burial depths (e.g. *Finney et al., 1988*). In sediments underlying areas of high productivity, accumulation of reactive organic matter induces reduction of Mn(IV) to the more soluble Mn(II) in the upper part of the sediment. Manganese released into the porewaters diffuses upward and reprecipitates in the oxic zone of the sediment, causing a high subsurface Mn oxide concentration (*Froelich et al., 1979; Burdige and Gieskes, 1983; De Lange et al., 1989*). Oxygenated bottom water conditions, therefore, ensure that no reactive Mn is lost from the sediment to the bottom water. Continued Mn cycling will build up the porewater Mn²⁺ concentration in the suboxic part of the sediment until a Mn carbonate phase starts to precipitate (*Thomson et al., 1986; De Lange, 1986; Middelburg et al., 1987; Calvert and Pedersen, 1993*). Under steady-state BWO conditions, all reactive (i.e. reducible) Mn initially deposited as Mn (hydr)oxides, is ultimately buried as Mn carbonates. Under suboxic to anoxic bottom water conditions, on the other hand, Mn oxides are reduced either in the water column or at the sediment water interface. Since no reactive Mn is buried, porewater Mn²⁺ concentrations remain low and no Mn carbonates are formed. Therefore, only the non-reactive Mn fraction, which is primarily associated with alumino-silicate minerals, is buried in these environments (*Calvert and Pedersen, 1993*).

In this chapter, Mn cycling in the Arabian Sea during the Late Quaternary is studied, comparing sediment records from deep basin and continental slope environments. First, we will discuss Mn diagenesis in the sediments of the Arabian basin. Subsequently, we will investigate whether Mn burial is influenced by Mn relocation processes, and whether the sedimentary Mn record from the deepest part of the basin can be used as an independent proxy to trace back variations of the OMZ in time.

Material and methods

Study area

The three piston cores selected for this study were taken during leg D2 and D3 of the Netherlands Indian Ocean program (NIOP) in 1992 (Table 1). Two piston cores (PC487 and PC458) were recovered from the Arabian Basin from water depths of 3574 m and 3001 m respectively, and are both located well below the base of the present-day OMZ. Piston core 455 (PC455) was taken from the continental slope of the Pakistan Margin from a water depth of 1002 m, which is presently located within the OMZ. The sample locations of the piston cores are shown in Figure 1. Bottom water oxygen concentrations were obtained from nearby CTD stations (Table 1). The sediments consist mainly of homogeneous, light-greenish hemipelagic muds interbedded with slightly darker organic-rich intervals. In PC455 most of the organic-rich intervals are finely laminated.

Pore water analysis

Porewater extractions were started on board within 24 hours of core collection following a standard shipboard routine (*Van der Weijden et al., 1994*). The sediment cores were sluiced into a glovebox, which was kept under low-oxygen conditions ($O_2 < 0.0005\%$) and at a constant in-situ bottom water temperature. Sediments were put into Reeburgh-type squeezers, and under a nitrogen pressure of up to 7 bar, pore waters were extracted. Shipboard analysis of alkalinity and pH were performed within 12 hours after the extraction of the porewater. Alkalinity was determined after titration using the Gran plot method (*Gieskes, 1973*). Precision on duplicate measurements was better than 1 %. Acidified porewater samples were taken back to the laboratory and measured for total dissolved Mn and Ca with a Inductively Coupled Plasma Atomic Emission Spectrometer (ICP-AES; Perkin Elmer Optima 3000). Precision of duplicate measurements was better than 3 %.

Table 1. *Position, water depth, core length, and present-day oxygen concentrations of the bottom water of the sampled piston cores.*

	Latitude (N)	Longitude (E)	water depth (m)	core length (m)	[O ₂] bottom water (μM)
PC487	19°55'9	61°42'8	3574	13.8	151
PC458	21°59'4	63°48'7	3001	16.31	124
PC455	23°33'4	65°57'0	1002	14.56	< 2

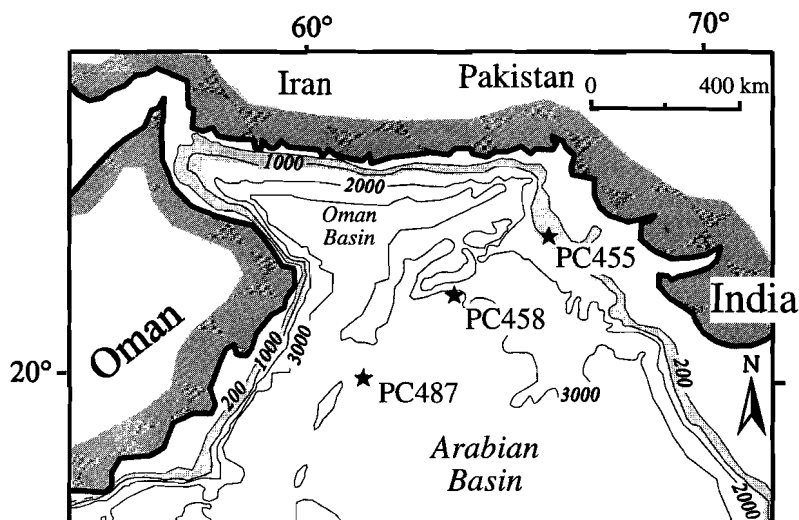


Figure 1. Locations of piston core sites 455, 458, and 487. PC458 and PC487 are located in the Arabian Basin, PC455 is located on the Pakistan Margin. The area where the present-day OMZ impinges on the continental slope is shaded.

Solid-phase analysis

Porosity and dry bulk density of the sediment were calculated by measuring weight loss of fixed volume samples after freeze-drying. After removal of inorganic carbon with 1 M HCl, the organic carbon content (C_{org}) was measured with a NCS analyser (NA 1500). Relative errors are smaller than 1 %. Bulk concentrations of Mn, Ca, Al, and Ba were determined by total digestion of 250 mg sample in 5 ml of a 6.5 : 2.5 : 1 mixture of $HClO_4$ (60%), HNO_3 (65%) and H_2O , and 5 ml HF (40%) at 90°C. After evaporation of the solutions at 190°C on a sand bath, the dry residue was dissolved in 25 ml 1 M HCl. The resulting solutions were analysed with ICP-AES. All results were checked using international (SO1, SO3) and in-house standards. Relative errors for duplicate measurement are better than 3 %.

The solid-phase speciation of Mn in PC487 was examined using a 6-step sequential extraction technique. The extraction steps were selected from known sequential extraction schemes, and where needed adjusted to obtain an optimal separation of a specific Mn phase (Table 2). Approximately 250 mg of dried and ground sediment were subsequently washed sequentially with 25 ml of the solvents. After each extraction step the sediment was rinsed twice with demineralised water. The extraction scheme was tested by extraction of rhodochrosite and sediment standards with a known Mn speciation. All solutions were analysed with ICP-AES. For sediment samples, recovery with respect to the total concentration of Mn, Al and Ca is 96%, 95% and 85% respectively. Relative reproducibility of Mn for each extraction step was generally better than 5 %.

Table 2. Details of the applied sequential extraction scheme and the extracted Mn fractions.

Step	Extractant	Mn phase extracted	Reference
1	<ul style="list-style-type: none"> • 6x 25 ml 2 M NH₄Cl (pH 7) • 2x 20 ml demin. water 	Mn carbonates	after <i>De Lange, 1992</i>
2	<ul style="list-style-type: none"> • 25 ml 0.17 M Na-citrate/ 0.6 M NaHCO₃/ 0.11 M ascorbic acid (pH 8) • 2x 25 ml demin. Water 	Amorphous Mn hydr(oxides)	<i>Kostka and Luther, 1994</i>
3	<ul style="list-style-type: none"> • 25 ml 1 M Na-acetate buffered to pH 5 with acetic acid • 2x 25 ml demin. water 	Mn carbonates	after <i>Rutten et al., 1999</i>
4	<ul style="list-style-type: none"> • 25 ml 0.2 M Na-citrate, 0.35 M Na-acetate, buffered to pH 4.8 with acetic acid, and 1.25 g Na-dithionite • 2x 25 ml demin. water 	Crystalline Mn hydr(oxides)	<i>Kostka and Luther, 1994</i>
5	<ul style="list-style-type: none"> • 20 ml 40 % HF • 1x 25 ml demin. water 	Mn associated with clay minerals	<i>Lord, 1982</i>
6	<ul style="list-style-type: none"> • 20 ml HF/HNO₃/HClO₄ 	Mn associated with pyrite	<i>Lord, 1982</i>

Oxygen isotope records for the piston cores were obtained from the analyses of ~30 handpicked specimens of *Neogloboquadrina dutertrei* per analysis. After roasting the samples for 30 minutes at 470°C under a helium flow to remove organic remains, they were transferred to an automated carbonate preparation unit (IsoCarb). The CO₂ was measured online on a VG SIRA 24 mass spectrometer. Values are reported relative to the Peedee belemnite (PDB) in standard δ notation; calibration is achieved through analyses of National Bureau of Standards (NBS) 19 reference materials. The mean standard deviation for $\delta^{18}\text{O}$ on triplicate samples was 0.08 ‰. The chronology of the piston cores is based on the $\delta^{18}\text{O}$ records (Fig. 2), using the procedure employed by *Reichert et al. (1998)*. Mass accumulation rates (MARs) were calculated by multiplying the linear sedimentation rates with the dry bulk densities.

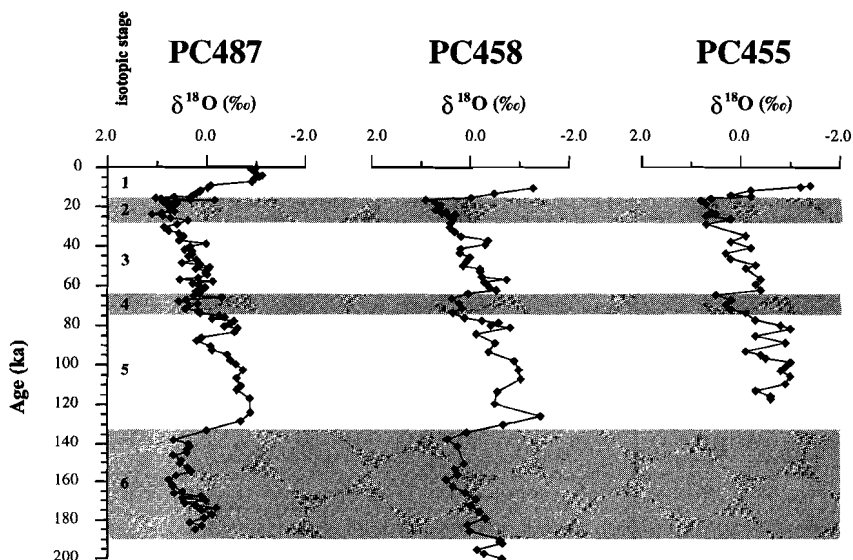


Figure 2. The $\delta^{18}\text{O}$ time series of *N. dutertrei* for PC487, PC458 and PC455, in ‰ relative to the PDB standard.

Results

Porewater results for PC487

The porewater concentration of Mn versus depth in PC487 sharply increases to 75 μM , followed by a gradual decrease to 15 μM in the deepest part of the core (Fig. 3). Alkalinity increases with depth, whereas porewater concentrations of Ca show a nearly linear decrease. The pH (not shown) remains constant at ~ 8.0 throughout the core. Saturation with respect to pure rhodochrosite (MnCO_3) in the porewaters of PC487 has been calculated as described in *De Lange (1986)*. The apparent solubility product of rhodochrosite (K'_{SO}) was calculated from K_{sp} in seawater (3.27×10^{-9} ; 25 °C, 1 bar; *Johnson, 1982*) for the in-situ pressure (368 bar) and temperature (1.3 °C), and equals 3.83×10^{-9} . The ion product (IP) of MnCO_3 was calculated as

$$\text{IP} = (\text{Mn}^{2+}) \times (\text{CO}_3^{2-})$$

where (Mn^{2+}) is the total or “analytical” concentration of Mn^{2+} measured in the porewater and (CO_3^{2-}) the in-situ CO_3^{2-} concentration, which has been calculated from pH (corrected for temperature and pressure) and alkalinity data (corrected for contributions of $\text{B}(\text{OH})_4^-$, HSiO_3^- ,

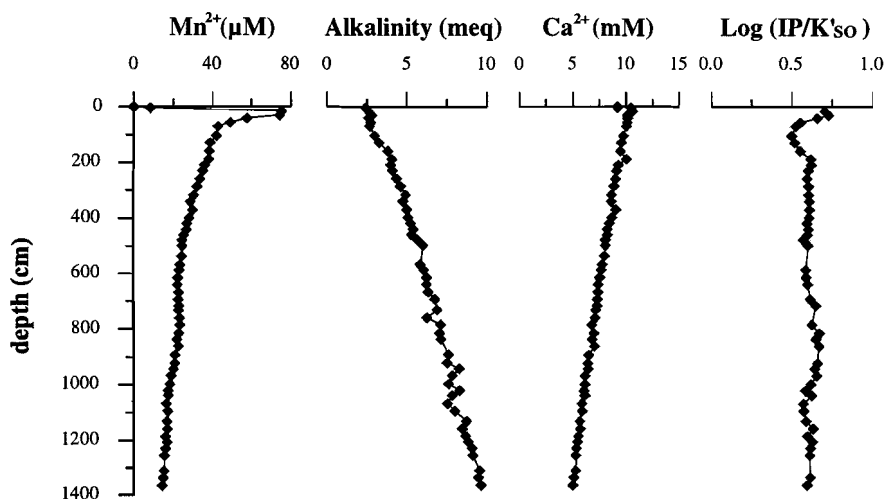


Figure 3. Porewater profiles for PC487: Mn^{2+} , alkalinity, Ca^{2+} and the degree of saturation of the porewater with respect to rhodochrosite, represented as $\text{Log}(IP/K'_{so})$ (see text). The small elevation in the Mn^{2+} concentration that occurs at 800 cm depth corresponds to an age of ~ 83 ka.

HPO_4^{2-} and NH_4^+). The degree of saturation with respect to rhodochrosite was calculated as

$$\text{Log } \Omega = \log(IP/K'_{so})$$

$\text{Log } \Omega$ is nearly constant with depth below 200 cm at a mean value of 0.6 (Fig. 3).

Solid phase

Organic carbon concentrations in PC487 and PC458 vary in a systematic way, with highest values up to 4 wt% (Fig. 4). In PC455 organic carbon concentrations are generally higher, but basically show the same pattern as for PC487 and PC458. The glacial mass accumulation rates (MARs) in PC487 are approximately twice as high as the interglacial MARs (Fig. 5). The pattern for MARs is approximately the same for PC458 and PC455 (not shown), whereas the MARs in PC455 are approximately twice as high as in the other two piston cores. Aluminum concentrations in PC487 are somewhat higher in the glacial period (Fig. 5).

The profile of total Mn in PC487 is characterized by a constant base level concentration of ~ 800 ppm (Fig. 4). Superimposed are several Mn maxima, which reach concentrations of up to 3750 ppm. These Mn spikes occur in the basal part of organic rich layers, with exception of enrichments at 44 and 102 ka. The spikes with the highest concentrations occur in interglacial stage 5. The Mn excess fluxes (mg Mn cm^{-2}), defined as the total excess Mn accumulated during a Mn spike, have been calculated by integrating the

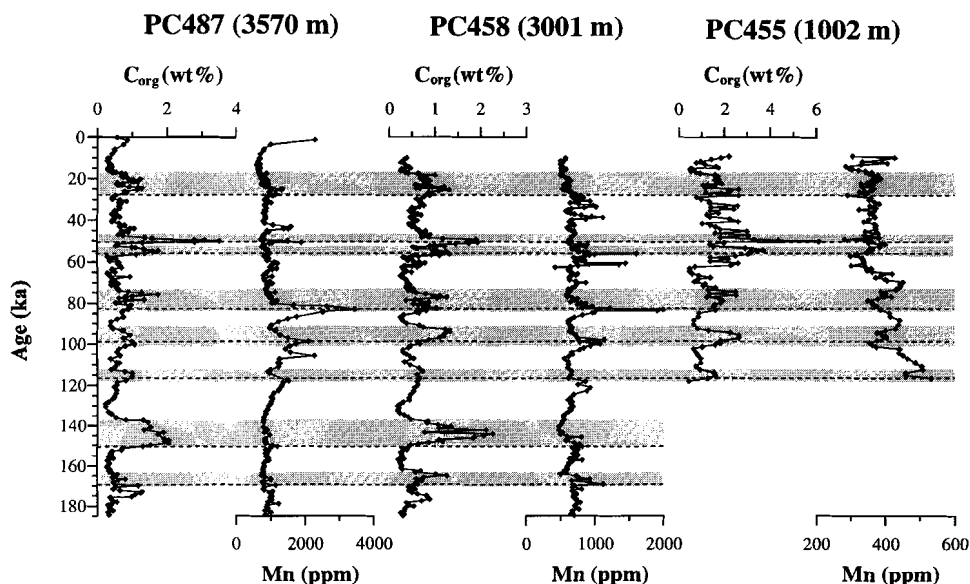


Figure 4. Records of organic carbon (wt%) and Mn (ppm) versus age for PC487, PC458 and PC455. Shaded intervals indicate organic-rich intervals, dotted lines indicate Mn spikes in PC487 and PC458, and Mn depletions in PC455.

product of the excess Mn concentration (i.e. the Mn concentration in spike minus Mn base level concentration), and the dry bulk density over the width of the Mn spike (see Appendix 2). The calculated Mn excess fluxes range between 1.9 and 4.3 mg Mn cm⁻² for glacial periods and between 9.7 and 15.8 mg Mn cm⁻² for the penultimate interglacial (Table 3). Mn enrichments in the lower part of organic-rich intervals are also found in PC458, although here the spikes have generally lower Mn concentrations (Fig. 4). The Mn spikes in PC487 and PC458 correlate relatively well. Small offsets between the two cores are probably due to inaccuracies in the age models. The calculated Mn excess fluxes for PC458 are of the same order of magnitude as in PC487 (Table 3). In contrast to PC458 and PC487, Mn concentrations in PC455 are much lower (300-500 ppm; Fig. 4) and are depleted in the organic-rich intervals.

Sequential extraction

The six-step sequential extraction for Mn was interpreted as representing three specific fractions: carbonates (steps 1 + 3), oxides (steps 2 + 4) and a residual fraction (steps 5 + 6), consisting of aluminosilicates and pyrite (Fig. 6). The Mn spikes consist for ~ 50 - 70 % of Mn associated with carbonates, with the exception of the near-surface enrichment, which

Table 3. The Mn excess fluxes calculated from the Mn spikes in PC487 and PC458, and the corresponding calculated vertical shifts (Δz) of the OMZ (see Appendix B).

Age (ka)	PC487		PC458	
	Mn flux (mg cm ⁻²)	Δz (m)	Mn flux (mg cm ⁻²)	Δz (m)
27	2.6	158	2.6	158
38	-	-	2.7	164
43	4.3	261	-	-
51	3.1	188	2.3	140
57	-	-	4.6	280
63	4.1	249	4.3	261
83	13.3	1087	15.4	1259
95	15.8	1291	4.3	351
116	9.7	793	3.6	294
150	1.9	116	2.3	140
167	2.2	134	3.2	195

Table 4. Results for the sequential extraction of standards: sediments standards with a known iron and manganese speciation (MMIN, MM91; A. Rutten, unpublished data), and rhodochrosite. Percentages are given relative to the total recovery for the three main fractions: carbonates (step 1 + 3), oxides (step 2 + 4), and a residual fraction (step 5 + 6). Rhodochrosite is not completely extracted in step 1 + 3 due to saturation of the solvents.

		Mn (%)		Al (%)		Ca (%)	
		observed	standard value	observed	standard value	observed	standard value
MMIN	carb.	20.5	23.5	0.2	0.0	93.6	98.6
	ox.	72.6	70.2	2.0	2.1	5.5	1.1
	res.	6.9	6.2	97.8	97.9	0.9	0.4
MM91	carb.	59.9	63.5	1.0	0.5	97.8	96.3
	ox.	21.0	18.4	12.2	8.5	1.3	2.6
	res.	19.1	18.1	86.8	91.0	0.9	1.1
Rhodochrosite	carb.	39.0	-	-	-	-	-
	ox.	0.8	-	-	-	-	-
	res.	60.2	-	-	-	-	-

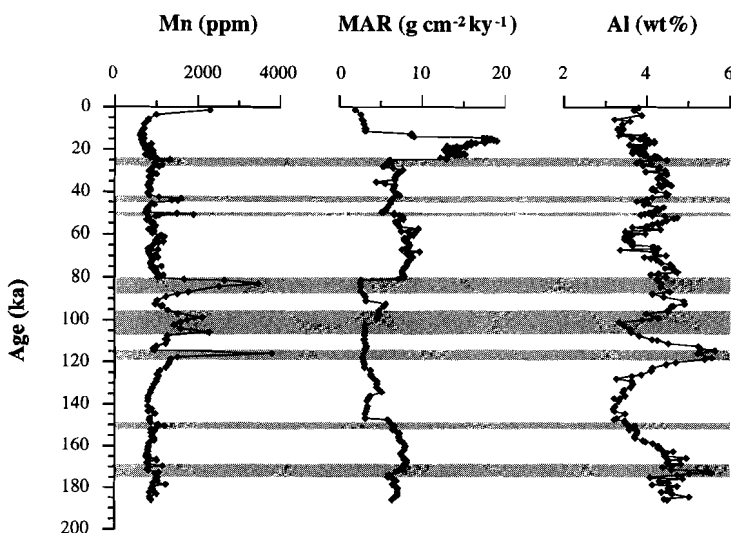


Figure 5. Records of Mn (ppm), mass accumulation rate (MAR; $\text{g cm}^{-2} \text{ky}^{-1}$), and Al concentration (wt%) versus age for PC487. The intervals with Mn enrichments are shaded.

consists primarily of Mn oxides. Mn oxides are also enriched in all Mn spikes. Manganese associated with carbonates is also the dominant fraction outside the Mn spikes, and increases slightly with depth. The Mn content in the residual fraction is more or less constant with depth. The Mn/Al ratio in step 5 (aluminosilicate fraction) is ~ 0.0066 . Mn associated with pyrite (step 6) usually constitutes less than 10 % of the Mn residual fraction.

The extraction results for the standards (Table 4) indicate that the sequential extractions adequately separated the different Mn phases. The high Mn concentration in the residual fraction for the rhodochrosite standard are attributed to saturation effects in step 1 and 3 in the solvents due to a relatively high solid/liquid ratio. However, it is conceivable that some remaining Mn carbonates have dissolved in step 2 (ascorbic acid extraction), and are thus incorrectly attributed to the Mn (hydr)oxide fraction. However, there are several arguments against this possibility: firstly, the solubility of Mn carbonates is primarily controlled by the pH of the extractant. Since the pH of the solvent in step 2 is higher (8.0) than in step 1 (7.0), insignificant amounts of Mn carbonates are expected to dissolve, as is clearly indicated by the low solubility of rhodochrosite in step 2 and 4 (Table 4). Secondly, the higher Mn concentrations observed in step 2 are associated with concomitant increases in Mn in step 4 (dithionite extraction). The low Ca and Mg concentrations in step 4 indicate that all carbonates have been dissolved in the previous steps, and, accordingly, these Mn enrichments can unquestionably be attributed to the Mn oxide fraction. Thirdly, the Mn porewater profile of PC487 shows a small elevation at 800 cm depth, which coincides with the interval where the highest Mn oxide spikes occur in the solid phase (~ 83 ka). These Mn porewater enrichments, therefore, can be explained by ongoing dissolution of Mn oxides.

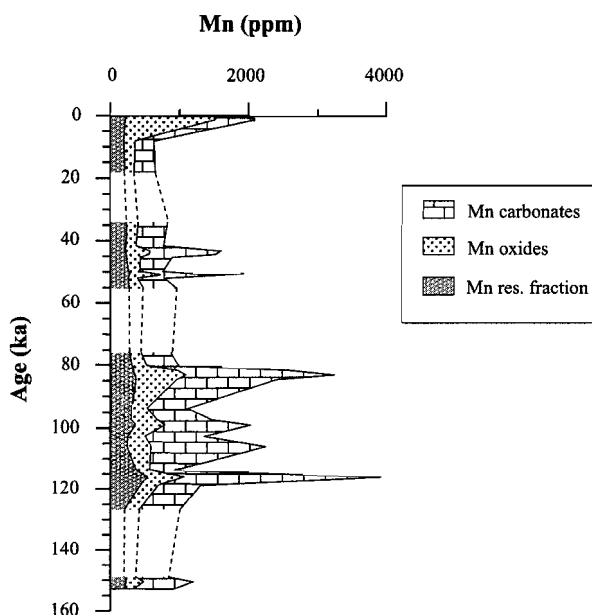


Figure 6. Stacked profile of the three Mn fractions (ppm) in PC487 versus age: Mn carbonate, Mn oxide, and a Mn residual fraction, consisting primarily of Mn associated with aluminosilicates.

Considering all these observations, we conclude that the observed Mn (hydr)oxides enrichments in the Mn spikes are not an artefact of the sequential extraction method.

Discussion

Mn carbonate precipitation in PC487

Presently, Mn oxides are being reduced in the upper part of the sediment, as is indicated by a decrease of Mn oxides with depth (Fig. 6) and a concurrent increase of porewater Mn^{2+} (Fig. 3). A detailed study on boxcore 487 (taken on the same location as PC487) showed that all free oxygen is consumed in the upper few centimetres of the sediment, and Mn (hydro)oxides start to be reduced at a depth of 4 cm (Passier *et al.*, 1997). The subsequent decrease of porewater Mn^{2+} with depth is often found in deep pelagic sediments (Li *et al.*, 1969; Pedersen and Price, 1982), and is indicative for the removal of Mn within the sediment by precipitation of Mn carbonates, probably as foraminiferal overgrowths (Boyle, 1983), or Mn adsorption to calcium carbonates (Thomson *et al.*, 1986).

Porewaters of sediments underlying oxygenated bottom waters are generally

supersaturated or close to saturation with respect to rhodochrosite (MnCO_3 ; *Li et al., 1969; Pedersen and Price, 1982; De Lange, 1986; Jakobsen and Postma, 1989; Calvert and Pedersen, 1996*). Saturation calculations indicate that this is also true for PC487 (Fig. 3). The composition of authigenic Mn carbonates in marine sediments, however, is highly variable with Ca carbonate percentages up to 50 wt% (*Pedersen and Price, 1982; Jakobsen and Postma, 1986; Middelburg et al., 1987*). Thermodynamic calculations and saturation experiments indicate that a kutnahorite ($\text{CaMn}(\text{CO}_3)_2$) like phase rather than pure rhodochrosite regulates Mn solubility in marine porewaters (*Middelburg et al., 1987; Mucci, 1988*). Since rhodochrosite is more soluble than kutnahorite (*Calvert and Pedersen, 1996*), the porewaters of PC487 can be considered to be (super)saturated with respect to a Mn-Ca carbonate phase. Equilibrium with a Mn-carbonate phase is also indicated by the constant ion activity product of MnCO_3 versus depth (Fig. 3).

The present-day rate of Mn carbonate precipitation in PC487 was estimated using the Mn porewater profile (Appendix A). The downward flux of Mn^{2+} was determined from the negative porewater concentration gradient in the upper part of the sediment, which was subsequently converted into a solid phase Mn carbonate concentration. This calculation yields a Mn concentration of ~ 470 ppm, which is somewhat higher than the observed concentration of ± 300 ppm Mn in the carbonate fraction in the top of the piston core (Fig. 6). Accordingly, the present-day downward flux of Mn is in reasonable agreement with the observed constant background level concentration of solid phase Mn-carbonate.

Origin of the Mn spikes in the sediment records of the deep Arabian basin

Mn carbonates have formed over the whole length of sediment core PC487. Since oxygenated bottom water conditions are essential for the diagenetic formation of Mn carbonates (*Calvert and Pedersen, 1993*), bottom waters of the deep Arabian basin must have remained oxygenated for at least the last 185 kyr. This is also indicated by the presence of bioturbation throughout the sediment record. Accordingly, no evidence was found for anoxic deep water in the Arabian Sea during the last glacial period, as postulated by *Sarkar et al. (1993)*. Furthermore, results from sediment cores from the Murray ridge demonstrate that the OMZ was significantly more intensive than the present situation during only two periods in the past 225 kyr (*Reichart et al., 1997*). In view of the present-day deep water circulation, it is unlikely that the OMZ extended to a depth of 3500 m during those two time periods. The deep pelagic sediments of the Arabian Sea, therefore, have not experienced extensive losses of reactive Mn to the bottom water during the last 185 kyr. The rather constant background level of Mn probably represents a steady-state situation in which the input of reactive Mn from the water column is balanced by burial of Mn carbonates.

The Mn spikes, which are superimposed on the constant background concentration, reflect a deviation from the steady-state situation. Sedimentary Mn enrichments have been associated with distinct transitions in lithology, such as turbidites or sapropels (*Colley et al., 1984; Wilson et al., 1986; De Lange et al., 1989*), ash layers, or other coarse grained sediments (*Pedersen and Price, 1982*). In PC487, macroscopical observations and geochemical analysis indicate that the sediment is undisturbed and rather homogeneous in composition, with the exception of some very thin turbidites that occur between 80 and

200 cm depth. Therefore, the Mn spikes must be attributed to an early diagenetic increase in the precipitation rate of Mn carbonates. The concurrence of Mn carbonate spikes with enrichments in Mn oxides (Fig. 6) suggests that Mn carbonates were formed by the in-situ transformation of Mn oxides, probably while being in the upper few centimeters of the sediment. If dissolution of Mn oxides had occurred deeper in the sediment, the process would have been slower, allowing more Mn^{2+} to diffuse away from the Mn spikes and causing a more evenly distribution of Mn carbonates over the sediments.

Higher carbonate alkalinity induced by bacterial sulphate reduction during early diagenesis may have augmented precipitation of Mn carbonates (Berner, 1970). Since the Mn spikes are located in the organic-rich layers which are enriched in pyrite, a rise of the porewater carbonate alkalinity may have triggered carbonate formation. Manganese carbonate precipitation, however, is principally controlled by the Mn^{2+} concentration rather than by carbonate alkalinity (Pedersen and Price, 1982, Calvert and Pedersen, 1996). The formation of the Mn spikes, therefore, must be associated with periods of increased Mn availability in the porewater. There are two potential mechanisms that could have caused higher Mn concentrations in the porewaters, namely 1) enhanced dissolution of Mn oxides that were initially precipitated through early diagenetic processes in the upper part of the sediment, or 2) an increased downward flux of particulate Mn from the water column.

1) Diagenetic redistribution

Manganese spikes in recent sediments are commonly interpreted to have an early diagenetic origin (e.g. Berger et al., 1983). In a steady-state situation, diagenetic Mn oxide peaks are not preserved in the sediment record, since they move upward with ongoing sedimentation (e.g. Burdige and Gieskes, 1982). Finney et al. (1988) proposed that Mn oxide enrichments can be preserved in the sediment record as the result of past variations of the redox conditions in the sediment: an increase in the rain rate of reactive organic matter flux will increase the oxidant demand and cause an upward movement of the Mn redox boundary. If the organic matter in the sediment is of low degradability, Mn oxide spikes can be trapped beneath the zone of active reduction, and can thus be preserved till considerable depth (Finney et al., 1988). In the Arabian Sea, where organic matter accumulation rates are higher than in the area of the Pacific ocean studied by Finney et al. (1988), an upward shift of the Mn redox boundary will bring Mn oxides in the reducing zone. As a result, Mn oxides will start to dissolve more rapidly (see Fig. 7). An intensification of the “manganese pump” will cause a higher production rate of Mn^{2+} in the porewaters, which may subsequently enhance Mn carbonate precipitation (Yang et al., 1995). Manganese is thus redistributed over the sediment as a function of the organic matter flux.

There are several indications that the Mn spikes observed in the sediments of the deep Arabian Basin are not the result of diagenetic redistribution. Firstly, the position of the Mn spikes is not in accordance with a diagenetic redistribution mechanism. If an increase of the reactive organic matter flux into the sediment causes an upward shift of the redox boundary, the Mn oxides beneath the newly forming organic rich layer will start to dissolve rapidly (Finney et al., 1988). Manganese carbonate precipitation, therefore, would mainly occur below the organic rich layers. With the exception of a Mn spike at 44 and 102 kyr in PC487,

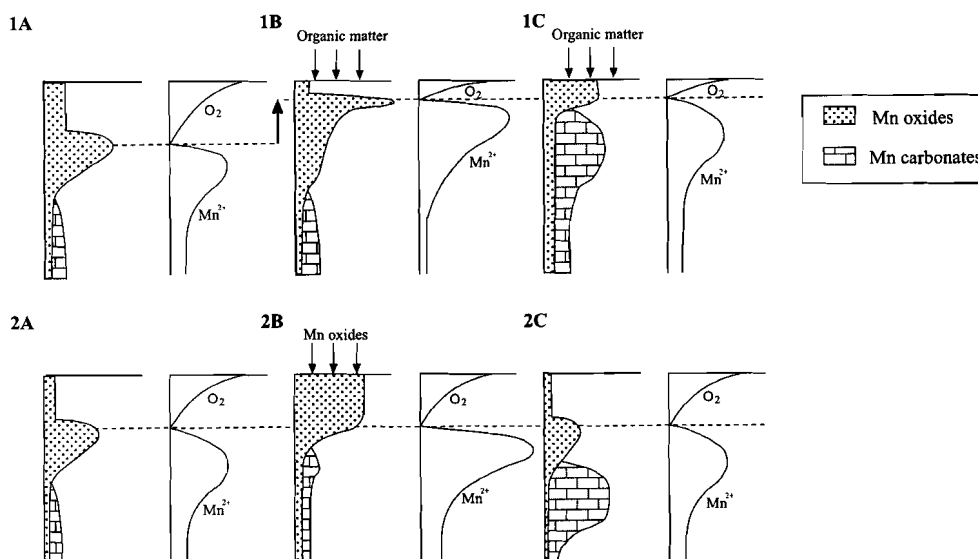


Figure 7. Schematic representation of the two possible mechanisms that may explain the formation of the Mn carbonate spikes in a deep, oxygenated basin environment: 1a, 2a) steady-state situation: Mn oxides are reduced with depth once the oxygen content in the porewater is depleted. The increase in Mn porewater concentration results in Mn carbonate precipitation. All reactive Mn initially deposited as Mn (hydr)oxides is ultimately buried as Mn carbonates.

1) Diagenetic redistribution: 1b) An increase of the organic matter rain rate causes an upward shift of the redox front, which enhances the dissolution of Mn oxides previously located above the redox front. 1c) A new steady-state situation is established, in which the diagenetic Mn oxide peak is located near the sediment surface. The increased Mn oxides dissolution rates have temporarily induced a higher precipitation rate of Mn carbonates.

2) Increased Mn flux from the water column: 2b) An increase of the reactive Mn oxides flux from the water column causes higher Mn^{2+} porewater concentrations, provided that enough labile organic matter is present to reduce all Mn oxides. 2c) In a new steady-state situation the Mn input has returned to previous values. The flux of increased Mn oxide input has been converted into Mn carbonates, and is buried as a Mn spike.

all Mn spikes observed in PC487 and PC458 occur within organic-rich layers. A diagenetic redistribution of Mn would also create depletions in solid-phase Mn directly above and below the manganese enrichments, which are not present. Secondly, in the case of Mn diagenetic redistribution, the mean Mn concentrations should have remained constant over long time periods, assuming that the sedimenting Mn flux is directly proportional to the MAR. In the

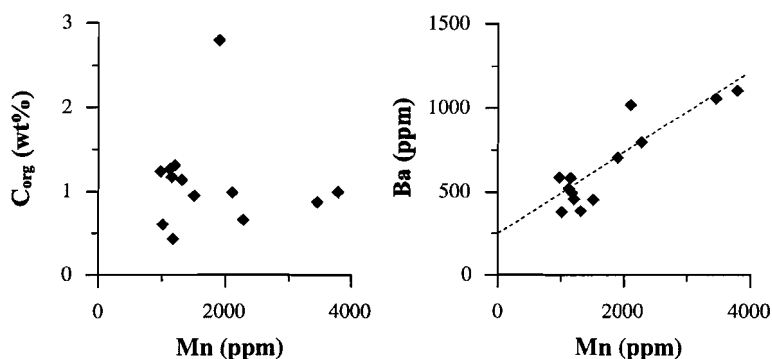


Figure 8. A plot of the Mn concentration in the Mn spikes of PC487 versus C_{org} and Ba. The dashed line represent the best linear fit.

penultimate interglacial (stage 5) the mean Mn concentration was approximately a factor 1.6 higher than in the glacial periods. In addition, the Mn spikes in stage 5 are rather thick, indicating that increased precipitation took place over relatively long time periods. Thirdly, Mn concentrations of the different spikes show no correlation with the organic carbon concentration values (Fig. 8), which would be expected, if burial of reactive Mn is governed by an upward shift of the Mn redox boundary. In contrast, a good correlation is observed between Mn and the paleoproductivity indicator Ba (Fig. 8), suggesting a link with water column processes. We conclude that it is not likely that the Mn record is shaped by diagenetic redistribution.

2) Increased Mn flux from the water column

A second mechanism to increase the release rate of Mn^{2+} during early diagenesis is a higher flux of Mn (hydr)oxides from the water column, provided that sufficient labile organic matter is present (see Fig. 7). These Mn oxides will be mixed by bioturbation into the shallow, reducing part of the sediment, resulting in higher Mn porewater concentrations and thus propagating higher precipitation rates of Mn carbonates. Accordingly, changes of the accumulating Mn fluxes in time are documented in the sediment record. This mechanism is partly analogous to the present-day formation of Ca-rich rhodochrosites in the Baltic Sea. In these sediments high rates of Mn carbonate precipitation are induced by high Mn oxides fluxes from the water column which are subsequently reduced in a low oxygen environment. (Sternbeck and Sohlenius, 1997).

We argue that the Mn spikes in PC487 and PC458 are best explained by periodic changes in Mn accumulation rates. Consequently, the Mn spikes are interpreted as indicators for periods of an increased reactive Mn flux to the sediment of the deep Arabian Basin.

Mn cycling in relation to OMZ Variability

An increase of the particulate manganese flux to deep basin sediments can originate from several different sources, namely a) enhanced hydrothermal activity, b) increased eolian and/or fluvial Mn input to the basin, c) rapid oxygenation of the OMZ, and d) redistribution of Mn from continental slope sediments to the deeper part of the basin due to an intensification of the OMZ.

A) Hydrothermal source

Manganese is supplied to the oceans by submarine hydrothermal vents such as those along the active oceanic spreading ridges (e.g. *Klinkhammer et al., 1986; Mandernack and Tebo, 1993*). A source of hydrothermal manganese in the Arabian Sea is the Carlsberg Ridge, an active spreading ridge which separates the Arabian Basin from the Somali Basin (*Demina and Choporov, 1986*). The northward movement of Antarctic bottom waters could transport these Mn-rich waters into the Arabian Basin. These deep bottom waters, however, are well oxygenated, and the formation of hydrothermal mineral deposits is restricted to the Carlsberg ridge (*Rona, 1984*). The depth of the Carlsberg ridge (>3500 m), the relative large distance from the high-productivity areas in the northern Arabian Sea and the pattern of deep water circulation make it improbable that oxygen depleted waters of the OMZ have ever engulfed the Carlsberg ridge. In addition, the orbital related pattern of Mn spike occurrences is unlikely to be related to pulses of hydrothermal Mn input. As a consequence, a hydrothermal control on the observed sedimentary Mn record is unlikely.

B) Increase of continentally derived Mn

The most important primary source of Mn to the oceans are the products of continental weathering, supplied by fluvial and atmospheric transport. Reactive Mn (hydr)oxides are partially recycled in estuarine and coastal sediments during anoxic or oxic diagenesis (*Heggie et al., 1987; Johnson et al., 1992*), and subsequently horizontally advected into the open ocean environment. These processes cause relatively high dissolved Mn concentrations in the uppermost part of the water column (*Martin and Knauer, 1984; Landing and Bruland, 1987; Saager et al., 1989*), which are kept in solution by photochemical reduction (*Sunda and Huntsman, 1988*). An increase of continental input will result in higher Mn concentrations of the surface waters, higher Mn scavenging rates, and, eventually, a larger Mn flux reaching the deep sea floor.

In the western part of the Arabian Sea deposition of eolian dust is high (*Sirocko and Sarnthein, 1989*), and accounts for 75 % of the burial of terrigenous material (*Chester et al., 1991*). Sedimentary records have shown that eolian transport has been the primary source for the lithogenic part of the sediments in the Arabian Sea for at least the past 370 kyr (*Clemens and Prell, 1990*). As a consequence, fluvial derived Mn, supplied from the Indus river and the Tigris/Euphrates, is considered to be less important than atmospheric derived Mn (*Chester et al., 1991*). Past variations in dust input are controlled by changes in the wind strength over the Arabian Sea and continental aridity (*Sirocko, 1991*). Mean grainsize records indicate that periods of precession-related intensification of the monsoonal wind strength correspond with increased wind-induced upwelling which result in higher primary productivity (*Clemens and*

Chapter 2

Prell, 1990). Dust fluxes to the Arabian Sea, however, are primarily controlled by glacial-interglacial variability due to changes in continental aridity (Clemens and Prell, 1990; Sirocko, 1991), which is also evident in the MAR records in PC487 (Fig. 5). The highest Mn enrichments occur in the interglacial periods when the MARs are lowest. Comparison of the Mn burial record with the Al content (Fig. 5) indicates that deposition of the Mn spikes is not correlated with periods of increased terrestrial input. Although continental derived Mn is the ultimate source of Mn buried in the sedimentary record, no direct relation exists between atmospheric dust deposition and the observed Mn burial record.

C) Oxygenation of the OMZ

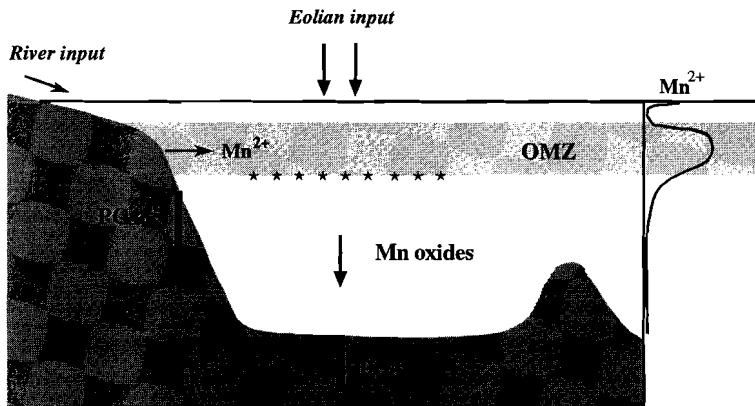
A rapid reventilation of an anoxic water column has been invoked to explain sedimentary Mn spikes in the Mediterranean at the end of the period of sapropel formation (e.g. Higgs *et al.*, 1994; Van Santvoort *et al.*, 1996), and in the Pacific and Atlantic oceans at the transitions from glacial to interglacial stages (Mangini *et al.*, 1990). The present Mn seawater concentration in the Arabian Sea OMZ does not exceed 6.4 nM (Saager *et al.*, 1989), which is low compared to Mn concentrations observed in enclosed anoxic basins such as the Black Sea (6-8 μM ; Landing and Lewis, 1991). Oxidation of the present OMZ (thickness ~ 1100 m) would yield a maximum Mn flux of 3.9×10^{-2} mg cm⁻², which is two orders of magnitude smaller than the calculated Mn excess fluxes for PC487 and PC458 (Table 3). Mangini *et al.*, (1990, 1994) suggested that the Mn concentration in the oceans during glacial periods was much higher due to anoxia of the deep waters. As discussed, the bottom waters of the deeper part of the Arabian Basin have remained oxygenated for at least the past 185 kyr. Since in this time period the OMZ has only twice been more intensive than it is in the present-day situation (Reichert *et al.*, 1997), it is unlikely that the Mn concentration in the water column has considerably exceeded present-day concentrations. One single re-oxidation event, therefore, cannot account for the Mn fluxes related to the Mn spikes. A succession of (partial) reoxidation events could, of course, have increased this flux, but to maintain a high Mn concentration the OMZ has to be refuelled with Mn from primary or secondary sources.

D) Intensification of the oxygen minimum zone

Presently, the OMZ in the Arabian Sea is intense in relation to the past and the low oxygen concentrations in the OMZ suggest that, besides denitrification (Naqvi, 1987), also Mn reduction occurs in the water column (Balakrishnan Nair *et al.*, 1999). It has been shown for the intense OMZ off central Mexico that the Mn maximum at intermediate water depth can only partly be explained by in-situ regeneration of Mn oxides (Martin and Knauer, 1984; Landing and Bruland, 1987). This, in combination with the observation that the Mn maximum at intermediate depths in the Arabian Sea decreases in an offshore direction (Saager *et al.*, 1989), indicates that the transport of Mn released from near-shore sediments could be an important source for Mn into the Arabian Basin. This is confirmed by sediment trap studies that indicate that atmospheric input alone cannot account for the high downward Mn fluxes below the OMZ (Balakrishnan Nair *et al.*, 1999).

We propose that periods of increased Mn deposition in the deep basin are associated

A: Steady state situation



B: Downward extension of the OMZ

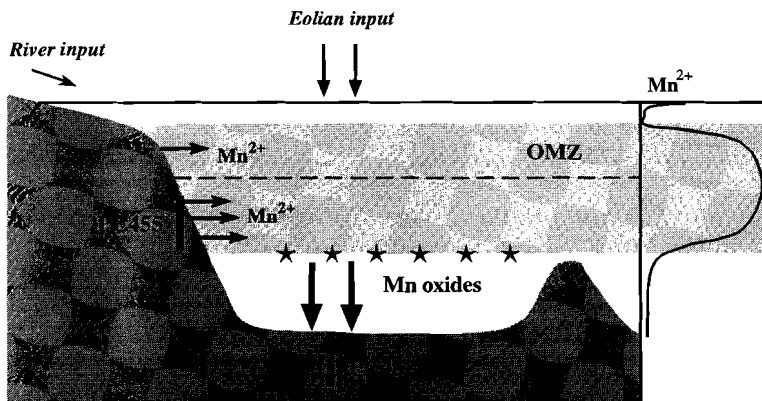


Figure 9. Schematic representation of Mn remobilisation from the continental slope due to a vertical shift of the lower boundary of the oxygen minimum zone. A: in a steady-state situation, the flux of Mn to the deep basin equals the input from the primary sources (rivers, eolian dust). B: A deepening of the base of the OMZ will mobilize Mn oxides which were previously deposited below the OMZ, causing higher Mn²⁺ concentrations in the OMZ and increased scavenging of Mn to the deep basin.

with a vertical extension of the OMZ. A deepening of the OMZ causes dysoxic conditions in the bottom water of slope sediments previously located below the OMZ (Fig. 9). Not only will this lower the Mn burial efficiency in these sediments, but also will it cause reduction of Mn oxides which were deposited and precipitated during a preceding period, in which the BWO concentrations were higher. The enhanced release of Mn from slope sediments will increase Mn concentrations in the OMZ. Subsequently, this Mn will be scavenged from the OMZ and ultimately result in higher Mn fluxes to the deeper part of the basin. The concept of Mn dissolution under low oxygen concentrations in the OMZ, transportation by diffusive and advective processes and subsequent reprecipitation in more oxygenated environments is known as “oxygen minimum zone redirection” (Klinkhammer and Bender, 1980; Johnson *et al.*, 1992). Relocation of Mn in Indian Ocean sediments has been observed in ODP cores taken from intermediate water depths (Dickens and Owen, 1994): depletions of labile Mn in sediments deposited during the Late Miocene to Early Pliocene were interpreted as the outward expansion of the OMZ in this period due to higher global productivity.

The importance of Mn regeneration along the continental margin as a source for the Mn maxima associated with OMZs was questioned by Johnson *et al.* (1992). These authors observed that the highest benthic Mn fluxes occurred in the oxic shallow continental shelf sediments, whereas lower benthic Mn fluxes were observed for sediments located within the OMZ. Model calculations show that in a steady-state situation Mn maxima at intermediate water depths can be explained by the reduction in the scavenging rate of Mn in the OMZ, and no additional source of Mn is necessary from continental slope sediments (Johnson *et al.*, 1996). This conclusion, however, is not in conflict with the mechanism presented in this study, since a deepening of the OMZ results in a deviation from the steady-state situation and relocation of Mn.

Past variations in OMZ intensity are primarily controlled by changes in paleoproductivity (Anderson and Gardner, 1989; Altabet, 1995; Reichart *et al.*, 1998). The organic matter patterns in PC487, PC458 and PC455 have been correlated in sediment cores throughout the Arabian basin, located both within the OMZ and in the more oxygenated deep basin (Shimmiel, 1992; Reichart *et al.*, 1998). This implies that the organic matter records are mainly related to precession-induced changes in surface water productivity (Reichart *et al.*, 1998). The onset of higher organic carbon concentrations in the sediment, therefore, indicates periods of the early extension of the OMZ, during which Mn is leached from previously oxygenated slope sediments. So, the proposed mechanism is in accordance with the position of Mn spikes in the lower part of organic-rich layers.

Evidence for Mn release from continental slope sediments comes from the sediment record of PC455 (1002 m), presently located within the OMZ. Due to its position, this record was directly influenced by changes in OMZ intensity, as is evidenced by its laminated intervals and sedimentary trace metal distribution (Reichart *et al.*, 1998; Den Dulk *et al.*, 1998). The mean Mn/Al ratio (~ 0.007) is slightly higher than the Mn/Al ratio of 0.005 measured for the residual Mn fraction in boxcore samples from the Arabian Sea (obtained with the same sequential extraction technique as presented in this study; unpublished data), indicating that Mn in this core is primarily present as a non-reactive phase. Consequently, most of the reactive Mn deposited on the continental slope has been lost to the water column.

The synchronous depletions of Mn in organic rich intervals of PC455 and burial of Mn spikes in PC458 and PC487 clearly points to relocation of Mn (Fig. 4). During periods of low organic carbon deposition, the Mn concentration in PC455 increases slightly. The presence of bioturbation in these intervals indicate that BWO concentrations were higher, reducing the loss of reactive Mn from the sediment and enabling the formation of some Mn carbonates.

Assuming that the Mn spikes in the deep Arabian Basin originate from Mn remobilization from continental slope sediments, a rough estimate can be made for the downward shift of the base of the OMZ. In these calculations, it is assumed that a) the OMZ, and thus transport of reactive Mn, did not extent beyond 10° N latitude, which is approximately the southern boundary of the Mn maximum in the present-day (intense) OMZ (Saager *et al.*, 1989), b) the contribution of reactive Mn from hydrothermal sources is negligible, and c) Mn is buried solely as a non-reactive fraction in the sediments located within the OMZ. For the calculations see Appendix B, the results are given in Table 3. During glacial periods relative small shifts of the OMZ are sufficient to produce the Mn spikes. The largest calculated shift (1291 m) is somewhat larger than the present extension of the OMZ. The largest downward shifts of the OMZ probably mobilized reactive Mn which was left undisturbed by the previous smaller shifts, thus overestimating the calculated vertical shift. These calculations, therefore, indicate that the mechanism of Mn mobilization from the continental slope can supply sufficient Mn to explain all observed Mn spikes. A comparison between PC487 and PC458 reveals the absence of certain Mn spikes and, particularly during stage 5, large differences in the calculated shifts (Table 3). These inconsistencies can partly be ascribed to the different settings of the two piston core locations (water depth, distance to the continental margin, regional differences in OMZ intensity). Furthermore, as has been discussed previously, diagenetic processes may have altered the Mn flux that is ultimately buried in the sediment. The calculated shifts, therefore, must be interpreted with care, but, in our opinion, can be used as a semi-quantitative proxy for the development of the OMZ through time.

The Mn spike record indicates that the largest vertical shifts in the OMZ occurred during interglacial stage 5. These observations are consistent with the observed correlation between the paleoproductivity indicator Ba and the Mn concentration in the spikes of PC487 (Fig. 8). The overall higher productivity during interglacial periods (Emeis *et al.*, 1995) probably caused the development of a more intensive OMZ during periods of precession minima. This is in reasonable agreement with other studies, which used paleoproxies all indicative for periods of weakened OMZ ($\delta^{15}\text{N}$, Altabet *et al.*, 1995; sedimentary Sr/Ca, foraminiferal species *G. truncatulinoides* and *G. crassaformis*; Reichert *et al.*, 1997, 1998). The record of Mn burial in deep basin sediments of the Arabian Sea can be used as an independent proxy to trace back variations of the redox conditions of the intermediate waters through time.

Conclusions

The sediments of the deep Arabian Basin have remained oxygenated for at least the last 185 kyrs, allowing precipitation of Mn carbonates and preventing loss of reactive Mn to the bottom waters. Manganese enrichments, which occur within the lower part of organic rich intervals, constitute a deviation from a steady-state situation. The Mn spikes are formed due to an increase of the reduction rate of Mn oxides during early diagenesis. The occurrence of Mn spikes in the sediments corresponds to periods of higher reactive Mn fluxes to the deep basin.

The coherence between the Mn spikes and organic matter enrichments points to a connection between Mn cycling in the water column and variations in paleoproductivity and OMZ variability. Periods of increased reactive Mn flux to the deep basin are associated with a vertical extension of the OMZ, which cause dysoxic conditions in the bottom water of slope sediments previously located below the OMZ. Remobilization of reactive Mn into the water column, and subsequent scavenging to the deeper, more oxygenated environment, resulted in the formation of Mn enrichments. Relocation of Mn is evidenced by the synchronous depletion of solid-phase Mn in the continental slope sediments. Calculations indicate that during glacial periods small vertical shifts of the OMZ are sufficient to explain all observed Mn spikes. The largest shifts in the OMZ occurred during interglacial stage 5, which are linked to higher productivity during periods of precession minima. The results of this study indicate that the record of Mn in deep basin sediments of the Arabian Sea can be used as a semi-quantitative proxy to reconstruct variations of the redox conditions of the intermediate waters.

Acknowledgements - The chief scientists on the NIOP cruises during the 1992-1993 Netherlands Indian Ocean Programme were W.J.M. van der Linden and C.H. van der Weijden. We want to thank J. van der Werf for his preparation of the foraminiferal samples. H. de Waard, A. Van Dijk en G. Nobbe are thanked for their contribution to the laboratory analyses, and G.J. van het Veld and G. Ittman for processing the micropaleontological samples. Critical reviews by C.H. van der Weijden, and A. Rutten significantly improved this manuscript.

Appendix A

The present downward Mn porewater flux and Mn carbonate burial concentration for NIOP station 487 was calculated assuming steady-state conditions, constant sedimentation rates and dry bulk densities, and no compaction, irrigation or bioturbation at the depth of Mn carbonate formation. The downward flux of Mn (J_{Mn}) ($\mu\text{M cm}^{-2} \text{s}^{-1}$) is given by (Berner, 1980) :

$$J_{Mn} = -\phi D_s (dC/dz)$$

where ϕ is the mean porosity, D_s the whole sediment diffusion coefficient for manganese, and dC/dz the linear concentration gradient. The whole sediment diffusion coefficient (D_s) ($\text{cm}^2 \text{s}^{-1}$) can be expressed by

$$D_s = D/\phi F$$

where D is the diffusion coefficient of Mn in seawater, and F the formation factor. D was corrected for the bottom water temperature of 1.6°C ($3.29 \times 10^{-6} \text{cm}^2 \text{s}^{-1}$, Li and Gergory, 1974). F has been estimated with the equation (Manheim and Watermann, 1974):

$$\log F = 0.110 - 1.80 \log \phi$$

The steepest negative gradient for manganese occurs between 30 and 70 cm depth (Fig. 3) and amounts to $31.2 \mu\text{M} / 40 \text{cm} = 0.79 \mu\text{M cm}^{-1}$. Applying a mean porosity in this interval of 0.65, the Mn flux annually amounts to $0.029 \mu\text{M cm}^{-2} \text{y}^{-1}$. This flux can be converted into a solid-phase Mn concentration (B_{Mn}) (ppm Mn):

$$B_{Mn} = J_{Mn} \times 54.9 \times 1000 / \text{SR} \times \text{dbd}$$

where SR is the sedimentation rate (3.1cm/ky , as measured in the boxcore 487), and dbd the mean dry bulk density (1.1g cm^{-3}). This yields a Mn concentration in the carbonate fraction of $\sim 470 \text{ppm}$.

Appendix B

The vertical shift of the lower OMZ boundary in the Arabian Sea has been calculated from the magnitudes of the Mn spikes as recorded in PC487 and PC458. The reactive Mn excess flux F (mg Mn cm^{-2}) is calculated by integrating Mn concentrations over the width of the Mn spike (from x_1 to x_2):

$$F = \int_{x_1}^{x_2} C_x \times \text{dbd}_x \, dx$$

Chapter 2

where C_x is the Mn concentration (ppm) and dbd_x the dry bulk density (gr cm^{-3}) at depth x . The total amount of Mn deposited in the deep basin ($[\text{Mn}_d]$) is calculated as:

$$[\text{Mn}_d] = F \times A_d$$

where A_d is the surface area of the basin deeper than 1500 m situated north of 10° latitude, the latter being approximately the southern boundary of the present (intense) OMZ (Saager *et al.*, 1989): $1.632.000 \text{ km}^2$.

The amount of Mn deposited in the deep basin must equal the amount of reactive Mn deposited on the continental slope during the time interval between two OMZ shifts. The total reactive Mn accumulation F_c , which would have been deposited on the continental slope in absence of the OMZ, has been estimated from the Al flux:

$$F_c = T \times \text{Al flux} \times (\text{Mn/Al})_{\text{reac}}$$

where T is the period during which reactive Mn was deposited, Al flux is the mean Al accumulation rate deposited during period T , and $(\text{Mn/Al})_{\text{reac}}$ the ratio of reactive Mn to Al of the primary sources. As the shifts in the OMZ are mainly controlled by the precession cycle (Reichert *et al.*, 1998), T was taken as 21 kyr. The mean Al accumulation rate, calculated from sediment record PC455, equals $610 \text{ mg Al cm}^{-2} \text{ ky}^{-1}$ for the interglacial (stage 5), and $820 \text{ mg Al cm}^{-2} \text{ ky}^{-1}$ for the glacial periods (stage 2,3,4 and 6). The mean Mn/Al ratio in Arabian Sea aerosols is 0.015 (Chester *et al.*, 1991), whereas the suspended material of the river Indus has a Mn/Al ratio of ~ 0.025 (Arain, 1987). Chester *et al.* (1991) calculated that the soluble atmospheric flux of Mn is twice the size of the fluvial Mn flux. Therefore, we used a mean Mn/Al ratio of 0.018, which after correction for the non reactive Mn fraction ($\text{Mn/Al} = 0.0052$), yields a $(\text{Mn/Al})_{\text{reac}}$ ratio of 0.0128. The surface area of the continental slope where reactive Mn is mobilized due to the downward shift of the OMZ (A_c) is calculated as

$$A_c = [\text{Mn}_d] / F_c$$

The vertical extension (Δz) of the OMZ can now be calculated as

$$\Delta z = \tan \alpha \times A_c / L$$

where α is the mean slope of the continental margin of the Arabian Sea between 200 and 1500 m water depth (2.7°), and L the length of the continental slope encircling the Arabian Basin (5700 km). α was obtained from the total surface area of the continental slope between 200 and 1500 m water depth (158000 km^2), which yields a mean width of 27.7 km for the continental slope. The results for Δz (m) are given in Table 3.

3

A 27 kyr record of monsoon variability and Oxygen Minimum Zone intensity from the Oman Margin coastal upwelling area

G.J. Reichart, S.J. Schenau, G.J. de Lange and W.J. Zachariasse

Abstract - In this chapter we present evidence for sub-Milankovitch variability in monsoon intensity from the Oman Margin, northern Arabian Sea. A high-resolution geochemical record combined with micropaleontological data, shows high-frequency variations in sea surface productivity caused by changes in the intensity of summer monsoon-induced upwelling. Changes in aridity on the Arabian Peninsula varied synchronously with the summer monsoon, periods with minimum monsoon intensity being driest. The local oxygen minimum zone (OMZ), which presently impinges on the Oman continental margin, was reconstructed using laminations, redox sensitive elements, aragonite preservation, and sulphur diagenesis. OMZ intensity varies together with monsoon strength, being weakest during periods of minimum summer monsoon intensity. Correlating summer monsoon variability to the northernmost part of the Arabian Basin, indicates that minima in summer monsoon intensity coincided with maxima in winter monsoon strength. Furthermore, the record from the Oman Margin again confirms the link between sub-Milankovitch variability in high and low latitude climate.

Introduction

During the last two decades, climate studies of the Indian Ocean monsoon have focussed on the Oman and Yemen upwelling area (*e.g. Prell, 1984; Shimmiel, 1992; Anderson and Prell, 1993; Sirocko et al., 1993; Emeis et al., 1995*). Using the fossil foraminiferal record and geochemical sediment signatures, the relation between global climate, insolation, and the response of the summer monsoon was reconstructed. Although it was shown that the monsoon climate system in the area off Oman is affected by abrupt changes (*Sirocko et al., 1993, 1996; Naidu and Malmgren, 1995*), no links to other parts of the climate system were established. Recently, sediment records from the northernmost Arabian Sea were used to portray changes in monsoonal climate with an unprecedented resolution (*Reichart et al., 1998; Schulz et al., 1998; Von Rad et al., 1999*). The summer monsoon productivity signal in this region, however, depends on the advection of nutrients from the coastal and open-ocean upwelling areas. Furthermore, productivity records offshore Pakistan may be the result of both summer and winter monsoon related surface water productivity (*Madhupratap et al., 1996*). Since the Oman Margin directly underlies the upwelling area, the sedimentary record can be expected to reflect summer monsoon variability more directly.

In this study, we present a high-resolution record for the last ~27 kyr of monsoonal change from the coastal upwelling area off Oman. Geochemical, paleontological, and sedimentological results are combined to resolve the monsoon-induced variability in paleoproductivity, Oxygen Minimum Zone (OMZ) intensity, and dust input. Sulphate reduction and pyrite formation in the sediments of the Oman Margin were investigated in order to reconstruct OMZ intensities. Changes in paleoproductivity and OMZ variability can be correlated to the northernmost Arabian Sea monsoon history, and show a remarkable correspondence to climate changes known from the Greenland ice cores.

Study area

Surface water productivity in the northern Arabian Sea shows a distinct response to the semi-annual reversal in monsoonal winds. During the Northern Hemisphere summer, heating of the Tibetan Plateau is at a maximum, resulting in a strong pressure gradient between the Tibetan low pressure cell and a belt of high pressure over the southern Indian Ocean. This pressure gradient drives warm and humid southwestern winds, causing coastal and open-ocean upwelling offshore Oman and Yemen. During the southwest monsoon, surface water productivity rises to values that are among the highest known for the open ocean (Wyrki, 1973; Smith and Bottero, 1977; Swallow, 1984; Brock *et al.*, 1992). In the winter period, cold northeastern winds blow from the high pressure cell above Central Asia to the region of low pressure associated with the inter tropical convergence zone (ITCZ) at $\sim 10^\circ$ S. These winds cause onshore Ekman transport, which suppresses coastal upwelling and productivity (Slater and Kroopnick, 1984).

Annual high surface water productivity (between 200 and 400 $\text{gC m}^{-2} \text{yr}^{-1}$; Kabanova, 1968; Qasim, 1982; Codispoti, 1991), in combination with moderate rates of thermocline ventilation (You and Tomczac, 1993), result in an intense OMZ between 150 and 1250 metres waterdepth (Wyrki, 1973; Deuser *et al.*, 1978; Olson *et al.*, 1993). Oxygen concentrations in the OMZ off Oman drop to values below 4.5 μM (*e.g.* Morisson *et al.*, 1999). The low bottom water oxygen concentrations strongly affect biological, geochemical and sedimentological processes at the sediment water interface (Schulz *et al.*, 1996; Jannink *et al.*, 1998; Van der Weijden *et al.*, 1999; Chapters 4 and 6).

Material and methods

Piston core 484 ($19^\circ 29'.8\text{N}$, $058^\circ 25'.7\text{E}$) was recovered from 516 metres water depth on the Oman Continental Margin during the Netherlands Indian Ocean Programme (NIOP) (Fig. 1). The top part of the sedimentary sequence at this station was studied in the trip core and the box core (527 mbss). Sediment at station NIOP484 consists of hemipelagic, foraminiferal muds, and show no evidence of turbidites or other types of sediment redistribution. The homogeneous, bioturbated sediments contain three finely laminated intervals (Fig. 2). Piston core 478 was recovered from the Pakistan Continental Margin ($24^\circ 12'.7\text{N}$, 065°E , 565 mbss, for details see Reichert *et al.*, 1998).

Cores were sub-sampled at 20 cm intervals for micropaleontological and sedimentological analyses, and at cm scale resolution for geochemical analyses. The water content of the sediment was determined by weight loss upon freeze-drying of fixed volume samples. These fixed volume samples were subsequently sieved into three size fractions, of which the 150-595 μm fraction was used for micropaleontological analyses. For each sample, using an Otto microsplitter, at least 200 planktonic foraminifers were picked out, identified, and counted. Pteropod preservation was defined by an index, which ranges from 0 to 4 (0 = no pteropods, 1 = some small fragments, 2 = trace amounts, 3 = fragments are common, 4 = abundant large-sized fragments). Oxygen isotope values were measured in 30 specimens

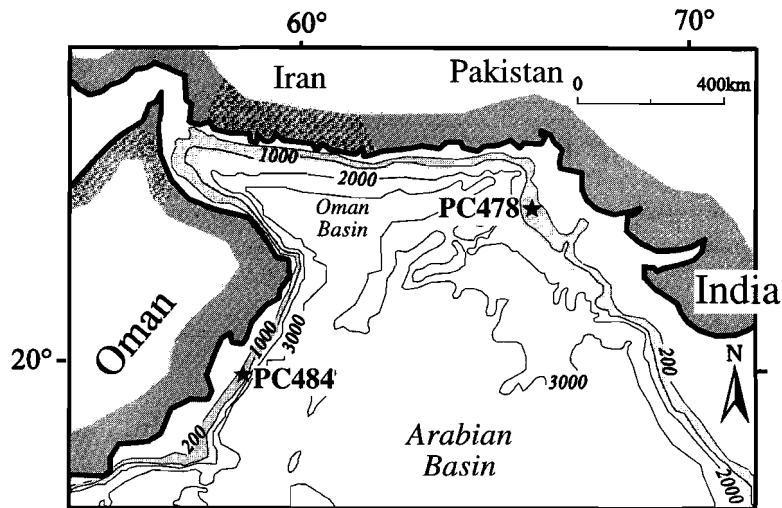


Figure 1. Location map of the northern Arabian Sea with the position of PC484 and PC478. The area where the present-day OMZ impinges on the continental slope is shaded.

of *N. dutertrei* and *G. menardii* per sample. Each sample was roasted for 30 minutes at 380°C under vacuum to remove organic remains, and transferred to an automated carbonate preparation unit (IsoCarb), after which the isotopes were measured on a mass spectrometer (VG SIRA 24). Values are reported relative to the Peedee belemnite (PDB) in standard δ notation; calibration is achieved through analyses of National Bureau of Standards (NBS) 19 reference materials. Precision for $\delta^{18}\text{O}$ measurements was better than 0.1‰.

A separate sub-sample was used for geochemical analyses. After freeze-drying, the sediment was thoroughly ground in a mortar before approximately 250 mg was dissolved in 5 ml of a 6.5 : 2.5 : 1 mixture of HClO_4 (60%), HNO_3 (65%) and H_2O , and 5 ml HF (40%). After reaction at 90°C the solution was evaporated to dryness at 190°C, and the residue was dissolved in 50 ml 1 M HCl. Elemental concentrations were subsequently measured using an Inductively Coupled Plasma Atomic Emission Spectrometer (ICP-AES) (Perkin Elmer Optima 3000), except for Mo (Perkin Elmer 4100 ZL ZGFAAS). Comparison with an international (SO1) and in-house standards revealed that the relative standard deviations, analytical precision and accuracy were better than 5% for all elements presented here. Another aliquot of the ground sample was used for organic carbon determination using a NCS analyser (Fisons NA 1500), after removal of carbonate. The carbonate was dissolved by mechanical shaking for 12 hours with 1 M HCl. Subsequently, samples were rinsed with demineralised water to remove CaCl_2 , and dried. The analytical precision and accuracy were determined by replicate analyses of samples, and by comparison with an international (BCR-71) and in-house standards. Relative standard deviations, analytical precision and accuracy were better than 3%. Particle sizes were determined on a carbonate-free basis, using a Malvern Series 2600 Laser Particle Sizer.

The solid-phase speciation of S and Fe was examined using a 3-step sequential extraction scheme (after *Lord, 1982*). Approximately 250 mg of dried and ground sediment was subsequently extracted with 1) 25 ml 1 M HCl (16h), 2) 20 ml 40 % HF (16h), and 3) 25 ml 14 M HNO₃ (16h). Accordingly, the carbonate, aluminum-silicate, and pyrite fractions were extracted. The reactive iron content of the sediments was determined separately using an extraction with 25 ml citrate-dithionite buffer (*Canfield, 1989*). This extraction dissolves the iron fraction that is highly reactive towards dissolved sulphide (amorphous and crystalline iron (hydr)oxides). All extracted solutions were analysed with ICP-AES for S, Fe and Al. Precision is generally better than 5 %.

Age model

The age model for core NIOP484 is based on AMS ¹⁴C dating (Table 1) and oxygen isotope records of both *Neogloboquadrina dutertrei* and *Globorotalia menardii*. Both species are thermocline dwellers (*Fairbanks et al., 1982; Ravelo et al., 1990*). Their similar depth preference is supported by the strong correlation between their oxygen isotope values ($r^2 = 0.97$). Small differences in $\delta^{18}\text{O}$ are most likely due to different vital effects. The two isotopic records were combined by converting $\delta^{18}\text{O}_{N.dutertrei}$ values to $\delta^{18}\text{O}_{G.menardii}$ values, using the best linear fit ($\delta^{18}\text{O}_{G.menardii} = 1.054 \times \delta^{18}\text{O}_{N.dutertrei} + 0.266$). Error bars in Fig. 2 indicate the $\delta^{18}\text{O}$ range between the two species in each sample.

Six AMS ¹⁴C ages for monospecific samples of *G. merardii* were corrected for changes in initial ¹⁴C content of the atmosphere (*Stuiver et al. 1986; 1998*) (Table 1, Fig. 2A). Although we realize that in an upwelling area, such as offshore Oman, reservoir ages can vary significantly as a function of the age of the upwelling waters, AMS ¹⁴C ages were corrected using a constant reservoir age of 400 yrs (*Bard et al., 1990*). Two AMS ¹⁴C ages for

Table 1. AMS ¹⁴C ages and calibration to calendar years for NIOP484 according to *Bard (1990)*, and *Stuiver et al., 1998*. Two ages acquired for the box core (BC484) were transferred to identical depths in the trip core in order to make a composite depth model.

	depth (cm)	AMS ¹⁴ C age (yr)	Calendar age (yr BP)
BC484	2	693 ± 39	373
	24,5	4485 ± 49	4672
PC484	2.5	11320 ± 80	12841
	7.5	10860 ± 60	12515
	92	13010 ± 80	15240
	339	20150 ± 150	23460
	430	21890 ± 170	25400

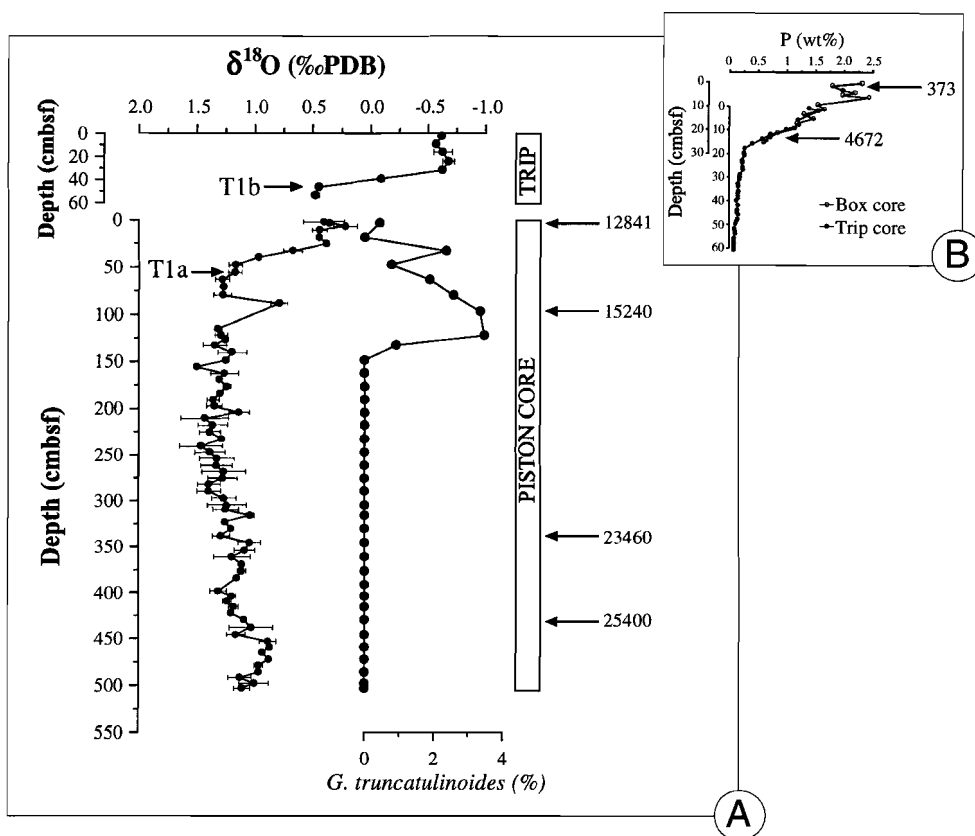


Figure 2. A) Downcore profiles of $\delta^{18}\text{O}$ and relative abundance of *G. truncatulinoides*. On the right hand side arrows indicate AMS ^{14}C calendar ages, corrected for reservoir age and changes in initial ^{14}C content of the atmosphere. The upper part of the record is from the trip core, the lower part was recovered from the piston core. Apparently, the sedimentary level at the base of the trip core corresponds to the top of the sediments from the piston core, possibly with a minor gap. B) Correlation between trip and box core using total solid-phase P. AMS ^{14}C ages are from the box core.

the box core were transferred to the trip core based on matching C_{org} and phosphorus profiles (Fig 2B). Two calibration points were added based on $\delta^{18}\text{O}$ stratigraphy (T1a (14700 ka) and T1b (11300 ka); Fairbanks, 1989; Bard et al., 1996). Ages for individual samples were calculated through linear interpolation between calibration points. An independent check on the age model comes from the short-term presence of *Globorotalia truncatulinoides* (Fig. 2A). This species is presently absent in the northern Arabian Sea, but proliferated during short periods in the past (Reichart et al., 1998). The timing of the *G. truncatulinoides* spike in PC484 is in good agreement with that of time equivalent spikes elsewhere in the

basin.

Linear sedimentation rates (LSRs) are greatly different in glacial and interglacial times (see also Fig. 5). Glacial sedimentation rates are up to 67 cm kyr^{-1} , whereas Holocene sedimentation rates are less than 5 cm kyr^{-1} . Sedimentation rates and sample spacing results in a resolution of $\sim 400 \text{ yrs}$ for the Holocene and $\sim 50 \text{ yrs}$ for glacial sediments.

Results

The sedimentary succession of NIOP484 can be divided into relatively organic-rich ($C_{\text{org}} > 0.75 \text{ wt}\%$) and organic-poor ($C_{\text{org}} < 0.75 \text{ wt}\%$) sediments (Fig. 3). The three glacial organic-rich intervals are distinctly laminated, whereas the Holocene sediments and the C_{org} maximum coinciding with the first part of the deglaciation (12.5-13.8 ka) are homogeneous. Records of Ba/Al and P/Al show a sharp increase from the glacial to the Holocene (Fig. 3). The P/Al values are much lower during the glacial period, and slightly higher in the laminated intervals. Ba/Al values are distinctly higher in the laminated intervals, but also

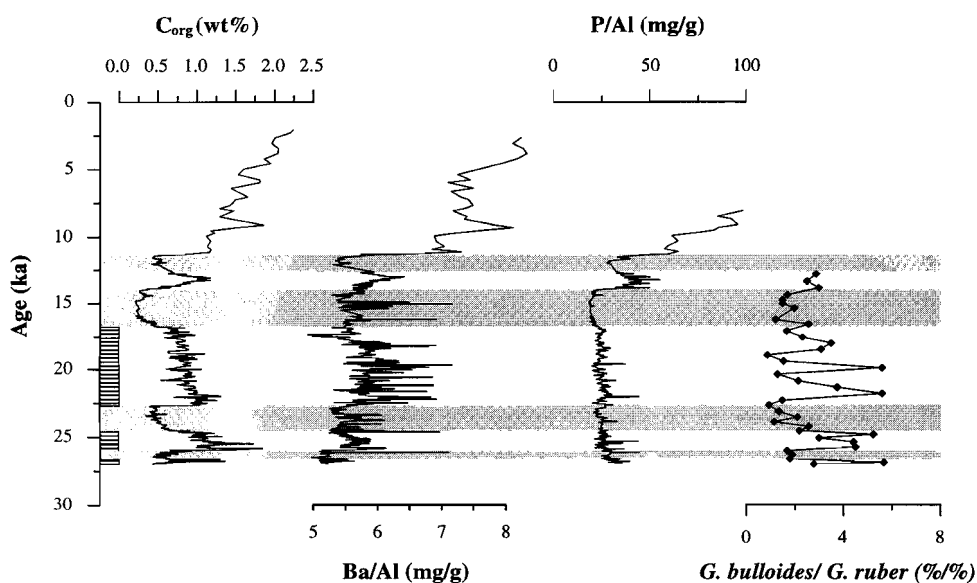


Figure 3. Records of organic carbon (wt%), P/Al (mg/g), Ba/Al (mg/g), and *G. bulloides*/*G. ruber* (%/%) ratios. P/Al is not shown in the upper part of NIOP484, where it rises to 700 mg/g (see Fig. 2). The shaded intervals indicate sediment depleted in organic matter. The laminated intervals are indicated at the left hand side.

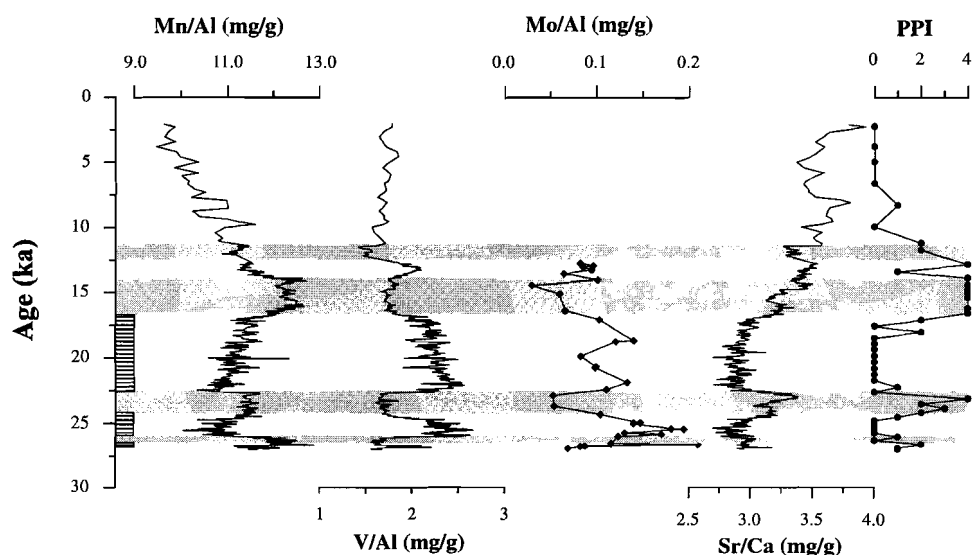


Figure 4. Records of sedimentary Mn/Al, V/Al, Mo/Al, Sr/Ca ratios (mg/g), and pteropod preservation index (PPI; see method section). The shaded intervals indicate sediment depleted in organic matter. The laminated intervals are indicated at the left hand side.

show a large scatter and maxima in the homogeneous intervals. The ratio of the planktonic foraminifers *Globigerina bulloides* to *Globigerinoides ruber* are generally higher in the laminated intervals (Fig. 3). Sediments rich in organic matter contain high concentrations of elements generally associated with bottom water dysoxia (V, Mo). No Mo data are available for the trip core. Sediments with a lower C_{org} content are enriched in Mn (Fig. 4), which is often associated with more oxygenated bottom water conditions. Sr/Ca and pteropod preservation is higher in the homogeneous intervals. Benthic foraminifers are present in both laminated and homogeneous intervals (not shown). There is a strong decrease in mass accumulation rate (MAR) at the transition from glacial to Holocene (Fig 5). Elements associated with the terrigenous fraction of the sediment, such as Al, show a corresponding drop in concentration. The grainsize distribution of the non-carbonate sediment fraction indicates that the homogeneous intervals contain relatively more coarse-grained terrigenous material. This is also indicated by the higher Ti/Al ratios in the homogeneous intervals, since Ti is usually concentrated in the coarse grained heavy mineral fraction of terrigenous sediments (Schmitz *et al.*, 1987; Shimmield, 1992).

Total solid-phase S (S_{tot}) concentrations show generally little variation with depth (0.4-0.5 wt%), with the exception of a distinct enrichment (up to 0.7 wt %) below the organic-rich interval in the top of the piston core (Fig. 6). Similar but lower sulphur spikes are also present below the laminated intervals. Pyritic-S (S_{pyr}) is present throughout the sediments of PC484 (Fig. 6). The distinct sulphur spike at 14.2 ka consists primarily of S_{pyr} . There is a close relationship between S_{pyr} and S_{tot} concentrations. Using the best linear fit

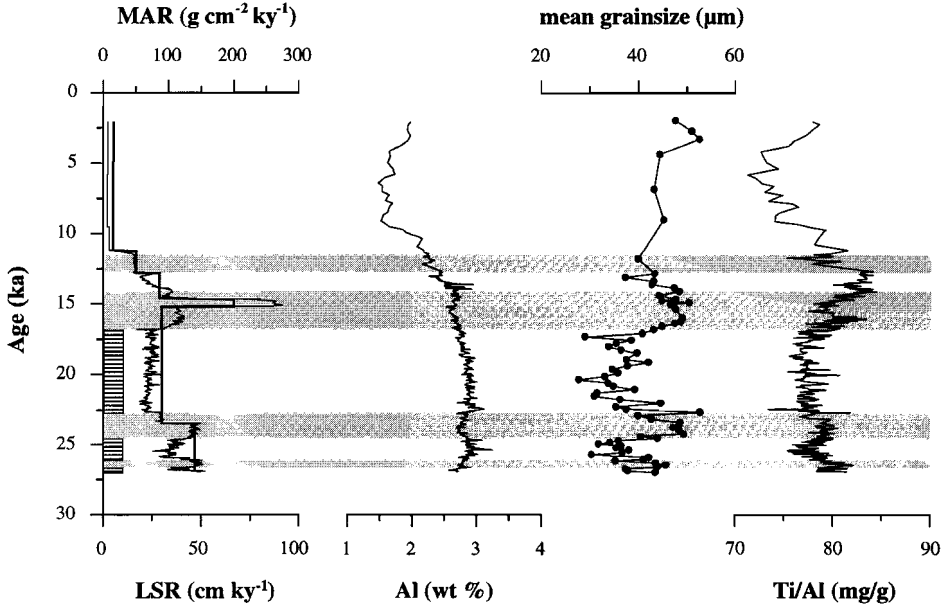


Figure 5. Records of the mass accumulation rate (MAR; $g\ cm^{-2}\ ky^{-1}$) and linear sedimentation rate (LSR; $cm\ ky^{-1}$), total aluminum content (wt%), mean grainsize of the decarbonated sediment fraction (μm), and Ti/Al ratio (mg/g). The shaded intervals indicate sediment depleted in organic matter. The laminated intervals are indicated at the left hand side.

($S_{pyr} = 0.94 \times S_{tot} - 0.13$; $r^2 = 0.95$), S_{pyr} concentrations were calculated for all samples, and plotted against the C_{org} content (Fig. 7a). Although the correlation between S_{pyr} and C_{org} is poor ($r^2 = 0.28$), a slope of -0.076 (i.e. a C/S ratio of 13.2), and a non-zero intercept on the S axis of ~ 0.23 wt% can be observed. C/ S_{pyr} ratios (wt%/wt%) are low (< 1.5) for organic-poor intervals and high (> 3.5) for intervals enriched in C_{org} .

Reactive iron contents (Fe_{rec}), here defined as the sedimentary iron fraction that is potentially available to react with H_2S to form pyrite (dithionite extractable Fe), are low throughout PC484 (500-1100 ppm). The degree of pyritization (DOP) is calculated with the equation (Berner, 1970):

$$DOP\ (\%) = 100 \times \frac{Fe_{pyr}}{Fe_{pyr} + Fe_{rec}} \quad (1)$$

where Fe_{pyr} is the iron concentration associated with pyrite. This parameter quantifies the extent to which reactive iron has been converted into pyrite. In this study dithionite

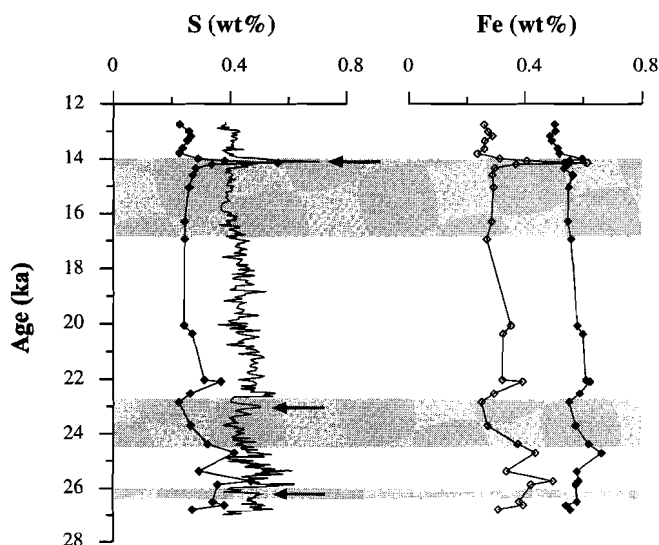


Figure 6. Records of total solid-phase S (solid line) and pyritic S (\blacklozenge) (wt%) versus age, and the pyritic Fe + reactive Fe concentration (\diamond) and estimated pyritic Fe + reactive Fe fraction ($Fe_{\text{reac}}(\text{exp})$) calculated with equation 2 (\blacklozenge) (see text), versus age. The shaded bands indicate organic-poor intervals. The arrows point to sulphur spikes located below organic rich layers.

extractable Fe was used to define Fe_{reac} instead of HCl-soluble Fe (Berner, 1970), which gives a better approximation of the degree of pyritization (Raiswell et al., 1994). Values for DOP are high (0.6-0.9) and independent of the C_{org} concentration (Fig. 7b).

Discussion

Paleoproductivity

Proxies related to sea surface productivity, such as Ba/Al, P/Al and C_{org} suggest that surface water productivity during the Holocene was significantly higher compared to the last glacial. This considerable increase in reconstructed productivity from the last glacial to the Holocene may partly be an artifact related to high glacial mass accumulation rates, which lowered both P/Al and Ba/Al values as a result of dilution with terrigenous material. On the other hand, Holocene C_{org} contents are relatively low compared to (sub) recent sediments from the same water depth at the Pakistan Margin ($C_{\text{org}} > 4$ wt%; Van der Weijden et al., 1999). This difference may be explained by the relatively low Holocene sedimentation rates on the Oman Margin, since slow burial of organic matter enhances its degradation (Müller and Suess,

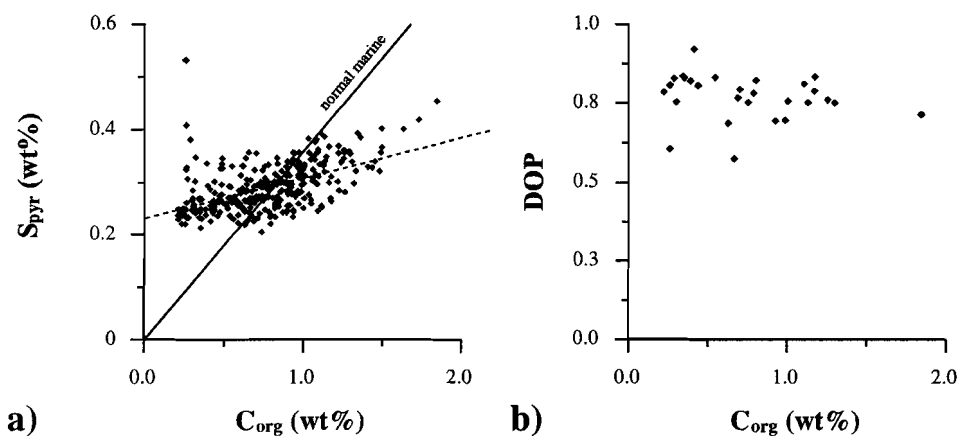


Figure 7. a) Plot of organic carbon content (C_{org}) versus pyritic S (S_{pyr}) content. The dashed line represents the best linear fit ($S_{pyr} = 0.076 \times C_{org} - 0.23$; $r^2 = 0.27$). The solid line through the origin represents the correlation observed in “normal” oxygenated marine sediments with a slope of 2.8 (Berner, 1984). b) Plot of the organic carbon content (C_{org}) versus degree of pyritization (DOP).

1979). Winnowing has been suggested to play an important role in organic matter degradation on the Oman Margin today (Pedersen *et al.*, 1992), but no independent evidence for winnowing was found for the sediments of NIOP484 (Chapter 4). On a precessional time scale, productivity seems to lack highest northern hemisphere summer insolation (11.5 ka) by, at least, several thousands of years. However, organic carbon, P/Al and Ba/Al values show a broad productivity maximum (Fig. 3), rather than a distinct interval with higher productivity.

Glacial sea surface productivity was relatively higher during periods of laminated sediment formation. The distinct Ba/Al peaks between the organic-rich intervals may be related to postdepositional redistribution of Ba caused by barite dissolution following pore water sulphate depletion (Van Os *et al.*, 1991; Von Breymann *et al.*, 1992). Pore water sulphate, however, was not completely exhausted in NIOP484 (unpublished data). The primary Ba signal, therefore, is still present, although probably somewhat attenuated. Further evidence for higher sea-surface productivity during glacial periods is derived from the ratio between the planktonic foraminifers *G. bulloides* and *G. ruber*. *G. bulloides* proliferates in the upwelling season, whereas *G. ruber* thrives all year round. High ratios of these species, therefore, are indicative for intensification of monsoon-induced upwelling (Conan and Brummer, *in press*). Summarizing, geochemical and paleontological proxy records indicate that sea surface productivity was higher during the Holocene, but that there were also distinct periods during the glacial with increased sea surface productivity. Higher productivity is attributed to increased upwelling, and is associated with deposition of laminated sediments during glacial times.

High-frequency variations in both C_{org} and Ba/Al (<100 yr) are recognized in the laminated intervals indicating rapid changes in monsoon induced upwelling. This variability

may have been present throughout the record, but was subsequently lost by bioturbation. Similar high-frequency variability has been observed in varved sediments from the late Holocene on the Pakistan Margin (Von Rad *et al.*, 1999), and seems an intrinsic part of the glacial and interglacial monsoonal climate system.

Variations in OMZ intensity

Laminations, redox-sensitive elements and Sr/Ca ratios

During the last glacial period the low BWO conditions resulted in the formation of laminated sediments. The continuous presence of benthic foraminifers in the laminated intervals indicates that bioturbation by meiofauna is unable to obliterate laminations if sedimentation rates are high. The absence of laminations in the organic-rich Holocene sediments may be related to a combination of very low sedimentation rates (< 5 cm/ky) and slightly higher bottom water oxygen concentrations. The higher Holocene upwelling rates, as well as bringing more nutrient-rich waters to the sea surface, possibly slightly enhanced bottom ventilation. This semi-annual upwelling-induced ventilation could have been sufficient to destroy laminations. Evidence for a semi-annual increase in bottom water oxygen concentration comes from oxygen profiles in the water column measured during the two monsoon seasons (Van Bennekom *et al.*, 1995; Morrison *et al.*, 1999). Whereas during winter oxygen concentrations at ~500 m are about 0.15 ml/l, this increases to about 0.29 ml/l in summer (Van Bennekom *et al.*, 1995). This slight increase in mid-water oxygen concentration during part of the year might enable the presence of benthos tolerant to low-oxygen conditions (e.g. the Galatheid Crab *Pleuroncodes*, which survives oxygen levels of 0.25 ml/L (Tyson, 1995)) to erase laminations.

Past BWO conditions can also be inferred from the down-core distribution of redox-sensitive elements. Mo and V are transported to the sediments as reduced species under dysoxic conditions in the water column (Ripley *et al.*, 1990; Breit and Wanty, 1991). Higher concentrations of Mo and V in the laminated intervals thus correspond to a more intense OMZ. The rather low Holocene V concentrations suggest that bottom waters were less dysoxic than during deposition of the laminated intervals. Manganese, which remobilizes and escapes to the water column under low BWO concentrations (Calvert and Pedersen, 1996), reaches highest concentrations in the homogeneous intervals. Manganese is only fixed in the sediments when surface sediments are oxygenated, and pore water Mn concentrations get sufficiently high to form Mn-carbonate phases (Calvert and Pedersen, 1996). The low Holocene Mn/Al values, therefore, indicate that bottom waters during the Holocene, although slightly more oxic than during the glacial, did not become fully oxygenated.

Aragonite has often a higher Sr content than calcite (Sutherland *et al.*, 1984) and, therefore, variations in the Sr/Ca ratio may reflect changes in the aragonite content of the sediment. This is confirmed by the distribution of pteropod shells, which consist primarily of aragonite. Past variations in aragonite preservation correlate well with laminations and redox-sensitive elements (Fig. 4). In the northern Arabian Sea, the aragonite compensation depth (ACD) is presently located at ~500 m (Berger, 1978), as a result of the intense OMZ (Canfield and Raiswell, 1991). Pteropods are indeed absent in the surface sediments at station

NIOP484. Consequently, high numbers of pteropods and increased Sr/Ca ratios reflect periods of a deeper ACD, and a weaker OMZ. Conversely, laminated sediments, being characterised by the absence of pteropods and low Sr/Ca values, have been deposited during periods with an intense OMZ. In the upper part of the record, however, Sr/Ca values are rather high, whereas no pteropods are present. This discrepancy may be related to the increased authigenic apatite formation during the Holocene, resulting in higher P concentrations in the surface sediments (**Chapter 4**). Authigenic apatite is known to contain relatively high amounts of Sr (*e.g. McArthur, 1985*).

The cool subtropical species *G. truncatulinoides* proliferates during periods of increased deep winter mixing, and thus a weakened OMZ. The peak occurrence of *G. truncatulinoides* in the homogeneous sediment interval directly above the upper laminated section (~17 to ~14 ka) (Fig. 2) is consistent with a weakened or even absent OMZ at that time.

Pyrite formation

C/S/Fe relationships in marine sediments have been used to determine paleoredox conditions in the environment of deposition (*e.g. Berner, 1970, Berner, 1984; Raiswell and Berner, 1985; Raiswell et al., 1988; Morse and Emeis, 1992; Passier et al., 1996*). Normal, oxygenated marine sediments are usually characterized by a positive correlation between sulphur and organic carbon, with a typical C/S ratio (g/g) of 2.8 ± 0.8 , because pyrite formation is controlled by the amount and reactivity of the organic matter. Conversely, in euxinic environments pyrite formation already commences in the water column (syngenetic pyrite). This results in relatively low sedimentary C/S ratios, and a positive S intercept in a S vs. C plot.

Considering the low BWO concentrations and the high rates of primary productivity on the Oman Margin, pyritic S concentrations in PC484 are unexpectedly low (average 0.3 wt%). These results are consistent with total reduced sulphur concentrations reported for ODP cores from the Oman Margin (on average 0.4 wt%; *Morse and Emeis, 1992*). The S vs. C distribution for PC484 (Fig. 7a) indicates a partial decoupling of pyrite formation from organic matter accumulation. The relatively high S concentrations in organic-poor intervals can be explained by postdepositional sulphidization (*Berner, 1969; Boesen and Postma, 1988; Middelburg, 1991; Leventhal, 1995; Passier et al., 1996*). In this situation, sulphide production by bacterial sulphate reduction in organic-rich intervals exceeds in-situ availability of reactive iron, and excess HS⁻ diffuses out of the interval. When reactive iron is present in the underlying, organic-poor interval, these sediments will be sulphidised by the downward migrating sulphide flux. Diagenetic sulphur enrichment induces low C/S ratios for organic-poor intervals, whereas organic-rich layers get relatively depleted in reduced S, resulting in high sedimentary C/S ratios (*Passier and De Lange, 1998*). Postdepositional sulphidization in PC484 is evidenced by the presence of iron sulphide enrichments just below the organic rich intervals (Fig. 6). These spikes are formed when the downward diffusion of sulphide is balanced by the upward migrating Fe²⁺ flux (Liesegang situation; *Berner 1969; Passier et al., 1996*). The distinct pyrite spike below the organic-rich layer in the top of PC484 may be related to the decrease in sedimentation rate at the end of the last glacial. A lowering of the accumulation rate of metabolizable organic matter, in combination with less

rapid burial of the organic matter may have caused relatively lower rates of sulphate reduction. As a result, the reduction rate of iron oxides could balance the H_2S production rate for a relatively long period of time. The presence of pyrite below the spike indicates that the sulphidization front eventually progressed further downward.

The occurrence of postdepositional sulphidization indicates that iron availability is limiting pyritization in the organic-rich intervals. This is also indicated by the high DOP values and the poor correlation between DOP and C_{org} (Fig. 7b; *Berner, 1970; Raiswell and Berner, 1985; Calvert and Karlin, 1991*). All easily reducible iron oxides in the sediments of PC484 have been converted into pyrite, leading to a complete sulphidization of the sediment. We argue that, in contrast to previous reports (*Emeis et al., 1991; Morse and Emeis, 1992*), Fe availability, rather than the reactivity of the organic matter, controlled the amount of pyrite formed in continental slope sediments of the Oman Margin during the last glacial period. The low pyrite concentrations in these sediments thus have to be attributed to iron limitation.

Iron limitation for pyrite formation is common for euxinic environments, where iron oxides are already reduced in the water column (*Raiswell and Berner, 1985; Boesen and Postma, 1988; Calvert and Karlin, 1991; Middelburg, 1991*), and organic-rich sediments, where high rates of bacterial sulphate reduction cause a rapid depletion of iron oxides (*Passier et al., 1996*). For the Oman Margin, iron limitation seems unexpected in view of the high input of dust and associated detrital iron minerals during glacial periods (*Clemens and Prell, 1990; Sirocko, 1991*), and the relatively low C_{org} contents in PC484 in comparison to sediments from euxinic basins and other upwelling zones (*e.g. Raiswell and Berner, 1985; Morse and Emeis, 1992*). Assuming that the detrital Fe deposition flux is proportional to that of aluminum, the expected initial reactive Fe concentration ($Fe_{react} (exp)$) can be estimated with the equation:

$$Fe_{react} (exp) = (Al) \times ((Fe/Al)_{tot} - (Fe/Al)_{unreact}) \quad (2)$$

where (Al) is the total sedimentary aluminum concentration, $(Fe/Al)_{tot}$ the Fe to Al ratio of the deposition flux, and $(Fe/Al)_{unreact}$ the Fe to Al ratio for the unreactive iron fraction. For the Oman Margin, reactive and unreactive iron are primarily supplied by eolian dust. The average Fe/Al ratio in Arabian Sea aerosols is 0.644 (*Chester et al., 1991*), which is consistent with $(Fe/Al)_{tot}$ ratios in Arabian Sea surface sediments that are unaffected by diagenetic enrichment or depletion (*Van der Weijden et al., 1999; Chapter 4*). The $Fe/Al_{unreact}$ ratio, which depends on the iron content in alumino-silicates, was obtained from the second step (HF extraction) in the sequential extraction (0.44). For all samples, there is a significant deficit between $Fe_{pyr} + Fe_{react}$ and calculated $Fe_{react} (exp)$ concentrations (Fig. 6). Apparently, a significant proportion of the reactive iron input was not preserved in the sediments. *Raiswell and Canfield (1998)* observed that oxic and dysoxic environments contained similar contents of the highly reactive Fe fraction (25-28 %; here defined as the sum of pyritic Fe and dithionite extractable Fe), as long as some oxygen is present in the bottom water. For PC484, the $Fe_{pyr} + Fe_{react}$ fraction constitutes only 9 % of the total solid-phase Fe. Consequently,

bottom waters on the Oman Margin must have been depleted in oxygen during certain time intervals to such an extent that this caused the reduction of iron oxides in the water column or at the sediment water interface. High dissolved iron concentration in the present-day OMZ (Saager *et al.*, 1989) are indicative for similar processes. The low oxygen concentrations of the intensive OMZ in the Arabian Sea are thus responsible for the iron limitation in continental slope sediments of the Oman Margin.

Euxinic environments are usually enriched in sedimentary pyrite contents compared to “normal” marine sediments, because a part of the settling detrital Fe flux is transformed into pyrite in the water column (Bernier, 1984; Raiswell and Canfield, 1998). The low pyrite S contents in PC484 indicate that no syngenetic pyrite has been formed, and that the water column on the Oman Margin thus contained no significant amounts of H₂S during the last glacial period or the Holocene. This is consistent with the continuous presence of benthic foraminifers, since prolonged exposure to sulphidic conditions would ultimately have decimated the benthic foraminiferal community (Moodley *et al.*, 1997). Bottom water conditions during deposition of the laminated intervals were probably similar, or slightly more intense than the present-day situation.

Dust sedimentation

Presently, the terrigenous fraction in Oman Margin sediments is exclusively of eolian origin (Nair *et al.*, 1989; Clemens *et al.*, 1991; Prins, 1999). Although in the past conditions on the Arabian peninsula have been more humid, the absence of major river systems draining this area makes a significant contribution of fluvial sediments highly unlikely. The record of the terrigenous fraction of NIOP484 is, therefore, controlled by the input of eolian material. The dust deposited on the Oman Margin originates from the Arabian Peninsula, from where it is transported to the Arabian Sea by the northwestern Shamal winds (Sirocko and Sarthein, 1989). Therefore, higher glacial MARs, and thus dust sedimentation, have to be attributed to more arid conditions on the Arabian Peninsula (*e.g.* Clemens and Prell, 1990; Shimmield, 1992). It can, however, not be excluded that dust sedimentation at site NIOP484 was also influenced by sea level, because the coring site is in close proximity of land. The lower sea-level during glacial times exposed a large portion of the continental shelf, making it a potential dust source area.

The grainsize distribution of the terrigenous sediment fraction has been used as a proxy for wind strength in the Arabian Sea (*e.g.* Clemens and Prell 1990; Clemens, 1998; Prins, 1999). The organic-rich intervals in NIOP484 are characterized by more fine-grained material, which is consistent with the lower Ti/Al ratios. The negative correlation between grainsize and organic carbon implies that the wind strength over the site 484 was diminished during periods of increased paleoproductivity. The opposite pattern is often found in sediment cores from the central and northern Arabian Sea: periods of high productivity correspond with deposition of more coarse grained material, as the strengthened summer monsoonal winds enhanced upwelling. The contrasting pattern in NIOP484 is probably related to a northwestward shift of wind trajectories during periods with an intense summer monsoon (Anderson and Prell, 1993; Sirocko *et al.*, 1993). Since dust is primarily transported to the Arabian Basin by the Shamal northwestern winds which override the southwestern

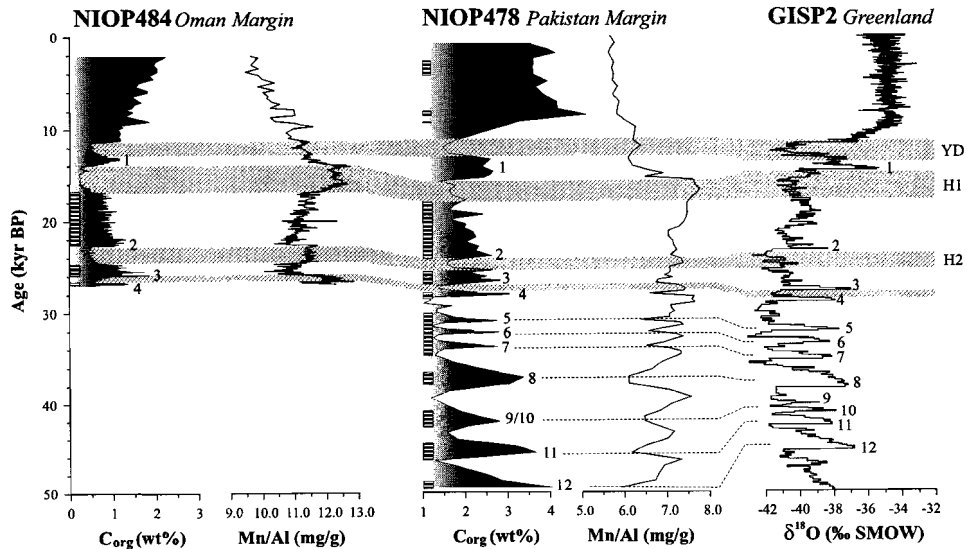


Figure 8. Correlation of high-frequency climate variability between marine sediment cores NIOP484 (Oman Margin), NIOP478 (Pakistan Margin), and the GISP2 icecore. From NIOP484 and NIOP478 are plotted organic carbon and Mn/Al ratios. Laminated intervals are indicated by the horizontal striped bars. Numbers indicate interstadials IS1 - IS12 (Dansgaard et al., 1993), and equivalent Arabian Sea monsoonal events. YD indicates Younger Dryas, H1 and H2 refer to northern Atlantic Heinrich meltwater events.

monsoon winds at the ITCZ, an inland shift of the wind trajectories could actually reduce the grainsize of dust fall at station NIOP484. Furthermore, a more inland position of the ITCZ would promote more humid conditions on the Arabian peninsula (Burns et al., 1998), thereby reducing dust formation.

Comparison with the Pakistan Margin record and the GISP2 ice core

Proxy records for continental aridity, summer monsoon intensity, wind strength, primary productivity, and OMZ intensity show variability on different timescales. Periods of high productivity, low BWO concentrations and a northward shift of the ITCZ alternate with periods characterised by the opposite conditions. This variability is clearly related to changes in summer monsoon strength on a sub-Milankovitch time scale at the Oman Margin.

Similar sub-Milankovitch variability has been recorded at the Pakistan Margin. The timing of these fluctuations at the Oman and Pakistan Margins is in good agreement with

climate changes recorded in the GISP2 ice core (Fig.8) (Grootes *et al.*, 1993; Dansgaard *et al.*, 1993; Meese *et al.*, 1994). Small offsets are attributed to uncertainties in the age models. For instance, the use of an average oceanic reservoir age in an upwelling area may introduce inaccuracies in the age model for NIOP484. Inaccuracies of about 3.5 kyr between 20 - 30 ka also exist in the age models for the ice cores, as is evident from the different timing of the Dansgaard Oeschger events in the GRIP and GISP2 ice cores (Hammer and Meese, 1993). Figure 8 shows that the glacial laminated intervals in 484 and 478 are time equivalent, and also that the glacial Mn/Al and C_{org} records can be calibrated in great detail. On the Pakistan Margin, however, laminations are also present in the Holocene. This is most likely due to the fact that the Pakistan Margin is not directly influenced by upwelling, and thus oxygen levels remain low throughout the year. In this part of the basin, summer productivity is dependent on nutrients that are advected from the upwelling areas. The organic carbon record from the Pakistan Margin has been calibrated to the $\delta^{18}\text{O}$ record of the GISP2 ice cores (Reichart *et al.*, 1998; Schulz *et al.*, 1998), with light coloured, bioturbated sediments and low C_{org} values, corresponding to cold air temperatures over Greenland, indicated by light $\delta^{18}\text{O}$ GISP2 values. During these periods intensity of the summer monsoon was reduced, whereas winter monsoon strength increased (Reichart *et al.*, 1998; Schulz *et al.*, 1998). The record from the Oman Margin shows a similar relationship with the GISP2 core (Fig. 8), and indicates that the ITCZ remained in a more southern position during cold Dansgaard-Oeschger events. These cold Dansgaard-Oeschger events also correspond to more arid conditions in the Arabian Peninsula.

Conclusions

High-resolution geochemical and micropaleontological records from the Oman Margin show high-frequency variations in sea surface productivity caused by changes in the intensity of summer monsoon induced upwelling. Changes in aridity on the Arabian Peninsula varied simultaneously with changes in summer monsoon, drier conditions being contributed to minimum monsoon intensity. Past variability in the intensity of the oxygen minimum zone (OMZ) was reconstructed using redox-sensitive elements, aragonite preservation and sulphur diagenesis. OMZ intensity varies together with summer monsoon strength, being weakest during periods of minimum summer monsoon intensity. Pyrite formation in the Oman continental margin sediments was limited by the availability of reactive iron. This was caused by the low oxygen concentrations of the OMZ, which resulted in the reduction of iron oxides in the water column or at the sediment water interface. However, no euxinic conditions developed in the OMZ at the Oman Margin. Calibrating the Oman Margin record with a record from the Pakistan Margin indicates that minima in summer monsoon intensity correspond with maxima in winter monsoon strength. Furthermore, the record from the Oman Margin again confirms the link between sub-Milankovitch variability in high and low latitude climate.

Chapter 3

Acknowledgements

We thank Captain J. de Jong, his crew and the skilled technicians of the NIOZ, Texel for help and good collaboration on board. W.J.M van der Linden and C.H. van der Weijden were chief scientists during the Utrecht NIOP cruises. A. Potjewijd is acknowledged for his help with the foram counting. Analytical support came from G. Nobbe, M.A. van Alphen, H. de Waard, G.J. Ittman, G. van het Veld, and A van Dijk. M.A. Prins is acknowledged for providing the grainsize data. Critical reviews by C.H. van der Weijden significantly improved this manuscript. This research was funded by the Netherlands Organisation for Scientific Research (NWO).

Part II:

**Sedimentary P cycling
in the Arabian Sea**

*“... Phosphorus has a very beautiful name (it means
'bringer of light'), it is phosphorescent, it's in the brain;
... without phosphorus plants do not grow; ... it is in
the tips of matches, and girls driven desperately by love
ate them to commit suicide; it is in will-o'-the-whisps,
putrid flames fleeing before the wayfarer,”*

P.Levi, The periodic Table, Schocken Books, New York,
1984.

4

Phosphogenesis and active phosphorite formation in sediments from the Arabian Sea Oxygen Minimum Zone

S.J. Schenau, C.P. Slomp and G.J. De Lange

Abstract - In this study, porewater chemistry, solid-phase analysis, and microscopical observations were combined to evaluate phosphogenesis in three boxcores located within the intensive oxygen minimum zone of the Arabian Sea. Three parameters, namely a decrease of the dissolved phosphate and fluoride concentrations with depth, saturation with respect to carbonate fluorapatite (CFA), and the presence of a solid-phase Ca-phosphate mineral, all indicate that phosphogenesis is currently taking place at all three sites. Authigenic apatite precipitation rates vary between 0.076 and 1.04 $\mu\text{mol P cm}^{-2}\text{y}^{-1}$, and are of the same order of magnitude as reported for other high productivity areas. Precipitation of an intermediate precursor precedes CFA formation in the continental slope sediments on the Karachi Margin. Results of a diagenetic P model indicate that phosphogenesis is induced by high rates of organic matter degradation. Dissolution of fish debris is likely to provide an substantial additional source of phosphate. Redox iron cycling does not influence phosphogenesis in these environments. Model results suggest that sediment mixing is essential in promoting early diagenetic phosphogenesis. The highest rate of CFA formation was observed in a boxcore taken on the Oman Margin, where it contributes to the formation of a Holocene phosphorite deposit. This observation contrasts with previous reports of only old phosphorites in this area. Phosphorites are presently forming on the Oman Margin as a result of a) deposition of older, reworked material from the continental shelf, which has undergone an earlier phase of phosphogenesis, b) a high input of reactive P (fish debris and degradable organic matter), c) a relatively low sediment accumulation rate, and d) the absence of winnowing on this location. Holocene phosphorite deposits may be less common on the Oman Margin than in other upwelling areas because of the narrowness of the shelf and the steepness of the slope, which is likely to limit the area where phosphorite formation may occur.

Introduction

Phosphogenesis is the early diagenetic precipitation of francolite, a carbonate fluorapatite mineral (CFA). Authigenic apatite formation is an important sedimentary sink for reactive phosphorus in the oceans (*Ruttenberg and Berner, 1993*). The major element composition of marine sedimentary apatite displays little variation (*e.g. Jarvis et al., 1994*), and approaches the simplified formula $\text{Ca}_{10}[(\text{PO}_4)_{6-x}(\text{CO}_3)_x]\text{F}_{2+x}$. In organic-rich sediments CFA precipitation is usually restricted to the uppermost part of the sediment because the increase of carbonate alkalinity with depth prohibits further formation of apatite (*Jahnke et al., 1983; Glenn and Arthur, 1988*), and because CFA formation requires fluoride, diffusing from the overlying bottom water (*Froelich et al., 1983*).

For the evaluation of P cycling in the oceans, it is important to understand the environmental conditions influencing phosphogenesis. Saturation of the interstitial water with respect to CFA is primarily controlled by the flux of reactive phosphorus transferred to the sediment (*e.g. Filippelli and Delaney, 1994*). Phosphate production in the porewater may originate from microbial degradation of organic matter (*e.g. Hartmann et al., 1973; Froelich et al., 1988; Ruttenberg and Berner, 1993*), desorption from iron oxides (*e.g. Sundby et al.,*

1992; Slomp *et al.*, 1998), and dissolution of fish debris (Suess, 1981). A second prerequisite for CFA precipitation is that sedimentary conditions have to permit the build up of phosphate in the porewater. High porosities enhance phosphate diffusion to the bottom water and reduce the capacity to retain reactive P in the sediment (Van Cappellen and Berner, 1988; Filippelli and Delaney, 1994). Early diagenetic iron cycling has been shown to promote phosphogenesis under oxygenated bottom water conditions (Sundby *et al.*, 1992; Slomp *et al.*, 1996). In addition, redox dependent cycling of phosphate by microorganisms (*e.g.* Ingall and Jahnke, 1994) and microbial mat communities at the sediment water interface (Williams and Reimers, 1983; Reimers *et al.*, 1990; Krajewski *et al.*, 1994) may play an important role in regulating the interstitial phosphate concentrations. Benthic P regeneration and consequent loss of phosphate to the water column appears to be more extensive under oxygen depleted bottom water conditions (Ingall and Jahnke, 1994). As a consequence, phosphogenesis is often associated to oxic to suboxic bottom water conditions (Heggie *et al.*, 1990; Ingall *et al.*, 1993; Jarvis *et al.*, 1994).

Upwelling areas are known to have sediments with high authigenic phosphorus contents, defined as phosphorites when containing more than 5 wt% P₂O₅ (*e.g.* Cook, 1984). These high sedimentary P concentrations are thought to result from high CFA precipitation rates during early diagenesis induced by high inputs of degradable organic matter and processes of sediment reworking (*e.g.* redeposition, winnowing; Burnett, 1977; Kolodny, 1981; Froelich *et al.*, 1988). Phosphorites have been found worldwide in numerous geological formations (*e.g.* Filippelli and Delaney, 1994; Föllmi, 1996; Trappe, 1998), but their recent formation is a relatively rare phenomenon (Jahnke *et al.*, 1983; Thomson *et al.*, 1984; Froelich *et al.*, 1988; Heggie *et al.*, 1990; Schuffert *et al.*, 1994, 1998). In addition to upwelling areas, phosphogenesis has been recognised in the sediments of shallow continental margins (Ruttenberg and Berner, 1993; Reimers *et al.*, 1996; Louchouart *et al.*, 1997), the continental slope underlying low productivity areas (Slomp *et al.*, 1996), and in deep-sea sediments (Lucotte *et al.*, 1994; Filippelli and Delaney, 1996).

The Arabian Sea is characterised by a high seasonal productivity (Qasim, 1982), which is caused by monsoonal induced coastal and open-ocean upwelling offshore Oman and Somalia. High vertical fluxes of organic matter, in combination with a sluggish ventilation owing to the semi-enclosed configuration of the Arabian Basin, result in an intensive Oxygen Minimum Zone (OMZ) between 150 and 1250 m water depth, with oxygen concentrations < 2 µM (*e.g.* Van Bennekom and Hiehle, 1994). Ancient phosphorite deposits, dating from the Miocene till Early Pleistocene, have been found in ODP cores recovered from the Oman Margin (Rao and Lamboy, 1995). Until now, recent phosphorite formation in this area has never been reported. This is surprising as the Oman upwelling area is in many aspects similar to that of Peru-Chile and Namibia.

In this study, we investigate phosphogenesis in three boxcores from the Arabian Sea located within oxygen depleted bottom waters, one recovered from the sediments underlying the Oman upwelling system, and two from the Pakistan Margin. We apply a diagenetic model for sedimentary P cycling developed by Slomp *et al.* (1996) to porewater and solid-phase P profiles to gain a better insight into the processes controlling phosphogenesis in these environments. In contrast to previous reports, we present evidence for Holocene phosphorite

formation on the Oman Margin.

Material and Methods

Sediment sampling and core description

During the Netherlands Indian Ocean program (NIOP, 1992) three boxcores were collected for this study: BC484 was recovered from the Oman margin from a depth of 527 m, BC451 and BC455 from the Karachi margin, from depths of 495 m and 1005 m respectively (Table 1; Fig. 1). All three boxcores are located within the OMZ and underlie an area of high primary productivity. In addition, a tripcore (TC484), taken on nearly the same location as BC484 (at a distance of ± 4 km.), was studied. Bottom water oxygen (BWO) concentrations were obtained from nearby CTD stations. ^{14}C Accelerator Mass Spectrometry (AMS) dating was performed on handpicked non-coated foraminifers (*Globorotalia menardii*), coated foraminifers, and phosphorite pellets. AMS ^{14}C ages were calibrated according to *Stuiver (1998)*, and corrected for a reservoir age of 400 yrs (Bard, 1990). Sedimentation rates (ω ; Table 1) were calculated from the ages of non-coated foraminifers.

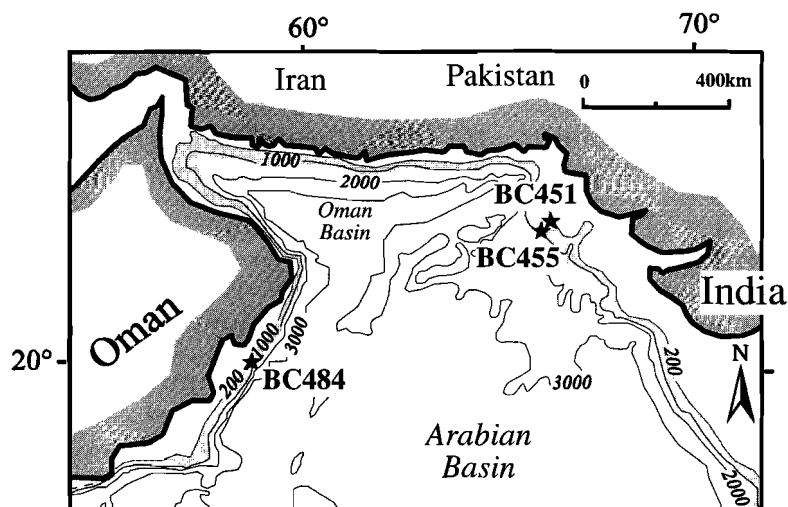


Figure 1. Positions of the boxcore sample sites. The area where the present-day OMZ impinges on the continental slope is shaded.

Table 1. Position, water depth, sedimentation rate (ω), organic carbon concentration in the top cm, oxygen concentration and bottom water temperature of the sampled boxcores.

Site	latitude (N)	longitude (E)	water depth (m)	ω (cm ky ⁻¹)	C _{org} top cm (wt%)	T bottom (C°)	[O ₂] bottom water (μ M)
BC484	19°30'.0	58°25'.8	527	5.6	2.24	12.3	< 2
TC484	19°29'.8	58°25'.7	516	-	-	-	-
BC451	23°41'.4	66°02'.9	495	28	4.37	12.6	< 2
BC455	23°33'.0	65°57'.4	1005	16	3.43	8.7	< 2

Pore water analysis

Porewater extractions were started on board within 24 hours of core collection according to shipboard routine (*De Lange, 1992a*). The boxcores were vertically sluiced into a glovebox, which was kept under low-oxygen conditions ($O_2 < 0,0005\%$) and at in-situ bottom water temperature. Under a nitrogen pressure of up to 7 bar, pore waters were extracted in Reeburgh-type squeezers. The shipboard pH measurements and nutrient analyses were performed within 12 hours after the extraction of the porewaters. Alkalinity was calculated after titration using the Gran plot method (*Gieskes, 1973*). Phosphate and ammonium were measured on a TRAACS 800 auto analyser, according to automated methods of *Strickland and Parsons (1968)* and *Solarzano (1986)* respectively. All analyses were performed in duplicate. Porewater fluoride concentrations were measured with a ion specific electrode. Relative errors were smaller than 2%.

Solid-phase analysis

The porosity and dry bulk density (dbd) were calculated from the weight loss after drying at 60°C, assuming a sediment density of 2,65 g cm⁻³. After removal of inorganic carbon with 1 M HCl, the organic carbon (C_{org}) content and total nitrogen content (N_{tot}) were measured with a NA 1500 NCS analyser. Relative errors were smaller than 0.4%. For the determination of total P, Ca, Al, Ti, and Zr, 250 mg of the sample was totally digested in 10 ml of a 6.5 : 2.5 : 1 mixture of HClO₄ (60%), HNO₃ (65%) and H₂O, and 10 ml HF (40%) at 90°C. After evaporation of the solutions at 190°C on a sand bath, the dry residue was dissolved in 50 ml 1 M HCl. The resulting solutions were analysed with an Inductively Coupled Plasma Atomic Emission Spectrometer (ICP-AES; Perkin Elmer Optima 3000). All results were checked using international (SO1, SO3) and in-house standards. Relative errors for duplicate measurement were better than 3%, except for Zr and Ti (5%). Particle sizes were determined on the bulk wet sediment and on carbonate and organic matter free fractions, using a Laser Particle Sizer (Malvern Series 2600).

The distribution of different phosphorus fractions in sediment samples was examined with a 6-step sequential extraction scheme, which is an adaptation of the SEDEX method developed by *Ruttenberg (1992)* with additional steps for selective Ca-carbonate extraction

Chapter 4

Table 2. *The P sequential extraction scheme and extracted fractions.*

step	extractant	P phase extracted	Reference
1	<ul style="list-style-type: none"> • 6× 25 ml 2 M NH₄Cl (pH 7) • 1× 25 ml demin. water 	P_{NH4Cl} <ul style="list-style-type: none"> • exchangeable or loosely sorbed P • carbonate associated P • fish debris 	<i>after De Lange, 1992b</i>
2	<ul style="list-style-type: none"> • 2× 25 ml • 1 M Na-acetate, buffered to pH 6 with acetic acid • 1× 2 M 25 ml NH₄Cl (pH 7) • 1× 25 ml demin. water 	<ul style="list-style-type: none"> • residual carbonate associated P 	-
3	<ul style="list-style-type: none"> • 1× 25 ml 0.15 M Na-citrate, 0.5 M NaCO₃ (pH 7.6), and 1.125 g Na-dithionite • 1× 2 M 25 ml NH₄Cl (pH 7) • 1× 25 ml demin. water 	P_{Fe} <ul style="list-style-type: none"> • easily reducible or reactive iron bound P 	<i>Ruttenberg, 1992</i>
4	<ul style="list-style-type: none"> • 2× 25 ml 1 M Na-acetate buffered to pH 4 with acetic acid • 1× 2 M 25 ml NH₄Cl (pH 7) • 1× 25 ml demin. water 	P_{CFA} <ul style="list-style-type: none"> • carbonate fluorapatite (CFA) 	<i>Ruttenberg, 1992</i>
5	<ul style="list-style-type: none"> • 1× 25ml 1 M HCl • 1× 25 ml demin. water 	P_{det} <ul style="list-style-type: none"> • detrital apatite 	<i>Ruttenberg, 1992</i>
6	<ul style="list-style-type: none"> • 20 ml HF/HNO₃/HClO₄ 	P_{res} <ul style="list-style-type: none"> • P adsorbed to clay minerals • organic P 	<i>Lord, 1982</i>

(Table 2). Approximately 250 mg of dried sediment was subsequently washed with 1) 25 ml 2 M NH₄Cl, pH=7 (6x), 2) 25 ml Na-acetate solution, pH=6, 3) 25 ml citrate dithionite buffer (CDB), pH=7.6, 4) 25 ml Na-acetate solution, pH=4, 5) 25 ml 1 M HCl, and 6) 20 ml HF/HNO₃/HClO₄ mixture. After extraction steps 2-5 the sediment was rinsed successively with 2 M NH₄Cl (pH=7) and demineralised water to prevent readsorption of HPO₄²⁻. The first extraction step differs from the SEDEX method in that 2 M NH₄Cl is used instead of 1 M MgCl₂ to dissolve carbonates prior to the other extraction steps (*De Lange, 1992b*). This has the advantage that carbonates are dissolved selectively, allowing a differentiation between CFA and more soluble calcium-phosphate minerals (**Chapter 5**). A separate

sequential extraction consisting of 8 times the 2 M NH_4Cl step was performed for some sediment samples. In this case, each extracted solution was analysed separately. The Na acetate (pH=6) extraction (step 2) was added to ensure complete carbonate removal, since incomplete dissolution of Ca-carbonates might cause precipitation of gypsum in the subsequent Na-dithionite extraction (step 3). All extracted solutions were measured for P with ICP-AES. Reproducibility was generally better than 5%, except for step 3 (10%). The recovery with respect to the total P concentration was 90%, 83%, and 90 % for BC484, BC451, and BC455 respectively. Fluoride concentrations in the extracted solutions of BC484 were measured with an ion specific electrode. For some samples, organic phosphorus (P_{org}) was determined according to the method of *Aspila et al. (1976)*.

Separate sediment samples were sieved into three fractions (65-150 μm , 150-595 μm , >595 μm). For BC484, these fractions were weighed and, after total digestion, analysed with ICP-AES. For all boxcore samples fish debris was quantified in the 150-595 μm fraction by counting the number of fish fragments in splits (using an Otto microsplitter). Coated foraminifers, dark brownish pellets, and fish debris in the top sediment of BC484 were hand picked from the 150-595 μm fraction. The bulk of these particles were analysed after total digestion with ICP-AES. A few particles were embedded in resin, photographed and analysed for Ca, P and F contents using an electron microprobe-scanning electron microscope (JEOL 8600).

Description of the model

A diagenetic model for P cycling developed by *Slomp et al. (1996)* was applied to the porewater and sequential extraction results for BC451 and BC455. This steady state model describes the concentration change with depth of porewater phosphate and three forms of solid-phase P, namely organic P, Fe-bound P, and authigenic P. The sediment column is divided into three zones: an oxidized surface zone (I: $0 \leq x \leq L_1$), a reduced sediment zone with bioturbation (II: $L_1 \leq x \leq L_2$), and a reduced sediment zone without bioturbation (III: $x > L_2$). The processes included in the model are 1) phosphate release from organic P due to organic matter degradation (zone I, II, III), 2) reversible sorption of phosphate to iron oxides (zone I), 3) phosphate release from Fe-bound P due to iron oxide reduction (zone II, III), and 4) authigenic P precipitation (zone II, III). Note that phosphate release from fish debris dissolution is not included in this model. The processes (1) to (4) are described as first order reactions, with reaction rate constants k_g , k_s , k_m , and k_a , respectively. The porewater equilibrium concentrations for sorption and apatite precipitation are C_s and C_a . The asymptotic Fe-bound P and organic P concentrations are equal to M_∞ and G_∞ . The molecular (D_s) and biodiffusion (D_b) coefficients, sedimentation rate (ω), reaction rate constants, and sediment porosity (ϕ) are assumed to be constant with depth in each relevant layer. In addition, the fluxes of organic P ($J_{\text{Gx}=0}$), Fe-bound P ($J_{\text{Mx}=0}$) and “authigenic” P ($J_{\text{ax}=0}$; i.e. the P fraction associated with fish debris, calcium carbonates, easily exchangeable P and resuspended authigenic apatite) from the water column to the sediment are assumed to be constant. Values of k_g , k_m , k_a , $J_{\text{Ax}=0}$, and $J_{\text{Gx}=0}$ were varied to fit the model to the experimental data. Variance-weighted sums of squares of the difference between the modelled and experimental values were minimized for all 4 components, i.e. phosphate, organic P,

Fe-bound P and authigenic P, simultaneously. Extra weight was assigned to the data points in the upper part of each profile and the whole authigenic P profile. The other parameters (L_1 , L_2 , D_s , D_b , ω , C_0 , C_s , C_a , k_s , $J_{Mx=0}$, M_∞ and G_∞) were fixed on the basis of existing data.

Results

Pore water

The phosphate concentration in BC484 is characterised by a sharp increase to 75 μM just below the sediment surface, followed by a decrease to 20 μM at the base of the boxcore (Fig. 2). In BC451 and BC455, the phosphate concentrations are lower, and the decrease of phosphate with depth is less pronounced (BC451), or absent (BC455). Fluoride concentrations decrease with depth in all three boxcores, whereas the ammonium concentrations and alkalinity increase almost linearly with depth (Fig. 2). BWO concentrations for all three boxcores are below the detection limit (2 μM ; Table 1).

Solid phase

The total P content is high in the top of BC484 (up to 2.0 wt%) (Fig. 3), corresponding to approximately 5 wt% of P_2O_5 , which classifies this sediment as a phosphorite. The P concentration in this core gradually decreases with depth to 4000 ppm. Phosphorus is concentrated in the coarse fraction of the sediment, namely, in concentrations up to 5.5 wt% in the 150-595 μm fraction. Approximately 20% of the solid-phase P is present in the fraction smaller than 65 μm , which constitutes 50 wt% of the bulk sediment. Total P contents in BC451 and BC455 are much lower (1000-2000 ppm) and increase with depth.

In BC484, the major fraction of P is extracted in step 4 (authigenic apatite). All P fractions in this core show a decrease of P with depth (Fig. 3). Probably, CFA is partially dissolving in the other extraction steps in this boxcore. This is confirmed by fluoride analysis in the solutions of step 2 till 5, which revealed a constant molar P/F ratio of 2.4. In BC451 and BC455, the P fraction responsible for the increase with depth of total solid-phase P was extracted during step 1 + 2 (Fig. 3). The P_{Fe} fraction in BC451 is low (~ 40 ppm). In the top of BC455, P_{Fe} is enriched up to 400 ppm. The P_{CFA} and P_{det} fractions are nearly constant with depth in both BC451 and BC455. The residual P fraction (P_{res}) decreases with depth in the top 10 centimeters of the sediment. The good correspondence between P_{org} (as determined with the Aspila method, not shown) and P_{res} contents, indicates that the P_{res} fraction is equal to organic P.

The sediments of BC451 and BC455 have higher organic carbon (C_{org}) contents than those of BC484 (Table 1). The $C_{\text{org}}/N_{\text{tot}}$ weight ratio in TC484 increases with depth till 18 cm, where it reaches a constant value of 10 (Fig. 4). A sharp upward increase of the P content occurs above this depth. The Ca-carbonate content is lower in the upper 12 cm of TC484, relative to the deeper part. Ti and Zr contents, which have been divided by Al to reveal changes not related to variations in terrestrial input, are fairly constant with depth. The mean grainsize of both bulk and decarbonated sediment samples is relatively constant with depth

Phosphogenesis and phosphorite formation

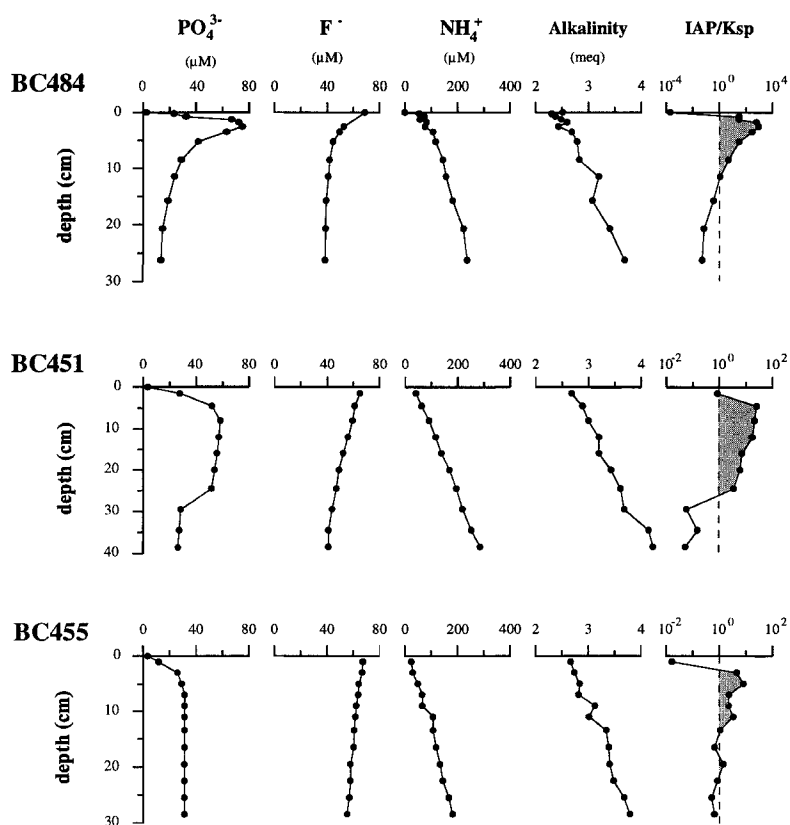


Figure 2. Porewater profiles for BC484, BC451, and BC455: phosphate, fluoride, ammonium, and alkalinity. The saturation state with respect to CFA in the porewaters was calculated as IAP (ion activity product) divided by the Ksp (solubility product of CFA). The shaded areas indicate saturation.

(Fig. 4). The fish debris concentration (numbers per gram of the 150-595 μM sieve fraction) decreases with depth in BC484 (Fig. 5), and correlates reasonably well with the total P concentration. The amount of detectable fish debris, however, constitutes only a minor fraction of the total P since other phosphatised particles are more abundant. The fish debris concentration in BC451 and BC455 show a larger variability with depth. The lower concentrations of fish particles in these sediments compared to BC484 can probably be attributed to dilution by detrital material supplied by the Indus river.

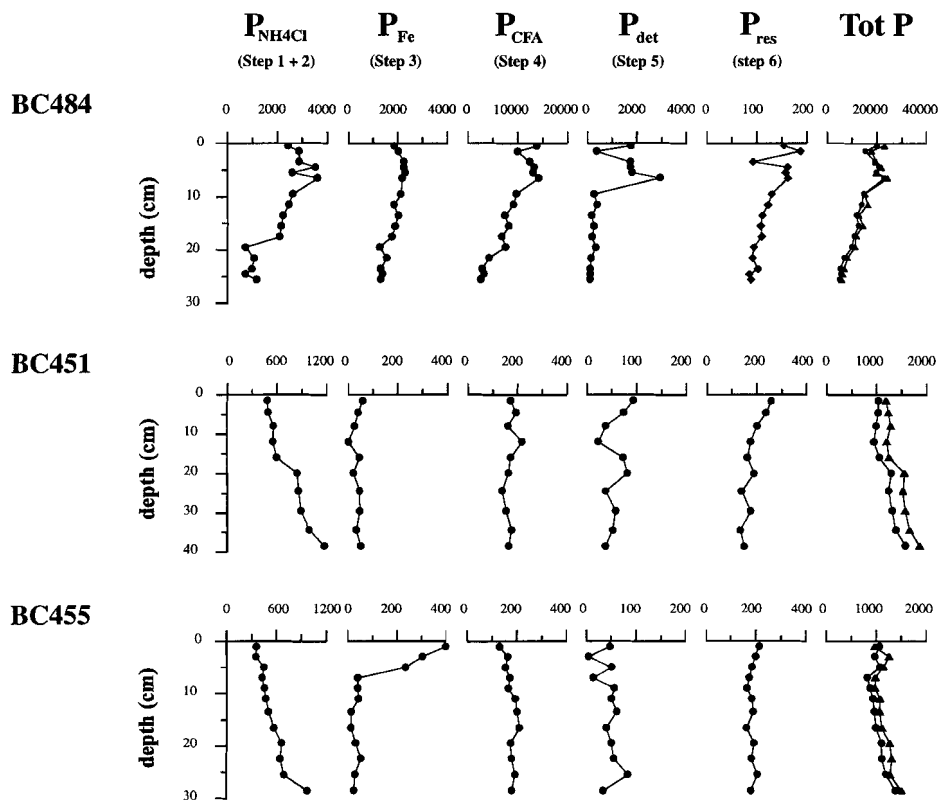


Figure 3. Profiles of extracted P phases (ppm): P_{NH_4Cl} (Step 1+2), P_{Fe} (Step 3), P_{CFA} (Step 4), P_{det} (Step 5), P_{res} (step 6+7), total P, as measured after total destruction (\blacktriangle), and the sum of all extracted P phases (\bullet). Note the different scales for BC484.

Microscopic observations, chemistry and calibrated ^{14}C ages of apatite macro particles in BC484

Microscopic observations and microprobe analysis allowed the identification of three types of apatite macro particles in BC484: coated foraminifers, phosphatised pellets and fish debris. A) *Coated foraminifers* constitute the bulk of the large phosphate grains (Fig. 6a). Most of the foraminifers in the top 10 cm of BC484 have a brown to black appearance caused by coatings and fillings. The foraminifer tests without coating look well preserved and do not show signs of calcite replacement or dissolution. Other particles consist of moulds, resembling the ovoid shape of the foraminifers. In the deeper part of the boxcore, coated foraminifers become less frequent. Calibrated ^{14}C ages for coated foraminifers are higher than “clean” (uncoated) foraminifers in the same sediment interval (Table 3).

B) *Phosphatised pellets* have ovoid to cylindrical shapes and a maximum length of ~ 3 mm (Fig. 6b). Their surface is blackish/brownish and usually smooth. Thin slides of samples reveal no internal structures indicating that the pellets are probably composed of apatite micro crystals. The number of phosphatised pellets decreases with depth, but they are still present in the deepest part of the boxcore. Phosphatised pellets at 2 cm depth have a calibrated ^{14}C age of 6890 yrs, and are thus slightly older than the coated foraminifers from the same depth (Table 3).

C) *Fish debris* is present in a range of forms and sizes (<2 mm) (Fig. 6c). The large parts are easily recognisable as vertebra (scales and bones) and have a spongy structure. Some particles are covered by small brown crystals consisting of CFA.

Table 3. Calibrated ^{14}C ages for non-coated foraminifers, coated foraminifers and phosphatised pellets in BC484 and pistoncore 484.

Core depth (cm)	pellets (yrs)	coated foraminifers * (yrs)	clean foraminifers (yrs)
2 cm	6890 ± 80	6385 ± 70 6200 ± 60	373 ± 40
24.5 cm	-	8800 ± 60	4672 ± 60
top pistoncore	-	-	12841 ± 60

* Calibrated ^{14}C age of total particles, i.e. including carbonate and apatite C.

The elemental composition of the phosphatised pellets and foraminiferal coatings/fillings (Table 4) indicates that both the pellets and coating/fillings consist primarily of CFA. Microprobe analyses show little variation in the chemical composition. The mean $\text{CaO}/\text{P}_2\text{O}_5$ and $\text{F}/\text{P}_2\text{O}_5$ ratios are similar to those reported for phosphatised particles in phosphorites (Price and Calvert, 1978; Thomson et al., 1984; Baker and Burnett, 1988). The $\text{F}/\text{P}_2\text{O}_5$ ratio of the pellets and coating/fillings is lower than the ratio for substituted francolite (0.148; McClellan et al., 1980). Low $\text{F}/\text{P}_2\text{O}_5$ ratios have been observed in relatively young phosphorites (Price and Calvert, 1978; Thomson et al., 1984; Baker and Burnett, 1988), but have also been related to CFA precipitation in organic-rich sediments (Jarvis et al., 1994). The $\text{F}/\text{P}_2\text{O}_5$ ratio of the pellets decreases towards the edge of these particles. This may reflect decreasing F concentrations in the porewater with ongoing formation of the pellets upon burial. The overall composition of the fish debris is very similar to that of apatite. However, the F concentration is lower than the mean concentration in francolites (5.04 wt%; McClellan, 1980), but higher than F concentrations of fresh fish debris (558–6850 ppm; Ke et al., 1970). This could be the result of fluoride adsorption in the water column and sediment.

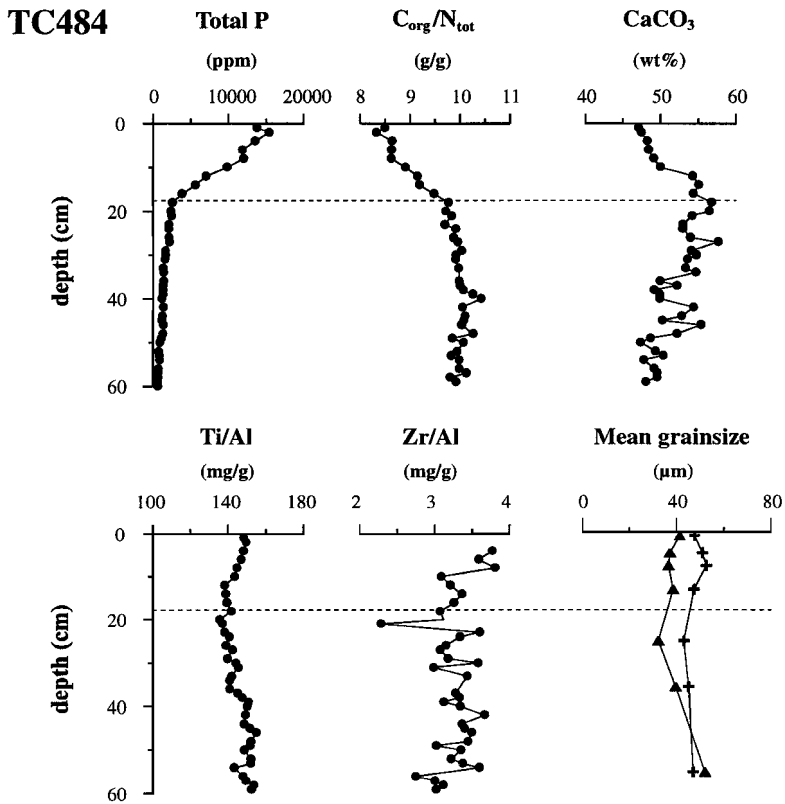


Figure 4. Profiles of total P (ppm), C_{org}/N_{tot} ratio (g/g), $CaCO_3$ (wt%), Ti/Al (mg/g), Zr/Al (mg/g), and mean grainsize (μm) (bulk (▲) and decarbonated (+) sediment) for tripcore 484 (TC484). The dotted line indicates the depth above which the P concentration increases sharply. The top 10 cm of TC484 were lost during core recovery.

Application of the model

The fixed parameters (L_1 , L_2 , ϕ , D_s , D_b , ω , C_0 , C_s , C_a , k_s , $J_{Mx=0}$, M_∞ and G_∞) used for the model and their sources are listed in Table 5. Considering the low BWO concentrations and the high sedimentary organic matter contents, oxygen will be consumed in the upper few millimeters in these sediments. Therefore, L_1 for BC451 was set at 1 mm. For BC455 L_1 is probably somewhat larger (~2 mm), as it is located near the base of the OMZ. The deposition rate of Fe-bound P ($J_{Mx=0}$) was estimated from the mass accumulation rate, an average reactive iron concentration of 6000 ppm (equal to the concentration in surface sediments below the OMZ), and an atomic Fe/P ratio of 20 for the newly deposited reducible iron particles.

The model fits agree reasonably well with the measured data (Fig.7), with the exception of the porewater profiles of BC451 and BC455. Fitted values for k_g , k_a , k_m , $J_{Ax=0}$,

Table 4. Chemical composition of apatite macro particles from BC484 (sample from 3 cm depth) as measured by ICP-AES (except for F, electron microprobe). The CaO/P₂O₅ ratios and P₂O₅/F ratios are weight ratios.

	Fish debris (ppm)	pellets (ppm)	coated foraminifers (ppm)
S	7550	7430	6480
P	124200	154300	139500
Fe	1490	1440	2750
Mg	9110	10130	10490
Al	130	1970	3320
Ca	315000	363000	353000
Y	45	18	77
Sr	2280	2840	2430
Na	1810	8010	4770
K	550	770	1130
F	15800	38800	28700
CaO/P ₂ O ₅	1.55	1.44	1.55
F/P ₂ O ₅	0.056	0.11	0.09

and $J_{Gx=0}$ are listed in Table 5. The calculated phosphate production and removal rates are given in Table 6.

Discussion

Authigenic apatite formation

Three indicators have been studied to examine whether phosphogenesis is currently taking place in the sediments located within the OMZ of the Arabian Sea (Ruttenberg and Berner, 1993): 1) pore water phosphate and fluoride concentrations, 2) the saturation state of CFA, and 3) solid-phase authigenic P concentrations.

1) *Porewater phosphate and fluoride concentrations.* A decrease in pore water phosphate and fluoride concentration with depth is indicative for P and F removal to the solid phase (Jahnke et al., 1983, Ruttenberg and Berner, 1993). The main sink for phosphate and fluoride in anoxic sediments is authigenic apatite (Froelich et al., 1983; Jahnke et al., 1983; Froelich et al., 1988; Ruttenberg and Berner, 1993). Consequently, the decrease in dissolved P and F with depth in BC484 and BC451 is interpreted as the result of CFA precipitation. The increase of ammonium and alkalinity with depth in all three boxcores implies that also dissolved phosphate is produced as the result of ongoing organic matter degradation. The

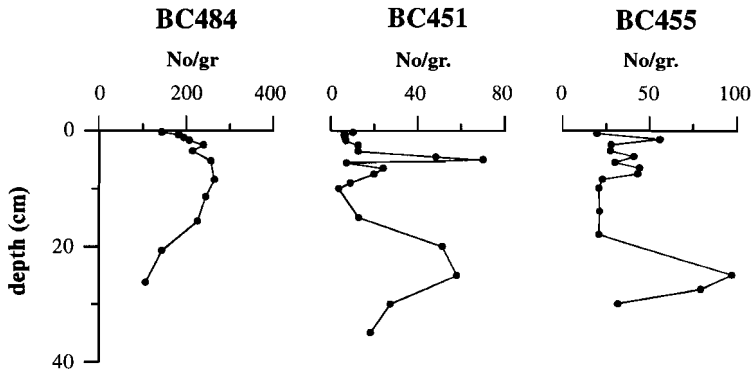


Figure 5. Concentration of fish debris in BC484, BC451 and BC455 (numbers per gram sediment).

rather constant phosphate concentration in BC455, therefore, indicates that also in this boxcore phosphate is removed and incorporated into a solid phase. In BC484 the negative porewater gradient of both phosphate and fluoride is non-linear, which implies that precipitation takes place in a zone comprising the upper 10 cm of the sediment. The nearly linear gradient of fluoride in BC451 and BC455 suggests that incorporation of F occurs at some greater depth.

Precipitation rates of CFA (or a precursor phase) were estimated from the downward diffusing phosphate and fluoride fluxes (see Appendix; Table 7). The fluoride flux (J_F) was converted into a P precipitation rate ($J_{P(F)}$), in order to enable a direct comparison with the phosphate flux (J_P). In BC484, J_P and $J_{P(F)}$ are similar at 4 cm depth, suggesting that the removal of phosphate and fluoride with depth is indeed due to CFA formation. The downward fluoride flux in the top cm is higher than at 4 cm depth (Table 7), which implies that CFA precipitation is also occurring in the top 4 cm of the sediment. In BC451 and BC455, J_P is lower than $J_{P(F)}$ (Table 7). A similar difference between interstitial phosphate and fluoride removal fluxes was observed by *Schuffert et al. (1994)* for sediments off western Mexico. The F flux into the sediment probably provides the best direct measure for CFA precipitation rates, because seawater is the dominant source for F in marine sediments (*Froelich et al., 1983*).

2) *The CFA Saturation state* has been calculated using pore water data, the stoichiometry of CFA ($\text{Ca}_{9.54}\text{Na}_{0.33}\text{Mg}_{0.13}(\text{PO}_4)_{4.8}(\text{CO}_3)_{1.2}\text{F}_{2.48}$; *Chien, 1972*), and the solubility product of carbonate fluorapatite (K_{sp}) (*Jahnke et al., 1983; Ruttenberg and Berner, 1993*). The solubility product of recently formed marine apatite has been shown to depend on the aqueous activity of CO_3^{2-} (*Jahnke, 1983*). Therefore, the solubility product has been calculated for each depth, using CO_3^{2-} concentrations estimated from pH and alkalinity data. In the top of the sediment of all cores the ion activity product (IAP) exceeds the solubility product, indicating supersaturation of the porewater with respect to CFA (Fig. 3). With depth, porewaters become undersaturated again. This suggests that precipitation of CFA or another

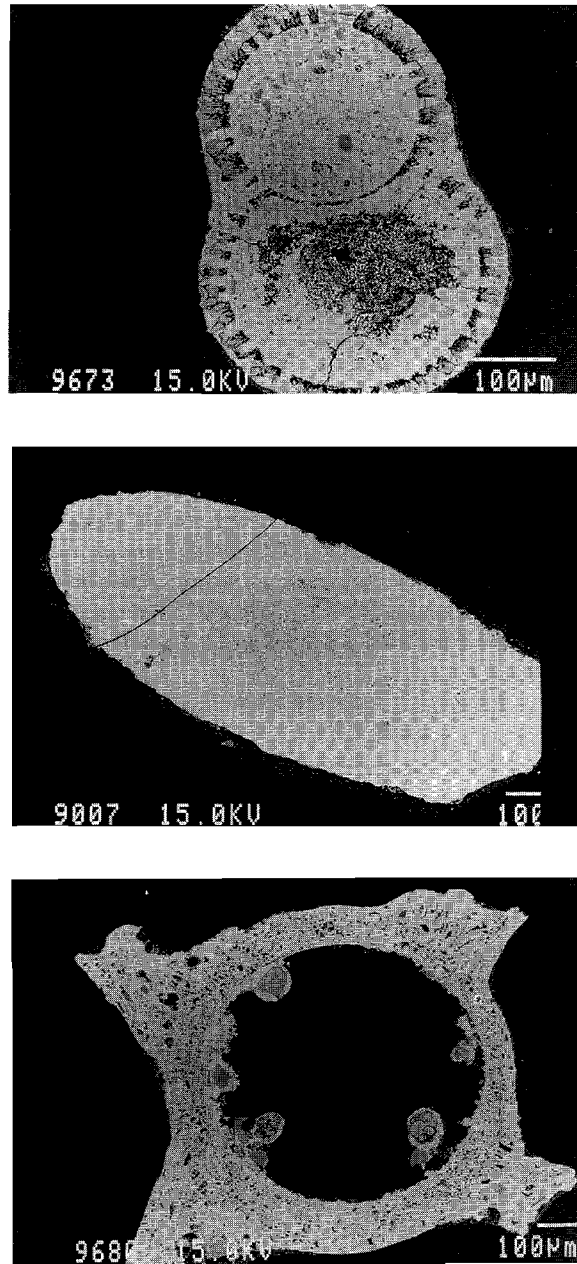


Figure 6. Microprobe backscatter photos of apatite macroparticles in BC484: a) a coated foraminifer, b) a phosphatised pellet, and c) fish debris.

Ca-phosphate mineral is most likely occurring in the upper 20 cm of the sediment.

3) *Solid-phase authigenic phosphorus*. The most direct indication for ongoing phosphogenesis is an increase of the solid-phase authigenic apatite fraction with sediment depth (Ruttenberg and Berner, 1993; Slomp et al., 1996; Louchouart et al., 1997). Although the P_{CFA} fraction remains constant in BC451 and BC455 (Step 4, Fig. 3), the $P_{\text{NH}_4\text{Cl}}$ concentrations increase with depth. To determine what P fraction is responsible for this increase, the 2 M NH_4Cl extraction was performed sequentially 8 times for some sediment samples from the base of BC455 and BC451. The release patterns for P and Ca show that the P concentration in the solvent starts to increase once the Ca concentration has dropped, indicating that the phosphorus fraction associated with $P_{\text{NH}_4\text{Cl}}$ starts to dissolve once all Ca-carbonates have been extracted (Fig. 8). Consequently, the $P_{\text{NH}_4\text{Cl}}$ fraction must be associated with a Ca-phosphate mineral. Fish debris, which consists primarily of hydroxyapatite, is, in contrast to authigenic or detrital apatite, highly soluble in 2 M NH_4Cl (Chapter 5). The number of fish debris as counted in the 150-595 μm sieve fraction, however, does not clearly increase with depth (Fig. 5). Consequently, it is unlikely that changes in the biogenic apatite contents can account for the observed $P_{\text{NH}_4\text{Cl}}$ profiles. In addition, an increase in sediment accumulation rates cannot be responsible for a possible dilution of the P fractions, as high resolution records on Arabian Sea sediment cores show that sedimentation rates during the Late Holocene remained constant (Sirocko et al., 1993). Therefore, we argue that the increase of the $P_{\text{NH}_4\text{Cl}}$ fraction with depth in BC451 and BC455 is the result of precipitation of an authigenic Ca- PO_4 mineral, which is more soluble than CFA.

Laboratory experiments have shown that CFA precipitation at high phosphate concentrations is a two-step process. First, an amorphous, F-poor precursor is formed, which subsequently acts as a substrate for CFA precipitation (Van Cappellen and Berner, 1991; Krajewski et al., 1994). This process is much faster than the direct nucleation of CFA from solution, which occurs at lower phosphate concentrations. The easily dissolvable Ca-phosphate in BC451 and BC455 may be identified as a precursor to CFA formation. This would also explain why fluoride incorporation occurs at a greater depth than the formation of the $P_{\text{NH}_4\text{Cl}}$ phase. Probably, a F-poor Ca-phosphate mineral precipitates in the top 10 cm of the sediment at the highest interstitial phosphate concentrations, and is converted into CFA deeper in the sediment. Uncoupling of interstitial phosphate and fluoride removal has previously been observed in Peru margin sediments (Froelich et al., 1988). Possibly, high concentrations of fish debris in the sediments of the Pakistan Margin are acting as a template for precipitation of a Ca-phosphate mineral (Föllmi, 1996), enabling rapid authigenic apatite precipitation under relatively low phosphate concentrations. Porewater profiles indicate that the transformation of the precursor into CFA takes at least a few thousand years.

Summarising, sequential extraction results and porewater flux calculations indicate that a Ca-phosphate mineral is precipitating in sediments located within the Arabian Sea OMZ during early diagenesis. In BC484, CFA precipitates in the upper 10 cm of the sediment. In BC451 and BC455, however, a precursor phase is formed, which is subsequently converted into CFA deeper in the sediment.

Table 5. Values for the fixed and fitted parameters for BC451 and BC455 as used in the diagenetic P model.

Fixed parameters	Units	BC451	BC455	Source
L_1	cm	0.1	0.2	see text
L_2	cm	2.8	3.8	Van der Weijden et al., 1999
φ	$\text{cm}^3 \text{cm}^{-3}$	0.82	0.84	average porosity
D_s	$\text{cm}^2 \text{d}^{-1}$	3.0×10^{-1}	2.8×10^{-1}	see appendix
D_b	$\text{cm}^2 \text{d}^{-1}$	5.0×10^{-3}	3.6×10^{-3}	Boudreau, 1994
ω	cm ky^{-1}	28	16	Table 1
C_0	μM	3.7	3.4	Bottom water concentration
C_s	μM	1	1	Froelich et al., 1988; Slomp and Van Raaphorst, 1993
C_a	μM	2.9	4.5	Atlas and Pytkowicz, 1977
k_s	d^{-1}	2.6×10^{-1}	2.6×10^{-1}	Slomp et al., 1996
$J_{\text{Mx=0}}$	$\mu\text{mol cm}^{-2} \text{y}^{-1}$	7.0×10^{-2}	4.0×10^{-2}	see text
M_w	$\mu\text{mol g}^{-1}$	1.1	1	conc. in bottom sample
G_w	$\mu\text{mol g}^{-1}$	4.8	5.8	conc. in bottom sample
Fitted parameters				
k_g	d^{-1}	3.0×10^{-3}	6.7×10^{-3}	
k_a	d^{-1}	7.4×10^{-4}	1.0×10^{-3}	
k_m	d^{-1}	2.3×10^{-4}	1.1×10^{-5}	
$J_{\text{Gx=0}}$	$\mu\text{mol cm}^{-2} \text{y}^{-1}$	5.7	2.9	
$J_{\text{Ax=0}}$	$\mu\text{mol cm}^{-2} \text{y}^{-1}$	2.5×10^{-1}	9.3×10^{-2}	

Implications of the model

The model results confirm that the increase of the solid-phase P with depth at stations BC451 and BC455 can be explained by early diagenetic phosphogenesis. The calculated CFA formation rates correspond reasonably well with the downward $J_{\text{P(F)}}$ fluxes (Table 7). The values of the rate constants k_m and k_a are in line with ranges estimated in other studies (Slomp et al., 1996; 1998). Fitted values for k_g correspond to rate constants for highly reactive organic matter (Boudreau, 1997; Boudreau et al., 1998). Model results suggest that phosphogenesis is fuelled by phosphate release from organic matter in the surface sediments.

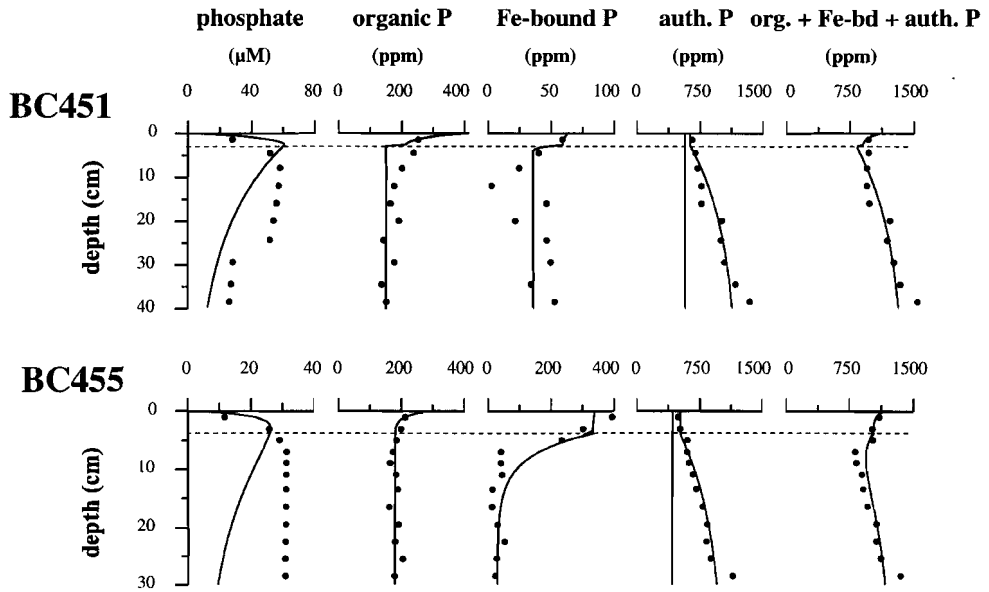


Figure 7. Model fits (solid lines) to the porewater phosphate, organic P (equal to P_{res}), Fe bound P (P_{Fe}), authigenic P (equal to $P_{NH4Cl} + P_{CFA}$), and the sum of these three solid-phase P fractions. The horizontal dotted line indicates the depth of bioturbation (L_2). The vertical solid line in the authigenic P profiles represents the $P_{NH4Cl} + P_{CFA}$ concentration which is not related with in-situ authigenic P formation (e.g. P associated with fish debris or carbonates, easily exchangeable P, or redeposited authigenic apatite).

In order to reproduce the high subsurface porewater phosphate concentrations organic P inputs of respectively 5.7 and 2.9 $\mu\text{mol P cm}^{-2} \text{y}^{-1}$ for BC451 and BC455 are required (Table 6). The potential organic carbon flux arriving at the sediment water interface ($J_{Cx=0}$; $\text{gC m}^{-2} \text{y}^{-1}$) can be estimated with the transfer equation (Berger and Herguera, 1992):

$$J_{Cx=0} = 2 PP^{0.5} \times (PP/100) \times (1/z + 0.025)$$

where PP is the primary productivity rate ($\text{gC m}^{-2} \text{y}^{-1}$), and z the water depth in units of 100 m. Assuming an average primary productivity rate of 300 $\text{gC m}^{-2} \text{y}^{-1}$ for the northern Arabian Sea (Qasim, 1982), the potential $J_{Cx=0}$ flux amounts to 23 and 13 $\text{gC m}^{-2} \text{y}^{-1}$ for BC451 and BC455 respectively. This corresponds to a potential $J_{Gx=0}$ flux of 1.7 and 0.9 $\mu\text{mol P cm}^{-2} \text{y}^{-1}$ respectively. Apparently, the values for the $J_{Gx=0}$ flux needed to reproduce the high subsurface phosphate concentrations are unrealistically high. There are three possible explanations for this. Firstly, the model describes organic matter decomposition with one first order rate constant. As a result, the model predicts that all degradable organic P is

mineralised in the upper few centimetres of the sediment (Fig. 7). This is an overly simplistic description because organic matter degradation continues deeper in the sediment, as is demonstrated by the increasing alkalinity and ammonium concentrations with depth (Fig. 2). When in the model calculations relatively more organic matter degradation and phosphate production would occur deeper in the sediment, a lower $J_{Gx=0}$ input flux would be sufficient. Secondly, the measured phosphate profiles may not represent a steady-state situation. In the Arabian Sea productivity is highly seasonal, and therefore deposition rates of reactive P, subsequent phosphate regeneration and authigenic P formation may vary through the year. This may also explain the discrepancy between the observed and the modelled phosphate porewater profiles. Thirdly, dissolution of fish debris in the upper few centimeters of the sediment may provide an additional source of phosphate.

Early diagenetic iron redox cycling has been shown to be important for phosphogenetic processes in certain marine environments (e.g. Heggie *et al.*, 1990; Sundby *et al.*, 1992; Slomp *et al.*, 1996). Phosphate liberated from organic matter degradation or fish debris dissolution is scavenged by Fe-hydroxides in the oxic part of the sediments. Upon burial, these iron oxides are transferred to the suboxic part of the sediment and will be reduced, resulting in desorption of phosphate. The porewater phosphate concentration will increase, until CFA or a precursor phase starts to precipitate. Model results indicate that phosphate sorption does not affect the benthic P flux leaving the sediments (Table 6). In addition, the phosphate desorption from iron oxides provides only a minor source relative to

Table 6. Phosphate production and removal rates for BC451 and BC455 as calculated with the diagenetic P model.

	BC451 ($\mu\text{mol cm}^{-2} \text{y}^{-1}$)	BC455 ($\mu\text{mol cm}^{-2} \text{y}^{-1}$)
Phosphate production		
- organic P release	5.66	2.85
- Fe-bound P desorption	0.1	0.13
Total	5.76	2.98
Phosphate removal		
- benthic P flux	5.44	2.75
- diffusive P flux at bottom	0.04	0.01
- authigenic P formation	0.24	0.13
- P adsorption to iron oxides	0.04	0.09
Total	5.76	2.98

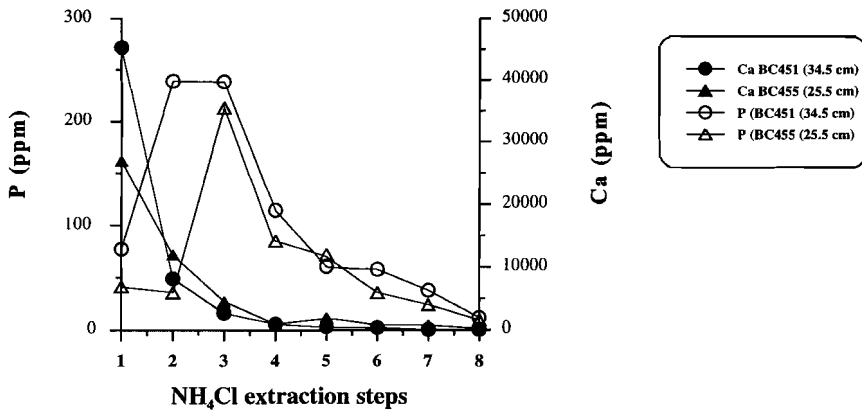


Figure 7. The P and Ca concentrations (ppm) in the solutions of the 8x NH₄Cl sequential extraction for two sediment samples (BC451, 34.5 cm depth; BC455, 25.5 cm depth).

organic matter degradation in BC451. The oxidized surface layer is too thin to induce effective iron cycling as a result of the low BWO concentrations and the high reactive organic matter contents. Early diagenetic iron cycling is relatively more important in BC455. However, reducing L_1 in the model to zero (i.e. no sorption of phosphate to iron oxides) and leaving all other parameters the same, results in a reduction of the CFA formation rate of only 11 %. Apparently, “iron pumping” is not driving phosphogenesis in the sediments located within the OMZ.

Holocene sediments of the Pakistan continental margin between 300 and 900 m water depth are frequently finely laminated, indicating lack of bioturbation (*Schulz et al., 1996; Von Rad et al., 1999*). In the sediments of BC451 and BC455, however, some benthic activity occurs as is demonstrated by the presence of benthic foraminifera (*Jannink et al., 1998*) and the absence of laminae. Extensive bioturbation of the upper part of the sediment enhances phosphate release to the water column, reduces the accumulation of dissolved phosphate, and thus inhibits phosphogenesis (*Filippelli and Delaney, 1994*). Model results, however, suggest that the occurrence of some bioturbation is essential to initiate CFA precipitation in these sediments. For example, limiting the zone of bioturbation (L_2) in BC451 from 2.8 cm to 2 mm would require a totally unrealistic 10-fold increase of the organic P input flux ($J_{ax=0}$; up to $54 \mu\text{mol cm}^{-2} \text{y}^{-1}$) to reproduce similar porewater and solid-phase P profiles. The same is true for a substantial decrease of the bioturbation rate constant (D_b). Downward mixing of reactive P is necessary to build up the subsurface phosphate concentrations. Without bioturbation, reactive P is primarily regenerated at the sediment surface and subsequently lost to the overlying bottom water. These results indicate that early diagenetic phosphogenesis rates may be seriously diminished under true anoxic bottom water conditions. This mechanism may reduce the phosphorus burial efficiency under oxygen depleted bottom water conditions, as has been observed by *Ingall and Jahnke (1994)*.

Summarising, model results indicate that phosphogenesis in sediments of the Pakistan

Margin located within the OMZ are controlled by high rates of phosphate release from organic matter degradation. Fish debris dissolution in the upper few centimeters of the sediment is likely to provide an substantial additional source of phosphate. The presence of some bioturbation is essential to initiate authigenic apatite formation in these sediments. Early diagenetic iron cycling plays only a minor role. The processes controlling phosphogenesis are probably analogous to those in other low-oxygen environments, for which similar CFA precipitation rates have been reported (Froelich *et al.*, 1988; Schuffert *et al.*, 1994).

Phosphorite formation in BC484

High CFA concentrations just below the sediment water interface as observed in BC484 have previously been documented for the continental margins of Peru (Burnett *et al.*, 1982; Froelich *et al.*, 1988), western Mexico, Baja California (Janhke *et al.*, 1983; Schuffert *et al.*, 1994, 1998), Namibia (Thomson *et al.*, 1984), eastern Australia (Heggie *et al.*, 1990), and western India (Rao and Lamboy, 1996). Many of these phosphorite deposits have been identified as lag deposits (Kolodny, 1981, Garrison and Kastner, 1990). Beside redeposition processes, winnowing has been suggested to play an important role in the formation of phosphorites (*e.g.* Glenn and Arthur, 1990; Glenn *et al.*, 1994). Since phosphorite particles have a higher specific gravity than the surrounding detrital particles, bottom currents could wash away the finer, lighter particles and thus concentrate P in the top of the sediment. Winnowing causes low sedimentation rates, which in turn may enhance the growth of phosphorite nodules by keeping them in the zone of active diagenesis. (Burnett *et al.*, 1983). On the other hand, the effects of winnowing may obstruct phosphogenesis, not only by reducing the flux of reactive P into the sediment by enhancing the degradation and removal of organic matter and fish debris at the sediment surface, but also by increasing the permeability and, therefore, inhibiting the build up of phosphate in the porewater (Van Cappellen and Berner, 1988; Filippelli and Delaney, 1994). To establish the origin of the phosphorite deposit in BC484, the processes of 1) winnowing and 2) redeposition have been examined.

1) Winnowing

The high phosphorus concentration in the top 20 cm of BC484 could be the result of winnowing, which is an important process affecting the continental slope sediments on the Oman Margin (Shimmield *et al.*, 1990; Pedersen *et al.*, 1992). Evidence for winnowing can be obtained from sedimentary C/N ratios, total carbonate concentrations, Ti/Al and Zr/Al ratios, and the grain size distribution. These parameters have been studied in TC484, a core that is longer than BC484 and, therefore, allows a better comparison between the phosphorite layer and the sediment beneath it. A comparison between BC484 and TC484 of the C_{org} and P_{tot} profiles revealed an offset of 10 cm. Probably, the top 10 cm of TC484 were lost during core recovery. It is noteworthy that the high P concentration is still present in TC484, despite the distance of 4 km to BC484. Obviously, the processes leading to phosphorite formation are not very localised. The C_{org}/N_{tot} ratio (wt%/wt%) in the upper centimetre of TC484 is 8.6, which falls in the range of 7-9 observed in the top sediments on the Oman Margin (Pedersen

Chapter 4

et al., 1992). These low C_{org}/N_{tot} ratios are common for many recent sediments that have not been subject to winnowing (e.g. *Calvert et al.*, 1995, *Van der Weijden et al.*, 1999). The C_{org}/N_{tot} ratio increases downcore to a constant value of 10, which reflects the normal pattern of preferential nitrogen release relative to carbon during organic matter degradation. This suggests that the organic matter in the top of the sediment has not been extensively degraded and thus has not been subjected to intense winnowing. Winnowed material often consists of coarse-grained skeletal carbonate (foraminiferal oozes). *O'Brien et al.* (1990) found a close correlation between bottom water current velocity and the $CaCO_3$ content of sediments on the East Australian continental margin. The $CaCO_3$ concentrations in the entire tripcore fall within the range of 25-50 wt%, observed for non-winnowed sediments on the Oman Margin (*Shimmield et al.*, 1990). The Ca concentration in the phosphorus-rich layer is in fact lower than deeper in the sediment, indicating that the top is not winnowed. Zr and Ti are enriched in heavy minerals, and will be concentrated in the coarse fraction of the sediment. High Zr/Al and Ti/Al sedimentary ratios on the Oman Margin have been associated with winnowed deposits (*Shimmield et al.*, 1990; *Pedersen et al.*, 1992). The rather constant values of these ratios in TC484 are another indication for the absence of active winnowing. Further evidence is provided by the mean grainsize of both the decarbonated fraction and the bulk sediment, which is also constant with depth. The high mean grainsize in this core is probably caused by the input of eolian material, since this site is in close proximity to the Arabian peninsula. We conclude that although located in an environment where physical concentration processes may occur, winnowing is not responsible for the high phosphorus concentrations in this sediment.

2) Redeposition

The continental slope of the Oman Margin is particularly steep (*Prell et al.*, 1990) and, therefore, redeposition processes are likely to occur. Seismic data taken during the retrieval of the sediment cores show that BC484 and TC484 were taken in a small depression, containing a thick cover of sediments. This depression is probably one of the small intrashelf basins previously observed on the Oman Margin (*Prell et al.*, 1990; *Shimmield et al.*, 1990), and could potentially have served as a trap for phosphorus-rich turbidites (*Kolodny and Garrison*, 1994). The calibrated ^{14}C ages for "clean" (i.e. un-coated) foraminifers indicate normal sedimentation for the last 13,000 years (Table 3). The "clean" foraminifers from the top sediment (0-2 cm depth) are dated at 373 years. Furthermore, the overall chemical composition of the sediment does not indicate any sharp, erosive boundaries or internal grading. The top 20 cm of the sediment is not homogenous in composition, as would be expected when it would have been deposited during one single redepositional event. The calibrated ^{14}C ages of the coated foraminifers and phosphatised pellets in the top 0-2 cm, conversely, are older than the "clean" foraminifers, suggesting a non-recent origin of these particles. This age difference is also observed deeper in the sediment. It is possible that during the early diagenetic precipitation of CFA part of the carbonate incorporated into the apatite is supplied by diffusion of "older" HCO_3^- from a deeper level in the sediment. This is in line with the increase of alkalinity with depth (Fig. 2). Phosphatisation of calcitic particles would thus lead to an increase in their ^{14}C ages, which would explain why the phosphatised nodules are older than the coated foraminifers. Age calculations, in which the

Table 7. Calculations for the downward flux of phosphate and fluoride (see Appendix).

boxcore	ϕ	z (cm)	-dP/dz $\mu\text{M cm}^{-1}$	-dF/dz $\mu\text{M cm}^{-1}$	J_p $\mu\text{mol cm}^{-2}\text{y}^{-1}$	J_F $\mu\text{mol cm}^{-2}\text{y}^{-1}$	$J_{P(F)}$ $\mu\text{mol cm}^{-2}\text{y}^{-1}$	J_p model $\mu\text{mol cm}^{-2}\text{y}^{-1}$
484	0.78	4.1	12.51	2.85	1.04	0.45	1.08	
484		1		7.1		1.08	2.6	
451	0.82		1.34	0.73	0.12	0.126	0.3	0.24
455	0.84		0.01	0.44	0.001	0.069	0.16	0.13

ϕ - average porosity.

z - depth of the of concentration gradient.

dP/dz - average linear negative porewater phosphate gradient.

dF/dz - average linear negative porewater fluoride gradient.

(For BC484 the phosphate/fluoride gradient was taken at a specific depth)

J_p - downward flux of phosphate (P removal rate by authigenic apatite formation).

J_F - downward flux of fluoride (F removal rate by authigenic apatite formation).

$J_{P(F)}$ - P removal rate by authigenic apatite formation, based on the downward flux of fluoride.

J_p model - the calculated authigenic P formation rate according to the diagenetic P model.

chemical composition of the samples is used to determine the individual age of the apatite and carbonate fraction, indicate, however, that this process can only partly explain the older ages: depending on the age of CFA coatings, the carbonate of the coated foraminifers must have been formed between 4 and 10 ky BP, and thus is not of a recent origin. A difference in calibrated ^{14}C ages for phosphatised particles and pure calcite at equal sediment depths was also reported for a modern phosphorite deposit on the Peru Margin (Burnett *et al.*, 1988), which was explained by the mixing of older pellets from a deeper level with recently formed pellets. This is not plausible for BC484, as no high P concentrations are present deeper in the sediment. The calibrated ^{14}C ages are therefore best explained by lateral transport of the phosphatised foraminifers to the location of NIOP station 484.

We propose that the phosphorite deposit in BC484 is the result of two successive phosphogenetic events. The first period of phosphogenesis probably took place on the continental shelf or upper slope of Oman. Assuming an average age of 6890 yrs for the CFA (the age of the CFA pellets), the calculated age of the carbonate for both coated foraminiferal samples from 2 cm depth is approximately 5700 yrs BP. This first period of phosphogenesis is possibly related with the intensification of the SW monsoon which took place between 10 and 5 ky and resulted in enhanced surface-water productivity offshore Oman (Naidu and Malmgren, 1996). Phosphorites consisting of phosphatised algal pellets, corals and pelletal limestones were formed on the western continental shelf and upper shelf of India during a relative short time period in the early Holocene (Rao and Lamboy, 1996). Formation of Holocene phosphorites on the continental shelf of Oman has not been reported, but

similarities in oceanic and climatic conditions between the two margins makes their occurrence plausible. After formation on the shelf, the phosphatised particles were transported downslope to be deposited in the small depression where BC484 was retrieved. The age difference between “clean” and “coated” foraminifers observed at both 2 and 24.5 cm depth implies that the downslope transport of phosphatised particles was a gradual process. The spherical and rounded pellets could be an indication for reworking (Glenn *et al.*, 1994), but their smooth surfaces could also be explained by an external development of microbes around the grains (Garrison and Kastner, 1990).

A second, present-day period of in-situ phosphogenesis is indicated by the porewater profiles of phosphate and fluoride. Assuming steady state, the downward fluoride (J_F) flux (Table 7) can be converted into a solid-phase authigenic P concentration, using the mass accumulation rate and a P/F ratio of 2.4. This results in a P concentration of 21.000 ppm. The downward flux of fluoride may thus account for the high solid-phase P content in the top of BC484. In-situ phosphogenesis, therefore, seems more important than the contribution of reworked phosphogenetic material. The calculated downward fluxes of phosphate and fluoride for BC484 (Table 7) are similar to estimates for modern phosphorite formation (Froelich *et al.*, 1988; Schuffert *et al.*, 1994). We conclude that the high phosphorus content is the result of both redeposition of phosphatised particles and high rates of in-situ phosphogenesis. The phosphorite in the top of BC484 can therefore be classified as a combination of an allochthonous and a pristine phosphate (Föllmi, 1996).

To the best of our knowledge, this is the first report of Holocene phosphorite formation on the Oman Margin. During ODP leg 117, old phosphorites were found predominantly on the upper continental slope (site 726 (330 m), located in the proximity of BC484), which were deposited during the Miocene till the Early Pleistocene (Rao and Lamboy, 1995). These phosphorite deposits consist of coprolites, faecal pellets, spherical and coated grains, micro-nodules, foraminifer infillings and fish bone fragments, which is similar to the phosphorite particle composition in BC484. A comparison with the Peru margin showed, however, that the number and thickness of Oman phosphorites is far less. Rao and Lamboy (1995) attributed this to 1) a less reactive nature of the organic matter, 2) high porewater alkalinity of the carbonate-rich sediments, 3) high sedimentation rates which inhibit hardground conditions, and 4) periods of a less pronounced OMZ.

The high present-day rates of phosphogenesis in BC484 can be attributed to three processes. First of all, the reworked coated foraminifers and phosphatised pellets probably provide reactive surface areas, which facilitate the precipitation of CFA. This explains why the “clean”, non-transported foraminifers have no CFA overgrowths. Secondly, the higher primary production on the Oman Margin in the Holocene (Naidu and Malmgren, 1996) has increased the flux of reactive P to the seafloor and, thus, has promoted higher rates of phosphogenesis. Part of the high concentration of fish debris in the top of BC484 may originate from transport from shelf sediments, supplying an additional source of reactive P. Thirdly, results from pistoncore 484, taken at the same location as TC484, show that sedimentation rates decreased sharply from the last glacial (ca. 30-50 cm/ky), into the Holocene (5.6 cm/ky) (Chapter 3). The Holocene drop in sedimentation rate could have contributed to the higher P content, because lower sediment accumulation rates will a) decrease the dilution of the precipitated CFA by other sediment components (Froelich *et*

al., 1988), b) increase the residence time of the sediment in the zone of active precipitation (at greater depth precipitation will be prohibited by a high alkalinity and lower porewater F concentrations), and c) concentrate the source of the phosphate (organic matter, fish debris) and, therefore, promote the build-up of phosphate in the porewater.

The fact that until now Holocene phosphorites have not been reported for the northern Arabian Sea may indicate that they are less common than in other upwelling areas. The narrow slope and shelf of the Oman Margin may limit phosphorite formation to a small area (ie. at the intersection with the OMZ). Furthermore, high rates of phosphogenesis may be restricted to the small intrashelf basins, where the sediment is protected from the effects of winnowing. On the Peru margin phosphorites were found to be irregularly distributed over the seafloor (Froelich *et al.*, 1988; Baker and Burnett, 1988). As a consequence, recent phosphorite formation on the Oman Margin may have remained unobserved thusfar. More detailed sampling is necessary to determine the extent of Holocene phosphorite formation on the Oman Margin.

Conclusions

Pore water and solid-phase P speciation results indicate that phosphogenesis is occurring in the surface sediments located within the OMZ of the Arabian Sea. The precipitation of a precursor precedes CFA formation in the sediments on the Karachi Margin. The highest rate of CFA formation was observed in a boxcore taken on the Oman Margin where it contributes to the formation of a Holocene phosphorite deposit. This observation contrasts with previous reports of only old phosphorites in this area. Application of a diagenetic P model revealed that phosphogenesis on the Pakistan Margin is induced by high rate of organic matter degradation and, probably, fish debris dissolution. Early diagenetic iron cycling does not significantly affect sedimentary P cycling in these environments. The occurrence of some bioturbation is essential to initiate phosphogenesis in these sediments. This implies that dysaerobic rather than fully anoxic bottom waters may be more effective in promoting early diagenetic phosphogenesis.

Phosphorites are presently forming on the Oman Margin as the result of a) deposition of older, reworked material from the shelf, which has undergone an earlier phase of phosphogenesis, b) a high Holocene input of reactive P (fish debris and degradable organic matter), c) a relatively low sedimentation rate, and d) absence of winnowing at this location, which would increase the permeability and enhance the degradation of organic material and the dissolution of fish debris.

Acknowledgements - The chief scientists on the NIOP cruises during the 1992-1993 Netherlands Indian Ocean Programme were W.J.M. van der Linden and C.H. van der Weijden. H. de Waard, A.F.M. de Jong and G. Nobbe are thanked for their contribution to the laboratory analyses, and G.J. van het Veld and G. Ittman for processing the

Chapter 4

micropaleontological samples. H.F. Passier is acknowledged for providing the porewater data of BC484. Critical reviews by C.H. van der Weijden and G.J. Reichart significantly improved this manuscript. This research was funded by the Netherlands Organization for Scientific Research (NWO).

Appendix

Porewater profiles have been used to estimate the downward fluxes of fluoride and phosphate (CFA precipitation rates), assuming steady state and constant bulk sediment compositions. Diffusive porewater fluxes (J) have been calculated with (*Berner, 1980*):

$$J = -\phi D_s (dC/dz) \quad (1)$$

in which ϕ is the mean porosity, D_s the whole sediment diffusion coefficient for phosphate and fluoride respectively, and dC/dz the linear concentration gradient at depth z . Whole sediment diffusion coefficients (D_s) ($\text{cm}^2 \text{s}^{-1}$) can be expressed by

$$D_s = D^*/\phi F \quad (2)$$

where D^* is the diffusion coefficient in seawater and F the formation factor. Diffusion coefficients ($7.34 \times 10^{-6} \text{ cm}^2 \text{ s}^{-1}$ for HPO_4^{2-} and $14.6 \times 10^{-6} \text{ cm}^2 \text{ s}^{-1}$ for F at 25°C) were corrected for the in-situ bottom water temperature with the Stokes-Einstein relation (*Li and Gregory, 1974*). The Formation factors were estimated with the equation (*Manheim and Waterman, 1974*):

$$\log F = 0.110 - 1.80 \log \phi \quad (3)$$

The downward fluxes were calculated from the average fluoride and phosphate gradients (for BC484 the phosphate/fluoride gradient was taken at a specific depth). The fluoride flux (J_p) was multiplied with the molar P/F ratio of authigenic CFA (2.4; as measured in the solvent of step 4 of the sequential extraction in BC484) to obtain ($J_{P(F)}$), which allows a direct comparison with the downward phosphate flux.

5

A novel chemical method to quantify fish debris in marine sediments: implications for interpreting phosphorus burial records

S.J. Schenau and G.J. De Lange

Abstract - Burial of fish bones, which consist primarily of hydroxyapatite, has been recognized as a mechanism to remove reactive phosphorus from the oceans. In this study, a new method is presented, which differentiates P associated with biogenous apatite (P_{fish}) from other P fractions. The method, consisting of a sequential chemical extraction with 2 M NH_4Cl , has been successfully tested on standard materials. It enables us, for the first time, to quantify fish debris in sediment records and to assess their importance for the marine phosphorus cycle.

The NH_4Cl extraction has been applied to sediment samples from the Arabian Sea. Preservation of fish debris is significantly higher in sediments located above 1200 m water depth than it is for deeper sediments. The distribution of P_{fish} contents in surface sediments is predominantly governed by the extent of fish debris regeneration, which is related to differences in water depth and sedimentation rates. In addition, a good correlation between high sedimentary P_{fish} contents and low oxygen bottom water concentrations suggests that the presence of the intense oxygen minimum zone may account for the enhanced preservation of fish debris in continental slope sediments. The burial history of P_{fish} has been investigated in two Late Quaternary sediment cores, one from the Pakistan Margin, the other from the deep Arabian Basin. Phosphorus associated with fish debris constitutes approximately 30% of total P buried in these sediments. Downcore variations in total solid-phase phosphorus concentrations are primarily related to changes in the contribution of the P_{fish} fraction. On the continental slope, changes in P_{fish} contents correspond with similar changes in paleoproductivity inferred from geochemical and paleontological proxies. In sediment records from the deep basin, however, phosphorus is less suitable as a paleoproductivity indicator due to the high regeneration rate of fish debris.

Introduction

Hard parts of marine fish (scales, bones, teeth) consist for 60 to 70 % of calcium phosphate crystals, which are embedded in an organic matrix largely composed of the fibrous protein collagen (*Posner et al., 1984; Newsly, 1989; Nemliher et al., 1997*). In addition, many marine invertebrates, such as cestods, inarticulate brachiopods, bivalves and gastropods, incorporate phosphate in their hard parts (*Lowenstam, 1972*). This inorganic material is best represented as hydroxyapatite ($\text{Ca}_{10}(\text{PO}_4)_6(\text{OH})_2$; *Newsly, 1989*). Large reactive surface areas, as well as crystal imperfections, make biogenic hydroxyapatite more soluble than well crystallized stoichiometric hydroxyapatite, which in turn is more soluble than fluorapatite (*Posner et al., 1984*). Seawater is undersaturated with respect to biogenous apatite (*Arrhenius, 1963; Atlas and Pytkowicz, 1977*). As a consequence, fish debris are subject to dissolution in the water column and in the upper part of the sediment. Fish bones may also be converted into the more stable carbonate fluorapatite (CFA; *Atlas and Pytkowicz, 1977; Newsly, 1989*), through substitution of hydroxyl ions by fluoride. Part of the fish debris will ultimately be buried in the

sediments. Fossil fish fragments have been found in geological deposits dating from the Early Paleozoic till the Present (e.g. Schmitz et al., 1991; Trappe, 1998).

Fish debris is found in high concentrations in sediments underlying areas of coastal upwelling (Diester-Haas, 1978, DeVries and Percy, 1982). In these environments, dissolution of fish debris in the sediment may play an important role in regulating benthic porewater phosphate fluxes and authigenic apatite formation (Suess, 1981; Van Cappellen and Berner, 1988; **Chapter 6**). Furthermore, burial of biogenic apatites has been recognized as a potentially important mechanism for reactive P removal in these areas (Suess, 1981). On a global scale, however, burial of biogenic apatites is generally considered to be an insignificant sink of reactive phosphorus compared to the other sedimentary P fractions (Froelich et al., 1982; Berner et al., 1993; Ruttenberg, 1993). Unfortunately, studies on fish debris in marine sediments are relatively scarce. Up to now, labourious handpicking was the only method to semi-quantify their presence (Suess, 1981; DeVries and Percy, 1982). Chemical extraction methods for phosphorus were not able to differentiate between biogenic and authigenic apatites (e.g. Ruttenberg, 1992).

In this study, we present a chemical extraction method, which, for the first time, enables the separation of P associated with biogenic apatite (fish debris) from other sedimentary P fractions. This extraction method has been applied to sediment samples from Arabian Sea box and piston cores. Here, we will concentrate on the application and results of the extraction of biogenic apatite, while detailed results of the other extraction steps are presented elsewhere (**Chapter 6 and 7**). The distribution and burial potential of fish debris in sediments will be discussed in relation to fish production and regeneration processes.

Material and Methods

Sample locations

During the Netherlands Indian Ocean program (NIOP) in 1992, sediment cores were taken in the northern Arabian Sea. For this study, we selected 11 box cores located on the Pakistan continental slope (stations 451, 452, 453, 454, 455), the Murray ridge (stations 463, 464), and the Arabian Basin (stations 458, 460, 466, and 487; Fig. 1, Table 1). Bottom water oxygen (BWO) concentrations were derived from oxygen measurements at near-by CTD-stations (Table 1). AMS ^{14}C dating of handpicked foraminifers from the base of the boxcores (Van der Weijden et al., 1999) was used to calculate the sedimentation rates (Table 1).

The sample locations of piston cores PC455 and PC487 correspond with their respective boxcores positions (Fig. 1). Piston core 487 was recovered in the Arabian Basin from a water depth of 3574 m, and is located below the present-day oxygen minimum zone (OMZ). Piston core 455 was taken from the Pakistan continental Margin at a water depth of 1002 m, which is presently located in a low-oxygen environment. The

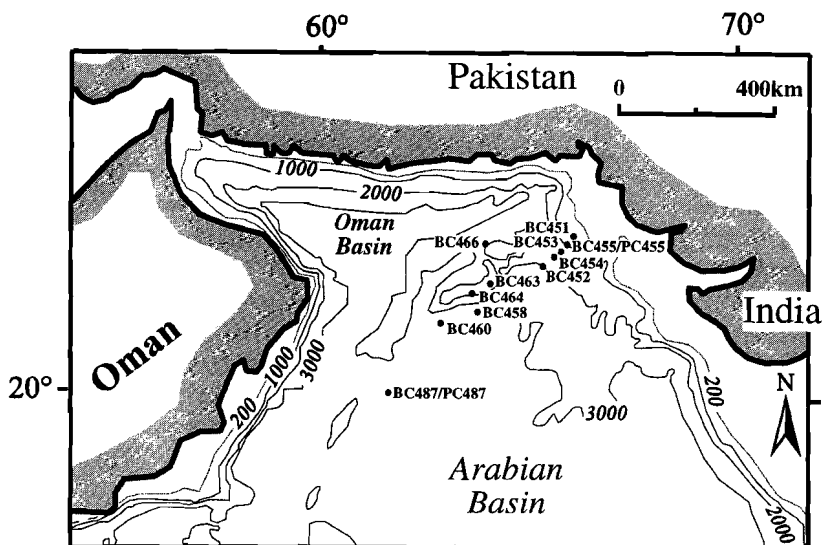


Figure 1. Sample locations in the northern Arabian Sea of the boxcores and pistoncores used in this study.

sediments of both cores mainly consist of homogeneous, light-greenish hemipelagic muds interbedded with darker organic-rich intervals. Most of the organic-rich intervals in PC455 are finely laminated.

Solid-phase analysis

The dry bulk density of the sediment samples was calculated by measuring weight loss of fixed volume samples after freeze-drying. Subsequently, samples were powdered in an agate mortar, and after homogenization, subsamples were taken for geochemical analyses. Bulk concentrations of P were determined by total digestion of 250 mg sample at 90°C in a 5 ml 6.5 : 2.5 : 1 mixture of HClO₄ (60%), HNO₃ (65%) and H₂O, and 5 ml HF (40%). After evaporation of the solutions at 190°C on a sand bath, the dry residue was dissolved in 25 ml 1 M HCl. The resulting solutions were analysed with a Perkin Elmer Optima 3000 Inductively Coupled Plasma Atomic Emission Spectrometer (ICP-AES). All results were monitored using international (SO1, SO3) and in-house standards. Relative errors for duplicate measurements were lower than 3 %. After removal of all carbonates with 1 M HCl, organic carbon contents (C_{org}) were measured with a NA 1500 NCS analyzer. Relative errors were less than 1 %.

Table 1. Location, water depth, present-day oxygen concentrations of the bottom water, mass accumulation rates, C_{org} and P_{fish} concentrations in the top 2 cm of the boxcores used in this study.

	latitude (N)	longitude (E)	water depth (m)	O ₂ bottom (μ M)	MAR ($g\ cm^{-2}\ ky^{-1}$)	C _{org} (wt%)	P _{fish} top 2 cm (ppm)
BC451	23°41'.4	66°02'.9	495	< 2	12.5	4.09	382
BC452	22°56'.4	65°28'.1	2001	87.1	3.8	1.07	158
BC453	23°14'.0	65°44'.0	1555	39.3	5.6	1.23	157
BC454	23°26'.9	65°51'.2	1254	12.5	6.0	3.36	189
BC455	23°33'.3	65°57'.2	998	< 2	6.8	4.28	320
BC458	21°59'.7	63°48'.8	3000	123.7	4.0	0.76	145
BC460	21°43'.2	62°55'.2	3262	125.3	-	0.86	205
BC463	22°33'.6	64°03'.3	970	< 2	5.2	5.67	310
BC464	22°15'.0	63°34'.7	1511	34.8	4.3	1.26	179
BC466	23°36'.1	63°48'.5	1960	75.4	5.9	0.89	143
BC487	19°54'.8	61°43'.3	3566	151.0	1.9	0.8	194

Sequential extraction analysis

The solid-phase speciation of phosphorus was examined using a 5-step sequential extraction scheme (after *Ruttenberg, 1992*). Approximately 125 mg of dried and powdered sediment was washed sequentially with several different solvents (Table 2). The 2 M NH₄Cl extraction (step 1), which has previously been applied to extract carbonate-associated P (*e.g. De Lange 1992b*), was included here to determine P associated with biogenic apatite (results reported in this study). After extraction step two, three and four, the sediment was rinsed successively with 2 M NH₄Cl (pH=7) and demineralized water to prevent readsorption of phosphate. All extracted solutions were measured by ICP-AES. The specificity and efficiency of each extraction step was tested by the extraction of standards, namely fish debris (vertebrae from a freshly killed whiting), ferromanganese nodule (iron-bound phosphate; collected from the Madeira Abyssal Plain), phosphorite nodule (authigenic apatite; collected from the Peru continental Margin), and detrital apatite (in-house mineral collection). Relative errors of P for duplicate measurements for each extraction step are given in Table 2. For sediment samples, recovery for P with respect to total P varied between 80 and 90%.

Fish debris and foraminiferal analyses

Sediments were sieved into three fractions (65-150 μ m, 150-595 μ m, >595 μ m). For all boxcore samples, fish debris was quantified in the 150-595 μ m fraction by counting the number of fish fragments in splits (using an Otto microsplitter). The chemical composition of the 65-150 μ m fraction for pistoncore samples was measured by dissolving

Chapter 5

Table 2. Details of the sequential extraction scheme, the extracted P fractions, and relative errors for duplicate measurements.

Step	Extractant	P phase extracted	Relative errors (%)	Reference
1	<ul style="list-style-type: none"> • 8x 25 ml 2 M NH₄Cl (brought to pH 7 with ammonia, 4 h) 	<ul style="list-style-type: none"> • exchangeable or loosely sorbed P • carbonate associated P • biogenic apatite 	< 4	This study
2	<ul style="list-style-type: none"> • 1x 25 ml 0.15 M Na-citrate, 0.5 M NaHCO₃ (pH 7.6, 16 h), and 1.125 g Na-dithionite • 1x 25 ml 2 M NH₄Cl (pH 7) • 1x 25 ml demin. water 	<ul style="list-style-type: none"> • easily reducible or reactive iron-bound P 	< 10	after <i>Ruttenberg, 1992</i>
3	<ul style="list-style-type: none"> • 1x 25 ml 1 M Na-acetate buffered at pH 4 with acetic acid (16 h) • 1x 25 ml 2 M NH₄Cl (pH 7) • 1x 25 ml demin. water 	<ul style="list-style-type: none"> • authigenic apatite 	< 10	after <i>Ruttenberg, 1992</i>
4	<ul style="list-style-type: none"> • 25ml 1 M HCl (16 h) • 1x 25 ml demin. water 	<ul style="list-style-type: none"> • detrital apatite 	< 7	<i>Ruttenberg, 1992</i>
5	<ul style="list-style-type: none"> • 5 ml of a 6.5 : 2.5 : 1 mixture of HClO₄ (60%), HNO₃ (65%) and H₂O, and 5 ml HF (40%) at 90°C (total digestion) 	<ul style="list-style-type: none"> • organic P • P adsorbed to clay minerals 	< 10	<i>Lord, 1982</i>

split samples of this fraction in 1 M HCl and analysing them subsequently with ICP-AES. The chronology of PC487 and PC455 is primarily based on $\delta^{18}\text{O}$ records (*Reichart et al., 1998; Chapter 2*). Mass accumulation rates (MARs) were calculated by multiplying the linear sedimentation rates with the dry bulk densities.

Results and discussion

The NH₄Cl extraction: differentiation between biogenic and authigenic apatite

Extraction results on fresh fish debris indicate that hard parts of fish are highly soluble in 2 M NH₄Cl: approximately 80 % of the total amount of P present in fish debris dissolves in this step (8x) (Fig. 2). The remaining P fraction of fish debris, which is extracted during steps 2 and 3, may result from incomplete dissolution in step 1 caused by saturation of the extraction fluid, slight differences in powdered particle sizes, or P associated with less easily dissolvable fractions in fish bones. In contrast, only small percentages of authigenic apatite, detrital apatite and iron-bound P are extracted in NH₄Cl (Fig. 2). Consequently, the sedimentary P fraction extractable in NH₄Cl (from hereon denoted as P_{fish}) is primarily associated with biogenic apatite. To further substantiate this observation, a separate sequential extraction was done on sediment and standard samples, analysing each of eight NH₄Cl steps separately (Fig. 3). For the two sediment samples (BC455, 0-2 cm and PC487, 329 cm), the P concentration starts to increase once the Ca concentration in solution has dropped (Fig. 3a), indicating that the P fraction associated with P_{fish} begins to dissolve once all Ca-carbonates have been extracted.

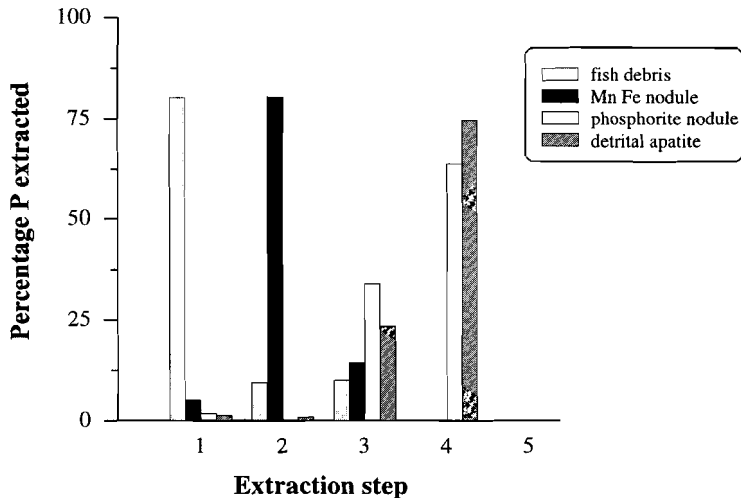


Figure 2. Percentage of P extracted for standard materials using the extraction schedule of Table 2; each step is given relative to the total extracted P for that standard. Standards used are fresh fish debris, a Mn-Fe nodule, a phosphorite nodule, and detrital apatite (in-house collection). Sample weights were ca. 50 mg. The relative low P recovery for the phosphorite nodule in step 3 can be attributed to saturation of the solvent due to a relatively high solid/liquid ratio.

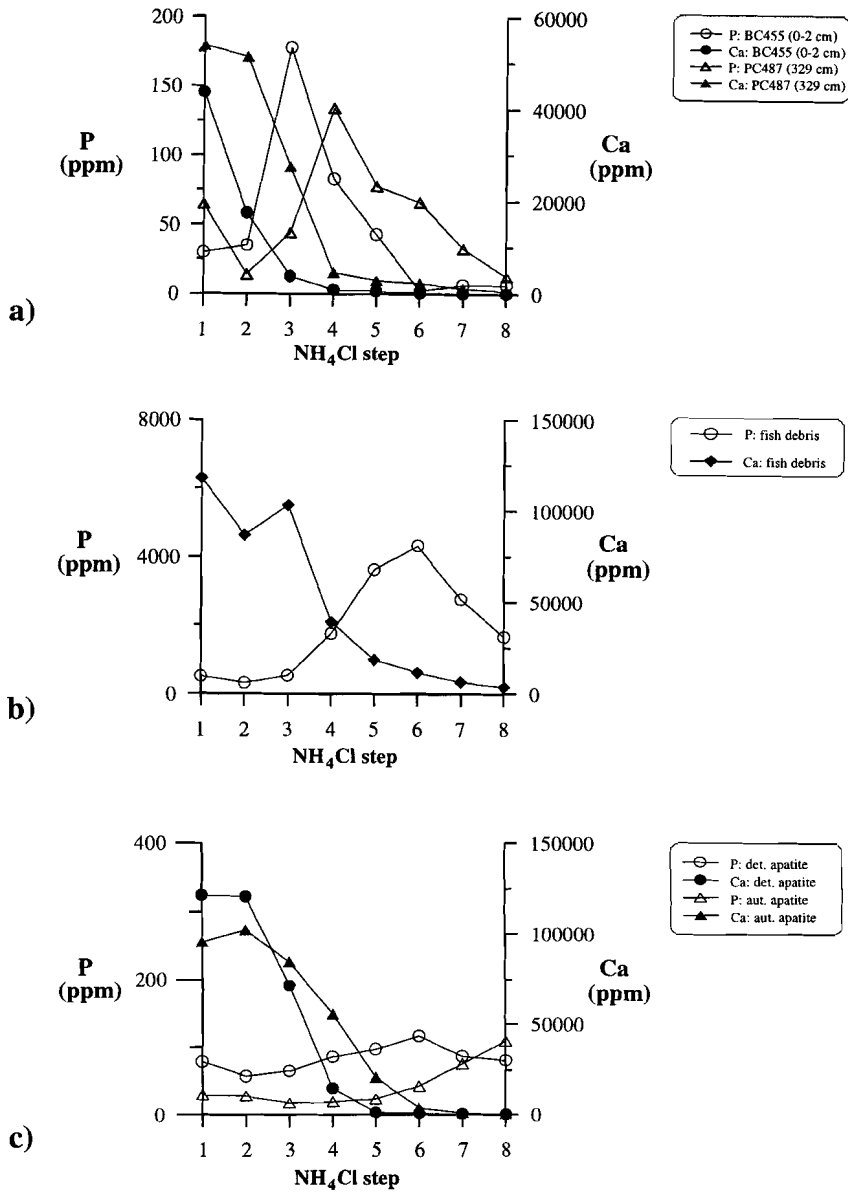


Figure 3. Extracted P and Ca concentrations (ppm) in each step of a 8-fold 2 M NH₄Cl sequential extraction for a) two sediment samples (BC455, 0-2 cm depth; PC487, 329 cm depth; ca. 125 mg), b) a sample consisting of calcite (ca. 50 mg) and fish debris (ca. 10 mg), and c) samples consisting of calcite (ca. 50 mg) and respectively detrital (ca. 10 mg) and authigenic apatite (ca. 10 mg).

Consequently, the P_{fish} fraction must be associated with a Ca-phosphate mineral phase. Furthermore, these results indicate that most of the extracted P is not directly related to Ca-carbonate associated P. The same release pattern of Ca and P can be discerned in the extraction of a sample consisting of pure calcite and a small addition of fish debris (Fig. 3b), indicating that the solubility of biogenic apatite is dependent on the Ca concentration in the solvent. Conversely, samples consisting of pure calcite and a small addition of respectively detrital apatite and authigenic apatite do not significantly respond to the drop in Ca concentration (Fig. 3c): the extracted P concentration remains low compared to the sample with fish debris. The similarity in the leaching patterns between sediment samples (Fig. 3a) and the calcite/fish debris sample (Fig. 3b) confirms that the P_{fish} fraction of sediment samples can be largely attributed to biogenic apatite.

Additional evidence for the association of the P_{fish} fraction with biogenic apatite is obtained by comparing the extraction results with fish debris counts in the 150-595 μm fraction. Boxcore samples with high numbers of fish debris also have high P_{fish} concentrations (Fig. 4a). However, the correlation is not straightforward, as samples with low fish debris contents still contain substantial concentrations of P_{fish} . The latter samples all originate from sample locations in the deep Arabian basin. The larger water depth and lower sediment accumulation rates may have enhanced the fragmentation of fish particles. As a consequence, fish debris may have become under-represented in the 150-595 μm fraction. This is consistent with microscopical observations of the 65-150 μm fraction, where small fish debris particles seem more abundant.

Microscopical observations in the sieve fractions (150-595 μm , 65-150 μm) of piston core samples also indicate that samples with the highest P_{fish} concentrations have high contents of fish debris. Besides fish debris, these sieve fractions predominantly contain foraminifers. All foraminifers have a clean appearance indicating that they have no coatings of iron oxides or authigenic apatite. Chemical analysis of samples from which fish debris was removed by handpicking, revealed that the P concentration of foraminiferal debris is indeed very low (< 20 ppm), which is consistent with the results of *Sherwood (1987)*. Consequently, the P concentration of these fractions must be directly related to the fish debris content. The correlation between the P_{fish} concentration (whole sample) and the total P content in the 65-150 μm fraction is good for both PC487 ($r^2 = 0.81$) and PC455 ($r^2 = 0.97$) (Fig. 4b). All these observations confirm the association of biogenic apatite with the P_{fish} fraction.

Other P fractions extracted in NH_4Cl are easily adsorbed P and porewater phosphate. Numerous studies (*De Lange, 1992b; Ruttenberg and Berner, 1993; Filippelli and Delaney, 1996; Eijsink et al., 1997*) have shown that the concentration of these fractions is usually low in marine sediments (< 30 ppm), particularly compared to the total P concentration. During early diagenetic phosphogenesis, precipitation of CFA is often preceded by the formation of a F-poor precursor (*Van Cappellen and Berner, 1991; Krajewski et al., 1994*). This precursor, which is precipitating in recent Arabian Sea sediments located within the OMZ, is also soluble in 2 M NH_4Cl (**Chapter 4**). Therefore, the NH_4Cl extraction cannot be used to differentiate between biogenic apatites and

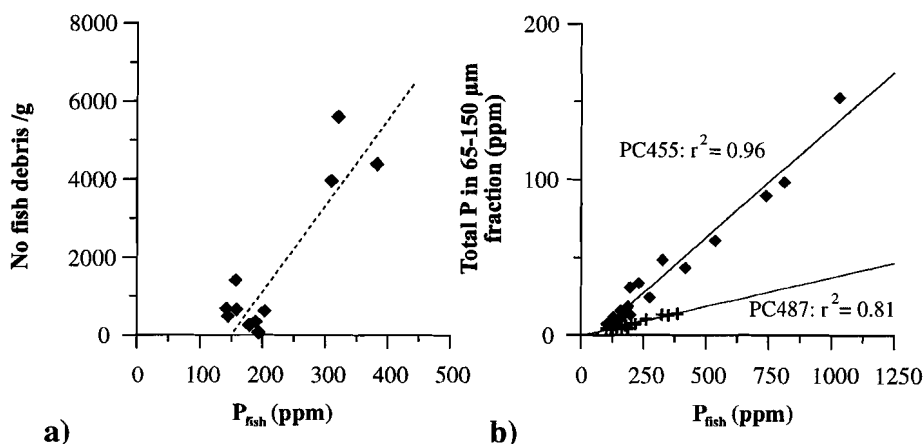


Figure 4. A plot of a) P_{fish} concentrations versus number of fish debris in surface sediment samples (150-595 μm sieve fraction; see Table 1), and b) P_{fish} concentrations in total samples versus total P contents of the 65-150 μm sieve fraction of the same samples from PC455 (\blacklozenge) and PC487 (+). The difference in slope for samples from these cores is related to a different fish debris distribution over the sieve fractions.

precursor apatite. In the sediment samples of this study, however, the contribution of such a precursor is insignificant (see below).

In conclusion, the NH_4Cl extraction is a good method to differentiate between CFA and more soluble biogenic apatites. Distinction between these two apatite phases has three advantages: 1) it enables the evaluation of the importance of fish debris burial in the marine phosphorus cycle, 2) it allows reconstruction of the deposition history of fish debris in sediment records, and 3) this method improves the determination of CFA burial rates. The results of this study indicate that the Ca-carbonate content of a sample is of ultimate importance in determining the step in which biogenic apatite is extracted. In traditional extraction schemes (e.g. SEDEX method; *Ruttenberg et al., 1992*), biogenic apatite may be extracted prematurely for sediment samples with low carbonate contents (for example during the Na-dithionite extraction), and may accordingly be attributed to the incorrect fraction.

Distribution of fish debris in recent Arabian Sea sediments

The NH_4Cl extraction has been applied to samples taken from surface sediments (upper 0–2 cm) of Arabian Sea boxcores. Because no (or very little) phosphogenesis takes place in the upper centimeter of these boxcores (**Chapter 4**), no interference of a possible precursor to CFA formation is expected for these samples. The P_{fish} concentrations are highest in sediments located at relatively shallow water depths (< 1200 m; Table 1). Because of dilution effects, the burial of fish debris is better represented by the

accumulation rates of P_{fish} , calculated as the product of the P_{fish} concentration and the mass accumulation rate. P_{fish} accumulation rates decrease rapidly with increasing water depth (Fig. 5a). In sediments deeper than 1200 m, P_{fish} accumulation rates decrease more gradually with depth. Furthermore, high P_{fish} concentrations are associated with organic-rich sediments (Fig. 5b).

In the next sections we will discuss the two factors governing the accumulation of P_{fish} namely, 1) fish production, and 2) regeneration of fish debris in water column and sediment. The sub-recent (pre-fishery) fish production in the Arabian Sea is estimated in order to calculate the preservation potential of biogenic apatite in the underlying sediments.

1) Fish production in the Arabian Sea

The Arabian Sea is one of the most productive areas in the world. Strong southwestern monsoonal winds cause coastal and open ocean upwelling off Somalia and Oman during the summer (e.g. Wyrski, 1973; Slater and Kroopnick, 1982). Upwelling nutrient-rich water masses are transported throughout the Arabian Sea, causing a high seasonal productivity (e.g. Qasim, 1982). High downward fluxes of organic matter, in combination with restricted deep water ventilation, result in an extensive Oxygen Minimum Zone (OMZ) between 150 and 1250 m depth (e.g. Slater and Kroopnick, 1984). The high biomass of phyto- and zooplankton induces high rates of fish production in the Arabian Sea (Peterson, 1991). The richest fishing areas are concentrated in the coastal waters of the Oman and Indian/Pakistan margins (Cushing et al., 1973; FAO, 1981; Venema, 1984). Good estimates for total demersal and pelagic fish resources in this region, however, are still lacking (FAO, 1997).

The size of fish populations in the oceans is dependent on several factors, such as primary productivity, water temperature, water depth, and, since recent times, the impact of increased fisheries (Sharp, 1988). Food availability, however, is generally considered as the most important factor determining fish production in the oceans (e.g. Bailey and Robinson, 1986). Numerous efforts have been made to estimate fish production based on trophic dynamic models (e.g. Ryther, 1969; Iverson, 1990). Uncertainty about the transfer efficiencies and food web structure, however, make good quantitative predictions for total fish production difficult (Haedrich and Merritt, 1992). Estimating fish production rates from primary productivity data in the Arabian Sea is even more complicated. First of all, the intensity of monsoon induced upwelling changes from year to year, and, as a consequence, the annual primary productivity rate in this area is variable. Abundances of oil sardine offshore southwestern India, for example, are closely tied to the onset time and strength of coastal upwelling (Longhurst and Wooster, 1990), and have varied significantly over the last century. Secondly, the vertical distribution of fish populations in the water column is influenced by the presence of low-oxygenated waters at mid-water depth (Banse, 1968; Röpke et al., 1993). Thirdly, dispersion processes may effect the distribution of fish populations over the surface waters, resulting in a distortion of the local food web (Sharp, 1988).

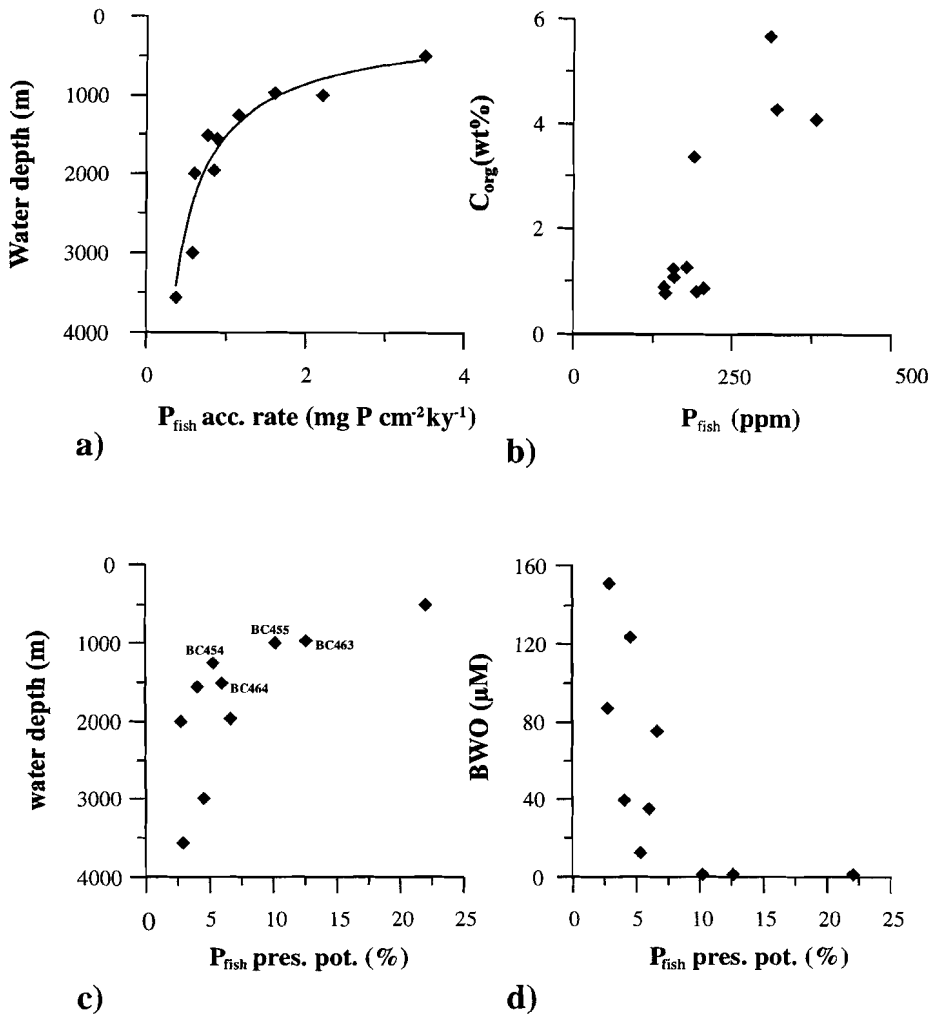


Figure 5. A plot of a) P_{fish} accumulation rates ($\text{mg P cm}^{-2}\text{ky}^{-1}$) in sediment surface samples (see Table 1) versus water depth (m), b) P_{fish} concentrations versus organic carbon concentrations (wt%), and a plot of P_{fish} preservation potential (%) in sediment surface samples versus respectively c) water depth (m), and d) bottom water oxygen concentrations (μM). The solid line in a) represents a best fit [P_{fish} accumulation rate] = $3745.9 \times [\text{water depth}]^{-1.124}$; ($r^2 = 0.93$).

Recognizing all these uncertainties, fish production (FP) ($\text{g m}^{-2} \text{y}^{-1}$, wet weight) in the Arabian Sea was estimated, by means of the trophic-dynamic model developed by *Iverson (1990)*, using the equation:

$$\text{FP} = (0.083 \times \text{ACP} - 3.08) \times E^n \times c_1 \times c_2 \quad (1)$$

where ACP is the phytoplankton annual carbon production ($\text{gC m}^{-2} \text{y}^{-1}$), E the transfer efficiency of nitrogen (0.28), n the number of trophic levels (2.5), c_1 the fish biomass C:N ratio (3.6:1), and c_2 the product of the ratio of fish dry weight to C (2.4) and the ratio of fish wet to dry weight (3.3), which equals 7.9. This model is based on the assumption that fish production is controlled by the amount of new N annually incorporated into phytoplankton biomass, which is subsequently transferred into the food chain. An average number of 2.5 for the trophic levels (n) has been found to apply to many marine environments (*Iverson, 1990*).

Estimates for present-day annual primary productivity in the northwestern Arabian Sea vary between 100 and 350 $\text{gC m}^{-2} \text{y}^{-1}$ (e.g. *Qasim, 1982; Olsen et al., 1993; Jochem et al., 1993*). Mean annual productivity for the coastal region of the Pakistan Margin is likely to be somewhat higher than in the central basin due to a deepening of the mixed layer during the winter, which injects nutrients into the surface waters (*Wyrki, 1973*). For this study, we have used the results of a photosynthesis-irradiance model (*Brock et al., 1994*), and have assumed a mean primary productivity rate of 180 $\text{gC m}^{-2} \text{y}^{-1}$ for the central Arabian Basin and 280 $\text{gC m}^{-2} \text{y}^{-1}$ for the Pakistan Margin. Applying these values to the model of *Iverson (1990)*, the calculated fish production for the Pakistan Margin and the central Arabian Sea amount to 23.8 $\text{g m}^{-2} \text{y}^{-1}$ and 14.0 $\text{g m}^{-2} \text{y}^{-1}$ respectively. These fish production rates are high compared to other oceanic and coastal regions (*Iverson, 1990; Haedrich and Merrett, 1992*), which can probably be attributed to the eutrophic nature of the Arabian Sea.

2) regeneration of fish debris in the water column and sediment

The amount of fish debris that eventually is buried is affected by dissolution occurring in the water column and in the sediment. Processes governing the dissolution of fish debris in the marine environment are not well-known. In the upwelling area offshore Peru approximately 10 wt% of P associated with fish bones produced in the surface waters is estimated to be preserved upon burial (*Suess 1981; Froelich et al., 1982*). Water depth, which determines the transit time through the water column, may be an important factor controlling preservation of fish debris. *DeVries and Pearcy (1982)* observed the highest concentrations of fish debris in sediments deposited at water depths < 600 m, whereas less well-preserved material was found in deeper water. On the other hand, fish particles are relatively large and have a high density compared to seawater, which will make them sink relatively fast to the seafloor, thereby limiting dissolution in the water column.

Dissolution of fish debris will continue after deposition in the sediment (e.g. *Nriagu, 1983*). High subsurface porewater phosphate concentrations observed in continental slope sediments often cannot be explained exclusively by phosphate release from organic matter degradation or iron oxide reduction (*Froelich et al., 1988; Van*

Cappellen and Berner, 1988; Schuffert et al., 1994; Chapter 6). Some of these high porewater phosphate concentrations, therefore, have been attributed to the dissolution of fish debris (*Suess, 1981; Van Cappellen and Berner, 1988; Chapter 6*). A significant fraction of P associated with fish debris may thus be regenerated during early diagenesis. Decomposition of fish bone apatite in sediments is dependent on many factors, including porewater pH, phosphate and calcium concentrations, destruction by micro-organisms, winnowing, and bioturbation (*Atlas and Pytkowicz, 1977; Newesly, 1989*). Furthermore, higher mass accumulation rates promote incorporation into the sediment before complete dissolution occurs (*Froelich et al., 1982*). Potentially, redox conditions of bottom water and pore water may effect the preservation of biogenic apatite. Organic matter remineralization under oxygenated conditions produces acidity, which induces the dissolution of carbonates and, possibly, biogenic apatite in deep-sea sediments (*e.g. Canfield, 1991; Thomson et al., 1998*). During suboxic (denitrification and Mn- and Fe-oxide reduction) and anoxic (sulphate reduction) diagenesis, however, no acidity is produced (provided that H₂S is consumed by pyrite formation; *Canfield, 1991*), potentially leading to less dissolution of fish debris. Furthermore, phosphate concentrations of the interstitial water of anoxic sediments are usually high due to high rates of organic matter degradation. This will also decrease the dissolution rate of fish debris. Consequently, sediments located within a suboxic environment may experience enhanced preservation of biogenic apatite.

To assess the factors controlling the burial of fish debris in the Arabian Sea, preservation potentials (pres%) of P_{fish} for the boxcore samples were calculated using the following equation:

$$pres\% = 100 \times \frac{P_{fish\ acc.}}{FP \times [P]_{fish} / c_3} \quad (2)$$

where P_{fish acc.} is the P_{fish} accumulation (gP m⁻² y⁻¹), FP the fish production rate (g m⁻² y⁻¹; as calculated with equation 1), [P]_{fish} the phosphorus dry weight fraction of marine fishes (0.03, *Anonymous, 1982*), and c₃ the ratio of fish wet weight % to fish dry weight % (3.3; *Iverson, 1990*). It should be noted that the preservation potential calculated with this equation incorporates only regeneration of P_{fish} during its transit through the water column and in the upper 2 cm of the sediment, and, therefore, is not equal to the total burial efficiency. The preservation potential, therefore, must be interpreted as a maximum value for the P_{fish} burial efficiency, because further dissolution may occur deeper in the sediment. The P_{fish} preservation potentials vary between 3 and 6 % for the boxcores located deeper than 1200 m (Fig. 5c). The three boxcores located at shallower water depths (BC451, BC455 and BC463) all have a significantly higher P_{fish} preservation potential (10-22%). The absolute values must be considered with some caution due to relatively large uncertainties for the calculated fish production rates and the value used for the dry weight P fraction of marine fishes. However, these results do demonstrate a distinct contrast in P_{fish} regeneration for different areas of the Arabian Sea.

Differences in P_{fish} accumulation rates are much larger than variations in fish production, indicating that the distribution of fish debris in the surface sediments of the Arabian Sea is predominantly governed by regeneration processes. This is also illustrated by the relatively large differences in P_{fish} preservation potential between BC455 and BC454, and between BC463 and BC464 (Fig. 5c). The sample sites of these boxcores are located in close proximity to each other, and, therefore, fish production in the water column must have been approximately the same. The higher preservation potentials in sediments of relatively shallow water depth can be attributed to shorter transit times through the water column, higher sedimentation rates, and lower BWO concentrations. It is not possible to determine the relative importance of each of these factors, but the close association between low BWO concentrations and high preservation potentials (Fig. 5d) suggests that more reducing bottom water conditions may have decreased dissolution of fish bone apatite. We therefore speculate that enhanced preservation of fish debris under oxygen depleted conditions may partly explain the high percentages of fish debris often observed in laminated sediments (Souter and Isaacs, 1974; De Vries and Percy, 1982; this study).

P_{fish} burial in the Arabian Sea during the Late Quaternary

The burial history of fish debris in the Arabian Sea has been studied in piston cores PC455 and PC487, which provide a continuous sediment record for the past 120 kyr (Reichart et al., 1998; **Chapter 2**). PC455 and PC487 were deposited in a continental slope and a deep marine environment respectively. The glacial mass accumulation rates (MARs) in both cores are approximately twice as high as the interglacial MARs, whereas the overall MARs in PC455 are about twice as high as those in PC487. The NH_4Cl extraction was applied to sediment samples from one interglacial (isotopic stage 5) and two glacial intervals (isotopic stage 2, 3, and 4). The high resolution of the time frames of the cores was used to select samples that were deposited contemporaneously (with the exception of two samples in the interglacial interval). The extraction results for P_{fish} are unlikely to have been affected by the presence of an early diagenetic precursor for CFA (see above), because all samples are older than 15 ky. The P_{fish} concentration in PC455 is highly variable with time, with concentrations varying from 100 to 1020 ppm (Fig. 6). P_{fish} accumulation rates in the glacial intervals are higher (3-10 $\text{mg P cm}^{-2} \text{ky}^{-1}$) than those in the interglacial interval and in the recent sediment of BC455 (2-4 $\text{mg P cm}^{-2} \text{ky}^{-1}$). The P_{fish} concentration in PC487 is nearly constant (150 ppm) in the glacial intervals, whereas higher concentrations (200-400 ppm) are observed in the interglacial interval (Fig. 6). The P_{fish} accumulation rates in PC487 are generally lower (0.8-2 $\text{mg P cm}^{-2} \text{ky}^{-1}$) than in PC455, but they are higher than present-day accumulation (0.37 $\text{mg P cm}^{-2} \text{ky}^{-1}$). Comparison with total solid-phase P concentrations (P_{tot}) (Fig. 6) indicates that P_{fish} constitutes an important fraction of total P burial in both cores (on average 37 % and 32 % for PC455 and PC487 respectively). P_{tot} correlates well with P_{fish} in PC455 ($r^2=0.98$). Although less distinct, the same is true for PC487 ($r^2=0.70$). Downcore variations in the total solid-phase P concentration in Arabian Sea sediment records, therefore, are primarily controlled by changes in the burial of the P_{fish} fraction.

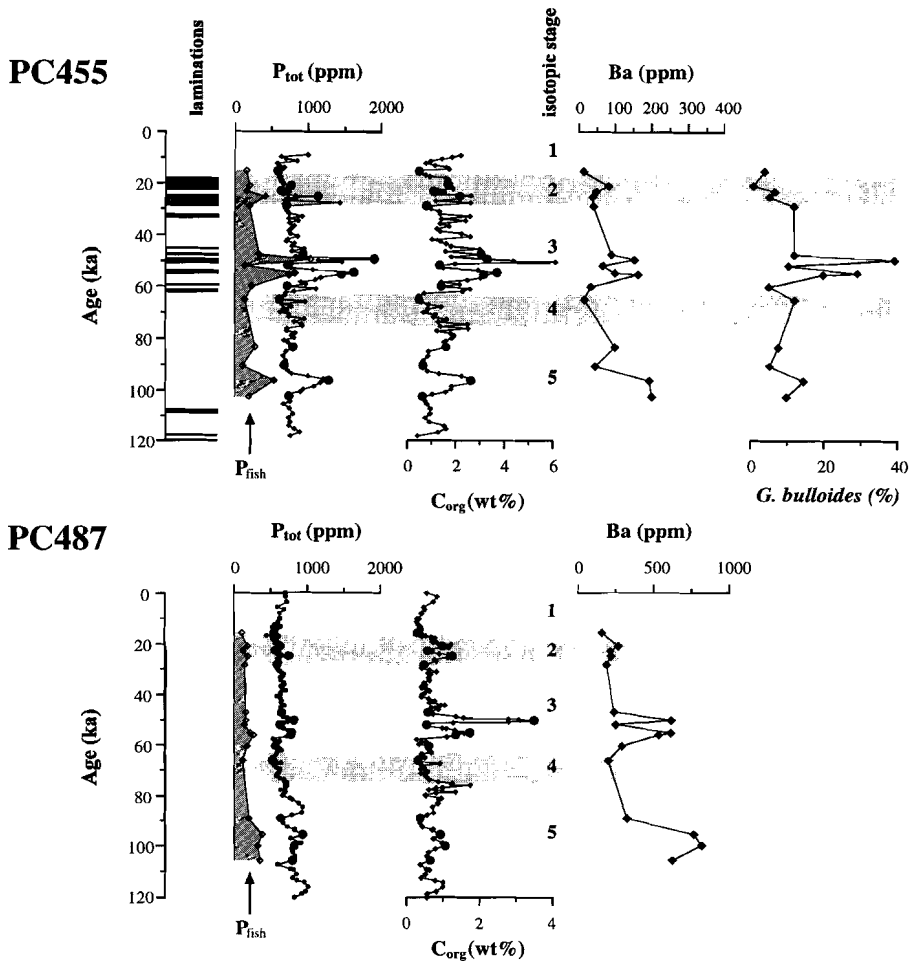


Figure 6. Sediment records of P_{fish} (ppm), total P (P_{tot} ; ppm), organic carbon (wt%), barite (ppm Ba), and *G. bulloides* (%) versus age for PC487 and PC 455. The shaded bands indicate isotopic stages.

Phosphorus in marine sediments is commonly associated with biogenic sources. Sediments underlying productive surface waters are often enriched in P, which is usually attributed to a high input of organic matter and high rates of authigenic apatite formation (e.g. Froelich *et al.*, 1988). The total solid-phase P concentration of marine sediments is, therefore, often used as an indicator for (paleo)productivity in the surface water (e.g. Brumsack, 1986; Tribovillard *et al.*, 1996; Kyte *et al.*, 1993; Reichart *et al.*, 1997). The identification of fish debris as the P fraction regulating the shape of the total solid-phase P records has important implications for the interpretation of P as a paleoproxy. Fish

production is primarily controlled by primary productivity in the surface water (Ryther, 1969; Bailey and Robertson, 1986; Iverson, 1990), and higher P_{fish} accumulation rates might thus be related to periods of increased productivity. However, the use of P_{fish} burial records for reconstructing paleoproductivity has some potential constraints, because a) the response of fish production to food availability may not have been constant over long time periods, and b) the degree of fish debris preservation may have varied as the result of to changes in mass accumulation rate and sedimentary diagenetic conditions.

Sediment records from the Arabian Sea have revealed strong fluctuations in paleoproductivity and OMZ intensity during the Late Quaternary, which have been linked to variations in orbital parameters (e.g. Emeis et al., 1995, Reichart et al., 1998). Results from frequency analysis indicate that the variability in paleoproductivity has a strong 23-kyr precession signal. During periods of a precession minimum, increased summer-monsoonal upwelling causes higher primary productivity in surface waters, resulting in increased organic matter accumulation rates and an intensified OMZ (Reichart et al., 1998). Besides the 23-kyr cyclicity, Arabian Sea records exhibit a glacial/interglacial variations. Glacial periods are characterized by relatively high MARs and low primary productivity compared to interglacial periods (Emeis et al., 1995). Periods of increased primary productivity are documented in PC487 and PC455 by organic-rich intervals (Fig. 6; Reichart et al., 1998; **Chapter 2**). These sediment cores, therefore, provide an excellent opportunity to explore the applicability of P_{fish} as a paleoproductivity proxy.

A good correlation is observed between the P_{fish} concentration and the organic carbon contents in PC455 ($r^2=0.76$; Fig. 6). Increased organic carbon contents in continental slope sediments of the northwestern Arabian Sea have been related to enhanced preservation of organic matter during periods of intensified OMZ (Reichart et al., 1998; Van der Weijden et al., 1999). Consequently, the potential of P_{fish} as a paleoproductivity indicator must be deduced by comparison with other independent productivity proxies that are unrelated to possible preservation artefacts. Abundances of the planktonic foraminifer *Globigerina bulloides*, which proliferates under eutrophic conditions (e.g. Prell et al., 1980), and barite enrichments (e.g. Dymond et al., 1992) in sediment records are commonly associated with increased paleoproductivity (Reichart et al., 1997, 1998; Den Dulk et al., 1998). P_{fish} concentrations correlate well with *G. bulloides* ($r^2=0.78$), whereas a correlation with barite contents is less apparent ($r^2=0.3$) (Fig. 6). This is probably related to the weakening of the Ba signal as a consequence of the relatively shallow water depth (von Breyman et al., 1992). In addition, some barite dissolution is likely to have occurred in these anoxic sediments due to early diagenetic sulphate reduction (e.g. Brumsack, 1989, De Lange et al., 1994). In conclusion, downcore fluctuations in the P_{fish} concentration in PC455 correlate with variations in paleoproductivity.

Downcore variations in the P_{fish} concentrations may have been affected by enhanced preservation of fish debris due to conditions related to low BWO concentrations. P_{fish} enrichments often coincide with laminated intervals (Fig. 6), which are indicative for deposition under more reducing bottom water conditions. During periods of OMZ intensification, preservation of fish debris may have been higher due to less oxygenated conditions in bottom water and sediment, which may partially explain the

Chapter 5

P_{fish} distribution in PC455. Comparison of the P_{fish} preservation potentials in boxcores located within and just below the OMZ (Fig. 5c), however, suggests that a difference in redox condition may cause a maximum preservation effect of a factor 2, whereas downcore P_{fish} accumulation rates vary by more than a factor 4. Moreover, not all P_{fish} enrichments co-occur with laminated intervals (for example at 95 kyrs; Fig. 6). Accordingly, it is unlikely that the downcore variability in P_{fish} can be attributed to changes in sedimentary redox conditions alone.

In contrast to PC455, the P_{fish} concentration in the glacial intervals of PC487 does not seem to respond to precessionally induced variations in paleoproductivity, as is indicated by the lack of a clear correlation between barite and organic carbon contents (Fig. 6). The high P_{fish} concentrations in the interglacial period, which co-occur with high barite concentrations, may be related to higher surface water productivity (*Emeis et al., 1995*), but could also be the result of the lower interglacial MARs, which might have reduced dilution of the P concentrations. The absence of a clear P_{fish} pattern in PC487 can be ascribed to the high regeneration rates of fish debris in the deep basin sediments relative to the more shallow continental slope sediments. Well-oxygenated bottom water conditions in the Arabian deep basin during the Late Quaternary (**Chapter 2**), and low MARs both contribute to lower burial efficiencies of P_{fish} . In addition, the different food web structure of the more oligotrophic open ocean environment (*Ryther, 1969*) may have made fish production less sensitive to changes in surface water productivity. In the sediments of the deep Arabian Basin, therefore, P_{fish} (and thus total solid-phase phosphorus), cannot be used to detect changes in paleoproductivity. Other productivity indicators, such as barite and possibly organic carbon concentrations, are better proxies for deep marine environments.

Summarizing, variations in P_{fish} concentrations in sediment cores from the continental margins of the Arabian Sea are directly linked to changes in primary productivity. In these marine environments organic carbon and barite concentrations are less suitable as paleoproductivity indicator. Consequently, P_{fish} may be the best presently available geochemical proxy for paleoproductivity in such environments. Fish production strongly responds to monsoonal induced upwelling, which has also been observed on a decadal time scale (*Longhurst and Wooster, 1990*). Neglecting possible preservation effects (i.e. assuming a constant maximum burial efficiency of 10 % calculated in BC455), fish production might have been as high as $100 \text{ g m}^{-2} \text{ y}^{-1}$ in the periods around 25, 50, and 55 kyr before present. This indicates that the Arabian Sea has sustained periodically much higher rates of fish production than at present. In deep marine sediments, high rates of biogenic apatite regeneration may obscure a paleoproductivity related signal. These observations indicate that total solid-phase P burial records are complex and have to be interpreted with caution. The observations made in this chapter urge for similarly detailed studies in comparable settings elsewhere in the world, which should yield further insights on using P_{fish} as a paleoproductivity indicator.

Conclusions

The 2 M NH_4Cl extraction has proven to be a good method to distinguish P associated with biogenic apatites (P_{fish}) from other sedimentary P fractions. Application of this method helps to identify the sedimentary phosphorus fractions, thereby improving the interpretation of total solid-phase phosphorus records in marine sediments. In low carbonate sediments, not using this extraction step may lead to erroneous inclusion of biogenic apatite in the Fe-related P fraction.

The P_{fish} accumulation rates in the surface sediments of the Arabian Sea are predominantly governed by differences in P_{fish} regeneration in sediment and water column. Preservation of fish debris is higher in sediments located at relatively shallow water depths, which is related to shorter transit times through the water column, higher sediment accumulation rates, and lower bottom water oxygen concentrations.

Phosphorus associated with fish debris constitutes approximately 30% of the total P buried in the Arabian Sea sediments. Downcore fluctuations in the total solid-phase P records are primarily related to changes in the contribution of the P_{fish} fraction. On the continental slope, changes in P_{fish} concentrations, and thus total solid-phase P, are directly coupled with variations in paleoproductivity. In sediment records of the deep Arabian basin, however, P contents cannot be directly related to changes in paleoproductivity as the result of higher regeneration rates of fish debris in these environments.

Acknowledgements - The chief scientists on the NIOP cruises during the 1992-1993 Netherlands Indian Ocean Programme were W.J.M. van der Linden and C.H. van der Weijden. H. de Waard, and G. Nobbe are thanked for their contribution to the laboratory analyses, and G.J. van het Veld and G. Ittman for processing the micropaleontological samples. G.J. Reichart is thanked for his assistance in the microscopical identification of fish debris. Critical reviews by C.H. van der Weijden, C.P. Slomp and A. Rutten significantly improved this manuscript. This research was funded by the Netherlands Organisation for Scientific Research (NWO).

6

Phosphorus regeneration versus burial in sediments of the Arabian Sea

S.J. Schenau and G.J. De Lange

Abstract - Solid-phase phosphorus (P) speciation and benthic phosphate fluxes have been determined in Arabian Sea sediments. Benthic phosphate fluxes are highest in the continental slope sediments, underlying bottom waters with low oxygen concentrations. Organic matter degradation and phosphate desorption from iron oxides do not produce sufficient phosphate to explain these high phosphate fluxes. The potentially high deposition of P associated with fish debris (P_{fish}) in the Arabian Sea, and a good correlation between benthic phosphate fluxes and P_{fish} accumulation rates indicate that benthic phosphate fluxes in these sediments are to a large extent governed by dissolution of biogenic apatite. Factors controlling dissolution and preservation of fish debris, therefore, play an important role in the burial and regeneration of P in continental margin sediments. A sharp decrease of the reactive P accumulation rate with increasing water depth, in combination with rather constant primary productivity rates throughout the northern Arabian Sea, indicates that P burial in continental margin sediments located within the OMZ is more efficient than in deep basin sediments. Consequently, no direct evidence was found in Arabian Sea sediments for more efficient P burial in oxic relative to dysoxic bottom water conditions. The effectiveness of P burial is primarily regulated by differences in P regeneration occurring in the water column and at the sediment water interface.

Introduction

Only a small fraction of particulate phosphorus exported from the euphotic zone is ultimately buried in the sediment, while the remainder is remobilized and reutilized by the marine ecosystem (Broecker and Peng, 1982). The quantity and form of P sequestered in sediments is strongly affected by early diagenetic processes (e.g. Krom and Berner, 1981, Sundby et al., 1992; Delaney, 1998). Processes regulating burial and regeneration of P in the marine environment have received much attention (e.g. Ruttenberg and Berner, 1993; Ingall and Jahnke, 1994, 1997; Slomp et al., 1996, McManus et al., 1997; Hensen et al., 1998), as the availability of dissolved P in seawater is thought to control biological productivity on geological time scales (Holland, 1978; Howarth et al., 1995; Tyrell, 1999).

The flux of particulate P arriving at the sediment water interface consists of a reactive and a non-reactive fraction. It is important to distinguish between these fractions because only the first may potentially be mobilized and become available again for utilization by the biosphere (Krajewski, 1994). Non-reactive P, primarily consisting of detrital apatite, usually represents only a small fraction relative to the total accumulating P flux (Ruttenberg and Berner, 1993; Filippelli and Delaney 1996). Reactive P is delivered to the sediment by three major sources (e.g. Froelich et al., 1988; Van Cappellen and Berner, 1988; Van Cappellen and Ingall, 1994): 1) organic matter, 2) iron oxides, which have a high sorption capacity for phosphate, and 3) fish debris. Accumulation of phosphorus incorporated into biogenic carbonates is insignificant compared to the other reactive P sources (Berner et al., 1993; Delaney, 1998).

Benthic phosphate regeneration in sediments is controlled by P recycling from biogenic debris, Fe redox cycling, and authigenic apatite precipitation (e.g. *Froelich et al., 1988; Van Cappellen and Berner, 1988; Föllmi, 1996*). Benthic phosphate fluxes have been reported to be much higher in continental margin sediments (*Krom and Berner, 1981; Jahnke et al., 1983; Froelich et al., 1988; Schuffert, 1994*), compared to deep pelagic sediments. The reactive P sources responsible for these high phosphate releases, however, have not yet been adequately identified (*Froelich et al., 1988; Van Cappellen and Berner, 1988; Schuffert et al., 1994*). *Ingall and Jahnke (1994)* have shown that benthic regeneration of reactive P is more extensive under oxygen depleted bottom waters, resulting in lower P burial efficiencies. Enhanced loss of P from sediments during periods of anoxic bottom water conditions will lead to an increased supply of P into the photic zone, and may stimulate higher rates of new primary productivity (*Ingall et al., 1993; Ingall and Jahnke, 1994; 1997*). Furthermore, sedimentary P cycling is influenced by the sediment accumulation rate, since P burial rates in the oceans are often controlled by the sedimentation rate (*Krajewski et al., 1994; Filippelli, 1997*).

In this study, P cycling was investigated in Arabian Sea surface sediments. The Arabian Sea is a marine environment characterized by a high monsoon-induced primary productivity and an intensive oxygen minimum zone (OMZ) between 150 and 1250 m water depth (e.g. *Wyrki, 1973; Slater and Kroopnick, 1984*). These properties make the Arabian Sea a suitable area to study the effects of surface water productivity, water depth, and bottom water oxygen (BWO) conditions on sedimentary P cycling. The investigated sediments from the continental slope and the deep basin underlie, respectively, suboxic and well-oxygenated bottom waters. We will focus on two aspects of sedimentary P cycling in Arabian Sea, namely 1) the origin of high benthic phosphate fluxes in continental slope sediments, and 2) the environmental factors controlling regeneration and retention of solid-phase P.

Material and Methods

Sample locations

During the Netherlands Indian Ocean program (NIOP) in 1992, boxcores were taken in the northern Arabian Sea. For this study, we selected 16 boxcores, located on the Pakistan continental slope (stations 451, 452, 453, 454, 455), the Murray ridge (stations 463, 464), the Arabian Basin (stations 409, 411, 458, 460 and 466), and Oman Margin (stations 484, 487, 494 and 497). Sample locations and details for the sample sites are given in Figure 1 and Table 1. BWO concentrations were derived from oxygen measurements at near-by CTD-stations. Sedimentation rates were calculated from AMS ¹⁴C dated foraminiferal samples from the base of the boxcores (*Van der Weijden et al., 1999; Passier et al., 1997; Table 1*), assuming a constant reservoir age of 400 yrs. The average mass accumulation rates (MAR) for each core were calculated as the product of the sedimentation rate and the mean dry bulk density.

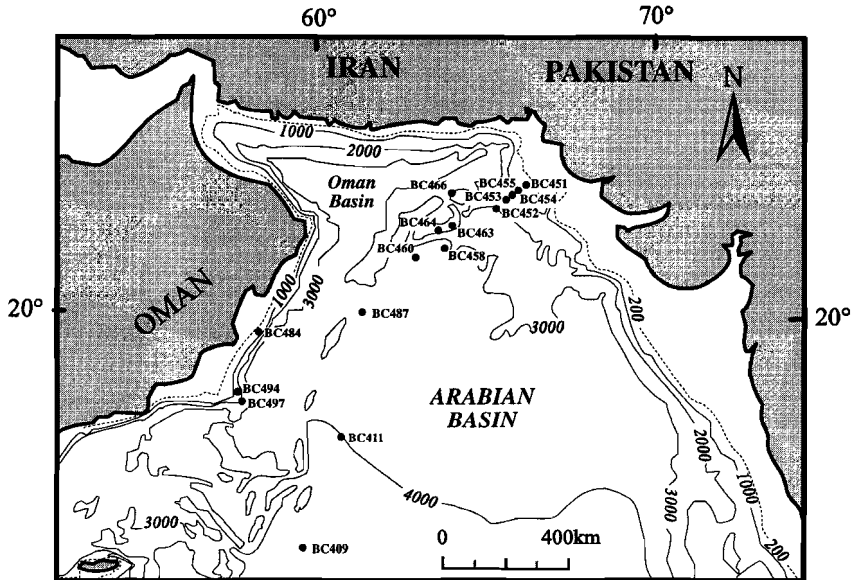


Figure 1. Sample locations in the northern Arabian Sea of the boxcores used in this study.

Pore water analysis

Porewater extractions started on board within 24 hours of core collection according to shipboard routine (De Lange, 1992a; Van der Weijden *et al.*, 1994). The boxcores were vertically sluiced into a glovebox. The glovebox was kept under low-oxygen conditions ($O_2 < 0.0005$ vol%) and at a constant near bottom temperature. The sediment was gradually extruded and slices of the extruded material were put into squeezers. Under a nitrogen pressure of up to 7 bar, the pore waters were extracted. The shipboard analysis of ammonium, alkalinity and phosphate started within 12 hours after the extraction of the porewaters. Alkalinity was measured by Gran titration (after Gieskes, 1973). Ammonium and phosphate were analysed on a TRAACS 800 auto-analyser, after the methods of Strickland and Parsons (1968) and Solarzano (1986) respectively. All determinations were done in duplicate. Acidified porewater samples were taken back to the laboratory and measured for iron on a Perkin Elmer 4100 ZL ZGFAAS. Relative errors for nutrients and alkalinity are better than 2%, for Fe 5%. The porewater iron data have previously been published by Van der Weijden *et al.* (1999).

Assuming steady state, diffusive (benthic) phosphate fluxes (J_p) were estimated with the equation (Berner, 1980):

$$J_p = \phi D_s (dC/dz) \quad (1)$$

Table 1. Location, water depth, bottom water oxygen concentration (BWO), bottom water temperature (T_{bottom}), mass accumulation rate (MAR), and organic carbon (C_{org}) concentration (in top 2 cm) of the box cores used in this study. Boxcores located in the OMZ are shaded.

	latitude (N)	longitude (E)	water depth (m)	BWO (μM)	T_{bottom} ($^{\circ}\text{C}$)	MAR ($\text{g cm}^{-2} \text{ky}^{-1}$)	$C_{\text{org top}}$ (wt%)
BC409	13°14'.2	59°30'.6	4338	158.8	1.6		
BC411	16°07'.7	60°45'.2	4016	156.8	1.6		
BC451	23°41'.4	66°02'.9	495	<2	12.6	12.5	4.1
BC452	22°56'.4	65°28'.1	2001	87.1	3.0	3.8	1.1
BC453	23°14'.0	65°44'.0	1555	39.3	5.0	5.6	1.2
BC454	23°26'.9	65°51'.2	1254	12.5	6.9	6.0	3.4
BC455	23°33'.3	65°57'.2	998	<2	8.7	6.9	4.3
BC458	21°59'.7	63°48'.8	3000	123.7	1.7	4.0	0.8
BC460	21°43'.2	62°55'.2	3262	125.3	1.7		0.9
BC463	22°33'.6	64°03'.3	970	<2	8.9	5.2	5.7
BC464	22°15'.0	63°34'.7	1511	34.8	5.3	4.3	1.3
BC466	23°36'.1	63°48'.5	1960	75.4	3.1	5.9	0.9
BC484	19°30'.0	58°25'.8	527	<2	12.3	3.8	2.3
BC487	19°54'.8	61°43'.3	3566	151.0	1.6	0.8	0.8
BC494	17°42'.0	57°43'.1	2437	88.0	2.2		
BC497	17°26'.7	57°57'.4	1890	82.8	3.4		

where ϕ is the mean porosity, D_s the whole sediment diffusion coefficient for phosphate, and dC/dz the concentration gradient at the sediment surface, determined as the concentration difference between the uppermost interstitial water sample and the bottom water, assuming a linear concentration gradient between these points. Whole sediment diffusion coefficients (D_s) ($\text{cm}^2 \text{s}^{-1}$) can be expressed by

$$D_s = D^*/\phi F \quad (2)$$

where D^* is the diffusion coefficient in seawater and F the formation factor. Diffusion coefficients ($7.34 \times 10^{-6} \text{ cm}^2 \text{ s}^{-1}$ for HPO_4^{2-} at 25°C) were corrected for the in-situ bottom water temperatures (*Li and Gergory, 1974*). Formation factors were estimated with the equation (*Manheim and Waterman, 1974*):

$$\log F = 0.110 - 1.80 \log \phi \quad (3)$$

Benthic flux calculations based on pore water gradients are subject to several inaccuracies. First, these calculations do not take into account phosphate regenerated at the sediment water interface, which directly diffuses back to the overlying bottom water.

Secondly, phosphate transport induced by macrobenthic irrigation is neglected. This may particularly cause an underestimation of the benthic fluxes in relative shallow continental margin sediments, where bioturbation is important (Glud *et al.*, 1994). For this reason, previous studies have confined benthic flux calculations to sample locations deeper than 1000 m (Zabel *et al.*, 1998; Hensen *et al.*, 1998). In this study, however, we included sample sites from 500 m water depth, because the low BWO concentrations inhibit vigorous bioturbation in these sediments (Jannink *et al.*, 1998; Van der Weijden *et al.*, 1999) and vertical diffusion can thus be assumed to be the dominant transport mechanism. Thirdly, porewater artifacts may have been introduced during core recovery, which may have decreased the phosphate concentrations (Jahnke *et al.*, 1982). This especially affects marine sediments with low interstitial phosphate concentrations (Zabel *et al.*, 1998; Hensen *et al.*, 1998). It should be noted that all these inaccuracies cause an underestimation of the benthic phosphate fluxes.

We recognize that these inaccuracies may also have affected the benthic phosphate fluxes presented in this study. However, the purpose of our calculations is to demonstrate regional differences in benthic fluxes in the Arabian Sea and to make some semi-quantitative estimates. In our opinion, the limitations listed above will not seriously hamper such interpretation. Possible consequences of the potential inaccuracy of calculated fluxes will be anticipated in the discussion.

Solid-phase analysis

The porosity and dry bulk density were calculated from the loss on drying at 60 °C, assuming a density of 2,65 g cm⁻³ for the sediment. For the determination of total solid phase P and Fe, 250 mg sample was digested in 10 ml of a 6.5 : 2.5 : 1 mixture of HClO₄ (60%), HNO₃ (65%) and H₂O, and 10 ml HF (40%) at 90°C. After evaporation of the solutions at 190°C on a sand bath, the dry residue was dissolved in 50 ml 1 M HCl. The resulting solutions were analysed by a Perkin Elmer Optima 3000 Inductively Coupled Plasma Atomic Emission Spectrometer (ICP-AES). All results were checked using international (SO1, SO3) and in-house standards. Relative errors for duplicate measurements are better than 3%. After removal of inorganic carbon with 1 M HCl the organic carbon content (C_{org}) was measured on a NA 1500 NCS analyser. Relative errors on duplicate measurements are better than 1 %.

The solid-phase speciation of P and Fe in the top 0-2 centimeters was examined using a 5-step sequential extraction scheme (for details see Table 2 in **chapter 5**). Approximately 125 mg of dried and ground sediment was subsequently washed with 1) 25 ml 2 M NH₄Cl, pH=7 (repeated 8 times), 2) 25 ml citrate dithionite buffer (CDB), pH=8, 3) 25 ml 1 M Na-acetate, pH=4, 4) 25 ml 1 M HCl, and 5) 20 ml HF/HNO₃/HClO₄ mixture. After extraction steps 2, 3 and 4 the sediment was rinsed with 2 M NH₄Cl and demineralised water. This extraction scheme is a modification of the SEDEX method developed by Ruttenberg (1992). The application of the 2 M NH₄Cl extraction enables the determination of P associated with biogenic apatite (fish debris; **Chapter 5**). The sum of all extraction steps varied between 80 and 90% with respect to the total P concentration. The deficit can be attributed to systematic errors in the measurements of the low P concentrations with ICP-AES. Precision for P was generally better than 5%, except for

steps 2 and 3 (10%). Iron oxide contents (reactive iron; Fe_{CDB}) were determined from the iron concentration extracted in step 2 (Na-dithionite). Organic phosphorus (P_{org}) was determined non-sequentially as the difference between P extractable in 1 M HCl before and after ignition of the sediment (550 °C, 2h; *Aspila et al., 1976*). All extracted solutions were analysed with ICP-AES. All measurements were done in duplicate (relative errors smaller than 2%). Precision for samples containing relatively low concentrations of organic P is low (relative errors up to 25 %), as it is calculated as the difference between two high concentrations.

Results

Porewaters

Interstitial phosphate concentrations increase rapidly with sediment depth to 30 - 80 μM in sediments located within the present-day OMZ (500-1000 m; Fig. 2). In two boxcores (BC451 and BC484) this increase is followed by a decrease with depth. Interstitial iron concentrations display the same pattern, but are generally lower than phosphate (Fig. 2). In sediments located below the OMZ (1200-3500 m), phosphate concentrations are lower (up to 15 μM) compared to sediments from 500-1000 m, and generally increase only slightly with depth. Dissolved iron concentrations gradually increase with depth in sediments from 1200-3000 m water depth, whereas sediments from the deepest part of the Arabian Basin (3000-4500 m) display low iron concentrations (1-5 μM) in the upper 5-10 cm sediment depth centimeters, below which depth they increase gradually.

The benthic phosphate fluxes are highest (0.3-6.4 $\mu\text{M cm}^{-2} \text{y}^{-1}$) in sediments located at intermediate water depths (500-1000 m), within the OMZ (Table 2; Fig. 3a). Below 1500 m water depth, benthic phosphate fluxes are lower, varying between 0.01 and 0.3 $\mu\text{M cm}^{-2} \text{y}^{-1}$. For one location (BC460) a negative P flux was calculated, which is possibly caused by artifacts introduced during core recovery (*e.g. Hensen et al., 1998*). In general, benthic phosphate fluxes in Oman Margin sediments are higher than in the northeastern Arabian Sea (Fig. 3a).

Solid phase

Organic carbon is enriched in the surface sediments located within the OMZ compared to deep Arabian Basin sediments (Table 1). Accumulation rates of reactive P (i.e. the amount of reactive P removed by burial; A_{Preac}) have been calculated as the product of the mass accumulation rate (Table 1) and the reactive P concentration (being the total solid-phase P concentration minus detrital P concentration) in the lowermost sample of each boxcore. It is assumed that MARs remained constant for the time period during which the sediments of the boxcores were deposited, as sedimentation rates were constant in the Arabian Sea during the Late Holocene (*Sirocko et al., 1993; Von Rad et al., 1999*). P_{reac} accumulation rates are highest in the shallowest boxcores (500-1000 m), and decrease with water depth (Fig. 3b). This trend is similar as that observed for the benthic phosphate

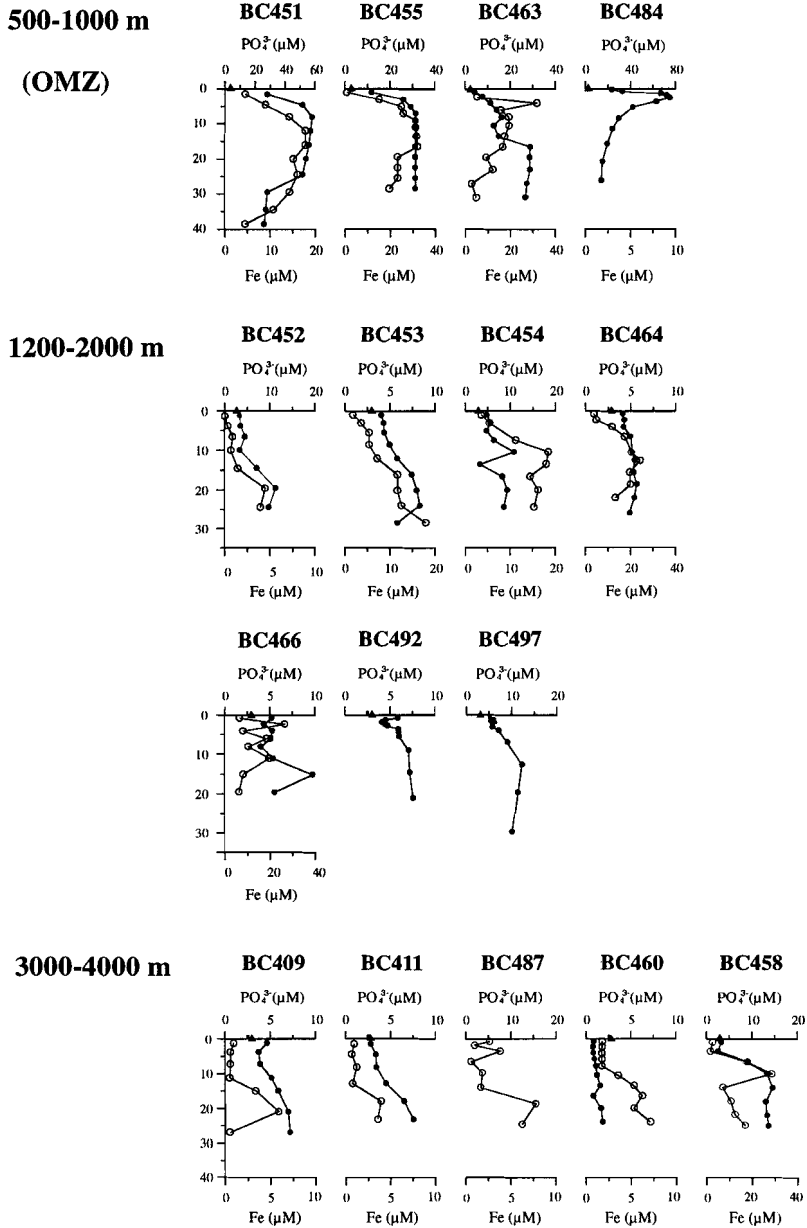


Figure 2. Porewater profiles of dissolved phosphate (●) and iron concentrations (○) (μM) for the box cores used in this study (Table 1). Phosphate bottom water concentrations are marked with a ▲. No porewater phosphate data are available for BC487, and no iron porewater data for BC484, BC492, and BC497.

Table 2. Benthic phosphate fluxes (J_p), reactive P accumulation rates (A_{Preac}), reactive P accumulation rates for the top 2 cm ($A_{Preac}(top)$), the deficit $A_{Preac}(top) - (J_p + A_{Preac})$, and the reactive P burial efficiency (PBE), as calculated with equation 7. Boxcores located in the OMZ are shaded.

	J_p	A_{Preac}	$A_{Preac}(top)$	$A_{Preac}(top) - (J_p + A_{Preac})$	PBE (%)
	$\mu\text{mol cm}^{-2}\text{y}^{-1}$	$\mu\text{mol cm}^{-2}\text{y}^{-1}$	$\mu\text{mol cm}^{-2}\text{y}^{-1}$	$\mu\text{mol cm}^{-2}\text{y}^{-1}$	
BC409	0.05				
BC411	0.01				
BC451	1.59	0.71	0.43	-1.88	30.9
BC452	0.03	0.07	0.08	-0.02	73.9
BC453	0.08	0.12	0.14	-0.05	60.8
BC454	0.13	0.16	0.21	-0.08	54.9
BC455	0.73	0.31	0.25	-0.79	30.1
BC458	0.03	0.07	0.08	-0.01	71.1
BC460	-0.1				
BC463	0.29	0.23	0.16	-0.36	43.8
BC464	0.09	0.07	0.09	-0.08	46.1
BC466	0.08	0.13	0.15	-0.06	63.0
BC484	6.44				
BC487	-	0.03	0.05	-0.33	
BC494	0.16				
BC497	0.12				

fluxes versus water depth (J_p ; Fig. 3a). P_{react} accumulation rates have also been calculated using the reactive P concentration in the upper two centimeters ($A_{Preac}(top)$; Table 2). For sediments located within the OMZ, $A_{Preac}(top)$ rates are lower than A_{Preac} (Table 2).

In general, the P speciation of Arabian Sea surface sediments (0-2 cm) does not vary much with water depth (Fig. 4). On average, each of the three major reactive P fractions (organic P, Fe bound P, P associated with fish debris) constitutes ~ 20-25 % of total extracted P. Organic P and P associated with fish debris are enriched relatively to the other P fractions in the sediments located within the OMZ. The iron-bound P fraction is relatively constant (ca. 25 %) for sediments below 1200 m, but variable for sediments located within the OMZ. Detrital apatite is a relatively more important fraction in the sediments from the deep basin. In all surface sediments, authigenic P contents (P_{CFA}) are low (20-100 ppm). The presence of P_{CFA} , however low, may indicate that some authigenic apatite has been redeposited, or is precipitating in these surface sediments. Alternatively, it is possible that the low amounts of extracted P_{CFA} can be attributed to partial dissolution of other P fractions, which would imply that no authigenic P phase is present.

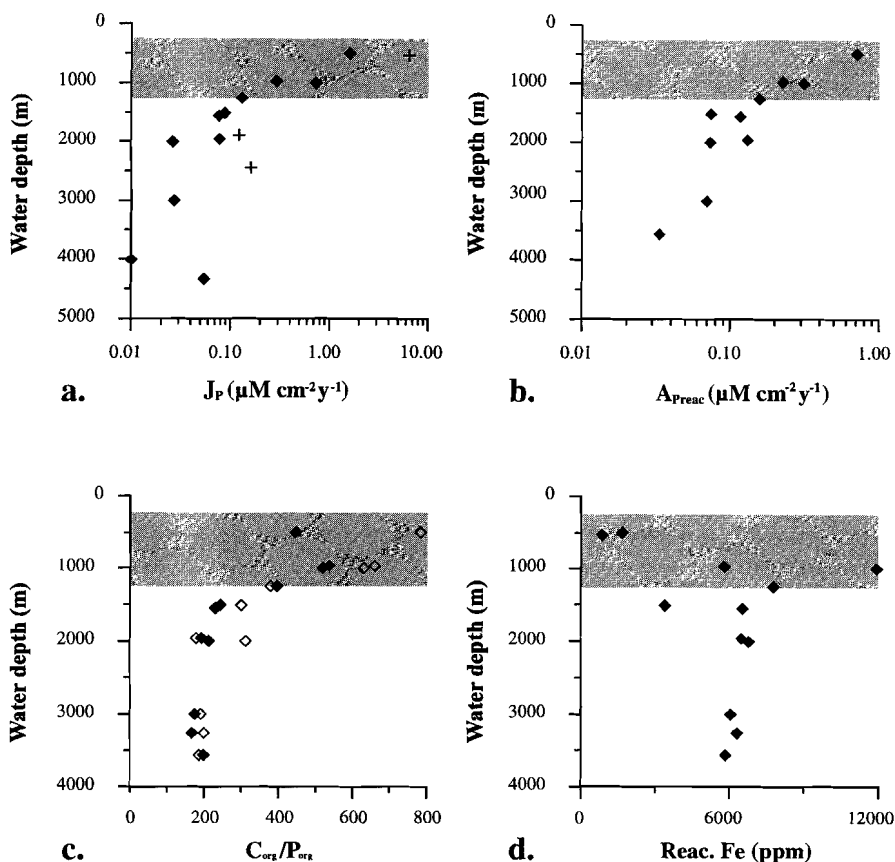


Figure 3. A plot of a) benthic P fluxes (J_P) versus water depth for sample locations from the northeastern Arabian Sea (◆) and the Oman upwelling area (+), b) reactive P accumulation rates ($A_{P_{\text{reac}}}$) versus water depth, c) sedimentary molar $C_{\text{org}}/P_{\text{org}}$ ratios versus water depth for surface samples (0-2 cm; ◆), and samples from the base of each boxcore (25-40 cm; ◇), d) reactive iron concentrations (Fe_{CDB}) in surface sediments (0-2 cm) versus water depth. The shaded area indicates the position of the OMZ (< 2 $\mu\text{M O}_2$).

Molar $C_{\text{org}}/P_{\text{org}}$ ratios in the surface sediments (0-2 cm) decrease with water depth from 400-500 at 500 m to 200 at 2000 m (Fig. 3c). Below this water depth, $C_{\text{org}}/P_{\text{org}}$ ratios remain fairly constant. $C_{\text{org}}/P_{\text{org}}$ ratios of sediments located within the OMZ samples are higher for deeper (25-40 cm) than for surface samples, indicating ongoing preferential loss of P relative to carbon upon burial. In contrast, molar $C_{\text{org}}/P_{\text{org}}$ ratios remain constant with sediment depth in the deepest part of the Arabian Basin. Dithionite-extractable (reactive) iron concentrations are constant in surface sediments below the OMZ (~6000 ppm; Fig. 3d). Around the base of the present-day OMZ, sedimentary reactive

iron is enriched in two boxcores (BC455 and BC454), while sediments from around 500 m water depth are depleted in reactive Fe. Molar Fe/P ratios in the dithionite-extractable fraction vary between 16 and 23 for all samples.

Discussion

The pattern of benthic P release with water depth in the Arabian Sea (Fig. 3a) is similar to that observed along the continental margins of California (*Ingall and Jahnke, 1994; McManus et al., 1997*) and the Southern Atlantic (*Zabel et al., 1998; Hensen et al., 1998*). The high benthic phosphate fluxes in upper continental slope sediments imply high rates of reactive P mobilization. According to the dissolved phosphate profiles, the source for this reactive P regeneration is located in the upper centimeters of the sediment. In a steady state situation, the flux of reactive P leaving the surficial sediment (i.e. $J_P + A_{\text{Preac}}$) should equal the reactive P flux that is deposited. A comparison between the $J_P + A_{\text{Preac}}$ flux and the accumulation of reactive P in the upper centimeter (A_{Preac} (top)) indicates a P input deficit for all boxcores (Table 2). This deficit is particularly high for sediments located within the OMZ. Furthermore, even if all of P in the top (A_{Preac} (top)) of the sediment was mobilized, insufficient reactive P is present to explain the observed benthic phosphate flux. Obviously, the observed solid-phase P contents do not concur with the estimated phosphate fluxes. A similar discrepancy has previously been reported for shallow coastal shelf sediments (*Krom and Berner, 1981*).

The inconsistency of the sedimentary P budget is not related to inaccuracies of the estimated pore water fluxes, as these probably cause an underestimation of the benthic phosphate fluxes. Possibly, the porewater fluxes are subject to seasonal variability (e.g. *Krom and Berner, 1981; Hensen et al., 1998*). The sediments were sampled between September and November, which is after the monsoon-induced period of high productivity. The estimated benthic fluxes may thus have been higher than the annual average. *Sayles (1994)*, however, showed that for most deep marine environments benthic fluxes show little seasonal variation. Moreover, even significantly lower annual benthic phosphate fluxes would not resolve the P input deficit. Consequently, the high benthic phosphate fluxes in continental margin sediments must be related to a large input of reactive P that, upon reaching the sediment water-interface, is rapidly regenerated (*Krom and Berner, 1981*). In order to produce high subsurface phosphate concentrations, some downward mixing of reactive P by benthic organisms is necessary (**Chapter 4**). When reactive P is continuously mixed into the sediment and is mobilized rapidly, it will not be detected as a distinct solid-phase P fraction in the top of the sediment. The low BWO concentrations significantly reduce the activity of benthic organisms (*Van der Weijden et al., 1999*), but the presence of benthic foraminifera (*Jannink et al., 1998*) and the absence of laminae indicate that some benthic activity does exist. Bioturbation may occur seasonally, namely during early summer when bottom waters are slightly less dysoxic (*Van Bennekom et al., 1995*), due to vigorous mixing of the upper layers of the water

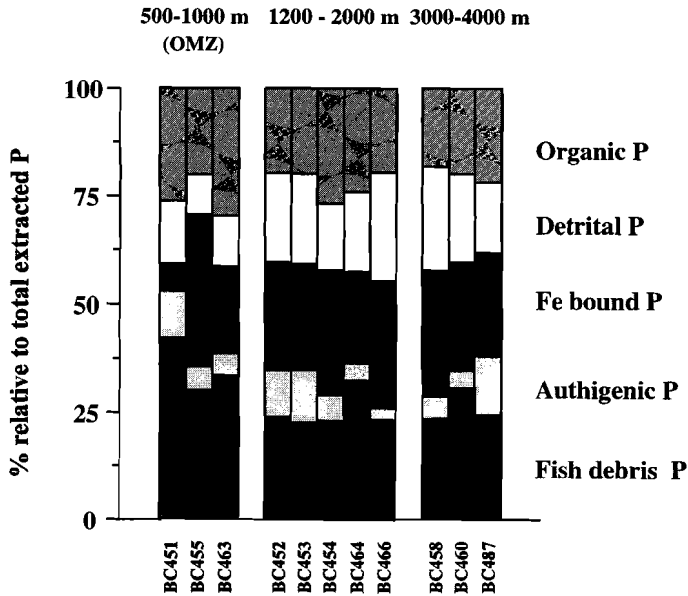


Figure 4. The solid-phase P speciation relative to total extracted P for the surface sediment samples (0-2 cm) of this study.

column. In addition to bioturbation, the higher sedimentation rates on the continental margin may promote a more rapid burial of reactive P.

Concluding, benthic phosphate fluxes are regulated by regeneration processes occurring briefly after deposition. As a consequence, the accumulation rates of reactive P in the top centimeters cannot be directly linked to benthic phosphate fluxes. The P speciation of the surface sediments thus only provides an indication of the contribution of each individual reactive P source. In the next section benthic phosphate fluxes will be related to the three principal sources of reactive P (organic matter, iron oxides, and fish debris), and to the subsequent diagenesis of these components, in order to identify the most important contributor of reactive P to the high benthic phosphate fluxes for sediments located within the OMZ.

1. Organic matter

Deposition of organic matter is quantitatively the most important mechanism by which reactive P is transferred to the sediment (Froelich *et al.*, 1982; Delaney, 1998). The average annual P export flux in the northern Arabian Sea amounts to $\sim 5.5 \mu\text{mol P cm}^{-2} \text{y}^{-1}$ (assuming an average export productivity of $70 \text{ g C m}^{-2} \text{y}^{-1}$ (Van der Weijden *et al.*, 1999) and a Redfield nutrient ratio). Burial of organic P, however, is not the foremost reactive P sink in most marine environments (Filippelli and Delaney, 1996; Delaney, 1998). This

also holds for Arabian Sea sediments, as is shown by the solid-phase P speciation (Fig. 4). Accordingly, a significant fraction of organic P is decomposed in the water column and in the top few centimeters of the sediment. In the Arabian Sea, organic carbon burial is higher in sediments located within the OMZ (Table 1). There is a good correlation between the benthic phosphate flux and the P_{org} accumulation rate (Fig. 5a), suggesting that the high benthic phosphate fluxes in these sediments may be linked to organic matter decomposition.

Phosphate production from organic matter decomposition for sediments located within the OMZ (BC451, BC455, BC463, BC484) can be estimated from ammonium porewater concentrations (Froelich *et al.*, 1988; Ruttenberg and Berner, 1993; Schuffert *et al.*, 1994; McManus *et al.*, 1997). An empirical fit was made to the ammonium porewater profiles, using the equation (Berner, 1980):

$$C = C_0 + \alpha_1(1 - e^{-\alpha_2 x}) \quad (4)$$

where C and C_0 are the concentrations of ammonium at depth x and 0 (cm) respectively, and α_1 and α_2 empirical constants. Considering the suboxic nature of these sediments, oxidation of ammonium can be neglected. Assuming that organic matter is decomposing stoichiometrically (i.e. α_2 for ammonium equals α_2 for phosphate), and has a Redfield nutrient ratio (C:N:P 106:16:1), the empirical constants α_1 for phosphate (α_{1P}) can be calculated with (Schuffert, 1994):

$$\alpha_{1P} = \alpha_{1N} \times D_N / 16 \times D_P \quad (5)$$

where D_N and D_P are the whole diffusion coefficient constants for respectively ammonium and phosphate corrected for the in-situ bottom water temperature (Li and Gregory, 1974).

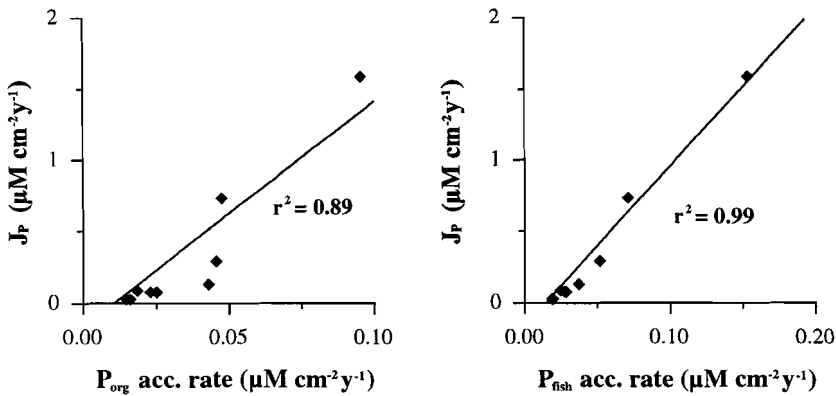


Figure 5. A plot of the benthic P flux (J_p ; Table 2) versus respectively a) the P_{org} accumulation rate, and b) P_{fish} accumulation rate.

Chapter 6

Possible contributions of the more refractory terrestrial organic P can be neglected, as accumulating organic matter in the sediments of the Arabian Sea is predominantly of a marine origin (Pedersen *et al.*, 1992; Van der Weijden *et al.*, 1999). The values for α_{1P} and α_2 were inserted in equation (4) and used to plot the calculated phosphate profile resulting from organic matter degradation, i.e. in absence of phosphate adsorption to iron oxides, phosphate incorporation into benthic biomass and authigenic apatite precipitation (Schuffert *et al.*, 1994). Subsequently, the maximum benthic flux resulting from organic matter decay ($J_{P_{org}}$) was calculated from the linear phosphate gradient in the upper part of the sediment in the modeled phosphate profiles using equations (1) and (2) (see method section). A comparison between the calculated $J_{P_{org}}$ fluxes and the real benthic phosphate fluxes (J_p ; Table 3) indicates that organic matter degradation in sediments located within the OMZ produces insufficient phosphate to explain the high benthic phosphate fluxes.

The C_{org}/P_{org} ratio for surface sediments (0-2 cm) located within the OMZ are higher than the Redfield ratio of organic matter (106), which can be attributed to preferential loss of organic P relative to carbon during organic matter degradation. As organic matter arriving at the sediment water interface is dominated by fast-sinking material and therefore still incorporates a nutrient ratio close to the Redfield ratio (Anderson and Sarmiento, 1994), preferential release of P must occur directly after deposition. The calculated P fluxes originating from organic matter decomposition ($J_{P_{org}}$) may thus have been underestimated. Assuming that approximately two thirds of the organic matter is rapidly decomposed after deposition (unpublished data) during which the C_{org}/P_{org} ratio increases from 106 to 500, it follows that C/P of the regenerated organic matter equals 75. As the result of preferential P release, the calculated $J_{P_{org}}$ fluxes may thus increase by a factor of at most 1.4. This is still insufficient to explain the observed benthic phosphate fluxes (Table 3).

We conclude that the high benthic phosphate fluxes in sediments located within oxygen depleted bottom waters can only partially (on average 25 %) be explained by high rates of sedimentary organic matter degradation and preferential P release. This finding is consistent with other studies concerning P cycling in continental margin sediments underlying low BWO concentrations (Froelich *et al.*, 1988, Van Cappellen and Berner, 1988; Heggie *et al.*, 1990; Schuffert *et al.*, 1994).

2. Iron oxides

A second potential carrier of reactive P to the sediment is iron (hydr)oxide, which is deposited as a detrital mineral and as surface coating on sedimentary particles (*e.g.* Berner, 1973; Froelich *et al.*, 1988). Under oxygenated conditions, iron oxyhydroxides have a large sorption capacity for phosphate (*e.g.* Lucotte and d'Anglejan, 1988). After burial in the suboxic zone of the sediment, iron oxides start to dissolve and the adsorbed phosphate is released into the interstitial water. Accumulation of iron-bound P and subsequent phosphate regeneration is principally regulated by the sediment accumulation rate (*i.e.* the deposition of detrital iron oxides) and the oxygenation state of the water column, bottom water and sediment.

Table 3. Calculated P fluxes for the box cores located within the oxygen minimum zone (BC484, BC451, BC455, BC463). First column : benthic P fluxes (J_p) as estimated from the porewater phosphate profile; second column : the estimated benthic P flux as the result of organic matter degradation (J_{Porg}), calculated from the ammonium porewater profiles assuming stoichiometric organic matter degradation according to a Redfield nutrient ratio (C:N:P 106:16:1; see text); Third column : potential input of P associated with reducible iron hydroxides, as calculated with equation 6 (J_{PFe} ; see text); Fourth column: the potential input of P associated with biogenic apatite (J_{Pfish}), as determined from fish production in the Arabian sea (see text); Fifth column : excess benthic P flux expected to diffuse out of the sediment under anoxic conditions as the result of redox dependent P cycling by microorganisms ($J_{Pexcess}$; see text).

	J_p $\mu\text{mol cm}^{-2}\text{y}^{-1}$	J_{Porg} $\mu\text{mol cm}^{-2}\text{y}^{-1}$	J_{PFe} $\mu\text{mol cm}^{-2}\text{y}^{-1}$	J_{Pfish} $\mu\text{mol cm}^{-2}\text{y}^{-1}$	$J_{Pexcess}$ $\mu\text{M cm}^{-2}\text{y}^{-1}$
BC451	1.59	0.16	0.07	0.7	0.13
BC455	0.73	0.15	0.04	0.7	0.07
BC463	0.29	0.20	0.03	0.4	0.07
BC484	6.44	0.14	0.02	“not determined”	0.02

In view of the low oxygen concentrations in the intermediate water column, it is questionable whether the accumulation of iron oxides may provide an efficient mechanism to transfer reactive P to sediments residing in the OMZ. Surface sediments from a water depth of ca. 500 m are characterized by an absence of reactive iron (Fig. 3d), indicating that iron oxides have already been reduced in the water column or at the sediment water interface. In contrast, sediments located near the lower boundary of the OMZ (1000-1250 m) have relative high concentrations of reactive iron. Bottom water oxygen concentrations are somewhat higher here, allowing the deposition of iron oxides. As the oxic-suboxic interface is located close to the sediment surface (*Van der Weijden et al., 1999*), reactive iron may become enriched due to reprecipitation of upward diffusing Fe^{2+} , mobilized in the deeper, suboxic part of the sediment. The sharp downcore increase of porewater Fe^{2+} observed in BC451, BC455 and BC463 (Fig. 2), indicates that iron oxides are being reduced upon deposition. Apparently, burial of some reactive iron occurs in the sediments located within the OMZ. The simultaneous increase of both dissolved phosphate and Fe^{2+} in these boxcores point to possible active phosphate desorption from iron oxides (*e.g. Slomp et al., 1996*).

The primary supply of P associated with reducible iron hydroxides (J_{PFe} , $\mu\text{mol P cm}^{-2}\text{y}^{-1}$) has been estimated using the equation (after *Ingall and Jahnke, 1997*):

$$1J_{PFe} = \frac{Fe_{CDB} \times MAR}{(Fe/P)_{red} \times 55800} \quad (6)$$

Chapter 6

where Fe_{CDB} is the concentration of iron oxides in the surface sediment as measured in extraction step 2 (ppm), MAR the mass accumulation rate ($\text{g cm}^{-2} \text{ky}^{-1}$, Table 1), and $(\text{Fe}/\text{P})_{\text{red}}$ the molar ratio of adsorbed phosphate in newly deposited reducible iron particles. The Fe_{CDB} concentrations in surface sediments within the OMZ, however, cannot be used to quantify the J_{PFe} flux, because iron oxides may already have been partly reduced at the sediment water interface, or have become enriched due to diagenetic iron cycling. Therefore, an estimate for the J_{PFe} flux was made based on the Fe_{CDB} concentrations recorded in the surface sediments located below the OMZ, which have probably not been subjected to significant diagenetic changes. The rather constant Fe_{CDB} concentrations (~ 6000 ppm), suggest that accumulation of iron oxides is directly proportional to the sediment accumulation rate. Previous estimates for the molar $(\text{Fe}/\text{P})_{\text{red}}$ ratio for newly buried iron oxides range from 20-26 (Lucotte *et al.*, 1994; Louchouart *et al.*, 1997; Anschutz *et al.*, 1998), which correspond with $(\text{Fe}/\text{P})_{\text{red}}$ ratios of surface sediments observed in this study. Assuming a Fe_{CDB} concentration of 6000 ppm and a $(\text{Fe}/\text{P})_{\text{red}}$ ratio of 20 (as found for deep basin sites), the J_{PFe} fluxes have been calculated for the boxcores located within the OMZ (Table 3). It should be noted that this calculation provides maximum values for the potential J_{PFe} flux, as it is assumed that no reduction of iron oxides occurs during their transit through the OMZ. Even so, the calculated J_{PFe} fluxes constitute only 4 to 10% of the observed benthic phosphate fluxes (Table 3). Another indication that the high subsurface phosphate concentrations in these sediments are not controlled by desorption from iron oxides, are the rather low molar porewater Fe/PO_4 ratios (0.1-1.5). If iron oxides were being reduced with a $\text{Fe}_{\text{CDB}}/\text{P}_{\text{CDB}}$ ratio of ~ 20 , much higher dissolved iron concentrations would be expected (*e.g.* Slomp *et al.*, 1996). Consequently, it is unlikely that burial and subsequent dissolution of iron oxides significantly contribute to the high benthic phosphate fluxes in the continental margin sediments. Van Cappellen and Berner (1988) and Ingall and Jahnke (1997) arrived at the same conclusion for continental margin sediments underlying low oxygenated bottom waters offshore California.

3. fish debris

The hard parts of fish (scales, bones, teeth) consist for 60 to 70 % of hydroxyapatite (*e.g.* Posner *et al.*, 1984). Crystal imperfections and a relative large reactive surface area make biogenic hydroxyapatite a more reactive and soluble mineral than well-crystallized stoichiometric hydroxyapatite, which in turn is more soluble than fluorapatite (Posner *et al.*, 1984; Newsly, 1989). Seawater is undersaturated with respect to biogenous apatite (Arrhenius, 1963; Atlas and Pytkowicz, 1977). As a result, fish debris can undergo dissolution in the water column and during early diagenesis. Only a fraction of biogenic apatite produced in the water column is ultimately buried in the sediments. The accumulation of fish debris has been recognized as a potentially important process to transfer reactive P to marine sediments (Suess, 1981; Van Cappellen and Berner 1988). There are few studies which consider dissolution of fish debris as a potential source for interstitial phosphate, which is probably due to the fact that (until now) they were not chemically distinguishable from other P fractions.

The high biomass of phyto- and zooplankton in the Arabian Sea induces high rates of fish production (e.g. *FAO, 1981*). Based on the trophic-dynamic model of *Iverson (1990)*, we have estimated a present-day fish production for the Pakistan Margin and the central Arabian Sea of respectively $23.8 \text{ g m}^{-2} \text{ y}^{-1}$ and $14.0 \text{ g m}^{-2} \text{ y}^{-1}$ (wet weight; **Chapter 5**). Assuming a phosphorus dry weight fraction of marine fish of 0.03 (*Anonymous, 1982*), and a ratio of fish wet weight % to fish dry weight % of 3.3 (*Iverson, 1990*), the potential production of P associated with biogenic apatite varies between 0.7 and $0.4 \mu\text{mol P cm}^{-2} \text{ y}^{-1}$ (Table 3). This calculation gives only a rough estimate for the potential vertical F_{Pfish} flux, but provides a reasonable order of magnitude. This calculated production of P associated with fish bones is approximately a factor 10 less than the export flux of organic P. Fish bone particles, however, are relatively large and have a high density compared to seawater, which will make them sink relatively fast to the seafloor. It is therefore plausible that dissolution of fish debris predominantly occurs after deposition. Accumulation of fish debris may thus potentially transfer a significant quantity of reactive P to the sediments of the Arabian Sea.

The application of the NH_4Cl extraction enables, for the first time, an evaluation of P_{fish} accumulation in marine sediments in relation to the other reactive P fractions. In the surface sediments of the Arabian sea, P_{fish} is an important reactive P fraction (Fig. 4). Particularly sediments located within the OMZ have relatively higher P_{fish} concentrations, which is confirmed by high numbers of fish particles in the 150-595 μm sieve fractions. This has been attributed to high fish production rates in the surface waters and reduced biogenic apatite dissolution rates in comparison to the deep Arabian Basin (**Chapter 5**). The P_{fish} accumulation rate correlates well with the benthic phosphate flux ($r^2 = 0.99$; Fig. 5b), suggesting that fish debris may be an important source for phosphate generation from these sediments.

Based on a) the good correlation between the benthic phosphate fluxes and the P_{fish} accumulation rates, b) the potentially high accumulation rate of P associated with fish in the Arabian Sea, and c) the insufficient contribution of other reactive P sources (organic matter and iron oxides), we conclude that the high benthic phosphate fluxes in continental margin sediments of the Arabian Sea are to a large extent the result of sedimentary fish debris dissolution. This finding may have important implications for P cycling in the oceans. Firstly, processes governing the dissolution and preservation of fish debris may control benthic P regeneration in many marine environments. Secondly, fish debris dissolution may drive CFA formation in continental shelf sediment underlying high productivity areas, as has previously been suggested by *Suess (1981)*, and thereby regulating P burial.

Phosphorus burial in the Arabian Sea

Benthic regeneration of P is generally considered to be more extensive under oxygen depleted bottom waters (*Ingall and Jahnke, 1994; 1997*). To evaluate regeneration and burial of P in sediments of the Arabian Sea, reactive P burial efficiencies (PBE) have been calculated using the equation (after *Ingall and Jahnke, 1994*):

$$\text{PBE (\%)} = 100 \times A_{\text{Preac}} / (J_{\text{p}} + A_{\text{Preac}}) \quad (7)$$

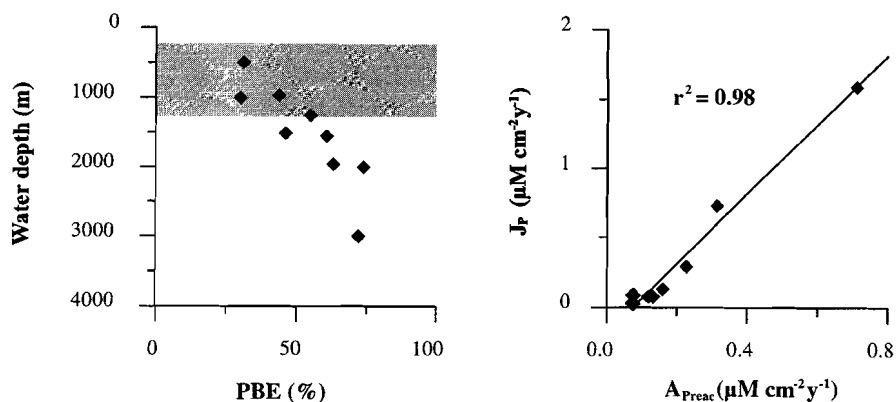


Figure 6. A plot of a) the P burial efficiencies (PBE) (%) versus water depth, and b) benthic P fluxes (J_p) versus reactive P accumulation rates (A_{Preac}). The shaded area indicates the position of the OMZ ($< 2 \mu\text{M O}_2$).

where A_{Preac} is the accumulation rate of reactive P and J_p the benthic phosphate flux (Table 2). The P burial efficiencies are lowest for the sediments located within the OMZ (BC451, BC455 and BC463) and decrease with water depth (Fig. 6a; Table 2). Although these results compare favourably with those in the study of *Ingall and Jahnke (1994)*, in general, the PBE found in the present study are higher. This may be attributed to the different method by which the benthic fluxes were obtained. *Ingall and Jahnke (1994)* used in-situ benthic chamber incubation measurements, which includes P mobilization at the sediment water interface, whereas our method does not. In addition, high rates of phosphogenesis in the continental margin sediments of the Arabian Sea (**Chapter 4**) may also result in higher PBEs.

The relatively low P burial efficiencies calculated for continental slope sediments compared to those in deep basin sediments seem contradictory to the high P_{reac} accumulation rates. Excluding the coastal upwelling area offshore Oman, primary productivity rates are very similar throughout the Arabian Sea (*Qasim, 1982; Banse, 1987, Van der Weijden et al., 1999*). The difference in surface water productivity and export production between the Pakistan coastal area and the open ocean region is probably less than a factor two (*Qasim, 1982; Brock et al., 1994; Pollehne et al., 1993*). Accordingly, the reactive P flux exported from the photic zone for these two areas is of the same order of magnitude. P_{reac} accumulation rates on the continental margin, however, are 5 to 20 times higher than in the deep Arabian Basin (Table 2). This would imply that reactive P is more efficiently buried in shallow, continental slope sediments located within the OMZ.

This conclusion, however, seems in conflict with the observed pattern of P burial efficiencies (Fig 6a) and the commonly held view that P regeneration is more efficient

under oxygen depleted bottom water conditions. In order to solve this paradox, we will first investigate two mechanisms that may explain higher P burial efficiencies under oxic conditions (*Ingall and Jahnke, 1994, 1997; Krajewski, 1994*), namely 1) phosphate cycling associated with reactive iron oxides, and 2) redox dependent P cycling of benthic microorganisms.

1) Phosphate cycling associated with reactive iron oxides

The diagenesis of P is closely linked to that of iron in sediments underlying oxic bottom water conditions (*Krom and Berner, 1981; Sundby et al., 1992; Slomp et al., 1996*). Phosphate liberated from organic matter degradation or fish debris dissolution is scavenged in the oxic part of the sediments by Fe-hydroxides. The presence of a distinct iron oxide sublayer may act as a near-surface trap for phosphate and reduce the loss of reactive P to the water column (*Mortimer, 1971*). In reality, however, benthic phosphate fluxes under oxic bottom water conditions are very variable, depending on the buffer capacity of the iron oxides and the oxygen penetration depth (*Sundby et al., 1993, McManus et al., 1997*). Upon burial in the suboxic part of the sediment, iron oxides are reduced, resulting in desorption of phosphate. Ongoing “iron pumping” will result in the build-up of the interstitial phosphate concentration below the oxic-anoxic boundary, until CFA (carbonate fluorapatite) or a precursor phase starts to precipitate (*Van Cappellen and Berner, 1988; Slomp et al., 1996*), thereby increasing the burial efficiency of P.

In the deep basin sediments of the Arabian Sea, active iron cycling is evidenced by a decrease of sedimentary Fe/Al ratios (*Van der Weijden et al., 1999*) and increasing interstitial Fe²⁺ concentrations with sediment depth (Fig. 2). However, dissolved iron and phosphate concentrations do not simultaneously increase with depth (with exception of BC458). Moreover, interstitial phosphate concentrations remain relatively low, indicating that iron redox cycling does not result in the build up of dissolved phosphate concentrations. In contrast, sediments located within the OMZ are all characterized by high dissolved phosphate concentrations, inducing precipitation of authigenic apatite (**Chapter 4**). It is, therefore, unlikely that P retention by authigenic apatite formation is more efficient for deep basin sediments. Phosphogenesis in deep basins may occur deeper in the sediment (*Lucotte et al, 1994; Filippelli and Delaney, 1996; Chapter 7*), but this process is not controlled by early diagenetic iron cycling. Furthermore, total solid-phase P concentrations decrease with sediment depth in all deep basin sediments (Table 2), which is probably primarily related to phosphate desorption from iron oxide during early diagenesis. Apparently, iron cycling cannot retain this pool of reactive P and prevent a significant loss of phosphate to the bottom water. This is consistent with the view that a surface layer of iron oxides should not be considered as a trap for phosphate, but rather as a regulator of the benthic phosphate flux (*Anschutz et al., 1998*). We conclude, therefore, that early diagenetic iron cycling is not responsible for the observed PBE pattern in Arabian sea sediments.

2) Redox dependent P cycling of microorganisms

A second mechanism that may explain higher P burial efficiencies under oxic bottom water conditions is related to the ability of benthic microorganisms to accumulate and

store P under aerobic conditions (Toerien, 1990). When the redox conditions become more reducing, the stored P will be used as an energy source and eventually be released to the porewater. During intense cycling of P by microorganisms under oxic conditions, refractory organic P compounds are produced that can no longer be recycled in the sediment (Gächter and Meyer, 1993). The presence of such refractory organic P compounds has been demonstrated by NMR studies in slowly depositing sediments (Ingall et al., 1990; Berner et al. 1993). Redox dependent P cycling of benthic microorganisms may partially explain the relatively low sedimentary C_{org}/P_{org} ratios under more oxygenated bottom water conditions (Fig. 3c; Ingall et al., 1993; Ingall and Jahnke, 1994).

The potential influence of redox dependent P cycling of microorganisms on the P burial efficiency can be estimated, assuming that the different sedimentary C_{org}/P_{org} ratios under oxic/anoxic conditions are solely the result of this process. The excess benthic phosphate flux expected to diffuse out of the sediment as the result of anoxic bottom water conditions ($J_{P_{excess}}$) is calculated with the equation:

$$J_{P_{excess}} = \frac{C_{org} \times MAR}{1.2} \times \left[\frac{1}{C_{org}/P_{org} (ox)} - \frac{1}{C_{org}/P_{org} (anox)} \right] \quad (8)$$

where C_{org} represents the organic carbon concentration (wt%; Table 1), MAR the mass accumulation rate (Table 1), and $C_{org}/P_{org} (ox)$ and $C_{org}/P_{org} (anox)$ the average C/P ratio of organic matter buried under oxic conditions (200) and anoxic conditions (500) respectively (this study). In this hypothetical situation it is assumed that the C_{org} accumulation rate does not change as a result of the different redox conditions (if we consider lower organic matter burial rates as the result of oxic organic matter degradation, estimates for $J_{P_{excess}}$ would become even less). Calculated $J_{P_{excess}}$ fluxes are all minor compared to the benthic phosphate fluxes (Table 3). Changing the C_{org}/P_{org} burial ratio, thus, only marginally effects the P burial efficiency. This is consistent with the conclusion that organic matter is not the main source of P regeneration in continental slope sediments.

Nature of the accumulating P flux

We propose that the decrease of P burial efficiency with water depth observed in this study (Fig 6a) is not related to differences in bottom water redox conditions, but rather is the result of differences in the quantity and quality of the reactive P flux arriving at the sediment surface. Not only the similar shapes of the benthic phosphate flux and the P_{reac} accumulation rate versus depth (Fig 3a,b), but also the high correlation between these parameters ($r^2 = 0.98$, corresponding with an average P burial efficiency of 28 %; Fig. 6b), suggest that benthic phosphate fluxes are generally controlled by the P deposition flux. This is consistent with the relatively higher benthic phosphate fluxes in

sediments underlying the upwelling area of the Oman Margin (Fig. 3a). For oxic sediments from the deep basin, the higher calculated PBEs are mainly due to the relatively low benthic phosphate fluxes. As discussed, this may partly be explained by the possible underestimation of the benthic phosphate fluxes. However, is it more plausible that the lower benthic phosphate fluxes are related to low input of reactive P in these sediments. The low P_{reac} accumulation rates in comparison with continental slope sediments indicate that reactive P remobilization occurred predominantly in the water column or at the sediment water interface. This is confirmed by sediment trap studies in the Arabian Sea that show a large reduction in the downward C_{org} flux (the prime carrier of P) in the upper 1000 m of the water column (Lee *et al.*, 1998). As a large fraction of reactive P is remobilised with increasing water depth, the nature of the remaining P will become more refractory, and, as a consequence, less phosphate regeneration will occur in the sediment. Absence of significant P mobilisation after burial in the deep basin sediments is clearly demonstrated by the low interstitial phosphate concentrations (Fig. 2) and the constant $C_{\text{org}}/P_{\text{org}}$ ratio with sediment depth (Fig. 3c). In contrast, more shallow sediments receive a much higher input of reactive P which will induce higher regeneration rates, and thus lower (sedimentary) P burial efficiencies. The effectiveness of P burial in the Arabian Sea, therefore, is primarily regulated by differences in P regeneration occurring in the water column and at the sediment water interface.

We conclude that the PBE pattern depicted in Figure 6a does not reflect the real P retention relative to the P produced in upper water column, because P regeneration processes occurring in water column and at the sediment water interface are not included. Based on the high P_{reac} accumulation rates we argue that P is more efficiently buried in continental margin sediments of the Arabian sea. This may be attributed to several processes, namely a) shallower water depths, resulting in higher deposition rates of reactive P, b) more rapid burial of P as the result of higher sediment accumulation rates, c) low BWO concentrations which may enhance the preservation of organic matter (*e.g.* Demaison and Moore, 1980; Canfield, 1993) and fish debris (Chapter 5), and d) high rates of phosphogenesis, induced by high interstitial phosphate concentrations. The exact role of bottom water redox conditions on sedimentary P cycling remains complex, but for Arabian Sea sediments no direct evidence was found for more efficient P burial under oxygen depleted bottom waters.

Conclusions

In the Arabian Sea, benthic phosphate fluxes are highest on the continental slope, underlying low bottom water oxygen concentrations. Reactive P regeneration in these sediments occurs briefly after deposition. Organic matter degradation and phosphate desorption from iron oxides provide insufficient phosphate to explain the high benthic phosphate fluxes in these marine environments. The good correlation between benthic phosphate fluxes and accumulation rates of P associated with fish debris in surface sediments, and the potentially high accumulation rate fish debris in the Arabian Sea

Chapter 6

indicate that dissolution of biogenic apatite largely governs the benthic phosphate fluxes in these sediments. Factors governing dissolution and preservation of fish debris thus play an important role in the burial and regeneration of P in continental margin sediments. Although benthic phosphate fluxes are much higher, P removal by burial is more efficient in continental slope sediments located within the OMZ than it is in deep basin sediments. The effectiveness of P burial is primarily regulated by P regeneration occurring in the water column and at the sediment water interface.

This study illustrates the complexity of P cycling in the marine environment. No direct evidence was found that P is more efficiently buried in oxic relative to dysoxic bottom water conditions in the Arabian Sea. P regeneration and burial is determined by the complex interplay of primary productivity in the surface water, composition of the accumulating P flux, water depth, sediment accumulation rate, redox conditions of the bottom water, and the possible occurrence of phosphogenesis.

Acknowledgements - The chief scientists on the NIOP cruises during the 1992-1993 Netherlands Indian Ocean Programme were W.J.M. van der Linden and C.H. van der Weijden. H. de Waard, A.F.M. de Jong and G. Nobbe are thanked for their contribution to the laboratory analyses. H.F. Passier is acknowledged for providing the porewater data of BC484 and BC487. Critical reviews by C.H. van der Weijden, I.A. Nijenhuis and A. Rutten significantly improved this manuscript. This research was funded by the Netherlands Organization for Scientific Research (NWO).

7

Factors controlling the Phosphorus burial efficiency in Arabian Sea sediments during the Late Quaternary

S.J. Schenau, G.J. Reichart, and G.J. de Lange

Abstract - In this study the response of sedimentary phosphorus (P) burial to changes in primary productivity and bottom water oxygen concentrations during the Late Quaternary was investigated, using two sediment cores from the Arabian Sea, one recovered from the continental slope and the other from the deep basin. The average solid-phase P speciation in both cores is similar: authigenic and biogenic (fish debris) apatite make up the bulk of the P inventory (ca. 70 %), whereas P adsorbed to iron oxides, organic P, and detrital apatite constitute minor fractions. Postdepositional redistribution has not significantly altered the downcore distribution of total solid-phase P. The phosphorus burial efficiency (PBE) is generally lower during periods of increased paleoproductivity. This is caused by a) partial decoupling of the P export flux, consisting primarily of particulate organic P, and the P burial flux, consisting primarily of biogenic and authigenic apatite, and b) the lack of increased rates of phosphogenesis during periods of higher P deposition. Fluctuations in bottom water oxygen content may have affected P burial on the continental slope sediments of the Arabian Sea, but the precise impact on the PBE remains unclear. The results of this study indicate that higher primary productivity induces more efficient P cycling, irrespective of the fact whether this leads to bottom water anoxia or not. On time scales exceeding the oceanic P residence time, this process may induce higher surface water productivity, thus creating a positive feedback loop. In the Arabian Sea, this feedback mechanism is likely to be active on (sub-) Milankovitch time scales, because P regenerated on the continental slopes of the Oman and Somalian coastal upwelling areas is reintroduced into the eutrophic zone relatively fast.

Introduction

Primary productivity in the oceans is governed by the availability of nutrients in the photic zone. Nitrogen is the limiting nutrient in most present-day coastal waters (Howarth, 1988). Phosphorus forms, in contrast to nitrogen, no important gaseous phases in the natural environment, and the oceanic P mass balance is solely governed by the input from fluvial and eolian sources and burial in sediments (e.g. Froelich et al., 1982; Delaney, 1998). Phosphorus availability is considered to be the main factor controlling net primary productivity in the oceans on geological time scales, because long-term shortages of nitrogen are replenished by nitrogen fixation from the atmosphere (Holland, 1978; Broecker and Peng, 1982; Howarth et al., 1995). Marine productivity, in turn, determines the burial of organic carbon, and controls the atmospheric CO₂ and O₂ contents. Detailed knowledge of phosphorus cycling in the oceans thus provides a better understanding of the biogeochemistry of the ocean and atmosphere on geological time scales (e.g. Van Cappellen and Ingall, 1994, 1996).

Phosphorus removal from the oceans is governed by the interplay between the supply of particulate P to the sediment surface, and P regeneration processes occurring in water column and sediment (e.g. Froelich et al., 1982; Krajewski et al., 1994; Föllmi, 1996). Sedimentary-P remobilisation processes include organic matter decomposition, phosphate desorption from iron oxides, and dissolution of fish debris (e.g. Froelich et al., 1988; Van

Cappellen and Berner, 1988). Phosphorus burial is dependent on several environmental factors, such as sedimentation rate, sediment porosity, microbial activity, the occurrence of authigenic apatite formation (phosphogenesis), and bioturbation rates (*e.g. Krajewski et al., 1944; Filippelli and Delaney, 1994*). Ingall and Jahnke (1994) have shown that benthic regeneration of reactive phosphorus is more extensive when bottom waters are oxygen-depleted, resulting in lower P burial efficiencies. Enhanced loss of P from sediments over long periods of bottom water anoxia (*i.e.* exceeding the oceanic P residence time) will lead to an increased supply of P to the surface waters and may promote higher biological productivity (Ingall *et al.*, 1993; Ingall and Jahnke, 1994, 1997). This positive feedback between water column anoxia, benthic P regeneration, and marine productivity may link organic-rich sediments to anoxic bottom water conditions (Ingall and Jahnke, 1994, 1997). On shorter time scales, enhanced P regeneration may also affect productivity in shallow coastal upwelling areas, where deeper waters are directly carried into the euphotic zone (Ingall and Jahnke, 1994).

We have investigated P burial in Arabian Sea sediments, using two cores taken from respectively the Pakistan continental slope and the deep Arabian Basin, both covering the last 120 kyr. The Arabian Sea is one of the most productive ocean basins of the world. During the Northern Hemisphere summer, strong southwestern monsoon winds cause intense upwelling offshore Somalia and Oman (*e.g. Wyrki, 1973; Slater and Kroopnick, 1984*). This causes a high seasonal productivity throughout the Arabian Sea (*e.g. Qasim, 1982*). High downward fluxes of organic matter, in combination with a sluggish intermediate water ventilation result in an intense Oxygen Minimum Zone (OMZ) between 150 and 1250 m water depth (*e.g. Slater and Kroopnick, 1984*), with bottom water oxygen (BWO) concentrations $< 2 \mu\text{M}$ (*e.g. Van Bennekom and Hiehle, 1994*). Sediment core studies have revealed large fluctuations in paleoproductivity during the Late Pleistocene (Shimmield, 1992; Emeis *et al.*, 1995; Reichart *et al.*, 1998). Frequency analysis has shown that paleoproductivity records from the Arabian Sea exhibit a strong 23-kyr signal, indicating that surface water productivity changes primarily reflect precession controlled changes in summer monsoon upwelling (*e.g. Clemens et al., 1991; Reichart et al., 1998*). The intensity and vertical extension of the OMZ have strongly varied during the Late Quaternary as a result of the differences in the organic carbon rain rate and deep winter mixing (Altabet *et al.*, 1995; Reichart *et al.*, 1997; Den Dulk *et al.*, 1998). Continental slope sediments have thus periodically experienced oxic and suboxic bottom water conditions. Sediment records from the Arabian Sea provide an excellent opportunity to elucidate the mechanisms that control P removal from the oceans under different paleoenvironmental conditions.

Material and methods

Sample locations

The two pistoncores selected for this study were taken during the Netherlands Indian Ocean Program (NIOP) in 1992. Pistoncore 455 (PC455) was taken on the continental slope of the Pakistan Margin ($23^{\circ}33'.3$, $65^{\circ}57'.2$) from a water depth of 1002 m, presently situated in a low oxygen environment ($BWO < 2 \mu M$). Pistoncore 487 (PC487) was recovered from the central Arabian Basin ($19^{\circ}54'.8$, $61^{\circ}43'.3$) from a water depth of 3574 m, and is located well below the present-day OMZ ($BWO = 151 \mu M$). The locations of the sample sites are shown in Figure 1. The sediments consist mainly of homogeneous, light-greenish hemipelagic muds alternated by darker organic-rich intervals. In PC455 most of these darker intervals are finely laminated.

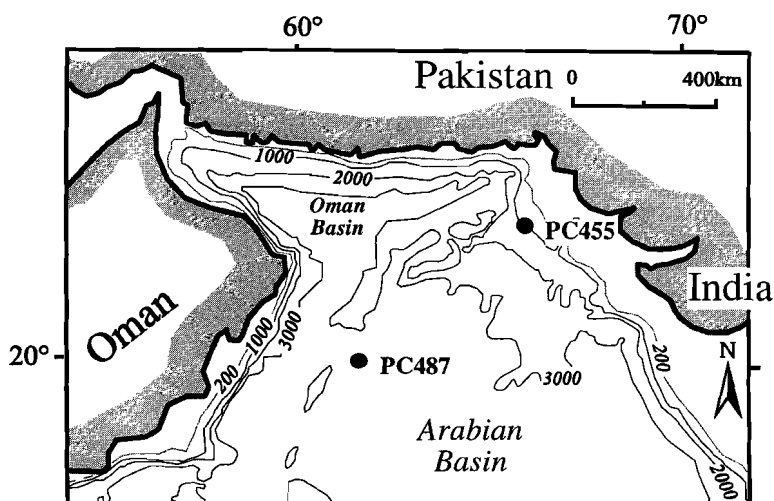


Figure 1. Sample locations of PC 455 (Pakistan Continental Margin) and PC 487 (Arabian Basin).

Pore water analysis

Porewater extractions were started on board within 24 hours of core collection according to shipboard routine (De Lange, 1992a). The sediment cores were sluiced into a glovebox, which was kept under low-oxygen conditions ($O_2 < 0.0005\%$) and at a constant in-situ bottom water temperature. Sediments were put into Reeburgh-type squeezers, and under a nitrogen pressure of up to 7 bar, pore waters were extracted. Shipboard analysis of ammonium, alkalinity and phosphate started within 12 hours after extraction of the pore waters. Alkalinity was measured by Gran titration (after Gieskes, 1973). Phosphate and

ammonium were measured on a TRAACS 800 auto-analyser, after the methods of *Strickland and Parsons (1968)* and *Solarzano (1986)* respectively. All analyses were performed in duplicate. Precision is better than 2%.

Solid-phase analysis

Samples for solid-phase analyses were taken at regular intervals of 5 to 10 cm, giving a temporal sample resolution of 0.5 to 2 kyr (depending on the linear sedimentation rate). Porosity and dry bulk density of the sediment were calculated by measuring weight loss of fixed volume samples after freeze-drying. Dried samples were ground in an agate mortar, and subsamples were taken for geochemical analyses after homogenization. After removal of inorganic carbon with 1 M HCl, organic carbon (C_{org}) and total nitrogen (N_{tot}) contents were measured with a NA 1500 NCS analyser (relative errors < 1 %). For the determination of bulk concentrations of P, 250 mg sample was digested in 5 ml of a 6.5 : 2.5 : 1 mixture of $HClO_4$ (60%), HNO_3 (65%) and H_2O , and 5 ml HF (40%) at 90°C. After evaporation of the solutions at 190°C on a sand bath, the dry residue was dissolved in 50 ml 1 M HCl. The resulting solutions were analysed with a Perkin Elmer Optima 3000 Inductively Coupled Plasma Atomic Emission Spectrometer (ICP-AES). All results were checked using international (SO1, SO3) and in-house standards. Relative errors for duplicate measurements are better than 3 %. The chronology of the pistoncores is based on $\delta^{18}O$ records (*Reichert et al., 1998*; **Chapter 2**). Mass accumulation rates (MARs) were calculated by multiplying linear sedimentation rates (LSRs) with dry bulk densities.

The solid-phase speciation of P and Fe was examined in sediment samples from one interglacial and two glacial intervals, using a 5-step sequential extraction method. The high resolution of the time frames was used to select samples that were deposited contemporaneously (with the exception of two samples in the interglacial interval). Approximately 125 mg of dried and ground sediment were subsequently extracted with 1) 25 ml 2 M NH_4Cl (pH=7, repeated 8 times), 2) 25 ml citrate dithionite buffer (CDB, pH=8), 3) 25 ml 1 M Na-Ac (pH=4), 4) 25 ml 1 M HCl, and 5) 20 ml HF/ HNO_3 / $HClO_4$ mixture (see Table 2 in **Chapter 5** for details). After extraction steps 2, 3 and 4, the sediment was rinsed with 2 M NH_4Cl (pH=7) and demineralised water to prevent resorption of phosphate. This extraction scheme is an adaptation of the SEDEX method developed by *Ruttenberg (1992)* for marine sediments. The 2 M NH_4Cl extraction (step 1) was inserted to determine the P fraction associated with biogenic (fish debris) apatite (**Chapter 5**). All extracted solutions were analysed with ICP-AES. Precision for P was generally better than 5%, except for steps 2 and 3 (10%). The recovery for all extraction steps with respect to total P varied between 80 and 90 %. This deficit is not caused by sample loss during the extraction procedure, but is due to systematic errors in the measurements of low P concentrations by ICP-AES. Iron oxide contents (reactive iron) were determined from the iron concentration extracted in step 2 (Na-dithionite). Organic phosphorus was determined as the difference between 1 M HCl extractable P before and after ignition of the sediment (550 °C, 2h; *Aspila et al., 1976*). All measurements were done in duplicate (precision better than 2 %). Relative errors for samples containing relatively low organic phosphorus concentrations are large (up to 50 %), because it is calculated as the difference between two large values.

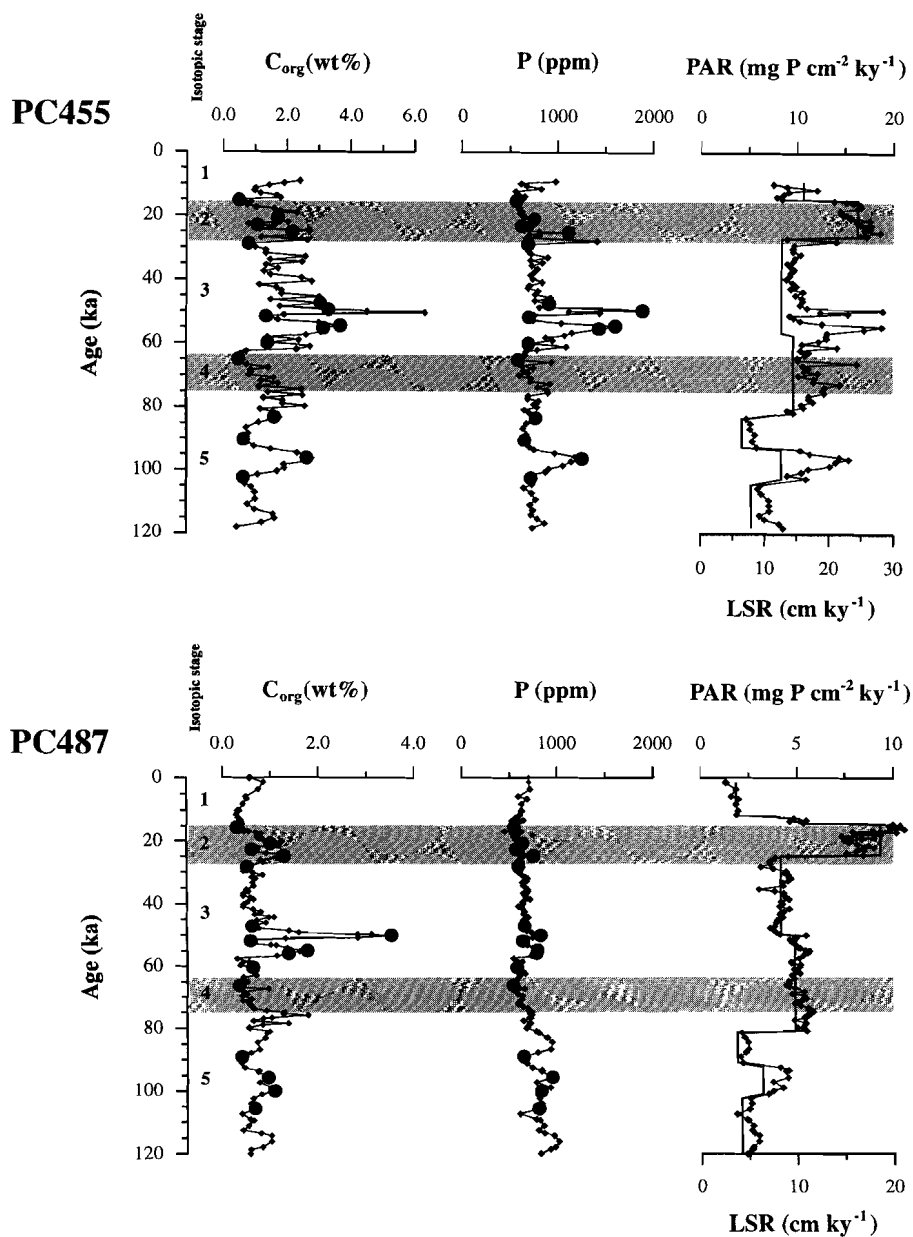


Figure 2. Sediment records of organic carbon (C_{org} ; wt%), total solid-phase P (ppm), P accumulation rate (PAR; mg P cm² ky¹), and linear sedimentation rate (LSR; cm ky¹) versus age for PC455 and PC487. The samples selected for sequential extraction analysis (Fig. 5) are indicated by the large filled dots. The shaded intervals indicate isotopic stages.

Results and Discussion

Burial of total solid-phase P

Total solid-phase P concentrations in PC455 vary from 700 - 2000 ppm, and are generally higher in the organic-rich intervals (correlation with C_{org} : $r^2=0.56$) (Fig. 2). In PC487, total solid-phase P concentrations are lower (600-1000 ppm), and show less variation with depth. In contrast to PC455, there is no apparent correlation between total solid-phase P and C_{org} in PC487 ($r^2 = 0.14$). Phosphorus accumulation rates (PARs), in particular those of PC487, are mainly regulated by variations in LSR, and vary between 5-25 for PC455 and 2-10 mg P cm⁻² ky⁻¹ for PC487 (Fig. 2). During the glacial period (isotopic stages 2, 3, and 4), PARs are approximately twice as high as for interglacial stage 5.

NIOB cores PC487 and PC455 have been intensively studied in order to reconstruct paleoenvironmental conditions in the Arabian Sea (Reichart *et al.*, 1998; Den Dulk *et al.*, 1998; **Chapters 2 and 5**). The downcore C_{org} patterns in these cores can be correlated with sediment cores throughout the Arabian basin. These C_{org} variations have been related to changes in paleoproductivity (Shimmiel, 1992; Emeis *et al.*, 1995; Reichart *et al.*, 1998), which is confirmed by independent geochemical (Ba, P) and paleontological (*G. bulloides*) proxies for paleoproductivity (Reichart *et al.*, 1998; Den Dulk *et al.*, 1998; **Chapter 5**). Accordingly, the organic-rich intervals in PC455 and PC487 represent periods of increased primary productivity. The bottom waters of PC455 have periodically experienced reduced BWO concentrations as the result of changes in OMZ intensity through time. This is shown by the alternation of laminated intervals, and the downcore distributions of redox-sensitive elements (Mn, V, Mo; Reichart *et al.*, 1998; **Chapter 2**) and benthic foraminifera (Den Dulk *et al.*, 1998). The bottom waters of PC487, on the other hand, have remained well-oxygenated during the last 185 kyr (**Chapter 2**), since the OMZ has never extended to the deepest part of the Arabian Basin.

To evaluate P burial under different paleoenvironmental conditions, we have reconstructed paleoburial efficiencies for P (i.e. the fraction of the depositional P flux that is preserved upon burial). In the oceans, reactive P is primarily delivered to the sediment as particulate organic matter (*e.g.* Delaney, 1998). Other vertical P fluxes, such as deposition of fish debris and iron-bound P are negligible compared to this flux (**Chapter 6**). The particulate P flux to the seafloor can thus be estimated by calculating the paleoexport productivity of organic phosphorus (PP_{export} ; gP m⁻² y⁻¹), for which the transfer function was used developed by Sarnthein *et al.* (1992):

$$PP_{export} = \frac{24.16 \times C_A^{0.493} \times z^{0.3} / LSR_{OCF}^{0.105}}{(C/P)_{org}} \quad (1)$$

where C_A is the organic carbon accumulation rate (g m⁻² y⁻¹), z the water depth (m), LSR_{OCF}

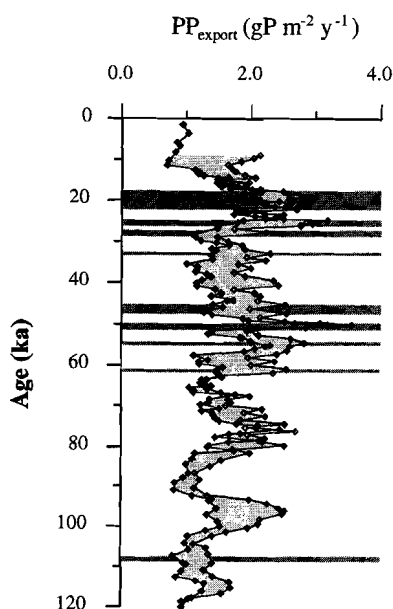


Figure 3. Records of calculated paleoexport fluxes of particulate organic P (PP_{export} ; $gP\ m^{-2}\ y^{-1}$) versus age for PC455 (\diamond) and PC487 (\blacklozenge). The shaded area between the two curves represents the difference in PP_{export} flux between PC455 and PC487. The dark shaded bands indicate laminated layers present in PC455.

the organic-carbon-free linear sedimentation rate ($cm\ ky^{-1}$), and $(C/P)_{org}$ the Redfield nutrient ratio of fresh organic matter (106) (Fig. 3). The phosphorus burial efficiency (PBE) can be calculated using the equation:

$$PBE\ (\%) = 100 \times \frac{[P] \times MAR}{10^5 \times PP_{export}} \quad (2)$$

where $[P]$ is the total solid-phase P concentration (ppm), and MAR the mass accumulation rate ($g\ cm^{-2}\ ky^{-1}$) (Fig. 4). Note that regeneration processes occurring during transit through the water column are included in the calculated PBEs. The PBEs in PC487 are generally lower during periods of increased productivity, although not distinguishable during stage 5 (Fig. 4). PC455 shows the same pattern, but somewhat less distinct than in PC487. For both cores, PBEs are higher during the glacial period. Before discussing the potential causes for the different modes of P burial, it must be established whether these PBE patterns are the

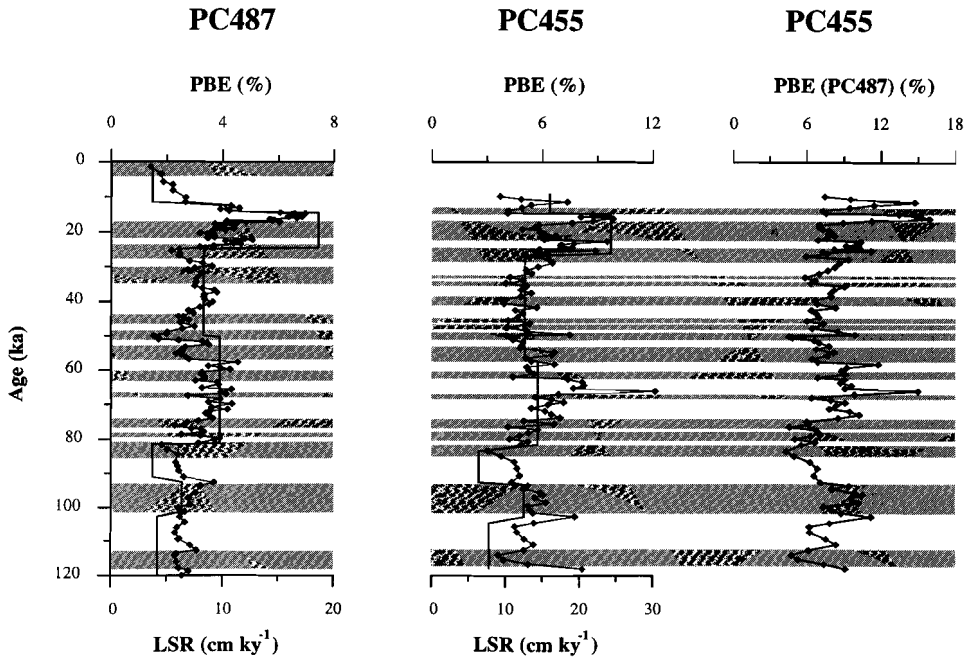


Figure 4. Records of burial efficiencies for phosphorus (PBE) versus age for PC455 and PC487, as calculated with equation 2 (see text). The LSR has been plotted to identify the shifts in PBE related to the abrupt changes of the mass accumulation rate. For PC455, the PBE has also been calculated using the calculated paleoexport fluxes for PC487 (Fig. 3) (PBE(PC487)). The shaded intervals indicate sediment enriched in organic matter deposited during periods of increased paleoproductivity.

result of changes in sedimentation rate or BWO conditions.

The PBEs calculated with equation 2 are sensitive to variations in MAR. Accordingly, the downcore PBE distributions show large shifts at the abrupt changes in LSR (Fig. 4). In the Arabian Sea, variations in sedimentation rates are primarily controlled by changes in dust input, which are related to glacial-interglacial variability in continental aridity (Clemens and Prell, 1990; Sirocko, 1991). The resolution of the time frame used in this study does not allow the resolution of variations in MAR on precessional or sub-Milankovitch time scales. Periods of precession-related productivity maxima are linked to intensified summer monsoon wind strength (Clemens and Prell, 1990). Intensification of the monsoon causes more humid climate conditions and reduces dust formation. Moreover, strong SW monsoonal winds cause a northward shift of the wind trajectories, which suppress the northwestern winds that carry dust from the Arabian Peninsula to the Arabian Sea (Anderson and Prell, 1993; Sirocko et al., 1993). Consequently, periods of increased productivity are associated with reduced sedimentation rates. Incorporating lower MARs for periods of high productivity in equation 2 would result in an even sharper contrast in PBE between periods of high and low

productivity. (Sub)-Milankovitch scale fluctuations in sedimentation rate thus cannot account for the calculated variations in PBE.

Calculation of paleoexport productivity rates with equation 1 is, in principle, only valid for pelagic sediments deposited in oxic environments with BWO concentrations above $50 \mu\text{M}$ (Sarnthein *et al.*, 1992). Dysoxic bottom waters may cause enhanced preservation of organic matter, resulting in an overestimation of the $\text{PP}_{\text{export}}$ flux. This may explain the overall higher calculated $\text{PP}_{\text{export}}$ fluxes for PC455 compared to PC487 (Fig. 3). However, the $\text{PP}_{\text{export}}$ fluxes in PC455 are not systematically higher in the laminated intervals, or in intervals deposited during increased productivity. To determine the potential effect of organic matter preservation in PC455, the PBEs were recalculated using the $\text{PP}_{\text{export}}$ fluxes calculated for PC487 (i.e. sediments deposited under oxic conditions), assuming that fluctuations in paleoproductivity were similar throughout the Arabian basin (Reichart, 1998). The recalculated values do not significantly alter the PBE pattern (Fig. 4). Periodical enhanced preservation of organic matter therefore does not induce the lower PBEs in the organic-rich intervals of PC455.

We conclude that the calculated PBE patterns reflect genuine differences in oceanic P cycling. The absolute values of the PBEs must be considered with some caution in view of the inaccuracies included when calculating $\text{PP}_{\text{export}}$ fluxes. However, the results display a distinct contrast in PBE under different paleoenvironmental conditions. In the next section, the burial behaviour of the different P fractions will be discussed, namely 1) organic P, 2) biogenic apatite, 3) P adsorbed to iron oxides, 4) detrital apatite, and 5) authigenic apatite, in order to determine the processes responsible for the lower PBE during periods of increased paleoproductivity.

Sedimentary P speciation

1) Organic phosphorus

Organic phosphorus (P_{org}) constitutes only a minor P fraction relative to total solid-phase P in PC455 and PC487 (on average respectively 6 and 12 %; Fig. 5). Consequently, organic P is a relatively unimportant reactive P sink in the Arabian Sea. This finding is consistent with P speciation results from other deep pelagic sediments (Lucotte *et al.*, 1994; Filippelli and Delaney, 1996; Delaney and Anderson, 1997; Table 1). During periods of high paleoproductivity, P_{org} concentrations increase in both cores (Figs. 5 and 6), in accordance with the higher organic matter contents (Fig. 2). In PC487, $\text{C}_{\text{org}}/\text{P}_{\text{org}}$ ratios are generally higher in the organic-rich intervals, indicating that burial of organic P relative to organic carbon is less efficient during periods of high productivity. A similar pattern is absent in PC455. The $\text{C}_{\text{org}}/\text{P}_{\text{org}}$ ratios in PC455 are higher (680-1470) than in PC487 (130-570).

Sedimentary $\text{C}_{\text{org}}/\text{P}_{\text{org}}$ ratios are usually higher than those of fresh marine planktonic organic matter (106; Redfield *et al.*, 1963), as the result of preferential regeneration of P relative to carbon during organic matter decomposition (e.g. Suess and Müller, 1980; Mach *et al.*, 1987; Ingall and Van Cappellen, 1990). At low sedimentation rates ($< 2 \text{ cm ky}^{-1}$), however, sedimentary $\text{C}_{\text{org}}/\text{P}_{\text{org}}$ ratios are relatively low (50-200) due to prolonged degradation

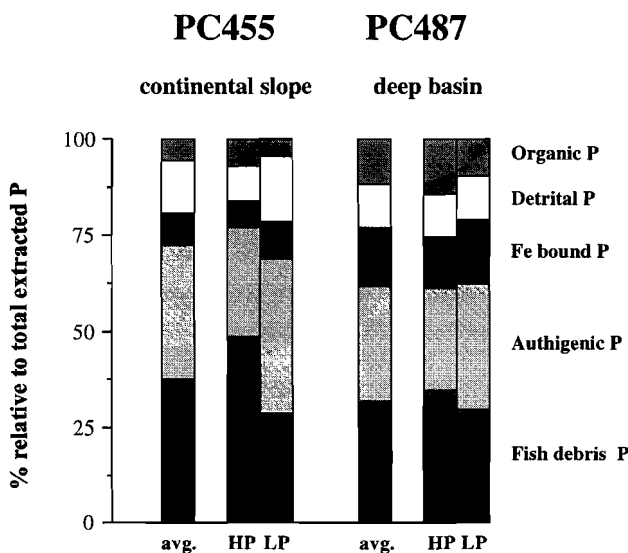


Figure 5. The solid-phase P speciation relative to total extracted P for sediment samples from PC455 and PC487. The average P speciation for all samples (avg.), and the average P speciation for periods of high (HP) and low paleoproductivity (LP) is given.

of the residual organic matter or high proportions of bacterial organic matter (Ingall and Van Cappellen, 1990). In addition, bottom water redox conditions affect the burial of P_{org} (Ingall et al., 1993). The fluctuations in sedimentary C_{org}/P_{org} ratios in PC487 cannot be attributed to these parameters, because the bottom waters of PC487 have remained well-oxygenated during the Late Quaternary, and sedimentation rates were lower during periods of increased productivity. Sedimentary C_{org}/P_{org} ratios may also be influenced by temporal admixing of terrestrial organic matter, which is depleted in P in comparison to marine organic matter (e.g. Ingall et al., 1993). Sedimentary organic matter in the northern Arabian Sea is primarily marine in origin (Pedersen et al., 1992; Den Dulk et al., 1998; Van der Weijden et al., 1999). Reichart (1997) found no evidence in Arabian Sea sediment records for enhanced input of terrestrial organic matter during periods of precessionally induced high productivity. Consequently, varying inputs of allochthonous organic matter are not likely to account for the fluctuations in the C_{org}/P_{org} ratios found in PC487. The most probable explanation for the C_{org}/P_{org} pattern in PC487 is different contributions of bacterial organic matter, which is characterized by low C_{org}/P_{org} ratios (~50; Reimers et al., 1990). During periods of low productivity, the organic matter deposited will be largely transformed into bacterial biomass. At higher organic matter accumulation rates, bacterial remains will be diluted with marine organic material deposited from the water column.

The relatively higher C_{org}/P_{org} ratios in continental slope core PC455 in comparison to PC487 are probably the result of the higher sedimentation rates, overall lower BWO

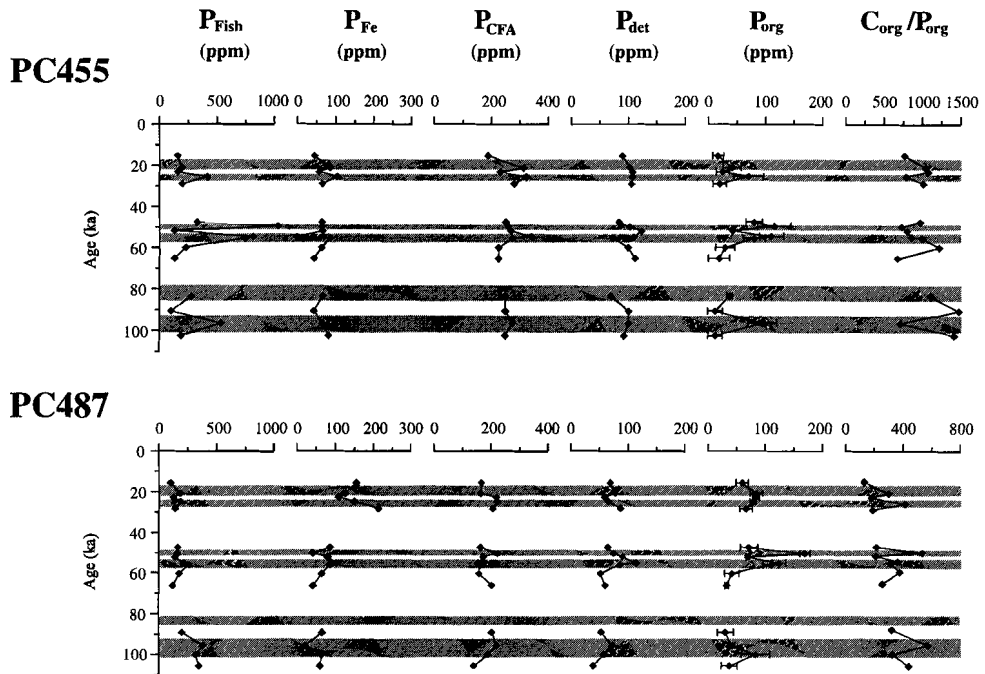


Figure 6. Records of solid-phase P speciation (ppm) and C_{org}/P_{org} molar ratios versus age for one interglacial and two glacial intervals from PC455 and PC487: P associated with fish debris (P_{fish}), iron-bound P (P_{Fe}), authigenic P (P_{CFA}), P associated with detrital apatite (P_{det}), and organic P (P_{org}). The shaded intervals indicate sediment deposited during periods of high paleoproductivity. The error bars for organic P indicate relative errors for duplicate measurements.

concentrations, and relatively lower bacterial organic matter contents. C_{org}/P_{org} ratios in PC455 show no consistent response with respect to changes in paleoproductivity or BWO conditions. Apparently, past fluctuations in BWO concentration have not substantially affected the C_{org}/P_{org} ratio in these sediments. We conclude that organic P retention is reduced in sediments of the deep Arabian Basin during periods of increased paleoproductivity, whereas no such trend is detected for continental slope sediments.

2) Biogenic apatite

At present, the Arabian Sea sustains relatively high fish production rates (FAO, 1981). The hard parts of fish consist primarily of amorphous hydroxy apatite (Posner et al., 1984), and burial of fish debris has been recognised as a potential mechanism for the removal reactive P from the oceans (Suess, 1981). The export flux of P associated with biogenic apatite is approximately a factor 10 less than that of organic P (Chapter 6). Phosphorus associated with fish debris (P_{fish}), however, constitutes on average the largest P fraction in the sediments of PC455 (37%) and PC487 (32%; Fig.5). This is remarkable, as fish debris are usually

considered to dissolve predominantly before burial, and, therefore, represent an unimportant sink of reactive P (e.g. Froelich et al., 1982; Table 1). The accumulation of P_{fish} is approximately 5 times more important than the accumulation of P_{org} (Fig. 5). Consequently, P regeneration from biogenic apatite in water column and sediment is relatively less intensive than that from organic matter. This may be explained by the relatively large size and high density of fish debris, which will make them sink fast to the seafloor. In addition, adsorption of fluoride occurring in water column and porewater makes biogenic apatites more resistant to dissolution.

The P_{fish} concentration in PC455 is enriched during periods of high paleoproductivity (Fig. 6; **Chapter 5**). Increased primary productivity rates induce higher rates of fish production, resulting in higher accumulation rates of fish debris. Additionally, P_{fish} concentrations in this core may have been subject to preservation effects related to the periodically reduced oxygen content of bottom water and top sediment. In contrast to oxic organic matter degradation, no acidity is produced during suboxic (denitrification, Mn- and Fe-oxide reduction) and anoxic (sulphate reduction) diagenesis (provided that H_2S is consumed by pyrite formation; *Canfield, 1991*), thereby reducing sedimentary dissolution of biogenic apatite. Moreover, phosphate porewater concentrations of anoxic sediments are usually high due to high rates of organic matter degradation, which will decrease dissolution of fish debris. Sediments located within a dysoxic environment, therefore, may experience enhanced preservation of fish debris (**Chapter 5**). In contrast to PC455, the P_{fish} concentration in the glacial intervals of PC487 is not significantly enriched during periods of high paleoproductivity (Fig. 6). This may be attributed to higher regeneration rates of fish debris in the deep pelagic site relative to the more shallow continental slope sediments as the result of lower MARs, larger water depth, and more oxygenated bottom water conditions (**Chapter 5**). In addition, the different food web structure of the more oligotrophic open ocean environment (*Ryther, 1969*), the high seasonality of primary productivity in the Arabian Sea, and the non-linear response of transfer efficiency to food availability (*Cushing, 1973*) causes fish production to be less sensitive to changes in surface water productivity

3) Detrital and iron-bound P

Iron oxides have a high adsorption capacity for phosphate (e.g. *Krom and Berner, 1981*), and iron-bound P constitutes an important P fraction in surface sediments overlain by oxic bottom waters (e.g. *Sundby et al., 1992; Slomp et al., 1996*). In PC455 and PC487, iron-bound P contents (P_{Fe}) are low compared to the other P fractions (8.5 and 15 % respectively; Fig.5), indicating that this fraction is an unimportant reactive P sink in Arabian Sea sediments. Low P_{Fe} contents are consistent with the low reactive iron oxide contents (Fe_{CDB}) in these sediments (2000-4000 ppm for PC487 and 1000-2000 ppm for PC455). As a result of a relatively high input of reactive organic matter, easily dissolvable iron oxides are reduced in the surface sediments of the continental slope (*Van der Weijden et al., 1999*) and the deep basin (**Chapter 6**) of the Arabian Sea during early diagenesis. The Fe_{CDB} fraction that remains below the zone of active iron oxide reduction consists of refractory iron oxides and some iron extracted from the partial dissolution of clay minerals (*Canfield, 1989; A. Rutten, personal communication*). The higher Fe_{CDB} contents of PC487 compared to PC455 are probably related to more oxygenated bottom water conditions and a lower reactivity of the sedimentary

Table 1. Partitioning of reactive P in sediments of the continental margin (Ruttenberg, 1993), the deep Pacific ocean (Filippelli and Delaney, 1996), and the Arabian Sea (this study), and estimates for the global average. Note that the P speciation (organic P, iron-bound P, and biogenic + authigenic P fractions) is similar for deep Pacific Ocean and Arabian Sea sediments. The global average for the reactive P partitioning in marine sediments (last column) was estimated using the P speciation results for the continental margin (Ruttenberg, 1993; second column) and the Arabian Sea (deep pelagic sediment; fourth column), assuming that the total annual sedimentary burial of reactive P in deep pelagic sediments is of the same magnitude as that in continental shelf areas (Froelich et al., 1984; Föllmi, 1996). The P fraction associated with biogenic apatite for continental margin sediments is assumed to constitute (likewise Arabian Sea sediments) half the authigenic + loosely sorbed P pool (31 %). Comparison with previous global estimates (Froelich et al., 1982; Ruttenberg, 1993) indicates that burial of authigenic and biogenic apatite fraction is relatively more important than previously assumed, whereas organic P burial is of less importance.

reactive P sinks				Estimated global average		
	Continental margin ¹	Pacific Ocean ²	Arabian Sea ³	Froelich (1982)	Ruttenberg (1993)	This study
organic-P	22 %	6 %	10 %	40 %	22 %	16 %
iron-bound P	16 %	11 %	12 %	11 %	22 %	14 %
loosely-sorbed	7 %	5 %	40 % ⁴	-	7 %	35.5% ⁴
carbonate-P	55 %	78 %		40 %	49 %	
fish-P				< 2 %		
authigenic P				38 %		

¹ Ruttenberg, 1993

² Filippelli and Delaney, 1996

³ Average from PC455 and PC487

⁴ Primarily consisting of P associated with biogenic apatite (fish debris). release with depth (Fig. 6).

organic matter. Burial of the P_{Fe} fraction in both cores is not affected by changes in paleoproductivity or BWO concentration (Fig.6). Apparently, also during periods of reduced organic carbon accumulation, sufficient reactive organic matter is present to ensure reduction of all easily reducible iron oxides.

Non-reactive, detrital apatite (P_{det}) is a small and rather constant P fraction in both cores (Figs. 5 and 6). The contribution of the non-reactive fraction, therefore, will not significantly influence the calculated PBEs. The higher P_{det} concentrations in PC455 are probably related to the higher content of lithogenic material.

4) Authigenic apatite

Phosphate released during diagenesis may be removed from the interstitial water by precipitation of an authigenic apatite phase (e.g. Jahnke et al., 1983; Froelich et al., 1988; Ruttenberg and Berner, 1993). Authigenic carbonate fluor apatite (CFA) is a relatively

important sink of reactive P in the sediments of this study (P_{CFA} ; Fig. 5). Interestingly, the average P_{CFA} fractions in the deep basin and continental slope core are of the same order of magnitude (35% and 29 % for PC455 and PC487 respectively). The P_{CFA} concentrations (Fig. 6) are similar to authigenic apatite contents reported for continental shelf sediments (Ruttenberg *et al.*, 1993; Louchouart *et al.*, 1997) and deep marine sediments (Lucotte *et al.*, 1994; Filippelli and Delaney, 1996; Table 1). A direct comparison is, however, not possible, since these latter studies did not distinguish between biogenic and authigenic apatite. The P_{CFA} concentrations do not (PC487), or barely (PC455) increase during periods of higher productivity (Fig. 6). Higher reactive P deposition rates, apparently, do not induce higher rates of in-situ phosphogenesis. This may be the result of postdepositional redistribution: phosphate liberated in intervals initially enriched in P diffuses away to precipitate as CFA outside these intervals. Hence, diagenetic redistribution of P may substantially have altered the downward distribution of solid phase P (Lucotte *et al.*, 1994), and thus the calculated PBEs.

Pore water chemistry may help to assess the importance of post-depositional redistribution processes. A subsurface maximum in the phosphate porewater concentration is present in PC487 and PC455 (Fig 7). These phosphate maxima ensure that all phosphate produced in the deeper part of the sediment (i.e. below the phosphate maxima) is buried as authigenic or adsorbed phosphate, instead of being lost to the water column. The subsequent decrease of the phosphate concentration with depth in both pistoncores (Fig. 7) indicates that dissolved phosphate is removed from the porewater and incorporated into a solid-phase in the top of the sediment column. In fact, in a more detailed study (including a boxcore taken on the same location as PC455) it was shown that authigenic apatite is presently forming in surface sediments of the Arabian Sea continental margins (Chapter 4). In deep pelagic environments phosphogenesis has been shown to originate from the gradual redistribution of P adsorbed to iron oxides or organic P into CFA (Lucotte *et al.*, 1994; Filippelli and Delaney, 1996), a process occurring over long time periods (up to millions of years). Interstitial phosphate concentrations in the deeper part of both pistoncores remain relatively low and constant (Fig. 7). Conversely, ammonium concentrations and alkalinity increase gradually with depth in both cores as the result of ongoing organic matter degradation. Dissolved phosphate concentrations, therefore, are also expected to rise with sediment depth. The gradual downcore increase of the $C_{\text{org}}/P_{\text{org}}$ ratio in PC487 also points to continued phosphate. The expected interstitial phosphate concentrations induced by organic matter degradation were calculated by making a best fit to the porewater data of ammonium (Ruttenberg and Berner, 1993; Schuffert *et al.*, 1994; Fig. 7), using whole sediment diffusion constants (Li and Gregory, 1974) and the nutrient ratios of decomposing organic matter (see caption of Fig. 7). It should be noted that these calculated phosphate concentrations are probably underestimated, since dissolution of fish debris and phosphate desorption from iron oxides may provide an additional source of interstitial phosphate. Nevertheless, a significant deficit between the observed and stoichiometrically calculated porewater phosphate is observed in both cores. This indicates that phosphate removal into the solid-phase by phosphogenesis or phosphate adsorption to sedimentary phases continues below the surface interval (Klump and Martens, 1987; Ruttenberg and Berner, 1993).

The P_{CFA} fraction in PC487 and PC455 does not increase with depth relatively to the

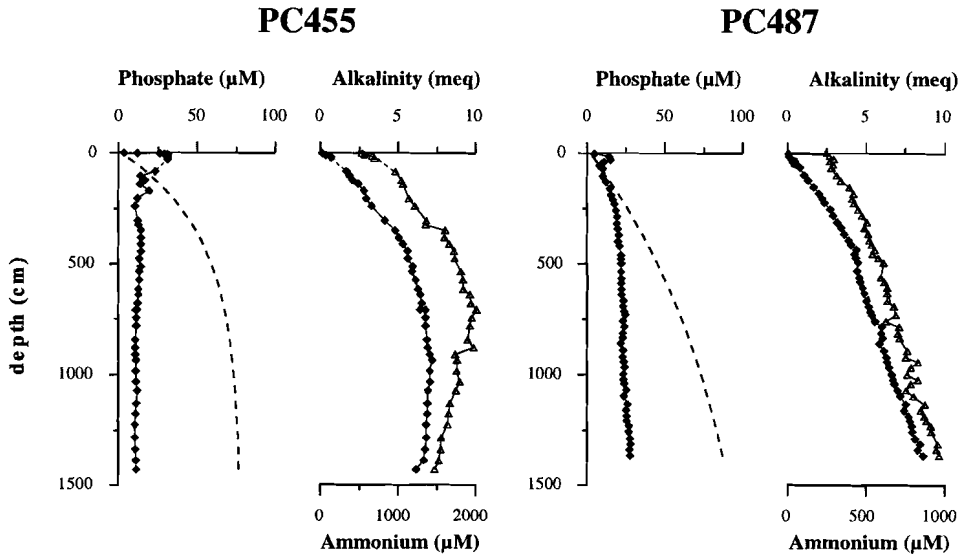


Figure 7. The porewater concentrations of phosphate, ammonium (\blacklozenge), and alkalinity (\blacktriangle) versus sediment depth in PC487 and PC455. The expected phosphate release as the result of organic matter degradation (dashed lines) was calculated using the ammonium porewater concentrations (Ruttenberg and Berner, 1993; Schuffert et al., 1994). Considering the suboxic conditions in the sediment, the ammonium concentrations have not been subject to oxidation. An empirical fit was made to the ammonium data with the equation (Berner, 1980): $C = C_0 + a(1 - e^{-\beta x})$, where C and C_0 are the concentrations of ammonium at depth x and 0 (cm) respectively, and a and β empirical constants. Assuming a nutrient ratio N:P of respectively 51.9 and 26.1 for PC455 and PC487 (determined from P_{org} and N_{tot} contents), and that organic matter is decomposing stoichiometrically (i.e. β for ammonium equals β for phosphate), the empirical constants α_p for phosphate was calculated with (Schuffert, 1994): $\alpha_p = \alpha_N * D_N / 16 * D_p$, where D_N and D_p are the whole diffusion coefficient constants for respectively ammonium and phosphate, corrected for the in-situ bottom water temperature (Li and Gregory, 1974).

other P fractions (Fig. 6). Precipitation of CFA is usually restricted to the uppermost part of the sediment because a) the increase of carbonate alkalinity with depth inhibits further formation of apatite (Jahnke et al., 1983; Glenn and Arthur, 1988), and b) CFA precipitation requires fluoride, which is mainly supplied by downward diffusion from the bottom water (Froelich et al., 1983). It can therefore be assumed that authigenic apatite precipitation takes place primarily in Arabian Sea surface sediments, in the deep basin as well as on the continental slope.

Although phosphogenesis appears to be chiefly restricted to the surface sediments, some downward diffusion of phosphate in the upper part of the sediment, as is currently occurring in PC455 and PC487 (Fig. 7), may alter the initially deposited solid-phase P contents. The impact of this process can be determined by examining the downcore P

distribution over longer (i.e. precessional) time intervals, because early diagenetic redistribution processes will transport phosphate only over relatively short distances. The rather constant P_{CFA} contents in PC455 and PC487 suggest that authigenic apatite precipitation rates remained fairly constant (relative to the MAR) over the last 120 kyr, but the number of data points presented in Fig. 6 is too small to fully corroborate this. For this reason, we have calculated average C_{org}/P_{react} ratios (i.e. the ratio of organic carbon to total reactive P) for precessional induced periods of high and low productivity (Fig. 8). Reactive P is here defined as all solid-phase P that may potentially be regenerated to the water column, which is equal to the total solid-phase P concentration minus detrital P concentration. Like the PBE calculated with equation 2, the C_{org}/P_{react} ratio gives an indication for the relation between input and burial of P (assuming that deposition of organic matter is the main supply of organic P), but has the advantage of not being affected by the abrupt shifts in LSR. For both cores, average C_{org}/P_{react} ratios for precessionally induced periods of increased productivity are consistently higher than for the intermediate intervals, indicating that relatively less reactive P is buried. Therefore, we argue that post-depositional redistribution

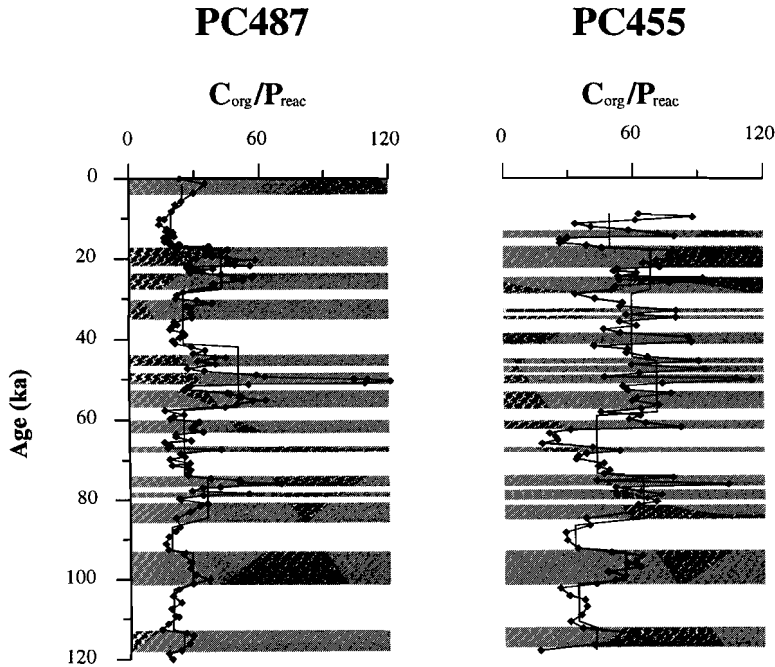


Figure 8. Records of the C_{org}/P_{react} ratios for PC455 and PC487 versus age. The solid lines represent average C_{org}/P_{react} ratios over precessional periods of high and low productivity. The shaded intervals indicate sediment enriched in organic matter deposited during periods of increased primary productivity.

has had only a limited effect on reshaping the downcore distributions of solid-phase P, and that this process cannot fully account for the lower PBEs during periods of high paleoproductivity.

Several other processes may explain the lack of response of P_{CFA} burial to changes in paleoproductivity. Firstly, an increase of the reactive P deposition flux may principally lead to more P regeneration and loss to the water column, and not cause the build-up of the interstitial phosphate concentration. This is particularly true for the deep pelagic sediments of the Arabian Sea, where the large water depth, oxic bottom waters, and relatively low sedimentation rates, cause reactive P regeneration to take place chiefly in the water column and at the sediment water interface (**Chapter 6**). A higher input of P will lead to burial of more refractory (bacterial) organic matter (as is indicated by the higher $C_{\text{org}}/P_{\text{org}}$ ratios in PC487), which will not induce higher rates of phosphogenesis. Secondly, phosphogenesis may be regulated by diagenetic iron cycling (Sundby *et al.*, 1992; Slomp *et al.*, 1996). During periods of reduced paleoproductivity, this process is more efficient in promoting phosphogenesis, because a reduced supply of reactive organic matter to the sediment increases the oxygen penetration depth and the sorption capacity of the iron oxides for phosphate (Sundby *et al.*, 1992; McManus *et al.*, 1997). In present-day surface sediments of the deep Arabian Basin, however, diagenetic iron cycling does not promote CFA formation because of the refractory nature of the deposited organic matter (**Chapter 6**). Thirdly, CFA formation rates may not be directly controlled by interstitial phosphate release, but may be dependent on other parameters, such as the downward diffusion rate of fluoride from the bottom water, precipitation kinetics, the permeability of the sediment, or microbial mediation (*e.g.* Filippelli and Delaney, 1994; Krajewski *et al.*, 1994). Fourthly, some bioturbation is necessary for the commencement of early diagenetic apatite formation (**Chapter 4**). Downward mixing of solid-phase reactive P in pelagic sediments is essential to prevent direct loss of phosphate to the bottom water, and to produce high subsurface phosphate concentrations. Accordingly, phosphogenesis rates may have been relatively reduced in the laminated intervals of PC455.

Cause of the higher PBE during periods of high productivity

Summarizing, close inspection of the solid-phase P speciation revealed that four processes may account for the reduced PBE in the Arabian Sea during periods of high productivity. Firstly, diagenetic redistribution may have changed the primary downcore distribution of sedimentary P, but, as discussed, this process has had only a limited effect on the calculated PBEs. Secondly, the export and burial flux of reactive P are largely decoupled. Whereas P is predominantly removed from the surface waters as particulate organic P, this P phase constitutes only a minor fraction in the underlying sediments in comparison to biogenic and authigenic apatite (Fig. 5; see also Table 1). In addition, authigenic P formation may, to a substantial extent, have been fuelled by dissolution of fish debris instead of organic matter degradation (**Chapter 4**). Accumulation of biogenic apatite rather than organic P is thus a more important mechanism to remove reactive P from the Arabian Sea. This is also shown by the sedimentary $C_{\text{org}}/P_{\text{reac}}$ ratios in PC487 and PC455, which are lower than the Redfield ratio for marine organic matter (106; Fig. 8). For deep pelagic sediments, P_{fish} burial does not

react proportionally to changes in paleoproductivity. Consequently, burial of reactive P becomes insensitive to productivity controlled changes in P fluxes to the seafloor. This decoupling is less effective for continental slope sediments, which explains why the PBE pattern for PC455 is somewhat less distinct than for PC487 (Fig. 4). Thirdly, authigenic P formation rates are not susceptible to changes in the rain rate of reactive P. Fourthly, more extensive P regeneration under oxygen-depleted bottom waters may have reduced P burial in continental slope sediments of the Arabian Sea (Ingall and Jahnke, 1994, 1997). Assessing the exact role of bottom water redox conditions on benthic P regeneration is problematic since periods of high productivity are often accompanied by bottom water anoxia. In addition, burial of the various reactive P fractions is differently affected by changes in BWO conditions. Retention of organic P is generally less efficient in sediments underlying anoxic bottom waters (Ingall *et al.*, 1993). Past variations in OMZ intensity, however, did not significantly affect organic P burial on the continental slope. Moreover, the potential impact of this process on the PBE is limited, as P_{org} constitutes only a minor sedimentary P fraction. In contrast to organic P, fish debris may have been subject to enhanced preservation during periods of bottom water anoxia, resulting in more efficient P burial. Finally, dysoxic bottom water conditions may both enhance (higher organic P and fish debris contents, reduced phosphate loss to the bottom water by bioturbation), or reduce (no or less efficient early diagenetic iron cycling, reduced downward mixing of sources by bioturbation) authigenic apatite precipitation rates. Fluctuating BWO contents have certainly influenced the quantity and quality of total solid-phase P burial in continental slope sediments of the Arabian Sea, but the precise impact on the PBE remains unclear. The results from Arabian Sea continental slope sediments, however, suggest that dysoxic bottom waters have rather enhanced P burial than reduced it.

Implications

Lower PBEs during periods of increased paleoproductivity imply more effective reactive P regeneration. When the regenerated phosphate is transferred back to the surface waters, it will stimulate higher rates of primary productivity (provided that phosphate is the bio-limiting nutrient). Increased surface water productivity, in turn, will increase the export flux of reactive P. Accordingly, a positive feedback loop is created between increased surface water productivity and enhanced P cycling. A similar feedback mechanism has previously been proposed for P cycling and water column anoxia (Ingall and Jahnke, 1994, 1997). The results of the present study, however, indicate that an increase in productivity, for example induced by more intense upwelling, automatically induces a positive feedback, irrespective of the fact whether higher organic matter accumulation rates cause oxygen depletion of the bottom waters or not. This conclusion has important implications for the assessment of the global cycle of P and its potential control on marine productivity and organic carbon burial.

According to box model calculations for the coupled geochemical cycles of P and organic carbon (Van Cappellen and Ingall, 1994), a positive feedback between enhanced phosphorus regeneration and higher primary productivity can only be effective on time scales equal or larger than the oceanic residence time of phosphate. On shorter time scales, the response of primary productivity to changes in P cycling may deviate significantly from the

predicted steady state situation (*Van Cappellen and Ingall., 1994*). Estimates for the oceanic residence time of phosphate vary between 16 and 80 kyr (*Froelich et al., 1982; Ruttenberg, 1993; Van Cappellen and Ingall., 1994*). Consequently, it is not evident whether the positive feedback is operative on precessional or sub-Milankovitch scale variations in paleoproductivity in the Arabian Sea. For example, in the present-day situation all regenerated phosphate released from deep basin sediments is taken up in the Antarctic bottom waters and is transported out of the Arabian Sea. Changes in P burial in the deep pelagic environment will thus not directly influence primary productivity in the basin itself. On the Oman and Somalian margins, however, upwelling waters originating from intermediate water depths provide a possible way to transfer phosphate more rapidly to the photic zone. The generally higher PBEs during the glacial period indicate less efficient P cycling and lower seawater phosphate concentrations. This is consistent with Cd/Ca and $\delta^{13}\text{C}$ data from the Arabian Sea, indicating more nutrient-depleted conditions during the last glacial maximum (*Boyle et al., 1995*), and is in accordance with the overall lower paleoproductivity rates compared to the interglacial periods (*Emeis et al., 1995*). During the Late Quaternary, (sub-) Milankovitch variations in paleoproductivity in the Arabian Sea may thus partly have been regulated by changes in P burial.

Conclusions

The average solid-phase P speciation in continental slope and deep marine sediments of the Arabian Sea is very similar. Authigenic and biogenic apatite (fish debris) make up the bulk of the P inventory (ca. 70 %), whereas P associated with iron oxides, organic P, detrital apatite constitute only minor fractions. The concentrations of all sedimentary P species generally do not increase during periods of high paleoproductivity, with the exception of organic P and, for continental slope sediments, the P fraction associated with fish debris.

The phosphorus burial efficiency (PBE) decreases during periods of increased paleoproductivity in deep marine and, though less pronounced, in continental slope sediments of the Arabian Sea. Postdepositional P redistribution has not significantly altered the downcore distribution of solid-phase P. Lower PBEs during periods of higher paleoproductivity are therefore explained by a) the partial decoupling of the P export flux, consisting primarily of particulate organic P, and the P burial flux, consisting primarily of biogenic and authigenic apatite, and b) the lack of higher rates of phosphogenesis during periods of increased reactive P deposition. Fluctuations in bottom water oxygen content may have affected P burial on the continental slope sediments of the Arabian Sea, but the precise impact on the PBE remains unclear. The results of this study indicate that a higher oceanic primary productivity induces more efficient P cycling in the oceans. On time scales exceeding the oceanic P residence time, this process may stimulate higher surface water productivity (assuming that P is the bio-limiting nutrient in the oceans), thus creating a positive feedback loop. In the Arabian Sea, such a feedback mechanism may also be active on sub-Milankovitch time scales as P regenerated on the continental slopes of the Oman and Somalian coastal

upwelling areas is transported to the photic zone relatively fast.

Acknowledgements - The chief scientists on the NIOP cruises during the 1992-1993 Netherlands Indian Ocean Programme were W.J.M. van der Linden and C.H. van der Weijden. H. de Waard, and G. Nobbe are thanked for their contribution to the laboratory analyses. Critical reviews by C.H. van der Weijden, A. Rutten and C.P. Slomp significantly improved this manuscript. This research was funded by the Netherlands Organization for Scientific Research (NWO).

List of abbreviations and chemical formulae

Chemical formulae

P	phosphorus
Mn	manganese
Fe	iron
C	carbon
N	nitrogen
S	sulphur
Ca	calcium
Mg	magnesium
Sr	strontium
Al	aluminum
Ba	barium
Ti	titanium
Zr	zirconium
V	vanadium
Mo	molybdenum
Cd	cadmium
F	fluor
PO_4^{3-}	phosphate
NH_4^+	ammonium
F ⁻	fluoride
NH_4Cl	ammonium chloride
HCl	hydrochloric acid
HF	hydrofluoric acid
HNO_3	nitric acid
CaCO_3	calcium carbonate

chemical fractions

C_{org}	organic carbon
P_{fish}	P associated with biogenic apatite
P_{Fe}	P adsorbed to iron oxides
P_{CFA}	P associated with carbonate fluorapatite
P_{det}	P associated with detrital apatite
P_{org}	organic phosphorus
P_{tot}	total solid-phase phosphorus
P_{reac}	reactive phosphorus (here defined as the sum of P_{fish} , P_{Fe} , P_{CFA} , and P_{org})
S_{pyr}	sulphur associated with pyrite
S_{tot}	total solid-phase sulphur
Fe_{pyr}	iron associated with pyrite
Fe_{reac}	reactive Fe (i.e. reactive iron oxides).

other

BWO	bottom water oxygen
OMZ	oxygen minimum zone
MAR	mass accumulation rate
PAR	phosphorus accumulation rate
LSR	linear sedimentation rate
dbd	dry bulk density
ϕ	porosity
CFA	carbonate fluorapatite
CDB	citrate dithionite buffer
BC	boxcore
PC	pistoncore
TC	tripcore
PBE	(reactive) phosphorus burial efficiency
DOP	degree of pyritization
PPI	pteropod preservation index
IAP	ion activity product
NIOP	Netherlands Indian Ocean Programme
ACD	aragonite compensation depth
ITCZ	inter tropical convergence zone
AMS	accelerator mass spectrometry
ICP-AES	inductively coupled plasma atomic emission spectrometer

References

- Anonymous, 1982. *Kirk - Othmer Encyclopedia of chemical technology*, third edition, Vol. 17. John Wiley and Sons.
- Altabet M.A., Francois R., Murray D.W. and Prell W.L., 1995. Climate-related variations in denitrification in the Arabian Sea from sediment $^{15}\text{N}/^{14}\text{N}$ ratios. *Nature* 373, 506-509.
- Anderson R.Y. and Gardner J.V., 1989. Variability of the Late Pleistocene-Early Holocene oxygen-minimum zone off northern California. *Geophysical Monograph* 55, 75-84.
- Anderson D.M. and Prell W.L., 1993. A 300 kyr record of upwelling off Oman during the Late Quaternary: evidence of the Asian southwest monsoon. *Paleoceanography* 8, 193-208.
- Anderson L.A. and Sarmiento, J.L., 1994. Redfield ratios of remineralization determined by nutrient data analysis. *Glob. Biogeochem. Cycles* 8, 65-80.
- Anschutz P., Zhong S., Sundby B., Mucci A. and Gobeil C., 1998. Burial efficiency of phosphorus and the geochemistry of iron in continental margin sediments. *Limnol. Oceanogr.* 43, 53-64.
- Arain R., 1987. Persisting trends in carbon and mineral transport-monitoring of the Indus river. In: *Transport of carbon and minerals in mayor world rivers - Part IV*. pp. 417-421.
- Arrhenius, G.O. , 1963. Pelagic sediments. In M.N. Hill. (Editor), *The Sea*, Vol..3. John Wiley and Sons, pp. 655-727.
- Aspila K.I., Agemain H. and Chau, A.S.Y., 1976. A semi-automated method for the determination of inorganic, organic and total phosphate in sediments. *Analyst* 101, 187-197.
- Atlas E. and R.M. Pytkowicz. 1977. Solubility behaviour of apatites in seawater. *Limnol. Oceanogr.* 22, 290-300.
- Baker K.B. and Burnett W.C., 1988. Distribution, texture and composition of modern phosphate pellets in Peru shelf muds. *Mar. Geol.* 80, 195-213.
- Balakrishnan Nair T.M., Ramaswamy V., Shankar R. and Ittekot, V., 1999. Seasonal and spatial variations in settling manganese fluxes in the Northern Arabian Sea. *Deep-Sea Res.* 46, 1827-1839.
- Banse K., 1968. Hydrography of the Arabian Sea Shelf of India and Pakistan and effects on demersal fishes. *Deep-Sea Res.* 15, 45-79.
- Banse K., 1987. Seasonality of phytoplankton chlorophyll in the central and northern Arabian Sea. *Deep-Sea Res.* 34, 713-723.
- Bailey T.G. and Robison B.H., 1986. Food availability as a selective factor on the chemical compositions of midwater fishes in the eastern North Pacific. *Mar. Biol.* 91, 131-141.
- Bard E., Hamelin B., Fairbanks R.G. and Zindler A., 1990. Calibration of the ^{14}C timescale over the past 30,000 years using mass spectrometric U-Th ages from Barbados corals. *Nature* 345, 405-410.
- Bard E., Hamelin B., Arnold M., Montaggioni L., Cabioch G., Faure G. and Rougerie F., 1996. Deglacial sea-level record from Tahiti corals and the timing of global meltwater discharge. *Nature* 382, 241-244.
- Bauer S., Hitchcock G.L. and Olson, D.B., 1991. Influence of monsoonally-forced Ekman dynamics upon surface layer depth and plankton biomass distribution in the Arabian Sea. *Deep-Sea Res.* 38, 531-553.
- Berger W.H., 1978. Deep-sea carbonate: pteropod distribution and the aragonite compensation

- depth. *Deep-Sea Res.* 25, 447-452.
- Berger W.H., Finkel R.C., Killingley J.S. and Marchig V. 1983. Glacial-Holocene transition in deep-sea sediments: manganese spike in the east-equatorial Pacific. *Nature* 303, 231-233.
- Berger W.H. and Herguera J.C., 1992. Reading the sedimentary record of the ocean's productivity. In: P.G. Falkowski and A.D. Woodhead (Editors), *Primary productivity and biogeochemical cycles in the sea*. Plenum Press, pp. 455-486.
- Berner R.A., 1969. Migration of iron and sulphur within anaerobic sediments during early diagenesis. *Am. J. Sci.* 267, 19-42.
- Berner R.A., 1970. Sedimentary pyrite formation. *Am. J. Sci.* 268, 1-23.
- Berner R.A., 1973. Phosphate removal from seawater by adsorption on volcanogenic ferric oxides. *Earth Planet. Sci. Lett.* 18, 77-86.
- Berner R.A., 1980. *Early Diagenesis: A theoretical approach*. Princeton Univ. Press. 241 p.
- Berner R.A., 1984. Sedimentary pyrite formation: An update. *Geochim. Cosmochim. Acta* 48, 605-616.
- Berner R.A., Scott M.R., and Thomlinson C. 1970. Carbonate alkalinity in the porewaters of anoxic marine sediments. *Limnol. Oceanogr.* 15, 544-549.
- Berner R.A., Rittenberg K.C., Ingall E.D. and Rao, J.-L., 1993. The nature of phosphorus burial in modern marine sediments. In: R. Wollast, F.T. Mackenzie and L. Chou (Editors), *Interactions of C, N, P, and S Biogeochemical Cycles and Global Change*. NATO ASI Series V. 14. Springer-Verlag, Berlin Heidelberg, pp. 365-378.
- Boesen C. and Postma D., 1988. Pyrite formation in anoxic environments of the Baltic. *Am. J. Sci.* 288, 575-603.
- Boudreau B.P., 1994. Is burial velocity a master parameter for bioturbation? *Geochim. Cosmochim. Acta* 58, 1243-1249.
- Boudreau B.P., 1997. *Diagenetic models and their implementation*. Springer, 141 pp.
- Boudreau B.P., Mucci A., Sundby B., Luther G.W. and Silverberg N., 1998. Comparative diagenesis at three sites on the Canadian continental margin. *J. Mar. Res.* 56, 1259-1284.
- Boyle E.A., 1983. Manganese carbonate overgrowths on foraminifera tests. *Geochim. Cosmochim. Acta* 47, 1815-1819.
- Boyle E.A., Labeyrie L. and Duplessy J.-C., 1995. Calcitic foraminiferal data confirmed by cadmium in aragonitic *Hoeglundina*: Application to the last glacial maximum in the northern Indian Ocean. *Paleoceanography* 10, 881-900.
- Breit G.N. and Wanty R.B., 1991. Vanadium accumulation in carbonaceous rocks: A review of geochemical controls during deposition and diagenesis. *Chem. Geol.* 91, 83-97.
- Brock J.C., McClain C.R., Anderson D.M., Prell W.L. and Hay W.W., 1992. Southwest monsoon circulation and environments of recent planktonic foraminifera in the northwestern Arabian Sea. *Paleoceanography* 7, 799-813.
- Brock J., Sathyendranath, S. and Platt T., 1994. A model study of seasonal mixed-layer primary production in the Arabian Sea. In D. Lal (Editor), *Biogeochemistry of the Arabian Sea*. Ind. Acad. Sci., pp. 65-78.
- Broecker W.S., 1982. Ocean chemistry during glacial time. *Geochim. Cosmochim. Acta* 46, 1689-1705.
- Broecker W.S. and Peng T.-H., 1982. *Tracers in the sea*. Eldrigio Press, 690 pp.
- Brumsack H.J., 1986. The inorganic geochemistry of Cretaceous black shales (DSDP Leg 41) in comparison to modern upwelling sediments from the Gulf of California. *Geol. Soc. Spec. Publ.* 21, 447-462.
- Brumsack H.J., 1989. Geochemistry of recent TOC-rich sediments from the Gulf of California

- and the Black Sea. *Geologische Rundschau* 78, 851-882.
- Burdige D.J. and Gieskes J.M., 1983. A pore water/solid phase diagenetic model for manganese in marine sediments. *Amer. J. Sci.* 283, 29-47.
- Burnett W.C., 1977. Geochemistry and origin of phosphorite deposits from off Peru and Chile. *Geol. Soc. Am. Bull.* 88, 813-823.
- Burnett W.C., Beers M.J. and Roe, K.K., 1982. Growth rates of phosphate nodules from the continental margin off Peru. *Science* 215, 1616-1618.
- Burnett W.C., Roe K.K. and Piper D.Z., 1983. Upwelling and phosphorite formation in the ocean. In: E. Suess and J. Thiede (Editors), *Coastal Upwelling, its sediment record, part A*. Plenum Press, New York, pp. 377-397.
- Burnett W.C., Baker K.B., Chin P.A., McCabe W. and Ditchburn R., 1988. Uranium-series and AMS ^{14}C studies of modern phosphatic pellets from Peru shelf muds. *Mar. Geol.* 80, 215-230.
- Burns S.J., Matter A., Frank N. and Mangini A., 1998. Speleothem-based paleoclimate record from northern Oman. *Geology* 26, 499-502.
- Calvert S.E. and Karlin R.E., 1991. Relationships between sulphur, organic carbon, and iron in the modern sediments of the Black Sea. *Geochim. Cosmochim. Acta* 55, 2483-2490.
- Calvert S.E. and Pedersen T.F. 1993. Geochemistry of recent oxic and anoxic marine sediments: Implications for the geological record. *Mar. Geol.* 113, 67-88.
- Calvert S.E., Pedersen T.F., Naidu P.D. and von Stackelberg U., 1995. On the organic carbon maximum on the continental slope of the eastern Arabian Sea. *J. Mar. Res.* 53, 269-296.
- Calvert S.E. and Pedersen T.F., 1996. Sedimentary geochemistry of manganese: Implications for the environment of formation of manganiferous black shales. *Econ. Geol.* 91, 36-47.
- Canfield D.E., 1989. Reactive iron in marine sediments. *Geochim. Cosmochim. Acta* 53, 619-632.
- Canfield D.E., 1993. Factors influencing organic matter preservation in marine sediments. *Chem. Geol.* 114, 315-329.
- Canfield D.E. and Raiswell R., 1991. Carbonate precipitation and dissolution, its relevance to fossil preservation. In P.A. Allison and D.E.G. Briggs (Editors), *Taphonomy: Releasing the data locked in the fossil record, Volume 9 of Topics in Geobiology*. Plenum Press. New York, pp. 411-453.
- Chester R., Berry A.S. and Murphy K.J.T., 1991. The distributions of particulate atmospheric trace metals and mineral aerosols over the Indian Ocean. *Mar. Chem.* 34, 261-290.
- Chien S.-S., 1972. Ion-activity products of some apatite minerals. *Ph.D. Thesis*, Iowa State University. 144 p.
- Clemens S.C., 1998. Dust response to seasonal atmospheric forcing: Proxy evaluation and calibration. *Paleoceanography* 13, 471-490.
- Clemens S.C. and Prell W.L., 1990. Late Pleistocene variability of Arabian Sea summer monsoon winds and continental aridity: eolian records from the lithogenic component of deep-sea sediments. *Paleoceanography* 5, 109-145.
- Clemens S.C., Prell W.L., Murray D.W. Shimmield G.B. and Weedon G., 1991. Forcing mechanisms of the Indian Ocean monsoon. *Nature* 353, 720-725.
- Clemens S.C., Murray D.W. and Prell W.L., 1996. Nonstationary phase of the Plio-Pleistocene Asian monsoon. *Science* 274, 943-948.
- Coale K.H., Johnson K.S., Fitzwater S.E., Gordon R.M., Tanner S., Chavez F.P., Ferioli L., Sakamoto C., Rogers P., Millero F., Steinberg P., Nightingale P.D., Cooper D., Cochlan W.P., Landry M.R., Constantinou J., Rollwagen G., Trasvina A. and Kudela R., 1996. A massive phytoplankton bloom induced by an ecosystem-scale iron fertilization experiment

- in the equatorial Pacific Ocean. *Nature* 383, 495- 501.
- Codispoti L.A., 1989. Phosphorus vs. Nitrogen limitation of new and export production. In: W.H. Berger, V.S. Smetacek, and G. Wefer (Editors), *Productivity of the oceans: present and past*. John Wiley & sons, pp. 377-394.
- Codispoti L.A., 1991. Primary productivity and carbon and nitrogen cycling in the Arabian Sea. In: S.L. Smith et al., (Editors) *U.S. JGOFS Planning report No. 13*. pp. 75-85.
- Colley S., Thomson J., Wilson T.R.S. and Higgs N.C., 1984. Post-depositional migration of elements during diagenesis in brown clay and turbidite sequences in the North East Atlantic. *Geochim. Cosmochim. Acta* 48, 1223-1235.
- Conan S.M.H. and Brummer G.J.A., in press. Fluxes of planktic foraminifera in response to monsoonal upwelling in the Somalia Basin.
- Cook P.J., 1984. Spatial and temporal controls on the formation of phosphate deposits - a review. In: J.O., Nriagu and P.B. Moore (Editors), *Phosphate minerals*. Springer Verlag, Berlin, pp. 242-274.
- Currie R.I., Fisher A.E. and Hargreaves P.M., 1973. Arabian Sea upwelling. In: B. Zeitzschel (Editor), *The biology of the Indian Ocean*. Springer Verlag, pp. 37-52.
- Currie R.I., 1992. Circulation and upwelling off the coast of South-East Arabia. *Oceanologica Acta* 15, 43-60.
- Cushing D.H., 1973. Production in the Indian Ocean and the transfer from the primary to the secondary level. In: B. Zeitzschel (Editor), *The biology of the Indian Ocean*. Springer Verlag, pp. 475-486.
- Dansgaard W., Johnson S.J., Clausen H.B., Dahl-Jensen D., Gundestrup N.S., Hammer C.U., Hvidberg C.S., Steffensen J.P., Sveinbjörnsdottir A.E., Jouzel J. and Bond G., 1993. Evidence for general instability of past climate from a 250-kyr ice-core record. *Nature* 364, 218-220.
- Delaney M.L., 1998. Phosphorus accumulation in marine sediments and the oceanic phosphorus cycle. *Glob. Biogeochem. Cycles* 12, 563-572.
- Delaney, M.L., and Anderson, L.D., 1997. Phosphorus geochemistry in Ceara Rise sediments. *Proc. ODP. Sci. Results* 154, 475-482.
- De Lange G.J., 1986. Early diagenetic reactions in interbedded pelagic and turbiditic sediments in the Nares Abyssal Plain (western North Atlantic): Consequences for the composition of sediment and interstitial water. *Geochim. Cosmochim. Acta* 50, 2543-2561.
- De Lange G.J., 1992a. Shipboard routine and pressure-filtration system for pore-water extraction from suboxic sediments. *Mar. Geol.* 109, 77-81.
- De Lange G.J., 1992b. Distribution of various extracted phosphorus compounds in the interbedded turbiditic/pelagic sediments of the Madeira Abyssal Plain, eastern North Atlantic. *Mar. Geol.* 109, 115-139.
- De Lange G.J., Middelburg J.J. and Pruyssers P.A., 1989. Middle and Late Quaternary depositional sequences and cycles in the eastern Mediterranean. *Sedimentology* 36, 151-158.
- De Lange G.J., Van Os B., Pruyssers P.A., Middelburg J.J., Castradori D., Van Santvoort P., Müller P.J., Eggenkamp H. and Prahl F.G., 1994. Possible early diagenetic alteration of palaeo proxies. In: R. Zahn et al. (Editors), *Carbon cycling in the glacial ocean; constraints on the ocean's role in global change*. NATO ASI Series I 17. Springer Verlag, pp. 225-258.
- Demaison G.J. and Moore G.T., 1980. Anoxic environments and oil source bed genesis. *Org. Geochem.* 2, 9-31.

- Demina L.L. and Choporov D.Ya., 1987. Plasma spectrometry of hydrothermal vents in the ocean. *Transections of the USSR Academy of Sciences: Earth Science Sections* 287, 170-173.
- Den Dulk M., Reichart G.J., Memon G.M., Roelofs E.M.P., Zachariasse W.J. and van der Zwaan G.J., 1998. Benthic foraminiferal response to variations in the surface water productivity and oxygenation in the northern Arabian Sea. *Mar. Micropal.* 35, 43-66.
- Deuser W.G., Ross E.H. and Mlodzinska Z.J., 1978. Evidence for and rate of denitrification in the Arabian Sea. *Deep-Sea Res.* 25, 431-445.
- DeVries T.J. and Percy W.G., 1982. Fish debris in sediments of the upwelling zone off central Peru: a late Quaternary record. *Deep-Sea Res.* 28, 87-109.
- Dickens G.R. and Owen R.M., 1994. Late Miocene-early Pliocene manganese redirection in the central Indian Ocean: Expansion of the intermediate water oxygen minimum zone. *Paleoceanography* 9, 169-181.
- Diester-Haas L., 1978. Sediments as indicators of upwelling. In: R. Boje and M. Tomczak (Editors), *Upwelling ecosystems*. Springer Verlag, pp. 261-281.
- Dymond J., Suess, E. and Lyle M., 1992. Barium in deep-sea sediment: a geochemical proxy for paleoproductivity. *Paleoceanography* 7, 163-181.
- Eijsink L.M., Krom M.D. and de Lange, G.J. 1997. The use of sequential extraction techniques for sedimentary phosphorus in eastern Mediterranean sediments. *Mar. Geol.* 139, 147-155.
- Emeis K.C., Morse J.W. and Mays L.L., 1991. Organic carbon, reduced sulphur, and iron in Miocene to Holocene upwelling sediments from Oman and Benguela upwelling systems. *Proc. ODP Sci. Results* 117, 517-527.
- Emeis K.-C., Anderson D.M., Doose, H., Kroon, D. and Schulz-Bull D., 1995. Sea-surface temperatures and the history of monsoon upwelling in the northwest Arabian Sea during the last 500,000 years. *Quat. Res.* 43, 355-361.
- Fairbanks R.G., Sverdrlove M., Free R., Wiebe P.H. and Be A.W.H., 1982. Vertical distribution and isotopic fractionation of living planktonic foraminifera from the Panama Basin, *Nature* 298, 841-844.
- Fairbanks R.G., 1989. A 17,000-year glacio-eustatic sea level record: influence of the glacial melting rates on the Younger Dryas event and deep-ocean circulation. *Nature* 342, 637-642.
- FAO 1981. *Atlas of the living Resources of the Sea*. FAO, Rome, 4th ed.
- FAO 1997. Review of the state of world fishery resources: marine fisheries. *FOA Fisheries circular No. 920 FIRM/C920*. FAO, Rome, Italy. WWWpage <http://www.fao.org/>
- FAO 1999. *FAOSTAT fisheries database*. WWWpage <http://www.fao.org/>
- Farrenkopf, A.M., Luther III, G.W., Truesdale, V.W. and Van der Weijden, C.H., 1997. Sub-surface maxima: evidence for biologically catalyzed redox cycling in Arabian Sea OMZ during the SW intermonsoon. *Deep-Sea Res. II* 44, 1391-1409.
- Filippelli G.M., 1997. Controls on phosphorus concentration and accumulation in oceanic sediments. *Mar. Geol.* 139, 231-240.
- Filippelli G.M. and Delaney M.L., 1994. Phosphogenesis and the controls on phosphorus accumulation in continental margin sediments. *Proc. 29th Int'l Geol. Congr. Part C*, 189-204.
- Filippelli G.M. and Delaney, M.L., 1996. Phosphorus geochemistry of equatorial Pacific sediments. *Geochim. Cosmochim. Acta* 60, 1479-1495.
- Finney B.P., Lyle M.W. and Ross Heath G., 1988. Sedimentation at Manop site H (eastern

- Equatorial Pacific) over the past 400,000 years: Climatically induced redox variations and their effects on transition metal cycling. *Paleoceanography* 3, 169-189.
- Föllmi K.B., 1996. The phosphorus cycle, phosphogenesis and marine phosphate-rich deposits. *Earth Science Reviews* 40, 55-124.
- Froelich P.N., 1984. Interaction of the marine phosphorus and carbon cycles. *Jet Propul. Lab. Publ., NASA* 84-21, 141-176.
- Froelich P.N., Klinkhammer G.P., Bender M.L., Luedtke N.A., Heath G.R., Cullen D., Dauphin P., Hammond D., Hartman B. and Maynard V., 1979. Early oxidation of organic matter in pelagic sediments of the eastern equatorial Atlantic: suboxic diagenesis. *Geochim. Cosmochim. Acta*, 43, 1075-1090.
- Froelich P.N., Bender M.L., Luedtke N.A., Heath G.R. and DeVries T., 1982. The marine phosphorus cycle. *Am. J. Sci.* 282, 474-511.
- Froelich P.N., Kim K.H., Jahnke R., Burnett W.C., Soutar A. and Deakin M., 1983. Pore water fluoride in Peru continental margin sediments: Uptake from seawater. *Geochim. Cosmochim. Acta* 47, 1605-1612.
- Froelich P.N., Arthur M.A., Burnett W.C., Deakin M., Hensley V., Jahnke R., Kaul L., Kim K.-H., Roe K., Soutar A. and Vathakanon C., 1988. Early diagenesis of organic matter in Peru continental margin sediments: phosphorite precipitation. *Mar. Geol.* 80, 309-343.
- Gächter R. and Meyer J.S., 1993. The role of microorganisms in sediment phosphorus dynamics in relation to mobilization and fixation of phosphorus. *Hydrobiologia* 253, 103-121.
- Garrison R.E. and Kastner M., 1990. Phosphatic sediments and rocks recovered from the Peru margin during ODP Leg 112. *Proc. ODP. Sci. Results* 112, 111-134.
- Gieskes J.M., 1973. Interstitial water studies leg15 - alkalinity, pH, Mg, Ca, Si, PO₄ and NH₄. *Init. Rep. DSDP*, US Gov. Print. Office, Washington 20, 813-829.
- Glenn C.R. and Arthur M.A., 1988. Petrology and major element geochemistry of Peru Margin phosphorites and associated diagenetic minerals: authigenesis in modern organic-rich sediments. *Mar. Geol.* 80, 231-267.
- Glenn C.R., Föllmi K.B., Riggs S.R., Baturin G.N., Grimm K.A., Trappe J., Abed A.M., Gall-Olivier C., Garrison R.E., Ilyin A.V., Jehl C., Rohrllich V., Sadaqah R.M.Y., Schidlowski, M., Sheldon R.E. and Siegmund H., 1994. Phosphorus and phosphorites: Sedimentology and environments of formation. *Eglogae Geol. Helv.* 87, 747-788.
- Glud R.N., Gundersen J.K., Jørgensen B.B., Revsbech N.P. and Schulz H.D., 1994. Diffusive and total oxygen uptake of deep-sea sediments in the eastern South Atlantic Ocean: in situ and laboratory measurements. *Deep-Sea Res.* 41, 1767-1788.
- Grootes P.M., Stuiver M., White J.W.C., Johnson S.J. and Jouzel J., 1993. Comparison of oxygen isotope records from GISP2 and GRIP Greenland ice cores. *Nature* 366, 552-554.
- Haedrich R.L. and N.R. Merrett., 1992. Production/biomass ratios, size frequencies, and biomass spectra in deep-sea demersal fishes. In: G.T. Rowe and V. Pariente (Editors), *Deep-sea food chains and the Global Carbon Cycle*. Kluwer Academic Publishers. pp. 157-182.
- Hammer C.U. and Meese D.A., 1993. Dating ice cores. *Nature* 363, 666.
- Hartmann M., Müller P.J., Suess E. and Van der Weijden, C.H., 1973. Oxidation of organic matter in recent marine sediments. *"Meteor"-Forsch.-Ergebnisse.* 12, 74-86.
- Heggie D.T., Klinkhammer G. and Cullen D., 1987. Manganese and copper fluxes from continental margin sediments. *Geochim. Cosmochim. Acta* 51, 1059-1070.
- Heggie D.T., Skyring G.W., O'Brien G.W., Reimers, C.E., Herczeg A., Moriarty D.J.W., Burnett W.C. and Milnes, A.R., 1990. Organic carbon and modern phosphorite formation on the East Australian continental margin: an overview. *Geol. Soc. Spec. Publ.* 52, 87-117.

- Hensen C., Landenberger H., Zabel M. and Schulz H.D., 1998. Quantification of diffusive benthic fluxes of nitrate, phosphate, and silicate in the southern Atlantic Ocean. *Global Biogeochem. Cycles* 12, 193-210.
- Higgs N.C., Thomson J., Wilson T.R.S., and Croudace I.W., 1994. Modification and complete removal of eastern Mediterranean sapropels by postdepositional oxidation. *Geology* 22, 423-426.
- Holland H.D., 1978. *The Chemistry of the Atmosphere and the Oceans*. Wiley-Interscience.
- Howarth R.W., 1988. Nutrient limitation of net primary production in marine ecosystems. *Ann. Rev. Ecol. Sys.* 19, 89-110.
- Howarth R.W., Jensen H.S., Marino R. and Postma, H., 1995. Transport to and processing of P in near-shore and oceanic waters. In: H. Tiessen (Editor), *Phosphorus in the global environment*. John Wiley and Sons. pp. 323-345.
- Huerta-Diaz M.A. and Morse J.W., 1990. A quantitative method for determination of trace metal concentrations in sedimentary pyrite. *Mar. Chem.* 29, 119-144.
- Ingall E.D. and Van Cappellen P., 1990. Relation between sedimentation rate and burial of organic phosphorus and organic carbon in marine sediments. *Geochim. Cosmochim. Acta* 54, 373-386.
- Ingall E.D., Schroeder P.A. and Berner R.A., 1990. The nature of organic phosphorus in marine sediments: New insights from ³¹P-NMR. *Geochim. Cosmochim. Acta* 54, 2617-2620.
- Ingall E.D., Bustin R.M. and Van Cappellen P., 1993. Influence of water column anoxia on the burial and preservation of carbon and phosphorus in marine shales. *Geochim. Cosmochim. Acta* 57, 303-316.
- Ingall E.D. and Jahnke R.A., 1994. Evidence for enhanced phosphorus regeneration from marine sediments overlain by oxygen-depleted waters. *Geochim. Cosmochim. Acta* 58, 2571-2575.
- Ingall E.D. and Jahnke R.A., 1997. Influence of water-column anoxia on the elemental fractionation of carbon and phosphorus during sediment diagenesis. *Mar. Geol.* 139, 219-229.
- Ittekkot V., Haake B., Bartsch M., Nair R.R. and Ramaswamy V., 1992. Organic carbon removal in the sea: the continental connection. *Geol. Soc. Spec. Publ.* 64, 167-176.
- Ivanenkov V.N. and Rozanov A.G., 1961. Hydrogen sulphide contamination of the intermediate waters of the Arabian Sea and the Bay of Bengal (in Russian). *Okeanologiya* 1, 443-449.
- Iverson R.L., 1990. Control on marine fish production. *Limnol. Oceanogr.* 35, 1593-1604.
- Jahnke R.A., Heggie D., Emerson S.R. and Grundmanis V., 1982. Pore waters of the central Pacific Ocean: nutrients results. *Earth Planet. Sci. Lett.* 61, 233-256.
- Jahnke R.A., Emerson S.R., Roe K.V. and Burnett, W.C., 1983. The present day formation of apatite in Mexican continental margin sediments. *Geochim. Cosmochim. Acta* 47, 259-266.
- Jakobsen R. and Postma D., 1989. Formation and solid solution behaviour of Ca-rhodochrosites in marine muds of the Baltic deep. *Geochim. Cosmochim. Acta* 53, 2639-2648.
- Jannink N.T., Zachariasse W.J. and Van der Zwaan G.J., 1998. Living (Rose Bengal stained) benthic foraminifera from the Pakistan continental margin (northern Arabian Sea). *Deep-Sea Res.* 45, 1483-1513.
- Jarvis I., Burnett W.C. Nathan Y., Almbaydin F.S.M., Attia A.K.M., Castro L.N., Flicoteaux R., Hilmy M.E., Husain V., Qutawnah A.A., Serjani A. and Zanin Y.N., 1994. Phosphorite geochemistry: State-of-the-art and environmental concerns. *Eclogae. Geol. Helv.* 87, 643-700.

- Jochem F.J., Pollehne F. and Zeitzschel B., 1993. Productivity regime and phytoplankton size structure in the Arabian Sea. *Deep-Sea Res. II* 40, 711-735.
- Johnson K.S., 1982. Solubility of rhodochrosite (MnCO_3) in water and seawater. *Geochim. Cosmochim. Acta* 46, 1805-1809.
- Johnson K.S., Berelson W.M., Coale K.H., Coley T.L., Elrod V.A., Fairey W.R., Iams H.D., Kilgore T.E. and Nowicki J.L., 1992. Manganese flux from continental margin sediments in a transect through the oxygen minimum. *Science* 257, 1242-1245.
- Johnson K.S., Coale K.H., Berelson W.M. and Gordon R.M., 1996. On the formation of the manganese maximum in the oxygen minimum. *Geochim. Cosmochim. Acta* 60, 1291-1299.
- Kabanova Y.G., 1968. Primary production in the northern part of the Indian Ocean. *Oceanology* 8, 214-225.
- Ke P.J., Power H.E. and Regier L.W., 1970. Fluoride content of fish protein concentrate and raw fish. *J. Sci. Fd Agric.* 21, 108-109.
- Klinkhammer G.P. and Bender M.L., 1980. The distribution of manganese in the Pacific Ocean. *Earth Planet. Sc. Lett.* 46, 361-384.
- Klinkhammer G., Elderfield H., Greaves M., Rona P.A. and Nelsen T., 1986. Manganese geochemistry near high-temperature vents in the Mid-Atlantic Ridge rift Valley. *Earth Planet. Sci. Lett.* 80, 230-240.
- Klump J.V. and Martens C.S., 1987. Biogeochemical cycling in an organic-rich coastal marine basin. 5. Sedimentary nitrogen and phosphorus budgets based upon kinetic models, mass balances, and the stoichiometry of nutrient regeneration. *Geochim. Cosmochim. Acta* 51, 1161-1173.
- Kolodny Y., 1981. Phosphorites. In: C. Emiliani (Editor), *The Sea, Vol. 7*. John Wiley and Sons, New York, pp. 981-1023.
- Kolodny Y. and Garrison R.E., 1994. Sedimentation and diagenesis in paleo-upwelling zones of epeiric sea and basinal settings: a comparison of the Cretaceous Mishash Formation of Israel and the Miocene Monterey Formation of California. In: A. Iijima, A.M. Abed and R.E. Garrison (Editors), *Siliceous Phosphatic and Glauconitic Sediments of the Tertiary and Mesozoic*. In: *Proc. 29th Int. Geol. Congr. Part C. VSP*, Utrecht, pp. 133-158.
- Kostka J.E. and Luther III, G.W., 1994. Partitioning and speciation of solid phase iron in saltmarsh sediments. *Geochim. Cosmochim. Acta* 58, 1701-1710.
- Krajewski K.P., Van Cappellen P., Trichet J., Kuhn O., Lucas J., Martin-Algarra A., Prévôt L., Tewari V.C., Gaspar L., Knight R.I. and Lamboy M., 1994. Biological processes and apatite formation in sedimentary environments. *Eclogae Geol. Helv.* 87, 701-745.
- Krom M.D. and Berner R.A., 1981. The diagenesis of phosphorus in a nearshore marine sediment. *Geochim. Cosmochim. Acta* 45, 207-216.
- Kyte F.T., Leinen M., Heath G.R. and Zhou L., 1993. Cenozoic sedimentation history of the central North Pacific: Inferences from the elemental geochemistry of core LL44-GPC3. *Geochim. Cosmochim. Acta* 57, 1719-1740.
- Landing W.M. and Bruland K.W., 1987. The contrasting biogeochemistry of iron and manganese in the Pacific Ocean. *Geochim. Cosmochim. Acta* 51, 29-43.
- Landing W.M. and Lewis B.L., 1991. Thermodynamic modelling of trace metal speciation in the Black Sea. In: J.W. Murray and E. Izdar (Editors), *Black Sea Oceanography. NATO ASI Series*. Dordrecht, Kluwer, pp. 125-160.
- Lee C., Murray D.W., Barber R.T., Buesseler K.O., Dymond J., Hedges J.I., Honjo S., Manganini S.J., Marra J., Moser C., Peterson M.L., Prell W.L. and Wakeham S.G., 1998. Particulate

- organic carbon fluxes: compilation of the results from the 1995 US JGOFS Arabian Sea Process Study. *Deep-Sea Res. II* 45, 2489-2501.
- Leventhal J.S., 1995. Carbon-sulphur plots show diagenetic and epigenetic sulfidation in sediments. *Geochim. Cosmochim. Acta* 59, 1207-1211.
- Li Y.-H., Bischoff J. and Mathieu G., 1969. The migration of manganese in the arctic basin sediment. *Earth Planet. Sci. Lett.* 7, 265-270.
- Li Y.-L. and Gregory S., 1974. Diffusion of ions in seawater and in deep-sea sediments. *Geochim. Cosmochim. Acta* 38, 703-714.
- Longhurst A.R. and Wooster W.S., 1990. Abundance of oil sardine (*Sardinella longiceps*) and upwelling on the southwest coast of India. *Can. J. Fish. Aquat. Sci.* 47, 2407-2419.
- Lord C.J. III 1982. A selective and precise method for pyrite determination in sedimentary materials. *J. Sed. Petr.* 52, 664-666.
- Louchouart P., Lucotte M., Duchemin E. and de Vernal A., 1997. Early diagenetic processes in recent sediments of the Gulf of St-Lawrence: phosphorus, carbon and iron burial rates. *Mar. Geol.* 139, 181-200.
- Lowenstam H.A., 1972. Phosphatic hard tissues of marine invertebrates: their nature and mechanical function, and some fossil implications. *Chem. Geol.* 9, 153-166.
- Lucotte M. and d'Anglejan B., 1985. A comparison of several methods for the determination of iron hydroxides and associated orthophosphates in estuarine particulate matter. *Chem. Geol.* 48, 257-264.
- Lucotte M., Mucci A., Hillaire-Marcel C. and Tran S., 1994. Early diagenetic processes in deep Labrador Sea sediments: reactive and nonreactive iron and phosphorus. *Can. J. Earth Sci.* 31, 14-27.
- Mach D.L., Ramirez A. and Holland H.D., 1987. Organic phosphorus and carbon in marine sediments. *Am. J. Sc.* 278, 429-441.
- Madhupratap M., Kumar S.P., Bhattathiri P.M.A., Kumar M.D., Raghukumar S., Nair K.K.C. and Ramaiah N., 1996. Mechanism of the biological response to winter cooling in the northeastern Arabian Sea. *Nature* 384, 549-552.
- Mandernack K.W. and Tebo B.M., 1993. Manganese scavenging and oxidation at hydrothermal vents and in vent plumes. *Geochim. Cosmochim. Acta* 57, 3907-3923.
- Mangini A., Eisenhouwer A. and Walter P., 1990. Response of manganese in the ocean to the climatic cycles in the Quaternary. *Paleoceanography* 5, 811-821.
- Mangini A., Rutsch H.-J., Frank M., Eisenhauer A. and Eckhardt J.-D., 1994. Is there a relationship between atmospheric CO₂ and manganese in the ocean? In: R. Zahn et al. (Editors), *Carbon cycling in the glacial ocean: Constraints on the ocean's role in the global change*. Springer Verlag, pp. 87-104.
- Manheim F.T. and Waterman, L.S., 1974. Diffusimetry (diffusion constant estimation) on sediment cores by resistivity probe. *Init. Rep. DSDP* 22, 663-670.
- Martin J.H. and Knauer G.A., 1984. VERTEX: manganese transport through oxygen minima. *Earth Planet. Sci. Lett.* 67, 35-47.
- Martin J.H., Fitzwater S.E. and Gordon R.M., 1990. Iron deficiency limits phytoplankton growth in antarctic waters. *Glob. Biogeochem. Cycles* 4, 5-12.
- McArthur J.M., 1985. Francolite geochemistry. - compositional controls during formation, diagenesis, metamorphism and weathering. *Geochim. Cosmochim. Acta* 49, 23-35.
- McClellan G.H., 1980. Mineralogy of carbonate fluorapatites. *J. Geol. Soc. London* 137, 675-681.
- McManus J., Berelson W.M., Coale K.H., Johnson K.S. and Kilgore, T.E., 1997. Phosphorus

- regeneration in continental margin sediments. *Geochim. Cosmochim. Acta* 61, 2891-2907.
- Meese D.A., Alley R.B., Fiacco R.J., Germani M.S., Gow A.J., Grootes P.M., Illing M., Mayewski P.A., Morrison M.C., Ram M., Taylor K.C., Yang Q. and Zielinski, G.A., 1994. Preliminary depth-agescale of the GISP2 ice core. *Special CRREL Report 94-1*, US.
- Middelburg J.J., De Lange G.J. and van der Weijden C.H., 1987. Manganese solubility control in marine porewaters. *Geochim. Cosmochim. Acta* 51, 759-763.
- Middelburg J.J., 1991. Organic carbon, sulphur, and iron in recent semi-euxinic sediments of Kau Bay, Indonesia. *Geochim. Cosmochim. Acta* 55, 815-828.
- Moodley L., Schaub B.E.M., van der Zwaan G.J. and Herman P.M.J., 1997. Tolerance of benthic foraminifera (Protista: Sarcodina) to hydrogen sulphide, *Marine Ecology Progress Series*, 169, 77-86.
- Morrison J.M., Codispoti L.A., Smith S.L., Wishner K., Flagg C., Gardner W.D., Gaurin S., Naqvi S.W.A., Manghnani V., Prosperie L. and Gundersen J.S., 1999. The oxygen minimum zone in the Arabian Sea during 1995. *Deep-Sea Res II* 46, 1903-1931.
- Morse J.W. and Emeis, K.C., 1992. Carbon/sulphur/iron relationships in upwelling sediments. *Geol. Soc. Spec. Publ.* 64, 247-255.
- Mortimer D.H., 1971. Chemical exchanges between sediments and water in the Great Lakes - speculations on probable regulatory mechanisms. *Limnol. Oceanogr.* 16, 387-404.
- Mucci A., 1988. Manganese uptake during calcite precipitation from seawater: Conditions leading to the formation of a pseudokutnahorite. *Geochim. Cosmochim. Acta* 52, 1859-1868.
- Müller P.J. and Suess E., 1979. Productivity, sedimentation rate and sedimentary organic matter in the oceans-I: Organic carbon preservation. *Deep-Sea Res.* 26, 1347-1362.
- Naidu P.D. and Malmgren B.A., 1995. A 2,200 years periodicity in the Asian monsoon system. *Geoph. Res. Lett.* 22, 2361-2364.
- Naidu P.D. and Malmgren B.A., 1996. A high-resolution record of Late Quaternary upwelling along the Oman Margin, Arabian Sea based on planktonic foraminifera. *Paleoceanography* 11, 129-140.
- Nair R.R., Ittekkot V., Manganini S.J., Ramaswamy V., Haake B., Degens E.T., Desai B.N. and Honjo S., 1989. Increased particle flux to the deep ocean related to monsoons. *Nature* 338, 749-751.
- Naqvi S.W.A., 1987. Some aspects of the oxygen-deficient conditions and denitrification in the Arabian Sea. *J. Mar. Res.* 45, 1049-1072.
- Nemliher J., Kallaste T. and Puura I., 1997. Hydroxyapatite varieties in recent fish scales. *Proc. Estonian Acad. Sci. Geol.* 46, 187-196.
- Newesly H., 1989. Fossil bone apatite. *Appl. Geochem.* 4, 233-245.
- Nriagu J.O., 1983. Rapid decomposition of fish bones in Lake Erie sediments. *Hydrobiologia* 106, 217-222.
- O'Brien G.W., Milnes A.R., Veeh H.H., Heggie D.T., Riggs S.R., Cullen D.J., Marshall J.F. and Cook P.J., 1990. Sedimentation dynamics and redox iron-cycling: controlling factors for the apatite-glaucanite association on the East Australian continental margin. *Geol. Soci. Spec. Publ.* 52, 61-86.
- Olsen D.B., Hitchcock G.L., Fine R.A. and Warren B.A., 1993. Maintenance of the low-oxygen layer in the central Arabian Sea. *Deep-Sea Res. II* 40, 673-685.
- Owens N.J.P., Burkill P.H., Mantoura R.F.C., Woodward E.M.S., Bellan I.E., Aiken, J., Howland R.J.M. and Llewellyn C.A., 1993. Size-fractionated primary production and nitrogen assimilation in the northwestern Indian Ocean. *Deep-Sea Res. II* 40, 697-709.

- Paropkari A.L., Babu C.P. and Mascarenhas A., 1992. A critical evaluation of depositional parameters controlling the variability of organic carbon in Arabian Sea sediments. *Mar. Geol.* 107, 213-226.
- Passier H.F., Middelburg J.J., van Os B.J.H. and de Lange G.J., 1996. Diagenetic pyritisation under eastern Mediterranean sapropels caused by downward sulphide diffusion. *Geochim. Cosmochim. Acta* 60, 751-763.
- Passier H.F., Luther III G.W. and De Lange G.J., 1997. Early diagenesis and sulphur speciation in sediments of the Oman Margin, northwest Arabian Sea. *Deep Sea Res. II* 44, 1361-1380.
- Passier H.F. and De Lange G.J., 1998. Sedimentary sulphur and iron chemistry in relation to the formation of eastern Mediterranean sapropels. *Proc. ODP Sci. Results* 160, 249-259.
- Pedersen T.F. and Price N.B., 1982. The geochemistry of manganese carbonate in Panama Basin sediments. *Geochim. Cosmochim. Acta* 46, 59-68.
- Pedersen T.F., Shimmield G.B. and Price, N.B., 1992. Lack of enhanced preservation of organic matter in sediments under the oxygen minimum on the Oman Margin. *Geochim. Cosmochim. Acta* 56, 545-551.
- Peterson, W.T., 1991. Zooplankton and nekton in the Arabian Sea. In: S.L. Smith et al., (Editors) *U.S. JGOFS Planning report No. 13*. pp. 75-85.
- Plinius Maior, *Naturalis Historia, Book IX*. The Loeb classical library, (London, etc., Heinman, etc, 1961-1971).
- Pollehne F., Zeitzschel B. and Peinert R., 1993. Short-term sedimentation patterns in the northern Indian Ocean. *Deep-Sea Res. II* 40, 821-831.
- Posner A.S., Blumenthal N.C. and Betts F., 1984. Chemistry and structure of precipitated hydroxyapatites. In: J.O. Nriagu and P.B. Moore (Editors), *Phosphate minerals*. Springer Verlag, Berlin, pp. 330-350.
- Prell W.L., 1984. Monsoonal climate of the Arabian Sea during the Later Quaternary: a response to changing solar radiation. In: A.L. Berger (Editor), *Milankovitch and Climate, part 1*. D. Riedel, Hingham, Mass, pp. 349-366.
- Prell W.L., Hutson W.H., Williams D.F., Be A.W.H., Geitzenauer K. and Molfino B., 1980. Surface circulation of the Indian Ocean during the Last Glacial Maximum, approximately 18,000 yr BP. *Quat. Res.* 14, 309-336.
- Prell W.L., and shipboard party of ODP Leg 117, 1990. Neogene tectonics and sedimentation of the SE Oman continental margin: results from ODP Leg 117. *Geol. Soc. Spec. Publ.* 49, 745-758
- Price N.B. and Calvert S.E., 1978. The geochemistry of phosphorites from the Namibian shelf. *Chem. Geol.* 23, 151-170.
- Prins M.A., 1999. Pelagic, hemipelagic and turbidite deposition in the Arabian Sea during the Late Quaternary. *Geologica Utraiectina* 168, Ph.D. thesis.
- Qasim S.Z., 1982. Oceanography of the northern Arabian Sea. *Deep-Sea Res.* 29, 1041-1068.
- Raiswell R. and Berner R.A., 1985. Pyrite formation in euxinic and semi-euxinic sediments. *Am. J. Sci.* 285, 710-724.
- Raiswell R., Buckley F., Berner R.A. and Anderson T.F., 1988. Degree of pyritization of iron as a paleoenvironmental indicator of bottom-water oxygenation. *J. Sed. Petr.* 58, 812-819.
- Raiswell R., Canfield D.E. and Berner R.A., 1994. A comparison of iron extraction methods for the determination of degree of pyritisation and the recognition of iron-limited pyrite formation. *Chem. Geol.* 111, 101-110.
- Raiswell R. and Canfield D.E., 1998. Sources of iron for pyrite formation in marine sediments.

- Am. J. Sci.* 298, 219-245.
- Rao V.P. and Lamboy M., 1995. Phosphorites from the Oman Margin. *Oceanologica Acta* 18, 289-307.
- Rao V.P. and Lamboy M., 1996. Genesis of apatite in the phosphatized limestones of the western continental shelf of India. *Mar. Geol.* 136, 41-53.
- Ravelo A.C., Fairbanks R.G. and Philander S.G.H., 1990. Reconstructing tropical Atlantic hydrography using planktonic foraminifera and an ocean model. *Paleoceanography* 5, 409-431.
- Redfield A.C., Ketchum B.H. and Richards F.A., 1963. The influence of organisms on the composition of seawater. In: M.N. Hill (Editor), *The Sea, Vol 2*. pp. 26-77.
- Reichart, G.J., 1997. Late Quaternary variability of the Arabian Sea monsoon and oxygen minimum zone. *Geologica Ultraiectina* 154, Ph.D. thesis.
- Reichart G.J., den Dulk M., Visser H.J., van der Weijden C.H. and Zachariasse W.J., 1997. A 225 kyr record of dust supply, paleoproductivity and the oxygen minimum zone from the Murray Ridge (northern Arabian Sea). *Palaeogeogr. Palaeoclimatol. Palaeoecol.* 134, 149-169.
- Reichart G.J., Lourens L.J. and Zachariasse W.J., 1998. Temporal variability in the northern Arabian Sea Oxygen Minimum Zone (OMZ) during the last 225,000 years. *Paleoceanography* 13, 607-621.
- Reimers C.E., Kastner M. and Garrison R.E., 1990. The role of bacterial mats in phosphate mineralization with particular reference to the Monterey Formation. In: W.C. Burnett and S.R. Riggs (Editors), *Phosphate deposits of the world, Vol 3*. Cambridge University Press, United Kingdom, pp. 300-311.
- Reimers C.E., Rutenber K.C., Canfield D.E., Christiansen M.B. and Martin J.B., 1996. Porewater pH and authigenic phases formed in the uppermost sediments of the Santa Barbara Basin. *Geochim. Cosmochim. Acta* 60, 4037-4057.
- Ripley E.M., Shaffer N.R. and Gilstrap M.S., 1990. Distribution and geochemical characteristics of metal enrichment in the New Albany Shale (Devonian-Mississippian), Indiana. *Econ. Geol.* 85, 1790-1807.
- Rona P.A., 1984. Hydrothermal mineralization on the slow-spreading Mid-Atlantic Ridge and Carlsberg Ridge. *Abstracts with Programs* 16, 638. (abstr.).
- Röpke A., Nellen W. and Piatkowski U., 1993. A comparative study on the influence of the pycnocline on the vertical distribution of fish larvae and cephalopod paralarvae in three ecologically different areas of the Arabian Sea. *Deep-Sea Res. II* 40, 801-819.
- Rutten A., De Lange G.J., Hayes A., Rohling E.J., De Jong A.F.M. and Van der Borg K., 1999. Deposition of sapropel S1 sediments in oxic pelagic and anoxic brine environments in the eastern Mediterranean: differences in diagenesis and preservation. *Mar. Geol.* 153, 319-335.
- Rutten A. and De Lange G.J., in prep. Sequential extraction of natural minerals applied to eastern Mediterranean sediments.
- Ruttenber K.C., 1992. Development of a sequential extraction method for different forms of phosphorus in marine sediments. *Limnol. Oceanogr.* 37, 1460-1482.
- Ruttenber K.C., 1993. Reassessment of the oceanic residence time of phosphorus. *Chem. Geol.* 107, 405-409.
- Ruttenber K.C. and Berner R.A., 1993. Authigenic apatite formation and burial in sediments from non-upwelling, continental margin environments. *Geochim. Cosmochim. Acta* 57, 991-1007.

- Ryther J.H., 1969. Photosynthesis and fish production in the sea. *Science* 166, 72-76.
- Saager P.M., De Baar H.J.W. and Burkill P.H., 1989. Manganese and iron in Indian Ocean waters. *Geochim. Cosmochim. Acta* 53, 2259-2267.
- Sarnthein M., Pflaumann U., Ross R., Tiedemann R. and Winn K., 1992. Transfer functions to reconstruct ocean palaeoproductivity: a comparison. *Geol. Soc. Spec. Publ.* 64, 411-427.
- Sayles F.L., Martin W.R. and Deuser W.G., 1994. Response of benthic oxygen demand to particulate organic carbon supply in the deep sea near Bermuda. *Nature* 371, 686-689.
- Sarkar A., Bhattacharya S.K. and Sarin M.M., 1993. Geochemical evidence for anoxic deep water in the Arabian Sea during the last glaciation. *Geochim. Cosmochim. Acta* 57, 1009-1016.
- Schenu S.J., Antonarakou A., Hilgen F.J., Lourens L.J., Nijenhuis I.A., van der Weijden C.H. and Zachariasse W.J., 1999. Organic-rich layers in the Metochia section (Gavdos, Greece): evidence for a single mechanism of sapropel formation during the past 10 My. *Mar. Geol.* 153, 117-135.
- Schmitz B., 1987. The TiO_2/Al_2O_3 ratio in Cenozoic Bengal abyssal fan sediments and its use as a pleostream energy indicator. *Mar. Geol.* 76, 195-206.
- Schmitz B., Åberg G., Werdelin L., Forey P. and Bendix-Almgren S.E., 1991. $^{87}Sr/^{86}Sr$, Na F, Sr and La in skeletal fish debris as a measure of the paleosalinity of fossil-fish habitats. Geological society of America Bulletin, 103, 786-794.
- Schuffert J.D., Jahnke R.A., Kastner M., Leather J., Sturz A. and Wing M.R., 1994. Rates of formation of modern phosphorite off western Mexico. *Geochim. Cosmochim. Acta* 58, 5001-5010.
- Schuffert J.D., Kastner M. and Jahnke R.A., 1998. Carbon and phosphorus burial associated with modern phosphorite formation. *Mar. Geol.* 146, 21-31.
- Schulz H., von Rad U. and von Stackelberg U., 1996. Laminated sediments from the oxygen-minimum zone of the northeastern Arabian Sea. *Geol. Soc. Spec. Publ.* 116, 185-207.
- Schulz H., von Rad U. and Erlenkeuser H., 1998. Correlation between Arabian Sea and Greenland climate oscillations of the past 110,000 years. *Nature* 393, 54-57.
- Sharma G.S., 1978. Upwelling off the southwest coast of India. *Indian Journal of Marine Sciences* 7, 209-218.
- Sharp G.D., 1988. Fish populations and fisheries, their perturbations, natural and man-induced. In: H. Postma and J.J. Zijlstra (Editors), *Continental shelves, ecosystems of the world 27*. Elsevier Science publishers, Amsterdam, pp.155-202.
- Sharp G.D., 1992. Climate change, the Indian Ocean tuna fishery, and empiricism. In: M.H. Glantz (Editor), *Climate variability, climate change and fisheries*. Cambridge University Press, pp. 377-416.
- Sherwood B.A., Sager S.L. and Holland H.D., 1987. Phosphorus in foraminiferal sediments from North Atlantic Ridge cores and in pure limestones. *Geochim. Cosmochim. Acta* 51, 1861-1866.
- Shimmield G.B., Price N.B. and Pedersen T.F., 1990. The influence of hydrography, bathymetry and productivity on sediment type and composition of the Oman Margin and in the Northwest Arabian Sea. *Geol. Soc. Spec. Publ.* 49, 759-769.
- Shimmield G.B., 1992. Can sediment geochemistry record changes in coastal upwelling palaeoproductivity? Evidence from northwest Africa and the Arabian Sea. *Geol. Soc. Spec. Publ.* 64, 29-46.
- Sirocko F., 1991. Deep-Sea sediments of the Arabian Sea: a paleoclimatic record of the Southwest-Asian summer monsoon. *Geologische Rundschau* 80, 557-566.
- Sirocko F. and Sarnthein M., 1989. Wind-borne deposits in the northwestern Indian Ocean:

- record of Holocene sediments versus modern satellite data. In: M. Leinen and M. Sarnthein (Editors), *Paleoclimatology and Paleometeorology: Modern and Past Patterns of Global Atmospheric Transport*. Kluwer Academic Publishers, pp. 401-433.
- Sirocko F., Sarnthein M., Erlenkeusers H., Lange H., Arnold M. and Duplessy, J.C., 1993. Century-scale events in monsoonal climate over the past 24,000 years. *Nature* 364, 322-324.
- Sirocko F., Garbe-Schönberg D., McIntyre A. and Molfino B., 1996. Teleconnections between the subtropical monsoons and high-latitude climates during the last deglaciation. *Science* 272, 526-529.
- Slater R.D. and Kroopnick P., 1984. Controls on dissolved oxygen distribution and organic carbon deposition in the Arabian Sea. p. 305-313. In: B.U. Haq, and J.D. Milliman (Editors), *Geology and oceanography of the Arabian Sea and Coastal Pakistan*.
- Slomp C.P., Epping E.H.G., Helder W. and Van Raaphorst W., 1996. A key role for iron-bound phosphorus in authigenic apatite formation in North Atlantic continental platform sediments. *J. Mar. Res.* 54, 1179-1205.
- Slomp C.P. and Van Raaphorst W., 1993. Phosphate adsorption in oxidized marine sediments. *Chem. Geol.* 107, 477-480.
- Slomp C.P., Malschaert J.F.P. and Van Raaphorst W., 1998. The role of adsorption in sediment-water exchange of phosphate in North Sea continental margin sediments. *Limnol. Oceanogr.* 43, 832-846.
- Smith R.L. and Bottero J.S., 1977. Nutrients as tracers of water mass structure in the coastal upwelling off northwest Africa. In: M. Angel (Editor), *A voyage of discovery*. Pergamon Press, pp. 291-304.
- Solarzano L., 1969. Determination of ammonia in natural water by phenol-hypochlorite method. *Limnol. Oceanogr.* 14, 799-801.
- Souter A. and Isaacs J.D., 1974. Abundance of pelagic fish during the 19th and 20th centuries as recorded in anaerobic sediments off the Californias. *Fish Bull.* 72, 257-274.
- Sternbeck J. and Sohlenius G., 1997. Authigenic sulfide and carbonate mineral formation in Holocene sediments of the Baltic Sea. *Chem. Geol.* 135, 55-73.
- Strickland J.D.H. and Parsons T.R., 1968. A practical handbook of seawater analysis. *Fish. Board Can. Bull.* 167. 311 pp.
- Stuiver M., Pearson G.W. and Braziunas T., 1986. Radiocarbon age calibration of marine samples back to 9000 cal yr BP. *Radiocarbon* 28, 980-1021.
- Stuiver M., Reimer P.J., Bard E., Beck J.W., Burr G.S., Hughen K.A., Kromer B., McCormac F.G., v.d. Plicht J. and Spurk M., 1998. INTCAL98 Radiocarbon Age Calibration, 24,000-0 cal BP. *Radiocarbon* 40, 1041-1083.
- Suess E., 1981. Phosphate regeneration from sediments of the Peru continental margin by dissolution of fish debris. *Geochim. Cosmochim. Acta* 45, 577-588.
- Suess E. and Müller P.J., 1979. Productivity, sedimentation rate and sedimentary organic matter in the oceans - II. - elemental fractionation. *Colloques Internationaux du C.N.R.S. no 293*, 17-26.
- Summerhayes C.P., Prell W.L. and Emeis K.-C., 1992. Upwelling systems: evolution since the early Miocene. *Geol. Soc. Spec. Publ.* 64, 1-5.
- Sunda W.G. and Huntsman S.A., 1988. Effect of sunlight on redox cycles of manganese in the southwestern Sargossa Sea. *Deep-Sea Res.* 35, 1297-1317.
- Sundby B., Gobeil C., Silverberg N. and Mucci A., 1992. The phosphorus cycle in coastal marine sediments. *Limnol. Oceanogr.* 37, 1129-1145.

- Sutherland H.E., Calvert S.E. and Morris R.J., 1984. Geochemical studies of the recent sapropel and associated sediment from the Hellenic Outer Ridge, eastern Mediterranean. I: Mineralogy and chemical composition. *Mar. Geol.* 56, 79-92.
- Swallow J.C., 1984. Some aspects of the physical oceanography of the Indian Ocean. *Deep-Sea Res.* 31, 639-650.
- Thomson J., Calvert S.E., Mukherjee S., Burnett W.C. and Bremner J.M., 1984. Further studies of the nature, composition and ages of contemporary phosphorite from the Namibian Shelf. *Earth Planet. Sci. Lett.* 69, 341-353
- Thomson J., Higgs N.C., Jarvis I., Hydes D.J., Colley S. and Wilson T.R.S., 1986. The behaviour of manganese in Atlantic carbonate sediments. *Geochim. Cosmochim. Acta* 50, 1807-1818.
- Thomson J., Jarvis I., Green D.R.H., Green, D.A. and Clayton T., 1998. Mobility and immobility of redox-sensitive elements in deep-sea turbidites during shallow burial. *Geochim. Cosmochim. Acta* 62, 643-656.
- Toerien D.F., Gerber A., Lötter L.H. and Cloete T.E., 1990. Enhanced biological phosphorus removal in activated sludge systems. In: K.C. Marshall (Editor), *Advances in Microbial Ecology* 11, 173-230. Plenum Press, New York.
- Trappe J., 1998. Phanerozoic phosphorite depositional systems, a dynamic model for a sedimentary resource system. *Lecture Notes in Earth Sciences* 76. Springer, Berlin. 316 pp.
- Tribovillard N.P., Caulet J.P., Vergnaud-Grazzini C., Moureau N. and Tremblay P., 1996. Lack of organic matter accumulation on the upwelling-influenced Somalia margin in a glacial-interglacial transition. *Mar. Geol.* 133, 157-182.
- Tyrrell, T., 1999. The relative influences of nitrogen and phosphorus on oceanic primary production. *Nature* 400, 525-531.
- Tyson R.V., 1995. *Sedimentary organic matter, organic facies and palynofacies*. Chapman and Hall, London, 615 pp.
- Van Bennekom J. and Hiehle M., 1994. CTD operations and calibrations during legs D1, D2 and D3 of the Netherlands Indian Ocean Programme. In: W.J.M. van der Linden and C.H. van der Weijden (Editors), *Geological study of the Arabian Sea Vol. 3*. National Museum of Natural History Leiden, pp. 37-65.
- Van Bennekom A.J., Hiehle J., Van Ooyen M.A., van Weerlee E. and van Koutrik M., 1995. CTD and hydrography. In: J.E. van Hinte, Tj.C.E. van Weering and S.R. Troelstra (Editors), *Tracing a seasonal upwelling*. Netherlands Geosciences Foundation, The Hague. pp. 41-54.
- Van Cappellen P. and Berner R.A., 1988. A mathematical model for the early diagenesis of phosphorus and fluorine in marine sediments: apatite precipitation. *Am. J. Sci.* 288, 289-333.
- Van Cappellen P. and Berner R.A., 1991. Fluorapatite crystal growth from modified seawater solutions. *Geochim. Cosmochim. Acta* 55, 1219-1234.
- Van Cappellen P. and Ingall, E.D., 1994. Benthic phosphorus regeneration, net primary production, and ocean anoxia: A model of the coupled marine biogeochemical cycles of carbon and phosphorus. *Paleoceanography* 9, 677-692.
- Van Cappellen P. and Ingall E.D., 1996. Redox stabilization of the atmosphere and oceans by phosphorus-limited marine productivity. *Science* 271, 493-496.
- Van der Weijden C.H., de Lange G.J. and Visser H.J., 1994. Porewater alkalinity, silica, phosphate, ammonia, nitrite and nitrate. In: W.J.M. van der Linden and C.H. van der

- Weijden (Editors), *Geological study of the Arabian Sea Vol. 3*. National Museum of Natural History Leiden, pp. 117-119.
- Van der Weijden C.H., Reichart G.J. and Visser H.J., 1999. Enhanced preservation of organic matter in sapropelic sediment deposited within the oxygen minimum zone in the northeastern Arabian Sea. *Deep-Sea Res.* 46, 807-830.
- Van Os B.J.H., Middelburg J.J. and De Lange G.J., 1991. Possible diagenetic mobilisation of barium in sapropelic sediment from the eastern Mediterranean. *Mar. Geol.* 100, 125-136.
- Van Santvoort P.J.M., De Lange G.J., Thomson J., Cussen, H., Wilson T.R.S., Krom M.D. and Ströhle K., 1996. Active post-depositional oxidation of the most recent sapropel (S1) in sediments of the eastern Mediterranean Sea. *Geochim. Cosmochim. Acta* 60, 4007-4024.
- Von Breymann, M.T., Emeis K-C. and Suess E., 1992. Water depth and diagenetic constraints on the use of barium as a paleoproductivity indicator. *Geol. Soc. Spec. Publ.* 64, 273-284.
- Von Rad U., Schaaf M., Michels K.H., Schulz H., Berger W.H. and Sirocko F., 1999. A 5000-yr record of climate change in varved sediments from the oxygen minimum zone off Pakistan, northeastern Arabian Sea. *Quat. Res.* 51, 39-53.
- Venema S.C., 1984. Fishery resources in the north Arabian Sea and adjacent waters. *Deep-Sea Res.* 31, 1001-1018.
- Williams L.A. and Reimers C.E., 1983. Role of bacterial mats in oxygen-deficient marine basins and coastal upwelling regimes: Preliminary report. *Geology* 11, 267-269.
- Wilson T.R.S., Thomson J., Hydes D.J., Colley S., Culkin F. and Sørensen J., 1986. Oxidation fronts in pelagic sediments: diagenetic formation of metal-rich layers. *Science* 232, 972-975.
- Woodward E.M.S., Rees A.P. and Stephens J.A., 1999. The influence of the south-west monsoon upon the nutrient biogeochemistry of the Arabian Sea. *Deep-Sea Res. II* 46, 571-591.
- Wyrski K., 1971. *Oceanographic atlas of the international Indian Ocean expedition*, Natl. Sci. Found., U.S. Gov. Print. Off., Washington D.C., 531 pp.
- Wyrski K. 1973. Physical Oceanography of the Indian Ocean. In: B. Zeitzschel (Editor), *The biology of the Indian Ocean*. Springer, pp. 18-36.
- Yang Y.-L., Elderfield H., Pedersen T.F. and Ivanovich M., 1995. Geochemical record of the Panama basin during the last glacial maximum carbon event shows that the glacial ocean was not suboxic. *Geology* 23, 1115-1118.
- You Y. and Tomczak M., 1993. Thermocline circulation and ventilation in the Indian Ocean derived from water mass analysis. *Deep-Sea Res.* 40, 13-56.
- Zabel M., Dahmke A. and Schulz H.D., 1998. Regional distribution of diffusive phosphate and silicate fluxes through the sediment-water interface: the eastern South Atlantic. *Deep-Sea Res.* 45, 277-300.

Samenvatting

Sinds lange tijd staat de Arabische Zee bekend om zijn rijkdom aan marien leven. De Grieken in de legers van Alexander de Grote, de ons eerst bekende Europeanen die in de vierde eeuw voor Christus de Arabische Zee bezeilden, merkten al de grote overvloed aan zeeleven op in vergelijking met de Middellandse Zee. Ze namen waar hoe met name tijdens de periode van de zonnwende “gierende wervelwinden, stortbuien en zware stormen, die van de bergruggen omlaag jagen, de zee van haar bodem omkeren en haar monsters uit de diepte in grote aantallen omhoogwentelen” (Plinius Maior, *Naturalis Historia*). Dit was waarschijnlijk de eerste keer, dat de hoge productiviteit van zeeleven in verband werd gebracht met de periode van moessonregens. Al eeuwen profiteert de lokale visserij van de grote scholen tonijn. Pas sinds de laatste eeuw wordt de Arabische Zee commercieel geëxploiteerd. De totale visvangst in de westelijke Indische Oceaan is toegenomen van ~ 0,5 miljoen ton in 1950 tot bijna 3,7 miljoen ton in 1997, waardoor deze visgronden zeer belangrijk zijn geworden voor de mondiale visvangst.

De overvloed aan leven in de Arabische Zee wordt veroorzaakt door het opwellen van nutriëntrijk water voor de kust van Oman en Somalië. Het is nog niet precies bekend welk nutriënt de primaire productie in de oceanen limiteert. Recentelijk is ontdekt dat de bio-beschikbaarheid van opgelost ijzer de groei van fytoplankton in enkele open-oceaan milieus bepaalt. Nitraat is het limiterende nutriënt in de meeste kustwateren, wat veroorzaakt wordt door de lage toevoer van nitraat door rivieren en het verlies door denitrificatie in de waterkolom en in het sediment. Fosfor (P) heeft, in tegenstelling tot stikstof, geen belangrijke gasfasen. De massabalans van P in de oceanen wordt daarom bepaald door enerzijds de aanvoer vanuit fluviaatiele en eolische bronnen, en anderzijds door de vastlegging in sedimenten. Fosfor is een structurele en functionele component van alle organismen en speelt een centrale rol in de opslag, het transport en het gebruik van energie. Deze eigenschappen maken fosfor een essentieel nutriënt voor de biosfeer. Op geologische tijdschalen wordt de beschikbaarheid van fosfor beschouwd als de voornaamste factor die de primaire productiviteit in oceanen controleert, omdat tekorten aan stikstof worden aangevuld door stikstofopname uit de atmosfeer. De productiviteit in de zee bepaalt de accumulatie van organisch koolstof en controleert daarmee de CO₂- en O₂-concentraties in de atmosfeer. De bio-beschikbaarheid van fosfor in de oceanen kan potentieel een belangrijke rol spelen in klimaatsveranderingen. Bovendien verschaft gedetailleerde kennis van de fosforcyclus in de oceanen een beter inzicht in de biochemische cycli van koolstof, stikstof, zwavel en andere elementen met een affiniteit voor organische fasen.

In dit proefschrift worden de fosfor- en mangaancycli in de Arabische Zee tijdens het Laat Kwartair bestudeerd, waarbij gebruik wordt gemaakt van de sedimentkernen die zijn verzameld in 1992 tijdens het Nederlandse Indische Oceaan Programma (NIOP). Het eerste deel heeft betrekking op de reconstructie van veranderingen in paleoproductiviteit en intensiteit van de zuurstofminimumzone. Speciale aandacht wordt besteed aan

mangaan- en zwavel-accumulatiepatronen om veranderingen in de redoxcondities van het bodemwater te bepalen. In het tweede deel van dit proefschrift wordt de fosforcyclus in de sedimenten van de Arabische Zee onderzocht. Poriewaterfluxen en gegevens over de vaste fase worden gecombineerd om de diagenetische processen te bepalen die de benthische regeneratie en vastlegging van P in sedimenten controleren. De zeer verschillende milieucondities van de Arabische Zee in het verleden en heden bieden een uitstekende mogelijkheid om de mechanismen vast te stellen die de onttrekking van P uit de oceanen bepalen en om de potentiële rol vast te stellen die de P-cyclus speelt in de veranderingen van de paleoproductiviteit op geologische tijdschalen.

Klimaat en hydrografie van de Arabische Zee

De Arabische Zee is een half-afgesloten bekken in de noordwestelijke Indische Oceaan. Het klimaat en de hydrografie worden sterk beïnvloed door het moesson-windsysteem. Tijdens de zomer op het noordelijke halfrond leidt het verschil in opwarming tussen het continent en de oceaan tot een intensief lagedrukgebied boven het Himalaya-gebergte en het Tibettaans plateau. Het grote luchtdrukverschil tussen Azië en de zuidelijke Indische Oceaan veroorzaakt een sterke zuidwestenwind boven de Arabische Zee (de ZW moesson). Deze winden, die zijn gebundeld in een nauwe straalstroom parallel aan de kust van Oman, Jemen en Somalië (de Findlater Jet), resulteren in transport van oppervlaktewater in een afluende richting. Hierdoor worden diepere nutriëntrijke watermassa's naar de oceaanoppervlakte gebracht, waardoor de biologische productiviteit in de gehele Arabische Zee wordt verhoogd. Tijdens de ZW moesson varieert de primaire productiviteit van $2.5 \text{ gC m}^{-2}\text{d}^{-1}$ voor het kustgebied van Oman tot $0.5 \text{ gC m}^{-2} \text{d}^{-1}$ in het meer oligotrofe centrale Arabische Bekken. Tijdens de winter op het noordelijk halfrond is de situatie omgekeerd. Hoge luchtdruk boven het Aziatisch continent veroorzaakt noordoostelijke passaatwinden, die over het algemeen zwakker zijn dan de ZW moesson. Deze winden resulteren in watertransport richting de kust van het Arabisch Schiereiland, die het opwellen van dieper water, en daarmee de biologische productie, vermindert. Schattingen van de jaarlijkse primaire productiviteit in de noordelijke Arabische Zee variëren tussen de 200 en $400 \text{ gC m}^{-2}\text{j}^{-1}$. Dit maakt de Arabische Zee een van de meest productieve gebieden van de wereld.

Een belangrijk kenmerk van de Arabische Zee is de intensieve zuurstof-minimumzone (ZMZ) die zich op een waterdiepte van 200 tot 1500 m bevindt. Zuurstofconcentraties in de ZMZ zijn het laagst in het noordoostelijk deel van de Arabische Zee ($< 4.5 \mu\text{M}$). Deze lage zuurstofconcentraties worden veroorzaakt door de combinatie van a) een hoge zuurstofconsumptie als gevolg van hoge mineralisatiesnelheden van het organisch materiaal, b) een sterke thermostratificatie van de bovenste 200 m van de waterkolom, c) een trage diepwaterventilatie, en d) het relatief lage zuurstofgehalte in de brongebieden (Indische Oceaan Centraal Water, Perzische Golf Water, Rode Zee Water) waar het water van de ZMZ wordt gegenereerd. De hoge biologische productiviteit en het zuurstofarme water van de ZMZ drukken hun stempel op de sedimenten van de Arabische Zee. Op de plaatsen waar de ZMZ de continentale

helling raakt, worden de sedimenten gekenmerkt door een hoog gehalte aan organisch-materiaal en een fijne laminatie. In het diepere deel van het Arabische Bekken, waar het bodemwater rijker is aan zuurstof, zijn deze gehalten over het algemeen een stuk lager.

Het unieke karakter van de Arabische Zee maakt dit gebied tot een belangrijk onderzoeksterrein voor verscheidene studies, betreffende de processen die het door de wind aangedreven opwellen veroorzaken, de invloed van het opwellen op de koolstofdioxideconcentratie in de atmosfeer, paleo-klimaatreconstructies, en de oorzaak van verhoogde accumulatie van organisch materiaal onder zuurstofarme bodemwatercondities.

Sequentiële extractietechnieken

De toepassing van sequentiële extractietechnieken vormt een belangrijk onderdeel van dit proefschrift. Sequentiële extracties worden gebruikt om de sedimentaire cyclus van verschillende elementen zoals S, N, P, Ca, Mg, Sr, Ba, Mn en Fe te bestuderen. Deze techniek is gebaseerd op het principe dat de verschillende vaste-fase-fracties van een bepaald element een ongelijk oplossingsgedrag vertonen ten opzichte van een reeks van reagentia. Sedimentmonsters worden achtereenvolgens geschud met een reeks oplosmiddelen om de verschillende fracties te extraheren, waarbij de meest reactieve fasen het eerst oplossen.

De speciatie van mangaan in de vaste fase is zeer gevoelig voor de redoxcondities in de waterkolom en het sediment. In **Hoofdstuk 2** wordt een extractieschema gepresenteerd om de drie belangrijkste Mn-fracties in mariene sedimenten te onderscheiden, namelijk 1) Mn-carbonaten, 2) Mn-oxiden en 3) een residufractie bestaande uit mangaan geassocieerd met aluminiumsilicaten en pyriet. Toepassing van dit extractieschema maakt het mogelijk om de paleo-redoxcondities vast te stellen en de aard van sedimentaire Mn-verrijkingen.

Als gevolg van de lage P-concentraties in mariene sedimenten zijn sequentiële extractietechnieken de enige beschikbare methoden om gedetailleerde informatie te verkrijgen over de samenstelling van P in sedimenten. Tijdens het laatste decennium is een sequentieel extractieschema ontwikkeld (de SEDEX-methode) dat een onderscheid kan maken tussen 1) makkelijk uitwisselbare P, 2) P geassocieerd aan ijzeroxiden, 3) authigeen apatiet, 4) detritisch apatiet, en 5) organisch P. Deze sequentiële extractiemethode is succesvol toegepast in verschillende pelagische milieus. In **Hoofdstuk 5** is de SEDEX-methode aangepast om, voor de eerste keer, een onderscheid te kunnen maken tussen P geassocieerd met biogeen apatiet (visresten) en authigeen apatiet. Tot op heden was het met de hand uitzoeken van visresten, wat een zeer tijdrovende bezigheid is, de enige beschikbare methode om hun aanwezigheid te kwantificeren. Toepassing van dit aangepaste extractieschema heeft drie voordelen. Ten eerste maakt het de evaluatie mogelijk van de accumulatie van visresten in de mariene fosforcyclus, ten tweede is het nu mogelijk om de accumulatiegeschiedenis van visresten in sedimenten te reconstrueren en ten derde verbetert de toepassing van dit extractieschema de bepaling van authigeen-apatietvorming in mariene sedimenten.

ZMZ variabiliteit in de Arabische Zee

Het moesson-klimaatstelsel van de noordelijke Indische Oceaan heeft grote veranderingen ondergaan tijdens het Laat Kwartair. De intensiteit van de moesson wordt primair gecontroleerd door precessiegedreven veranderingen in de zomerinsolatie. Studies aan sedimentkernen laten zien dat de paleoproductiviteit variaties vertoont met een cycliciteit van 23.000 jaar. Bovendien wordt de intensiteit van de zomer-moesson beïnvloed door glaciale/interglaciale klimaatveranderingen. In de Arabische Zee worden de glaciale perioden gekarakteriseerd door relatief hogere sedimentatiesnelheden en een hogere primaire productie in vergelijking met interglaciale perioden. Als gevolg van verschillen in de depositie van organisch materiaal en het convectief mengen in de waterkolom hebben de intensiteit en de verticale extensie van de ZMZ tijdens het Laat Kwartair sterke variaties ondergaan.

Mangaan is een belangrijk element voor de reconstructie van variaties in de zuurstofconditie van het bodemwater in het verleden. In **Hoofdstuk 2** worden Mn accumulatie patronen onderzocht in Arabische-Zee-sedimenten die zijn afgezet tijdens het Laat Kwartair, om zodoende de variabiliteit van de ZMZ te reconstrueren. De aanwezigheid van Mn-carbonaten in de sedimenten van het diepe Arabische Bekken toont aan dat het bodemwater gedurende minstens 185.000 jaar zuurstofhoudend is geweest. Op bepaalde sedimentdieptes bevinden zich in het onderste deel van de organisch-rijke lagen verrijkingen van Mn. De timing van de Mn-pieken komt overeen met de perioden van verhoogde reactief-Mn-fluxen naar het diepe bekken. Een verticale extensie van de ZMZ resulteerde in versterkte remobilisatie van reactief Mn in de sedimenten van het continentale plat naar de waterkolom en het daarop volgende transport naar het diepere, meer zuurstofrijke milieu.

Gedurende de laatste 20 jaar hebben klimaatstudies betreffende de moesson in de Indische Oceaan zich toegespitst op het opwellinggebied van Oman en Jemen. In **Hoofdstuk 3** wordt de sub-Milankovitch variabiliteit van de moessonintensiteit bestudeerd in het kustgebied van Oman. Geochemische en micropaleontologische accumulatiepatronen laten hoogfrequente veranderingen zien in de mariene productiviteit veroorzaakt door veranderingen in de intensiteit van het door de moesson geïnduceerde opwellen van dieper water. De intensiteit van de ZMZ varieerde synchroon met de sterkte van de zomer-moesson, waarbij de ZMZ het minst intensief is tijdens perioden van minimale zomer-moessonintensiteit. Het zuurstofarme water van de ZMZ veroorzaakt de reductie van ijzeroxiden in de waterkolom en/of het sediment-water-grensvlak. Als gevolg hiervan wordt pyrietvorming in de continentale-plat-sedimenten van Oman gelimiteerd door de beschikbaarheid van reactief ijzer. De veranderingen van de zomer-moesson kunnen goed gecorreleerd worden met synchrone veranderingen in het noordelijkste deel van de Arabische Zee. Bovendien bevestigen deze gegevens eerdere studies die een connectie suggereren tussen klimaatveranderingen op hoge en lage breedtegraad.

De sedimentaire P-cyclus in de Arabische Zee

Fosfor wordt uit de oceanen verwijderd door middel van accumulatie in sedimenten. Fosfor dat wordt vastgelegd in het sediment bestaat uit een reactieve en niet-reactieve component. Alleen reactief P kan opnieuw worden gemobiliseerd en weer beschikbaar komen voor opname in de biosfeer. Accumulatie van reactief fosfor vindt plaats door de sedimentatie van 1) organisch materiaal, 2) ijzeroxiden, die een hoge adsorptiecapaciteit hebben voor fosfaat, en 3) visresten (biogeen apatiet). De niet-reactieve fosforfractie in het sediment, die voornamelijk bestaat uit detritisch apatiet, vertegenwoordigt meestal slechts een klein deel van de totale accumulerende P-flux. De hoeveelheid en vorm waarmee P wordt vastgelegd in het sediment wordt sterk beïnvloed door vroeg-diagenetische processen. De afbraak van organisch materiaal, de reductie van ijzeroxiden en het oplossen van visresten resulteert in het vrijkomen van fosfaat in het poriewater. Dit opgelost fosfaat zal óf omhoog diffunderen naar de water kolom, óf neerslaan als een carbonaatfluorapatiet-mineraal (fosfogenese). De vorming van authigeen apatiet in sedimenten is geïdentificeerd als een potentieel belangrijke manier om reactief fosfor uit de oceanen te verwijderen. Met name sedimenten gelegen onder opwellingsgebieden worden dikwijls gekenmerkt door hoge concentraties van authigeen fosfor (zogenaamde fosforietafzettingen).

Voor een beter inzicht in de P-kringloop binnen de oceanen is het belangrijk om de omvang en de milieucondities te bepalen waarbij fosfogenese plaatsvindt. In **Hoofdstuk 4** worden fosfogenese en fosforietvorming onderzocht in de oppervlaktensedimenten van de Arabische Zee die zich thans in de zuurstofminimumzone bevinden. Poriewaterprofielen en een toename met de sedimentdiepte van de concentratie van een Ca-fosfaat-mineraal tonen aan dat fosfogenese op dit moment plaatsvindt in deze sedimenten. Resultaten van een diagenetisch model laten zien dat fosfogenese in de sedimenten voor de kust van Pakistan wordt veroorzaakt door een hoge afbraak van organisch materiaal en, waarschijnlijk, het oplossen van visresten. Vroeg-diagenetische reductie van ijzeroxiden heeft echter weinig invloed op de P-cyclus in deze sedimenten. Verder laten de modelresultaten zien dat dysoxische bodemwatercondities meer effectief zijn in het bevorderen van fosfogenese dan milieus met volledig zuurstofloze bodem waters. In een boxcore genomen vlak voor de kust van Oman werd de hoogste vormingssnelheid van authigeen apatiet waargenomen, hetgeen bijdraagt tot de vorming van een fosforiet afzetting. Dit is de eerste keer, dat de recente vorming van een fosforietafzetting is vastgesteld voor dit opwellingsgebied. Fosforietvorming vindt op dit moment plaats voor de kust van Oman als gevolg van a) de depositie van oud, herbewerkt materiaal van het continentale plat, dat een eerdere fase van fosfogenese heeft ondergaan, b) de hoge aanvoer van reactief P tijdens het Holoceen (visresten en afbreekbaar organisch materiaal), c) een relatief lage sedimentatiesnelheid en d) de afwezigheid van sterke waterstromingen op de zeebodem.

Over het algemeen wordt verondersteld dat de accumulatie van visresten in sedimenten een onbelangrijke rol speelt in de mariene P-kringloop. In de **Hoofdstukken 5, 6, en 7** worden de begraving en regeneratie bestudeerd van P geassocieerd met visresten (P_{vis}) in de sedimenten van de Arabische Zee. In recente oppervlaktensedimenten

is de accumulatie van visresten significant hoger boven 1200 m waterdiepte in vergelijking met diepere sedimenten (**Hoofdstuk 5**). De verdeling van P_{vis} over de oppervlakesedimenten wordt voornamelijk bepaald door de mate waarin visresten oplossen, wat is gerelateerd aan verschillen in waterdiepte en sedimentatiesnelheden. Bovendien kunnen de lage zuurstofconcentraties van het bodemwater een grotere preservatie van visresten hebben veroorzaakt. In **Hoofdstuk 6** wordt de vaste-fase-speciatie van P en de benthische fosfaatfluxen in recente Arabische-Zee-sedimenten besproken. Benthische P-fluxen zijn het hoogst in sedimenten op de continentale helling die zich thans in de ZMZ bevinden. Afbraak van organisch materiaal en fosfaatdesorptie van ijzeroxiden produceren niet voldoende fosfaat om deze hoge benthische fluxen te kunnen verklaren. De potentieel hoge accumulatie van visresten in de Arabische Zee en een goede correlatie tussen benthische fosfaatfluxen en P_{vis} -accumulatiesnelheden wijzen erop, dat de benthische fosfaatfluxen in deze sedimenten voornamelijk worden bepaald door oplossing van visresten tijdens de vroege diagenese.

De geschiedenis van de accumulatie van visresten tijdens het Laat Kwartair is onderzocht in sedimentkernen van het Pakistaanse continentale plat en van het diepe Arabische Bekken (**Hoofdstuk 7**). De gemiddelde vaste-fase-speciatie van P in deze twee verschillende milieus vertoont veel overeenkomsten: fosfor geassocieerd met visresten en P geassocieerd met authigeen apatiet vormen elk ongeveer 30% van de totale P-concentratie, terwijl P geassocieerd met ijzeroxiden, organisch P en detritisch apatiet slechts kleine fracties vormen. Variaties in de totale P-concentraties van de vaste fase zijn primair gerelateerd aan veranderingen in de bijdrage van de P_{vis} -fractie (**Hoofdstuk 5**). Op de continentale helling komen veranderingen in de P_{vis} -concentratie overeen met fluctuaties in de paleoproductiviteit. In deze mariene milieus is de P_{vis} -concentratie (en dus P in de vaste fase) een betere indicator voor paleoproductiviteit dan bijvoorbeeld organisch koolstof of bariet. In sedimenten van het diepe bekken, daarentegen, zijn fosforgehalten minder geschikt als indicator voor de paleoproductiviteit vanwege de hogere regeneratie van visresten.

Het afgelopen decennium is er een aanmerkelijke belangstelling geweest voor de omgevingsfactoren die de begravingsefficiëntie van P in de oceanen reguleren. Ingall en Jahnke (1994) hebben aangetoond dat de benthische regeneratie van reactief fosfor extensiever is in sedimenten die zich onder zuurstofarm bodemwater bevinden, wat resulteert in een lagere P-begravingsefficiëntie. Een verhoogde afgifte van fosfaat uit het sediment gedurende lange perioden van bodemwateranoxia (d.w.z. voor perioden langer dan de verblijftijd van fosfaat in de oceanen), zal op den duur leiden tot een hogere toevoer van fosfaat naar de fotische zone, wat nieuwe primaire productiviteit zal bevorderen (aannemende dat P het biolimiterende nutriënt is). Deze positieve terugkoppeling tussen zuurstofloosheid van de waterkolom, benthische fosfaatregeneratie en primaire productiviteit in de oceanen kan de dikwijls waargenomen aanwezigheid van organisch-rijke sedimenten onder zuurstofloos bodemwater verklaren. In de **Hoofdstukken 6 en 7** zijn de milieucondities onderzocht die P-accumulatie bepalen in de Arabische Zee. De scherpe afname van de accumulatie van reactief P in oppervlakesedimenten met toenemende waterdiepte, in combinatie met constante primaire-productie-snelheden in de hele Arabische Zee, toont aan dat de P-begraving efficiënter is in sedimenten gelegen binnen de ZMZ dan in sedimenten van het diepe

bekken (**Hoofdstuk 6**). Bijgevolg is in de Arabische-Zee-sedimenten geen direct bewijs gevonden voor efficiëntere P-begraving in zuurstofrijke ten opzichte van zuurstofarme bodemwatercondities. De effectiviteit van P-begraving wordt primair bepaald door de verschillen in P-regeneratie in de waterkolom en op het sediment-water-grensvlak.

In **Hoofdstuk 7** wordt de invloed besproken die veranderingen in paleo-productiviteit en redoxcondities van het bodemwater hebben gehad op de begravingsefficiëntie van fosfor tijdens het Laat Kwartair. De efficiëntie van fosforaccumulatie is over het algemeen lager tijdens perioden van hogere mariene productiviteit. Dit kan worden verklaard door a) de gedeeltelijke ontkoppeling van de P-exportflux, die voornamelijk bestaat uit organisch P, en de P-accumulatieflux, die voornamelijk bestaat uit biogeen en authigeen apatiet en b) de relatief lagere snelheden van de vorming van authigeen apatiet tijdens perioden van hogere P-depositie. Hogere primaire productiviteit leidt tot een efficiëntere P-kringloop in de oceanen. Op geologische tijdschalen kan dit proces een hogere productiviteit stimuleren (aannemende dat de beschikbaarheid van P de productiviteit in de oceanen bepaalt) en op deze manier dus een positieve terugkoppeling creëren. In de Arabische Zee kan deze terugkoppeling ook actief zijn op sub-Milankovitch tijdschalen, omdat P dat vrijkomt uit de sedimenten op de continentale helling van de Oman en Somalische kust relatief snel naar de fotische zone wordt getransporteerd.

Acknowledgments

Many people have contributed to the realization of this Ph.D. thesis. With these words I want to thank them all for their cooperation and support during the past five years.

First of all, I want to thank Cees van der Weijden and Gert de Lange for giving me the opportunity to do this research. Their input and constructive remarks were of great value to me. My thanks also go to the members of the dissertation committee Dr. C.P. Slomp, Dr. M. Schlüter, prof. Dr. P. Van Cappellen, Prof. Dr. J.W. De Leeuw, and Prof. Dr. K.B. Föllmi for reading my thesis.

All the sediment samples used for this thesis were collected during the Netherlands Indian Ocean Programme in 1992. I am indebted to Captain J. de Jong, his crew, the technicians of the NIOZ, Texel, and all other participants of this cruise, for collecting this excellent material. For their hard work in obtaining the porewater samples (as I was recently able to experience for myself) I thank Arthur Schmidt, Arian Steenbruggen, Janet Meima, Keimpe Sikkema, and Guido Ypenburg.

I could never have done all my work in the laboratory without the analytical support from all the skillful laboratory assistants and technicians at Utrecht University. I am grateful to Gijs Nobbe, Dineke van de Meent, Mark van Alphen, Paul Anten, Arnold van Dijk, Marjan Reith, Pieter Kleingeld, Tilly Bouten, Helen de Waard (for all those countless ICP analyses), Geert Ittman, Gerrit van het Veld, and Ton Zalm for all their professional help. Anko Potjewijd and John van der Werf are acknowledged for their help with the foram counting.

I appreciated the good cooperation with my colleagues from the micropaleontology (Maryke den Dulk, Jan-Willem Zacheriasse, Lucas Lourens and Joris Steenbrink) and sedimentology department (Maarten Prins and Jan-Berend Stuu). Arie de Jong is thanked for his discussions on the interpretation of the ^{14}C datings. Thanks are also due to Caroline Slomp for letting me use her model for early diagenetic P cycling.

Furthermore, I wish to thank all my colleagues at the department of geochemistry, who made my stay here a pleasant one. I especially thank Arthur Schmidt, Mariëtte Wolthers, Gerard van der Berg, Hendrik-Jan Visser, Thomas Keijzer, Dick Schipper, Hilde Passier, Peter Pruyzers, Hans Hage, Gernot Nehrke, Dorinda van der Linden, Niels Hartog, Gerben Mol, Peter van der Linde, Marijke de Klein, Marcel Hoefs, Caroline Slomp, and Ralph Haese.

Three persons I want to mention in particular. My room mate at the university during the first years and good friend Ivar Nijenhuis I would like to thank for our joint start in marine research (on the boat in Crete that would not leave). His continuing interest and support during all these years helped me to see this work finished. For construction of the sequential extraction methods and many pleasant discussions, I am indebted to Arrian Rutten. I highly appreciated his countless rereads of earlier drafts, which greatly improved their quality. My second room mate Gert-Jan Reichart is thanked for his fruitful and stimulating discussions about the Arabian Sea and all his assistance, that proved indispensable in the realization of this thesis. I particularly remember his suggestion, some three years ago now, "that it might be a good idea to count fish debris". Without that remark this thesis would have looked very differently.

Finally, I want to thank my family and friends (including of course Olaf and Boris) for their continuous support during the last years. Special thanks are due to my parents, for their love, attention and encouragement, and for always being there when I needed them.

Curriculum Vitae

Sjoerd Johannes Schenau werd op 25 oktober 1971 in Gorinchem geboren. In 1984 begon hij met het VWO aan het gymnasium Camphusianum te Gorinchem. Na het behalen van het gymnasium diploma in 1990 begon hij aan de studie Geologie aan de Universiteit Utrecht, waarvan het propedeutisch examen werd behaald in 1991 (*cum laude*). Daarna legde hij zich toe op de studie exogene Geochemie. Deze studie werd in 1994 afgesloten met het doctoraal examen geochemie (*cum laude*). Aansluitend werd hij door de Nederlandse Organisatie voor Wetenschappelijk Onderzoek bij de Faculteit Aardwetenschappen te Utrecht aangesteld als Onderzoeker in Opleiding. In deze functie verrichtte hij geochemisch onderzoek aan Arabische Zee sedimenten, waarvan de resultaten in dit proefschrift zijn beschreven.

“Vancouver, Vancouver, this is it !”

